Faculty of Science and Engineering
School of Electrical and Computing Engineering
Department of Electrical and Computer Engineering

Analysis and Solutions of Congestion of Vehicles using DTCA, FUZZY logic, and ITS on Highways

Ahmed S. AlGhamdi

This thesis is presented for the Degree of
Doctor of Philosophy

Curtin University

October 2013

Declaration

To the best of my knowledge and belief, this thesis contains no material previously published by any other person except where due acknowledgment has been made.

This thesis contains no material which has been accepted for the award of any other degree or diploma in any university.

Signature:

Date: 11/11/2013

Abstract

Automotive technology has become an important part of life on both individual and collective levels. As a part of modern civilization and global economic development over the years, traffic congestion has become a serious issue for all nations. Therefore, to date many researchers have considered traffic flow issues seriously by using different techniques. Some traffic system researchers focus on experimental techniques, while others focus on mathematical descriptions and simulation models. The models could be classified depending on whether they are submicroscopic, microscopic, mesoscopic, or macroscopic modelling, and on temporal factors like continuous or discrete time descriptions. Cellular Automata (CA), adapted in this work, is one of the models developed for studying traffic flow. It uses discrete steps for processing updating the movement of vehicles. Contrastingly, different types of controllers, such as the FUZZY Logic Controller (FLC) and the PID, have been used commonly to describe and control vehicle behaviour. The FLC uses instantaneous and integral data, which does not need to be highly accurate to perform actions similar to those of a human driver. Therefore, FLC has commonly been used to simulate human driving behaviour. Recently, it has been recognised that communication among vehicles could assist traffic flow and could provide solution for traffic congestion and there are systems running on trial basis. Among several communication systems, the Information Transportation System (ITS) is the most common type. Inter-vehicular communication not only helps to alleviate congestion, but also reduces fuel consumption and toxic gas emission into atmosphere.

In this research, CA model has been improved further, and the new model is referred to Dynamic Traffic Cellular Automata (DTCA). Cells in DTCA are eliminated for the applicable vehicles. DTCA model changes information on the position and movement of the vehicles from a discrete to continuous form. For the conventional individual cell model, the dawdling probability of the vehicle velocity has been modified to three factors, namely: acceleration, deceleration, and vehicle and driver reaction, to improve the real vehicle behaviours in the simulation. In addition, it has been shown that the acceleration and deceleration factors play key roles in DTCA model. This model clearly shows that the conflicting of speeds between the lead

vehicle and the following vehicle significantly affects relative velocity and relative position. In addition, the start-up vehicles from stationary position, the delay modelling has been tested and applied in the DTCA model, and it has been shown to improve the traffic flow. As a result, the DTCA model has been improved to describe the traffic flow in a mathematical matrix form using acceleration, velocity, and position.

This study has been extended by inclusion of the driver behaviour using FUZZY Logic Controller (FLC). Four types of human driver behaviour characteristics have been considered, as:

- Normal human driver behavior as mathematically described in literature,
- Asymmetric auto driving conditions for simulating automatic vehicles of different brands and models,
- Symmetric auto driving conditions for simulating automatic vehicles of similar brands and models,
- Human driver behaviour with information available from Information Transportation Systems (ITS).

The Human Driver Behaviour, Asymmetric Auto Driving and Symmetric Auto Driving simulation models reflect different types of driving scenarios where vehicles are driven without any communication between them. It has been shown that these non-communicative models create isolated pockets of congestions or clusters of vehicles. The only difference between these models is the intensity of traffic congestion and magnitude of clusters. It has also been shown that the congestion in Human Driver Behaviour scenario worsens over time, while there is no significant change in the congestion in the Auto Driving scenario. But, significant improvements have been recorded when ITS has been applied.

In order to capitalize on the benefit of using ITS, using the Human Driver Behaviour, the vehicle behaviour has been modified based on the information about the congestions. In this case, appropriate vehicle controllers have been activated to adjust inter-vehicular gap. This helps the reduction of traffic flow density for the vehicles approaching congestion ahead. Consequently, the velocity is reduced and inter-vehicular gap is increased allowing new vehicles to arrive at the congestion site in a controlled manner to reduce the intensity of congestions. The inter-vehicle gap

controller receives the signal and converts it to a suitable signal and sends it to the Human Driver Behaviour Model controller. The gap controller modifies the gap otherwise would have caused by the Human Driver Behaviour Model. The modified control forces the Human Driver Behaviour Model to reduce the velocity of the vehicle. After a certain laps of time, congestion starts dissolving because the number of vehicles leaving the congestion becomes higher than the number of vehicles arriving. It can easily been seen that, at some stage, there is an equilibrium where arriving vehicles are equal to those leaving the congestion, called the critical density point.

After having investigated various mathematical models, this project considered other factors such as: average distance covered by each vehicle, average of instantaneous traffic flow, total fuel consumption, and total gas emission into the atmosphere. It has been shown that the average distance covered per unit time in Human Driver Behaviour with the ITS Model is less than the Asymmetric Auto Driving Model and Symmetric Auto Driving Model because velocity is controlled to avoid congestions. The Asymmetric Auto Driving Model and Symmetric Auto Driving Model leads to better stability in traffic flow. In Human Driver Behaviour Model traffic flow is much reduced because of an increase in the congestion size, and more frequent clusters. However, the Human Driver Behaviour utilising ITS Model gradually rises traffic flow if the average velocity of the system is relatively higher, say 100 km/h instead of 40 km/h. Fuel consumption and emission indicate that the Human Driver Behaviour utilising ITS Model has the lowest amount of fuel consumption and emission, producing in all vehicles an average or per certain distance average.

HIGHLIGHT

- Cellular Automata (CA) is modified to Dynamic Traffic Cellular Automata (DTCA) to simulate traffic flow with its congestion. DTCA model has Acceleration factor, deceleration as controlling factors in the acceleration and deceleration. In addition, reaction factor is controlling the making decision.
- Traffic flow matrix has been modified to understand the relation among the vehicles to reduce the congestion.
- Modifying FUZZY Logic as a common controller to control the vehicles has Astrom first-order model. The vehicles are running in one lane loop to make

traffic flow with initiated congestion. There are four scenarios has been established: Human Driver Behaviour, Asymmetric Auto Driving, Symmetric Auto Driving and Human Driver Behaviour with utilising ITS models.

- The benefit of using the communication network technology among vehicles to sense the distance and speed of others on the road has been investigated. There are many benefits has been done: solving the congestion, reducing the fuel consumption and reducing the emissions.

Acknowledgements

I would like to acknowledge the direct and indirect help and support of many people for the production of this thesis. I would like to express my sincere gratitude to my supervisor, Dr Halit Eren, for his patience, guidance and belief in my abilities, which kept me constantly motivated and truly helped in completing this task.

I would also like to thank my co-supervisor, Dr Ali Mansour, for motivating me and providing his invaluable suggestions to this thesis.

I would also like to acknowledge the Saudi Arabian government for the 'King Abdullah Scholarship', which supported me and my family's financial needs during my research.

I would also like to express my appreciation to all my post-graduate colleagues for the formal discussions we had regarding our projects. I would especially like to extend my heartfelt appreciation to a very special friend, who prefers to remain anonymous due to personal reasons, for helping me many times to get back on track.

I would like to thank my parents for the unconditional love and inspiration they provided, despite their being far away. They never let me realise that they are living on the other side of the world.

I would like to thank my brother and sisters, Salem, Mohrah, Maha, Seham and Fatemah, for their support during my study away from home.

Last, I would like to thank my beloved wife, Reem AlGhamdi, for her endless patience and everlasting support. I also wish to express my gratitude to our children, Juri, Hala, Fajer and Abdullah, for their love and being a source of everyday inspiration for all the work I have put into this thesis.

Publications Resulting from This Thesis

1. AlGhamdi, Ahmed S., Eren, Halit, and Hariani Pakka. 'Microscopic Analysis of Highway Congestion by DTCA Model'. *International Journal of Modelling and Optimization* 2 (2012).
2. AlGhamdi, Ahmed Saeed, Eren, Halit, and Ali Mansour. 'Application of Fuzzy Logic control in automated transport systems'. *Sensors Applications Symposium (SAS), 2010 IEEE*. 2010, pp. 216-219
3. AlGhamdi, A., Eren, H., and H. Pakka, 'Dynamic Traffic Cellular Automata model to express the congestion at one lane highway traffic system', in International Proceedings of Computer Science & Information Tech, Perth, WA, 2012, pp. 69.
4. AlGhamdi, Ahmed S., and Halit Eren. 'Highway Traffic Flow Equation Depending on DTCA'. *Human System Enteractions (HSI), 2012 5th Enternational Conference on. IEEE,* 2012. pp. 130-136
5. Eren, H., Pakka, H. M. T., AlGhamdi, A. S., & Yue, Y. (2013, May). Instrumentation for safe vehicular flow in intelligent traffic control systems using wireless networks. In *Instrumentation and Measurement Technology Conference (I2MTC)*, 2013 IEEE International. pp. 1301-1305.
6. AlGhamdi, Ahmed S., Eren, Halit, and Abdulwahed Salem. 'FLS Modelling and Using ITS to Adopt Traffic Congestion'. Intelligent Systems Modelling & Simulation (ISMS), 2013 4th Enternational Conference on. IEEE, pp. 112-115
7. A. AlGhamdi and H. Eren, 'Using Fuzzy Logic to Control Vehicles' Velocity in Traffic Systems', in The Enternational Federation of Automatic Control (IFAC), Gold Coast, Australia, 2013, pp. 54-59.

TABLE OF CONTENTS

FIGURES

APPENDIX FIGURES

TABLES

APPENDIX TABLES

NOMENCLATURE

a	Acceleration
a_{max}	Maximum acceleration
A	Frontal cross-sectional area of vehicle
ACC	Adaptive cruise control
ADAS	Advanced Driver Assistance Systems
ADASE2	European project of Advance Driver Assistance Systems
$ADRT$	Acceleration/Deceleration Reaction Time
Age	Driver age
b	Maximum deceleration
b_0 to b_6	Acceleration vehicle-specific regression coefficients
c	Resistance constant
C	Air drag coefficient
CA	Cellular automata
CAMP	Crash Avoidance Matrices Partnership
CAS	Collision Avoidance System
CICAS	Cooperative Intersection Collision Avoidance Systems Initiative
CICASSLTA	CICAS-Signalized Left-Turn Assist
CICASTSA	CICAS-Traffic Signal Adaptation
CICAS-SSA	CICAS-Stop Sign Assist
CICAS-V	CICAS-Violation Warning System
CO	Carbon monoxide
$\mathrm{CO_2}$	Carbon dioxide
CTCR	Congestion Thickness Change Rate
dec_{max}	Maximum deceleration
DTCA	Dynamic Traffic Cellular Automata model
d_0 to d_6	Deceleration vehicle-specific regression coefficients
D_{ramp}	Delay at the ramps imposed by IMP
DOT	U.S. Department of Transportation
E	Acceleration force
F	Force
FLC	FUZZY Logic Controller
$\mathrm{FLC_{out}}$	FLC output
FRF	Frequency Response Function
G	Gravity
G_F	Gradient
$Gender$	Driver gender
G_{min}	Jam distance
GNP	Gross National Product
GPS	Global Positioning System

H	Any added curvature resistance
H_c^{in} & H_c^{out}	vehicle's dynamic
H_d^{in} & H_d^{out}	drive Frequency Response Function (FRF)
ICT	Information and Communication Technologies
IDM	Intelligent Driver Model
IMP	Idealized ramp Metering control Policy
IR	Infrared
ITS	Information Transportation System
j	Gap a head in CA
$k_{i,0}^{e}$	Cruising vehicle-specific regression coefficients
L	Length of vehicle
m	Number of the vehicle in cluster queue
M	Mass of the vehicle
MAC	Medium Access Control layer
MANET	Mobile ad hoc network
$\mathrm{MOE_e^{decel}}$	fuel consumed, or pollutants emitted while decelerating
$\mathrm{MOE_e}^{cruise}$	fuel consumed, or pollutants emitted while cruising
$\mathrm{MOE_e}^{accel}$	fuel consumed, or pollutants emitted while acceleration
n	Vehicle order number on queue
N_2	Nitrogen
NAAQS	National Ambient Air Quality Standards
NO_2	Nitrogen dioxide
O_2	Oxygen
O_3	Ozone
p	Given probability and Reaction factor
P_m	Propulsive force
PDF	Probability Density Function
PHY	Physical layer
PID	Proportional, Integrative and Derivative controller
PM-10	Particulate matter
R	Desired speed
r	Fuel rate
R_m	Inherent resistance to motion
SO_2	Sulfur dioxide
t	Time
T	Safety time gap
TCTCR	Traffic Congestion Thickness Change Rate
TF	Traffic flow on the highway
TF_{in}	Traffic flow going to the congestion zone
TF_{out}	Traffic flow leaving the congestion zone
U	Coefficient of rolling resistance for automobiles
v	Velocity
v_0	Initial velocity at leaving point

V_{des}	Desired velocity
V_{min}	Minimum velocity
V_{max}	Maximum velocity
v_{rel}	Relative velocity
$\dot{v}$	Acceleration
$\dot{v}_{free}$	Acceleration on a free road
v_{lead}	Velocity of lead vehicle
VANET	Vehicular Ad Hoc Networks
VHT	Total number of vehicle hours traveled over the section over some time interval
VHT_{imp}	total travel time under IMP
VMT	Total number of vehicle miles traveled
VT-Micro	Virginia Tech to compute mode specific fuel consumption and emission rates
V-2-I	Vehicle to Infrastructure
V-2-V	Vehicle to Vehicle
W	Total propulsive work
WLAN	Wireless Ad-hoc and Local Area Networks
x	Position
x_{des}	Desired minimum gap
x_{min}	minimum gap
$x_{min\ \_rel}$	Minimum head gap in the cluster
x_{rel}	Distance gap to a head vehicle (Relative distance)
z	fuel consumption

GREEK SYMBOLS

δ	Acceleration exponent constant
η	Efficiency
α	Acceleration factor
β	Deceleration factor
Γ	Weight of vehicle
ρ_{air}	Air density
θ	Ascent angle
θ_v	Vehicle angle of inclination from the horizontal plan
Λ	Friction coefficient for dry seal roads
φ	Safety factor
ϕ	Combination of α and β
$\gamma_1, \gamma_2, \gamma_3, \gamma_4\ \gamma_5$	Regression coefficient
ρ	Traffic density
ρ_{in}	Input traffic density
ρ_{out}	Output traffic density

Chapter 1

Introduction

The invention of the vehicle left an indelible mark on the welfare of the individuals and society at large. With the development of high level automotive technology, the vehicles have become an important part of life on the individual and collective level. Now, we can measure the well-being and prosperity of a society with the quality of the vehicles used for travelling. Modern and industrialised societies need an efficient transportation system to improve the quality of life [1]. Part of the challenges facing the societies are traffic safety, traffic flow, environmental issues, and energy consumption, and the growing demands placed on roads [2]. Moreover, in the last few decades, the traffic has grown much faster than the transportation infrastructure. Traffic congestion is expected to become a severe problem worldwide. The costs of traffic congestion in the European Union countries approximated 1.5% of its Gross National Product (GNP) in 2010. In 2005, congestion costs totalled about €55 billion in the USA, which was about 0.7% of the GNP [3, 4]. Researchers are looking for solutions in which the capacity of the roads could be improved for more efficiency.

These solutions start at partly automated driver assistance systems such as Adaptive Cruise Control (ACC) and range to fully automated vehicle control systems like Information and Communication Technologies (ICT) [3]. In this thesis, we attempt to find solutions to ease highway traffic congestion by using ICT and Fuzzy Logic Controller (FLC). In addition, the environmental and energy consumption implications of using ICT and FLC are studied.

This background provides a starting point for the next part of the introduction. In the following section, 1.1, an overview of actual driver assistance systems will be provided. In section 1.2, mathematical models for describing driving behaviour and traffic flow dynamics will be expressed. This introductory chapter will be completed with an outline of the thesis structure and an overview of the remaining chapters in section 1.4.

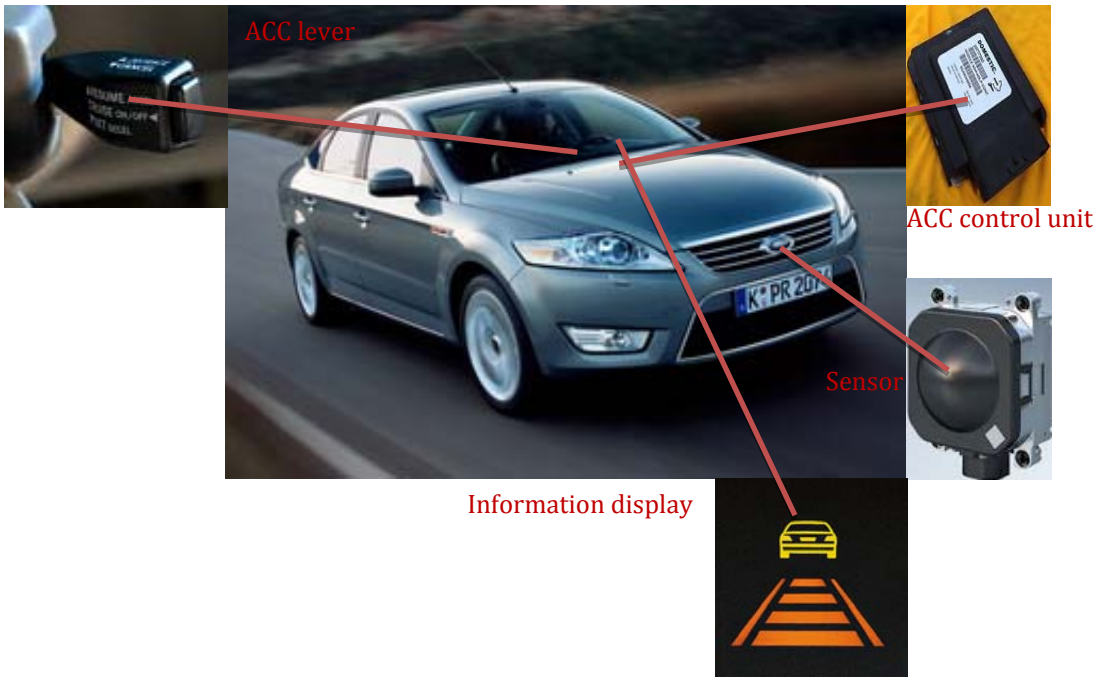

Figure 1-1: Parts of Adaptive Cruise Control (ACC) system

1.1. Driver Assistance Systems

Vehicle technology is rapidly increasing in solid-state electronics, sensors, computer technology and control systems [5]. Automotive manufacturers have deployed a variety of driver assistance systems to improve vehicle control and automate driving operations. Driver assistance systems will continue to develop with the evolution of Advanced Driver Assistance Systems (ADAS), which hold great potential in increasing the safety, convenience and efficiency of driving. ADAS come in many forms, from a navigation system, lane departure warning and lane-keeping assistance system, collision warning systems and active pre-crash assistance, intelligent speed adaptation, infrared technology, driver condition/drowsiness monitoring systems and automatic parking. One of the essential driver assistance systems is Adaptive Cruise Control (ACC); see Figure 1-1. ACC systems are exclusively designed to increase driving comfort and are expected to become more common [6]. Acceleration may be controlled via an electronic actuated mechanism that exercises control over an engine or motor that propels the vehicle. A vehicle propelled by an internal combustion engine may have an electronic throttle control that changes the amount of engine throttle opening to apply the corresponding acceleration force to the vehicle via the drive train. In contrast, deceleration may be applied to a vehicle via its service brakes. In vehicles with hydraulic-actuated service brakes at the wheels and an ABS system for operating the brakes, an adaptive cruise control may apply deceleration force to the vehicle via the ABS hydraulic system [7]. In contrast, merging, lane changing or creating gaps for other vehicles still need the intervention of the driver. Therefore, the driver is still fully responsible and can cancel the system at any time.

Driver assistance systems are developed with the aim of improving of automatic vehicle control systems, parameter estimation, signal processing, inter-vehicular communications, vehicle networks, and so forth. The improvement of the driver assistance systems led to an increase on the objectives of many researchers. Therefore, it has been suggested that the ACC system must meet the expectations of the human driver to a certain degree [8]. Because of some advantages to FUZZY Logic, it has been applied in vehicle following models [9]. The FUZZY Logic Controller (FLC) model for the vehicle following is based on the deviation of the

ratio of vehicle distance to the desired vehicle distance together with the relative speed of two vehicles [10].

1.2. Modelling of Driver Behaviour and Traffic Dynamics

Research and experiments with real-life traffic flow could help to improve traffic systems [11]. However, apart from the scientific problem of reproducing such experiments, costs and safety play a role of dominant importance as well. Due to the complexity of the traffic flow system, analytical approaches may not provide the desired results. Therefore, traffic flow (simulation) models designed to characterise the behaviour of complex traffic flow systems have become an essential tool in traffic flow analysis and experimentation.

Mathematical modelling of the dynamics of traffic flow has a long history. Since the 1930s, scientists have studied the fundamental relations of traffic flow, velocity and density. Dynamic macroscopic and microscopic models have been utilised to describe the physical propagation of traffic flows since the 1950s [12, 13]. During the 1990s, the availability of better traffic data and higher computational power for numerical analysis made traffic modelling grow rapidly [14].

There are two types of transportation modelling, traffic flow modelling and the approach used for transportation planning. Dynamic flow models describe the physical propagation of traffic flows in a road, while transportation planning models are the link between traffic and the economic, social and cultural activities of travelers [15]. For our purposes, the most important is the dynamic flow model. There are two major methods in expressing the propagation of traffic flow:

- Macroscopic traffic flow models (Figure 1-2) shown on color coded

  These focus on traffic dynamics such as traffic density, flow or average velocity as a function of space and time corresponding to partial differential equations.

- Microscopic traffic models (Figure 1-2)

  These express the motion of each individual vehicle, such as accelerations, decelerations and the lane changes of each driver.

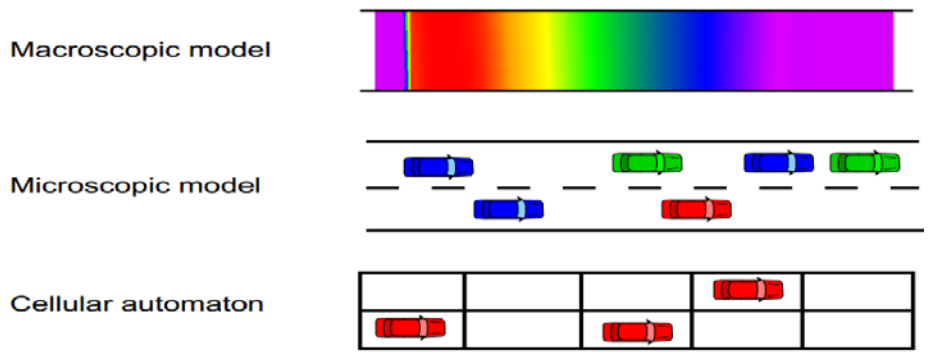

Figure 1-2: Different traffic models [3]

Microscopic traffic models can be distinguished into the following subclasses:

- Time-continuous models are formulated as differential equations, and consequently, space and time are treated as continuous variables.
- Cellular automata (CA) use integer variables (cells) to describe the dynamic state of the system (Figure 1-2).
- The function of iterated coupled maps is between CA and time continuous models.

This is the starting point for this thesis, in which the question of the impact of individual and automated driving behaviour on traffic dynamics will be assessed. Before this, this thesis will deal with methodological fundamentals. Time-continuous microscopic models will be presented, and evolving system dynamics will be studied numerically. Traffic simulation software has been developed, which will be described particularly with regard to the traffic simulations of traffic flows.

1.3. Scope and Objectives of Project

Over time with the economic developments, land transportation has become increasingly essential. The number of vehicles on the road has risen dramatically since the first car was manufactured. Recently, road congestion is evident in big cities worldwide and causes extensive problems related to gross national product (GNP), the environment, the public health. Expanding the roads is the first step towards minimising traffic congestion; however, this is very limited and insufficient. Therefore, researchers have begun to investigate the practical and effective methods of solving congestion issues.

Vehicles traffic congestions may occur due to a number of reasons. Many researchers worked on and identified those reasons, they configured mathematical and simulation models, also tested the theory with practical operations. Other researchers have worked on improving the road condition. But, we can confidently claim that the transportation world is moving to intelligent traffic systems. Intelligent traffic systems are claimed to improve traffic flow and safety. The specific objectives of the present study are as following:

- To develop traffic flow matrix to get the relation with other vehicles to reduce the congestion.
- To develop FUZZY Logic controller to control vehicle velocity.
- To develop communication network among vehicles to sense the distance and speed of vehicle among others on the road to reduce the congestion.
- Investigate the benefit of using the communication technology in traffic system

1.4. Thesis Overview and Outline

This thesis consists of two major parts. In Part I, the methodological fundamentals will be developed, which will deal with the microscopic model, Cellular Automata (CA), for traffic flow behaviour. The focus will be on future ACC systems and their abilities for solving traffic congestion-based intelligent transportation systems (Part II). This relates to the collective characteristics of traffic flow, which only can be answered by computer simulations and requires an integrated microscopic simulation approach.

Chapter 2 will introduce a brief explanation of the historical development of traffic flow, ITS communication, the FUZZY Logic Controller (FLC), energy consumption and emissions.

Chapter 3 will express the relation among vehicles by using the Dynamic Traffic Cellular Automata (DTCA), which improves CA. The mathematic equation of the relationship in one lane has been expressed. Drivers behave to increase or decrease velocity, which is defined as acceleration and deceleration factors. Those factors affect a vehicle's reaction. Also, the reaction factor states the driver should take action.

In **Chapter 4,** a methodology will be presented that calibrates a vehicle following model with respect to realistic microscopic data. This chapter will express three models: traffic system, individual vehicle and controller.

Chapter 5 reveals simulation results, which are discussed for the Human Driver Behaviour Model for different desired speeds, from 20 Km/hr to 140Km/hr, the Asymmetric Auto Driving Scenario Model with 120 Km/hr speed and the Symmetric Auto driving Scenario Model with 120 Km/hr speed.

In **Chapter 6,** the results of Human Driver Behaviour utilising the ITS Model will express one way of alleviating congestion by adding the x_{rel}signal controller.

In **Chapter 7,** the total distance has been passed, traffic flow, fuel consumption and emissions in the four scenarios will be expressed to compare those scenarios.

Chapter 2

Literature Review

2.1. Introduction

During the past several years, many researchers have considered traffic flow issues is different ways. Some researchers focus on such phenomena as traffic flow stability, safety rules such as pedestrian safety rules, Information Transportation Systems (ITSs) and using new technology in traffic systems such as ACC, fuel consumption, emissions like vehicle carbon monoxide (CO) and so on [16-19].

In this part of the thesis, I would like to give a brief explanation of the historical development of traffic flow in section 2.2, ITS communication in section 2.3, FUZZY logic in section 2.4, energy consumption in section 2.5 and emissions in section 2.6.

2.2. Traffic Flow

Research and experiments in the fields of real-life traffic flow can improve traffic systems [11, 20]. The models have been utilised for reproducing observed collective, self-organised traffic dynamics, including phenomena such as breakdowns of traffic flow, the propagation of stop-and-go waves (with a characteristic propagation velocity), capacity drop, and different spatiotemporal patterns of congested traffic due to instabilities and nonlinear interactions [11, 14, 21-29]. Levels of detail, operationalisation and representation of processes categorised traffic flow models [11, 30]. These have been classified based on the level of detail, such as submicroscopic, microscopic, mesoscopic and macroscopic modelling approaches [11, 30]. According to Hoogendoorn [11], submicroscopic simulation models provide a highly detailed description of vehicles' subunits functioning and their interaction with their surroundings. Microscopic simulation models are highly detailed descriptions with distinguishing and tracing individual entities. Mesoscopic and macroscopic models show medium and low detail, respectively. Traffic flow models could be dynamic traffic management, the design and testing of transportation facilities, operational flow models serving as a sub-module in other tools such as model-based traffic control, and training of traffic managers [11, 30]. For a quantitative description and assessment of the collective traffic dynamics of mixed traffic flows emerging from the driving behaviour of individuals, one must start with traffic models, which capture the nature of automated and manual driving to a realistic degree [6]. We focus on the submicroscopic and microscopic traffic flow models that are separated into vehicle following models, microscopic simulation models, submicroscopic simulation models, cellular automaton models and particle models [11].

A microscopic traffic flow model describes the motion of each vehicle [3]. The calculation of the first-time derivative of the position to make the speed of the individual vehicle is the definition of microscopic traffic. It can be written as [31]:

$$\tilde{v}(\tilde{x}^0, t) = \left.\frac{\partial \tilde{x}(\tilde{x}^0, t)}{\partial t}\right|_{\tilde{x}^0} \tag{2-1}$$

$\tilde{x}^0$ is the initial position of the n[th] vehicle, and $\frac{\partial \tilde{x}(\tilde{x}^0,t)}{\partial t}\Big|_{\tilde{x}^0}$ is the speed of the vehicle at $\tilde{x}^0$.

According to Kesting, Treiber and Helbing [12], microscopic traffic models can be divided into three major subclasses:

- Time-continuous models are ordinary or delayed differential equations. Consequently, space and time are treated as continuous variables. Vehicle following models are the most prominent examples of this approach [32-34]. In general, these models are deterministic, but stochasticity can be added in a natural way [35, 36].
- Cellular automata use integer variables to describe the dynamic state of the system. The time is discretised, and the road is divided into cells, which can be either empty or occupied by a vehicle. Besides rules for accelerating and braking, most CA models require additional stochasticity. The first CA for describing traffic was proposed by Nagel and Schreckenberg [26]. Although CA lacks the accuracy of time-continuous models, they can reproduce some traffic phenomena [37, 38]. CA can be implemented to simulate large road networks efficiently [39].
- Iterated coupled maps are between CA and time-continuous models. In this model class, the updated time is considered an explicit model parameter rather than an auxiliary parameter needed for numerical integration. Consequently, the time is discretised while the spatial coordinate is still continuous. Popular examples are the Gipps model and the Newell model [40, 41].

We aim to develop a mathematical model of traffic flow to determine the relationship among the vehicles, clusters of vehicles to reduce congestion; therefore, a historical novel about CA and traffic systems will be taken as the base as described in Sections 2.2.1 and 2.2.2.

2.2.1. Cellular Automaton

Cellular Automaton is one of the more recent additions to the development of microscopic traffic flow theory [11, 26, 42-44]. Pattern cells, with a size equal

to 7.5m, is the definition of CA models [11, 26, 42]. It has been proven that the CA technique can approximate the solutions of hydrodynamic partial differential equations [45]. Discrete time and velocity is the base of the movement of the vehicle in the CA model. The vehicle's velocity ranges from zero to V_{max} [11, 26, 42].

According to Hoogendoorn and Bovy, the process can be split up into three steps [11]:

- **Acceleration**

  Each vehicle with a velocity of less than V_{max}, accelerates to $v + 1$.

$$v \leftarrow min\,(V_{max}, v + 1) \qquad (2\text{-}2)$$

- **Deceleration**

  If the velocity is more than the distance gap (x_{rel}) to the preceding vehicle, then the vehicle will decelerate.

$$v \leftarrow min\,(v, x_{rel}) \qquad (2\text{-}3)$$

- **Dawdling**

  With given probability (p), the velocity of a vehicle decreases randomly.

$$v \leftarrow max\,(v - 1, 0) \qquad (2\text{-}4)$$

But Nagel and Schreckenberg have added the fourth step [26]:

- **Vehicle motion**

  In each step, v cells advance with each vehicle.

The CA model has been used to simulate traffic operations, traffic assignments and traffic forecasting because of the minimising set of driving rules. The ability to apply parallel computing makes the CA model very fast [11].

The classical CA vehicle-following model is proven by Wu and Brilon, who proposed an alternative multilane CA model by using time-oriented vehicle

following rules that were more realistic and saving all the positive features of the original CA model [11, 28].

CA models have been verified on different systems and show fairly realistic results on a macroscopic scale, especially in the case of urban networks in terms of the reproduction of empirical speed density curves [28, 46, 47]. CA models combine the advantages of compound microscopic simulation models yet remain computationally efficient. Moreover, they are too simple to describe and study the microscopic details of traffic flow like overtaking and merging, which is sufficiently accurate from a single driver's perspective. However, CA models with space- and time-oriented vehicle following rules lack intuitive appeal, and their exact mechanisms are not easily interpretable from the driving task perspective [11].

One of the other microscopic traffic flow models, which describes the motion of each individual vehicle, is the Intelligent Driver Model (IDM). IDM assumes that the dominant influence on driving behaviour comes from the vehicle ahead, called the leading vehicle, Figure 2-1 [3, 48].

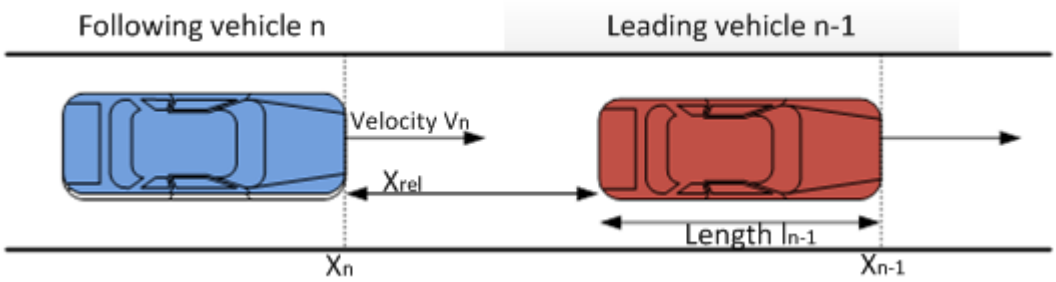

Figure 2-1: The input quantities of a vehicle model

The front bumper to rear bumper distance between a vehicle n and $(n-1)$ in front is given by

$$x_{rel} = x_{n-1} - x_n - l_{n-1} \tag{2-5}$$

Where (x_{rel}) is the front bumper to rear bumper distance, (l_n) is the vehicle length and (x) is the vehicle position on the considered stretch of road. The relative velocity is defined as:

$$v_{rel} := v_n - v_{n-1} \tag{2-6}$$

Where (v_{rel}) is the relative velocity.

The superposition of the acceleration is

$$\dot{v}_n(x_{rel}, v_n, \Delta v_n) = a\left[1 - \left(\frac{v_n}{v_{des}}\right)^{\delta} - \left(\frac{\mathrm{X}_{des}(v_n, v_{rel})}{x_{rel}}\right)^2\right] \tag{2-7}$$

Where ($\dot{v}_n$) is the acceleration as the result of the maximum acceleration (a_{max}). The acceleration exponent constant (δ) illustrates how the acceleration decreases when approaching the desired velocity. This expression, ($\dot{v}_{free}$), is a superposition of the acceleration on a free road to be

$$\dot{v}_{free}(v) = a[1 - (v/v_{des})^{\delta}] \tag{2-8}$$

However, the braking deceleration reflects an interaction when vehicle comes too close to the vehicle ahead. Where v_n/v_{des}=1, which leads to

$$-\dot{v}_{int}(x, v, \Delta v) = a(\mathrm{x}_{des}/x_{rel})^2 \tag{2-9}$$

The deceleration term depends on the ratio between the effective and desired minimum gap (x_{des}). The minimum gap (x_{min}) in congested traffic is significant for low velocities only.

$$x_{des}(v, \Delta v) = x_{min} + vT + \frac{v\Delta v}{2\sqrt{ab}} \tag{2-10}$$

Where a_{max} and b is maximum acceleration and deceleration respectively, while the main contribution in stationary traffic is the term vT, which corresponds to following the leading vehicle with a constant 'safety time gap', T. The last term is only active in non-stationary traffic with $v_{rel} \neq 0$ and implements intelligent driving behaviour including a braking strategy that, in nearly all situations, limits braking decelerations to the comfortable deceleration, b. Moreover, the IDM braking strategy guarantees collision-free driving.

Table 2-1: IDM parameters together with a typical setting and reasonable parameters of different drivers and situations [3]

IDM parameters	**Typical value**	**Reasonable range**
Desired velocity v_{des} [km/h]	120	$20 - 200$
Safety time gap T [s]	1.5	$0.9 - 3$
Jam distance G_{min} [m]	2.0	$1 - 5$
Maximum acceleration a_{max} [m/s^2]	1.4	$0.3 - 3$
Desired deceleration b [m/s^2]	2.0	$0.5 - 3$

The five IDM parameters, with typical values for freeway traffic together with their reasonable ranges, are listed in Table 2-1. An important feature of the IDM is its few parameters, which additionally have an intuitive meaning. According to Kesting, all parameters are measurable, and the best values are in a realistic range. The IDM can be calibrated essentially independently with respect to the behaviour in stationary situations and with respect to the stability of traffic flow.

2.2.2. Traffic System

It is believed that congestion occurs because the number of vehicles exceeds a road's capacity, so many people support initiatives to change roads or change the use of the road [49, 50]. Authorities would like to implement more highway construction projects into their areas. But environmentalists encourage making public

transportation more attractive or making private vehicles more costly [49, 50]. Improving traffic flow and road safety is the goal of the advanced traffic management system [51, 52]. The efficiency (η) of any highway section is one of the ways of measuring specifications and can be written as [49]:

$$\eta = \frac{VMT/v_{des}}{VHT} \tag{2-11}$$

Where VMT is the total number of vehicle miles traveled.

VHT is the total number of vehicle hours traveled over the section during a given time interval.

The Idealised ramp Metering control Policy (IMP) holds vehicles back at on ramps so the occupancy on each highway section is maintained at its critical level. The total travel time under IMP (VHT_{imp}) is the sum of highway travel time (at 100% efficiency, v_{des} mph) and the delay at the ramps imposed by IMP:

$$VHT_{imp} = \frac{VMT}{v_{des}} + D_{ramp} \tag{2-12}$$

Where D_{ramp} is the delay at the ramps imposed by IMP.

Therefore, the travel time saving from IMP is

$$VHT_{saved} = VHT - VHT_{imp} \tag{2-13}$$

Comparing the actual travel time to some standard is the way to measure congestion delay [49]. There are two defensible standards. One is travel time under free-flow conditions (v_{des} mph). The other is travel time under maximum flow. From that definition and from Equation 2-12 and Equation 2-13, one can find the congestion delay with the following:

$$Congestion\ delay = VHT_{saved} + Delay_{ramp} \tag{2-14}$$

It is very essential to understand occupancy, which is passing distance during time.

$$Occupancy = \frac{VPH(\text{Vehicle/hr}) \times l(\text{mile})}{v\ (\text{mile/hr})} \quad (2\text{-}15)$$

Building new road infrastructure is becoming increasingly difficult while congestion costs are growing rapidly [53, 54]. Congestion affects both the speed of travel and the reliability of travel conditions [55]. Here, in this research, we would like to find a solution for congestion rather than modify the roads or the behaviour of drivers by using new technology to rise the traffic flow and safety with decline of fuel consumed and emission.

2.3. ITS Communications

The Intelligent Transport System has been produced because of symbiosis between communication technologies and transport infrastructure [56]. Societies will be affected by the role of ITS, in which "each automotive vehicle will be a unique node on a global and ubiquitous vehicular communications network in the future" [56]. These intelligent communication systems will support scenarios in which interactions within the vehicle, with the surrounding environment and directly with nearby vehicles will offer real-time communication among thousands of vehicles daily crossing cities and highways and opening new opportunities to many challenging applications dealing with security, management and entertainment on the road in a highly efficient way [48, 56, 57]. For many purposes, the U.S. Department of Transportation (DOT), for example, recognised the ITS to "enhance mobility and safety and to reduce fuel consumption and emissions without the formerly exclusive reliance on an expanding physical infrastructure" [48].

One of the objectives of this project has been the reduction of traffic congestion by developing inter-vehicular communication network to enable vehicles to sense the distances and speeds of other vehicles in the vicinity. Therefore, ITS refers to the integrated application of communication and control systems with the aid of information processing technologies in vehicles and in the transportation infrastructure [49]. These technologies will allow safe, tightly spaced vehicle

clusters or platoons, coordinate safe lane merges, collision avoidance in intersections and under limited-visibility conditions. The technology is moving in such a way that wireless communication will directly be applied between vehicles [57] for efficiency and economy,. ITS can be [49,58-62]:

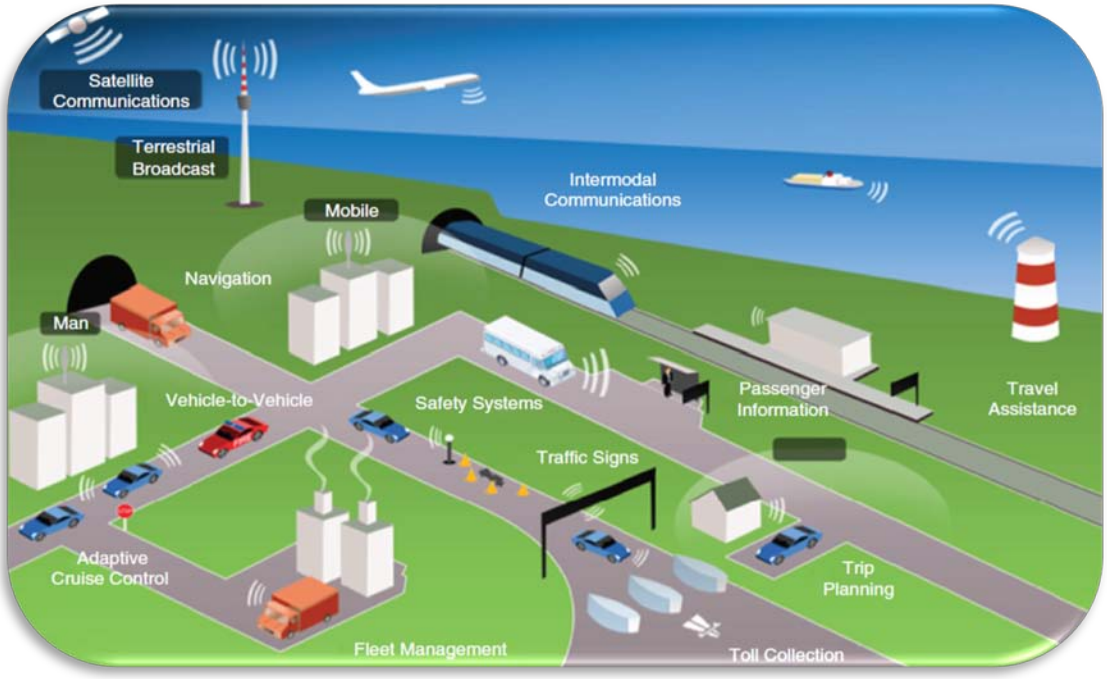

Figure 2-2: Overview of ITS [63]

a) **Navigational aid** is provided by a set of on-board sensors, including a speed gauge and compass; indicators for travel distance, time, location, remaining distance and time to destination; turn-by-turn guidance for drivers; and real-time traffic information. The global positioning system (GPS) is becoming an essential component of navigational aid.
b) The **lane departure warning system** is a driver assist technology that is designed to alert a driver when the vehicle begins to depart from its lane without the proper use of a turn signal. There are two types of these systems: i) systems that only warn the driver using visual, audio or vibration feedback and ii) systems that warn the driver. If no action is taken, the latter automatically takes steps to ensure the vehicle keeps in its lane.
c) The **drowsy driver warning system** monitors the driver's eye movements and detects when a driver is showing signs of fatigue. The system then sends

audio, visual or vibration alarm feedback to the driver to help avoid dangerous driving situations.

d) The **blind spot monitor** is a warning system on a vehicle that detects other vehicles entering its blind spot on the sides and rear of the vehicle.
e) **Adaptive Cruise Control (ACC)** maintains the vehicle's specific speed and can automatically adjust speed to maintain a safe following distance. ACC uses forward radar to detect the distance and speed of the vehicle ahead.
f) **Traffic sign recognition** is a technology of sensors and computation that enables a vehicle to recognise traffic signs on roadways, such as speed limit, turn ahead or traffic signals.
g) The **Collision Avoidance System (CAS)** represents a change of focus in the way vehicle manufacturers look at automotive safety. Traditionally, the emphasis has been on injury mitigation for those involved in a collision, for example, by providing stronger vehicle frames, seat belts and airbags.
h) An **automatic crash notification system** uses on-board units, such as airbag deployment or other sensors, to detect evidence of a collision. When the vehicle's sensors detect a collision, the crash notification system automatically communicates with a call center and transmits information about the accident and the vehicle's location.

2.3.1. Adaptive Cruise Control (ACC)

Adaptive Cruise Control is partly automated driving for basic driving tasks such as accelerating and decelerating with the recent advent of advanced driver assistance systems. ACC scientific activity had its beginnings in the 1930s. During the 1990s, the number of scientists engaged in traffic modelling grew rapidly because of the availability of better traffic data and higher computational power for numerical analysis [64]. The ACC system is the first driver assistance system with the potential to influence traffic flow characteristics [6, 65]. Adaptive Cruise Control is an intelligent system that automatically adjusts vehicle speed to maintain a driver-selected distance from the vehicle ahead in the same lane [66, 67]. Using all the data, ACC does intelligent computations to determine the desired acceleration of the host vehicle and achieve it with help from the throttle and braking system [68]. ACC can detect the leading vehicle and determine its speed and distance by using sensors such

as radar to measure the vehicle velocity and calculate the desired acceleration of the vehicle. Adaptive Cruise Control can also regulate the vehicle speed and decide the mode of operation like speed control or distance control [66].

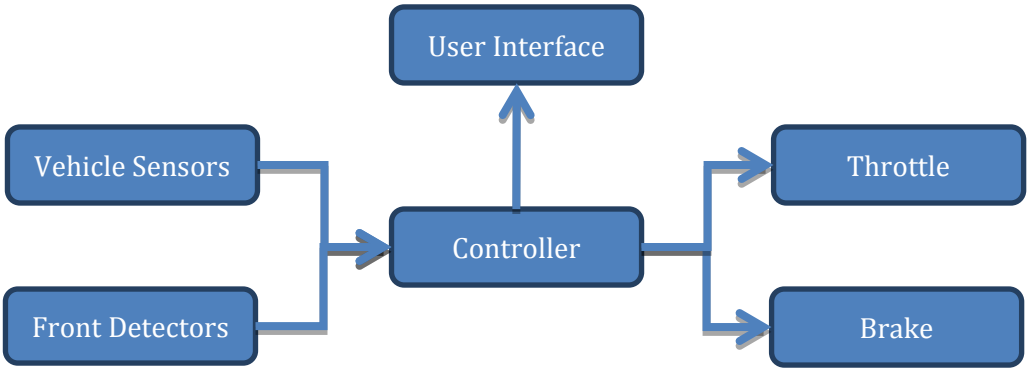

Figure 2-3: Block diagram of ACC

Front detectors supervise the road from the front side and could help guide the automobile. There are two purposes for detectors: identifying white lines on the road, that is, lane limits, and observing static and dynamic obstacles in the path.

There are a variety of sensors that could be used: 1) High-resolution point grey Bumblebee stereo camera [69], 2) Vertical scanning SICK LMS-291 LIDAR [69], 3) Infrared (IR) camera to detect lanes [70], 4) Mobile eye camera, a new type of camera used to warn the driver and detect the distance to obstacle [71, 72].

2.3.2. Vehicular Ad Hoc Networks (VANET)

IEEE 802.11, released in 1997, contains Vehicular Ad hoc Network (VANET) standards for computer communication in different frequency bands and “defines a Medium Access Control (MAC) layer and physical (PHY) layer” [73, 74]. As an example of WALAN, Mobile Ad hoc Networks (MANET) are many of routing protocols. No fixed network topology is used, and the system provides a kind of wireless communication in which nodes are mobile to reach all multicast members in the neighborhood in a single transmission. [75, 76]. It facilitates such an atmosphere to the mobile nodes in which they can connect anytime anywhere to communicate

among themselves [77]. VANET are a subclass of MANET [78] and a special kind of MANET [79]. VANET is one of the influencing areas for the improvement of ITS to provide safety and comfort to road users [80, 81]. VANET communication has various applications in improving traffic efficiency and infotainment such as weather information, mobile e-commerce, Internet access and other multimedia applications such as Advance Driver Assistance Systems ADASE2, crash avoidance matrices partnership (CAMP), VEHICLETALK2000 and Fleet Net [77, 82]. VANET helps vehicle drivers avoid any critical situation through Vehicle-to-Vehicle communication such as roadside accidents, traffic jams, speed controls, free passage of emergency vehicles and unseen obstacles [81]. Those applications have been developed with the cooperation of various governments and major vehicle manufacturers [82].

VANET has two applications, V-2-V and V-2-I, which are commonly regarded as an enabling technology for future ITS [81]. It is expected that vehicles will be prepared with onboard units with wireless interfaces and antennas since these have low costs, common availability and wide deployment [81]. Communication-based intersection safety has been utilised in Europe, Japan and the U.S., which is addressed in the cooperative intersection collision avoidance systems initiative (CICAS) [83]. CICAS uses ITS technologies including in-vehicle positioning, roadside sensors, intersection maps and two-way wireless communication [83]. CICAS has developed four main applications:

1. CICAS-violation warning system (CICAS-V).
2. CICAS-stop sign assist (CICAS-SSA).
3. CICAS-signalised left-turn assist (CICASSLTA).
4. CICAS-traffic signal adaptation (CICASTSA).

However, communication-based intersection safety technologies warn about traffic light violations, turning and crossing-path collisions, rear-end collisions, traffic signal adaptations for an emergency, prioritised road users and traffic efficiency [83].

2.4. FUZZY Logic

For accurate control of highly nonlinear systems with time varying parameters, an intelligent or a hybrid technique must be considered. The aim has been to develop an effective way of controlling vehicle velocity. For this a well-known and widely accepted artificial intelligence technique is used. The subset of artificial intelligence proposed by Lotfy Zadeh in 1965 [84] is the FUZZY logic controller (FLC).

There are some benefits of using FLC compared with conventional controllers, as expressed below [84-88]:

1) Compared to conventional PID controllers, FLCs are more robust since they can cover a much wider range of operating conditions than PID can and can operate with noise and disturbances of a different nature.
2) Developing an FLC is cheaper than developing a model-based or other controller to do the same thing.
3) Since it is easier to understand and modify their rules, FLCs are customisable, which not only uses a human operator's strategy but also are expressed in natural linguistic terms.
4) They are attractive because it is easy to learn how FLCs operate and how to design and apply them to a concrete application.
5) It can easily handle multiple inputs.
6) FLC is an automatic controller, a self-acting or regulating mechanism that controls an object to perform a desired behavior.

Designing an FLC can be described in the following steps [84, 89, 90]:

1) Determine the inputs and the value of output that should be achieved.

2) Define the condition interface, that is, fix the way in which observations of the process are expressed as FUZZY sets.

3) Design the rule base to determine which rules are to be applied under which conditions. This is usually easier if designed with a table model. This can be said to be part of the inference engine.

4) Design the computational unit and supply algorithms to perform FUZZY computations. Those will generally lead to fuzzy output.

5) Determine rules according to which FUZZY control statements can be transformed into crisp control actions. This is also part of the defuzzification process of the fuzzy output.

In FLC, there are four, most-common membership functions as is illustrated in Figure 2-4, Figure 2-5, Figure 2-6 and Figure 2-7.

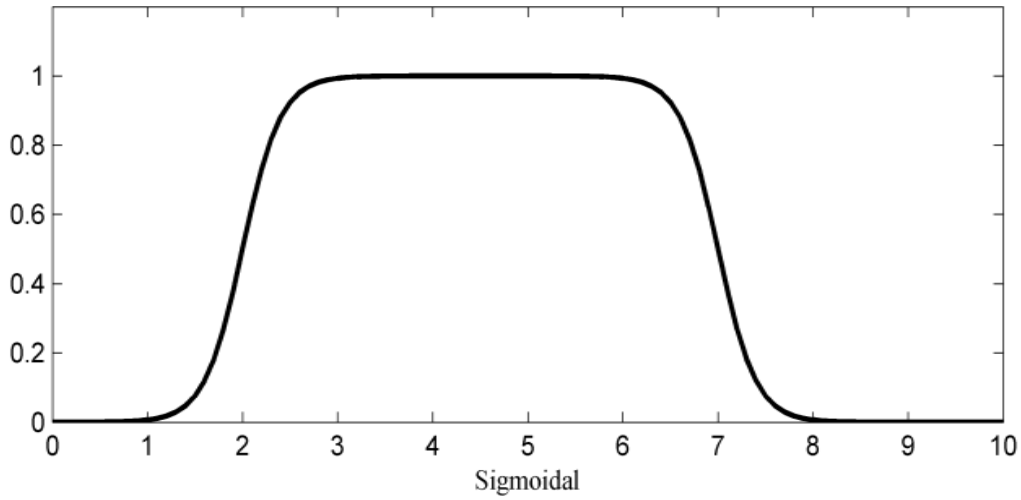

Figure 2-4: Sigmoidal membership function of FUZZY logic

Sigmoidal curve Figure 2-4 can be obtained from Equation 2-16.

$$f(x: a, c) = \frac{1}{1 + e^{-a(x-c)}} \tag{2-16}$$

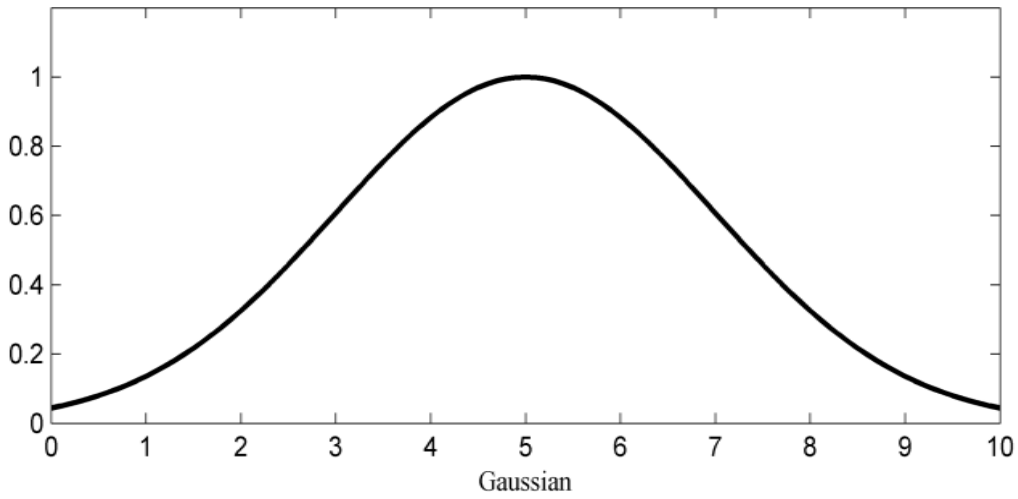

Figure 2-5: Gaussian membership function of FUZZY logic

Gaussian curve Figure 2-5 can be obtained from Equation 2-17.

$$f(x:\sigma,c) = e^{\frac{-(x-c)^2}{2\sigma^2}} \tag{2-17}$$

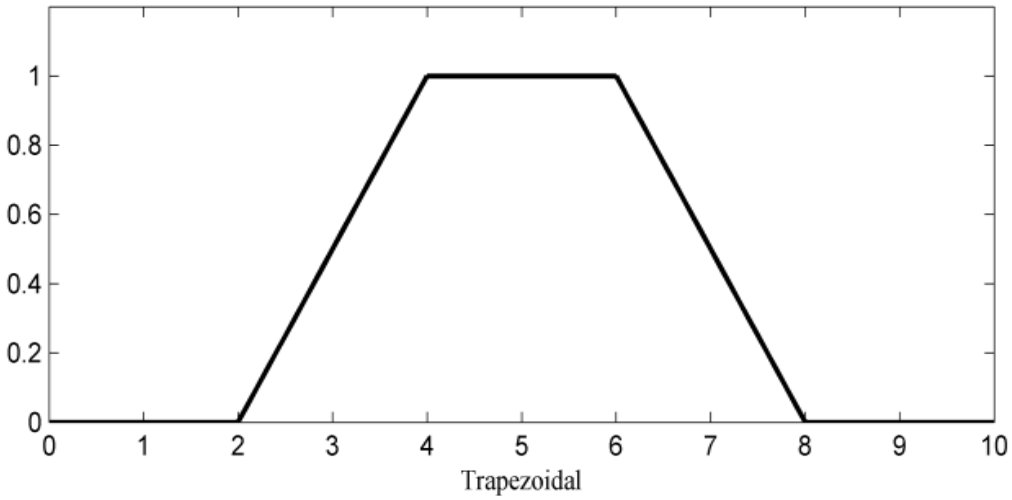

Figure 2-6: Trapezoidal membership function of FUZZY logic

Trapezoidal curve Figure 2-6 can be obtained in Equation 2-18 and Equation 2-19.

$$f(x,a,b,c,d) = \begin{cases} 0, & x \le a \\ \dfrac{x-a}{b-a}, & a \le x \le b \\ 1, & b \le x \le c \\ \dfrac{d-x}{d-c}, & c \le x \le d \\ 0, & d \le x \end{cases} \tag{2-18}$$

Or more compactly, by

$$f(x,a,b,c,d) = max\left[min\left[\frac{x-a}{b-a}, 1, \frac{d-x}{d-c}\right], 0\right] \tag{2-19}$$

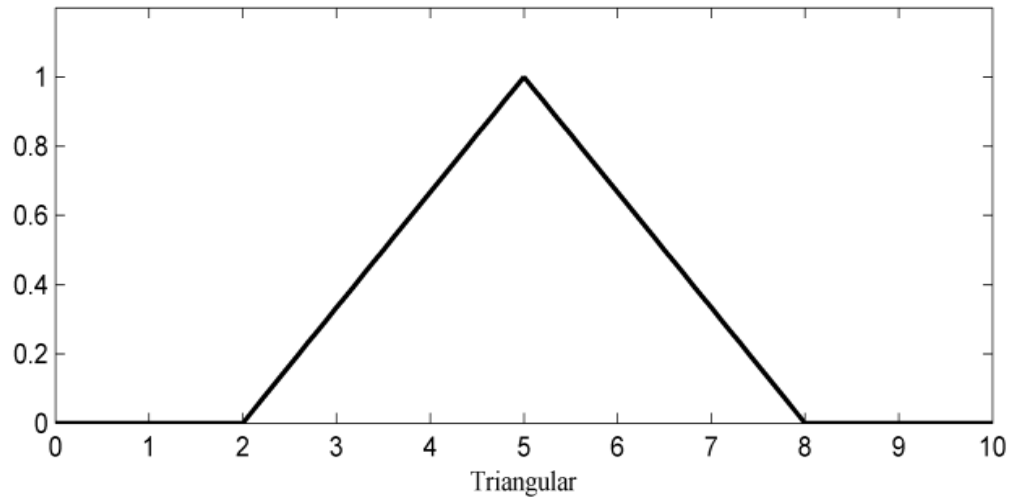

Figure 2-7: Triangular membership function of FUZZY logic

Triangular curve Figure 2-7 can be obtained from Equation 2-20 and Equation 2-21.

$$f(x,a,b,c) = \begin{cases} 0, & x \le a \\ \dfrac{x-a}{b-a}, & a \le x \le b \\ \dfrac{c-x}{c-b}, & b \le x \le c \\ 0, & d \le x \end{cases} \qquad (2\text{-}20)$$

Or more compactly, by

$$f(x,a,b,c) = max\left[min\left[\frac{x-a}{b-a}, \frac{c-x}{c-b}\right], 0\right] \qquad (2\text{-}21)$$

Triangular or trapezoidal (piecewise linear) and sigmoidal functions have proven to be more popular with FUZZY logic theoreticians and practitioners rather than higher order-based functions such as quadratic, cubic etc. [84].

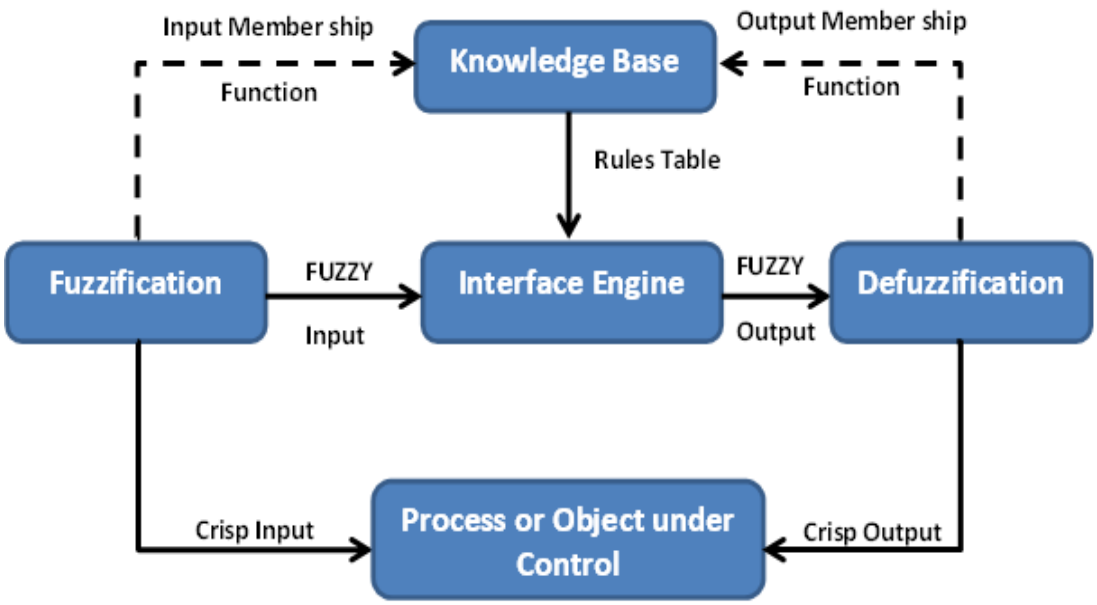

Figure 2-8: Typical structure of an FLC

In this project, we will examine many different FLC models in Figure 2-9, Figure 2-10 and Figure 2-11.

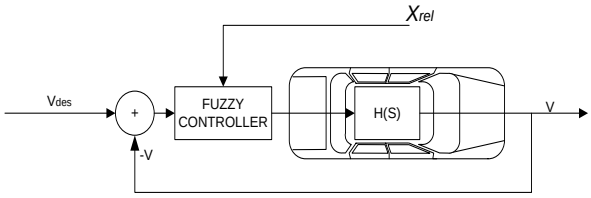

Figure 2-9: ACC model with using FLC

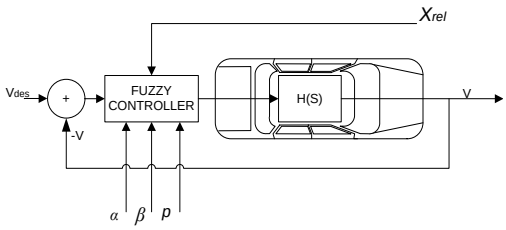

Figure 2-10: ACC model with using FLC and disturbance ($\boldsymbol{\alpha}, \boldsymbol{\beta}$ and $\boldsymbol{p}$) added to the controller

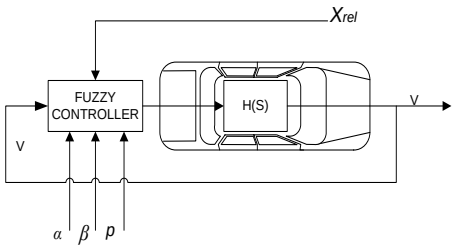

Figure 2-11: ACC model with using FLC and disturbance ($\boldsymbol{\alpha}, \boldsymbol{\beta}$ and $\boldsymbol{p}$) added to the controller and no V_{des} as reference. (This is a human driver modeler.)

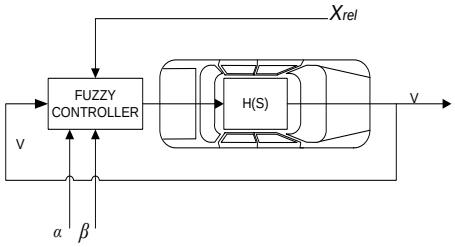

Figure 2-12: ACC model with using FLC and disturbance ($\boldsymbol{\alpha}, \boldsymbol{\beta}$) added to the controller and no V_{des} as reference. (This is an automatic driver modeler.)

2.5. Energy Consumption

Identifying the virtue and the benefits of the project is one of the aims of the thesis to assess if the objectives have been met. It has been shown that saving energy is one of the benefits of this project. Therefore, studies on energy consumption of vehicle and aggregate of vehicles have been included in the literature review.

Propulsive work (W), which is the work implemented by the propulsive force as the vehicle moves along its path, will be used as proportional to fuel consumption (z) [91, 92].

$$z = W * r \tag{2-22}$$

Where r is the fuel rate and W is the total propulsive work performed by propulsive force ($P_m(x)$) in travelling from x_1 to x_2 would be:

$$W = \int_{x_1}^{x_2} P_m(x)dx \tag{2-23}$$

Where P is the total resistance of the vehicle plus the acceleration force (E):

$$P_m(x) = \max(E, 0) \tag{2-24}$$

$$E = R_m + H + G_F + M\dot{v} \tag{2-25}$$

Where M is mass of the vehicle, $\dot{v}$ is the acceleration of the vehicle, R_m is inherent resistance to motion, H is any added curvature resistance and G_F is the gradient. R_m will be:

$$R_m = \Gamma U + CA(\rho_{air}/2)v^2 \tag{2-26}$$

Where Γ is the weight of the vehicle, U is the coefficient of rolling resistance for automobiles, C is air drag coefficient, A is the frontal cross-sectional area of vehicle, ρ_{air} is air density, and v is velocity [91]. F is:

$$F = \Gamma * \sin\theta \tag{2-27}$$

Where θ is the ascent angle.

As mentioned, propulsive work is proportional to fuel consumption. Fuel consumption has been studied by many researchers such as Ahn [19], who produced many models to predict fuel consumption or emission rates, as shown in Appendix (A). Yue [93] began his model from the general format of the VT-Micro mode, which was developed at Virginia Tech to compute mode-specific fuel consumption and emission rates [94].

$$MOE_e = \begin{cases} \sum_{i=0}^{3}\sum_{j=0}^{3} e^{k_{i,j}^{e} v^i a^j} & for\ a \geq 0 \\ \sum_{i=0}^{3}\sum_{j=0}^{3} e^{l_{i,j}^{e} v^i a^j} & for\ a < 0 \end{cases} \tag{2-28}$$

Equation (2-28) is distributed into three parts:

1. **Deceleration Mode** is the instantaneous manoeuvre from a pre-defined cruise speed to a complete stop that Equation (2-28) has modified to be

$$MOE_e^{decel} = d_0 + d_1 v_c + d_2 v_c^2 + d_3 v_c^3 + d_4 v_c^4 + d_5 v_c^5 + d_6 v_c^6 \quad (2\text{-}29)$$

Where MOE_e^{decel} is the fuel consumed or pollutants emitted while decelerating (L/s, or mg/s, respectively), v is the vehicle speed (km/h), and d_0, d_1, d_2, d_3, d_4, d_5 and d_6 are vehicle-specific regression coefficients.

In this project, the model that has been used is for high-emission vehicles with engine sizes of less than 5.7 litres [93] to recognise the differences in consumption between the models. Therefore, the coefficient used by Yue is in Appendix (B) [93].

2. **Idling and Cruise Modes** are the instantaneous speed of 0 km/h and an instantaneous acceleration rate of 0 km/h/s[1].

$$MOE_e^{cruise} = exp\left(k_{0,0}^e + k_{1,0}^e v + k_{2,0}^e v^2 + k_{3,0}^e v^3\right) \quad (2\text{-}30)$$

Where MOE_e^{cruise} is the fuel consumed or pollutants emitted while cruising (L/s, or mg/s, respectively) and $k_{i,0}^e$ is vehicle-specific regression coefficients.

Similar to the deceleration model, the model that has been used is the high-emission vehicle [93] and regression coefficients in Appendix (B).

3. **Acceleration Mode** is the fuel consumed and pollutants emitted by a vehicle during an acceleration event.

$$MOE_e^{accel} = b_0 + b_1 v_c + b_2 v_c^2 + b_3 v_c^3 + b_4 v_c^4 + b_5 v_c^5 + b_6 v_c^6 \quad (2\text{-}31)$$

[1] $Km/hr/s$ has been used as acceleration measuring unit such as Yasunobu, Miyamoto and Ihara and [95] S. Yasunobu, *et al.*, "A fuzzy control for train automatic stop control," *Trans. of the Society of Instrument and Control Engineers*, vol. 2, pp. 1-9, 2002. Also has been used by Ahn, Rakha, Trani and Aerde [96] K. Ahn, *et al.*, "Estimating vehicle fuel consumption and emissions based on instantaneous speed and acceleration levels," *Journal of transportation engineering*, vol. 128, pp. 182-190, 2002..

Where $\mathrm{MOE}_{\mathrm{e}}^{accel}$ is the fuel consumed or pollutants emitted during acceleration (L/s, or mg/s, respectively) and b_0, b_1, b_2, b_3, b_4, b_5 and b_6 are vehicle-specific regression coefficients.

Similar to the previous models, the model used is the high-emission vehicle [93] and regression coefficients that are in Appendix (B).

2.6. Emissions

Environmental issues are one of the major global interests. This project shows the reduction of vehicle emissions, which can be considered as one of the benefits.

The universe is comprised of chemicals. The air that we breathe contains a mixture of Nitrogen ($\mathrm{N_2}$), Oxygen ($\mathrm{O_2}$), vehicle-borne dioxide ($\mathrm{CO_2}$) and trace amounts of other gases. The breakdown of air into its constituents gives us an $\mathrm{N_2}$concentration in the air of 78.08%, while $\mathrm{O_2}$is 20.9% and $\mathrm{CO_2}$is 387 ppm by volume [97, 98]. Under natural conditions, the animal kingdom can survive on the existing air composition [99]. However, because pollution is changing the air available for human consumption, the air is not as healthy as it used to be. Some sources say that, if the concentration of oxygen in the air decreases to less than 19.5%, humans will have difficulty living [100, 101]. There are different studies on the universe's gases. Some focus on the particular gas; others, on the impacts and benefits and so on [73, 100-109].

Chemical gases affect people, overall, in two ways. The first one is the indirect impact on humans through chemical gases, as these change with climate change [102]. The second is the direct impact, namely, the direct effects on human beings and the systems within the human body. The person is affected by chemical gases most often through one of four ways: (1) breathing, (2) ingestion, that is, the toxin entering the stomach, (3) through coming into contact with the eyes and (4) through being absorbed through the skin [102].

The National Ambient Air Quality Standards (NAAQS) provide threshold concentrations for six pollutants: vehicle-borne monoxide (CO), lead (pb), nitrogen dioxide ($\mathrm{NO_2}$), ozone ($\mathrm{O_3}$), particulate matter (PM-10) and sulfur dioxide ($\mathrm{SO_2}$) [93, 103].

Vehicle fuel consumption and emission rates are the main goal of many approaches that have been developed [93]. Based on VT-Micro model, Equation (2-8) and similar to fuel consumption models, Ahn [19] produced many models to predict fuel consumption or emission rates, as shown in Appendix (A). Furthermore, Yue [93] developed Equation (2-8), and dividing it into three parts:

1. **Deceleration Mode** is the instantaneous maneuver from a pre-defined cruising speed to a complete stop. As in fuel consumption, Yue created Equation (2-29) with different regression coefficients. It has utilised the coefficient used by Yue in Appendix (B) [93].

2. **Idling and Cruise modes** are an instantaneous speed of 0 km/h and an instantaneous acceleration rate of 0 km/h/s. From Equation (2-30) and Yue [93], the regression coefficients of idling and cruise modes appear in Appendix (B).

3. **Acceleration Mode** is the fuel consumed and pollutants emitted by a vehicle during an acceleration event. From Equation (2-31) and Yue [93], the regression coefficients of the acceleration model appear in Appendix (B).

Chapter 3

Mathematical Modelling

3.1. Introduction

Several studies have replicated traffic in the microscopic model. For example, there is a simulation model of a vehicle with a fuzzy theory, neural network and cellular automata (CA) model [110].

The CA model, developed by Nagel and Schreckenberg in 1992, was earlier used to study congestion on one-lane highways [26]. Later, the model was improved to analyse congestion on two- and three-lane highways [42, 111-113]. Originally, the CA model contained a one-dimensional array of L number of cells. Each cell was 7.5m and may or may not have been occupied. The velocity of the i^{th} vehicle v_i is an integer between '0' to maximum speed. (V_{max}) updating is vehicleried out if the system consists of the following steps:

(1) **Acceleration:** If the velocity v_i of a vehicle is lower than V_{max} and if the distance to the next vehicle ahead is larger than v_{i+1}, the speed is advanced by one [$v_i \rightarrow v_i + 1$].

(2) **Slowing down (due to other vehicles):** If a vehicle i sees the next vehicle at site $i + j$, where j is the gap ahead, (provided $j \leq v_i$), it reduces its speed to be $[v_i \rightarrow j - 1]$.

(3) **Randomisation:** With probability p, the velocity of each vehicle (if greater than zero) is decreased by one $[v_i \rightarrow j - 1]$.

(4) **Vehicle motion:** Each vehicle is advanced *v* cells.

This chapter investigates congestions on the one-lane highway traffic system by using the Dynamic Traffic Cellular Automata (DTCA) model [26, 42, 113, 114] .

A brief explanation about CA has been presented in the introduction chapter of this thesis. Section 3.2 provides details about DTCA and the new concept, congestion. Finally, section 3.3 defines the flow of traffic equations.

3.2. Microscopic Model Dynamic Traffic Cellular Automata (DTCA)

The DTCA that has been suggested in this chapter can be compared with the original CA model. DTCA offers three main differences:

1) In CA, the road is divided into equal-length cells, each cell being $7.5\ m$. A cell may or may not be occupied. The CA model assumes that a vehicle is restricted by a fixed position, while the position of the vehicle in DTCA is not limited with fixed cells on the highway. However, the vehicle in CA is viewed as a $7.5\ m$ cell moving through the highway.

2) Nagel and Schreckenberg [26] used fixed magnitude of acceleration and declaration equal to 1 cell ($\pm 7.5\ \mathrm{m/s^2}$). According to Bansal and Brar, maximum deceleration is explained by [115].

$$dec_{max} = G(\Lambda \cos\theta_v + \sin\theta_v) \qquad (3\text{-}1)$$

Where G is the gravity (9.81 $\mathrm{m/s^2}$), Λ is friction coefficient for dry sealed roads (0.6) and θ_v is the vehicle angle of inclination from the horizontal plan. Assuming flat highways, θ_v is set to '0'. Bansal and Brar indicate that declaration cannot be greater than -5.886 $\mathrm{m/s^2}$ while the Nagel and Schreckenberg model assumes this value to be equal to the cell length of -7.5 $\mathrm{m/s^2}$ [26, 115]. Different deceleration values are achieved by different driver habits and road and traffic conditions. These differences

are stated by deceleration factor (β). β gives the proportion of the dec_{max}, and it will be within the range $0 \leq \beta \leq 1$.

Similarly, the maximum acceleration (a_{max}) is 4.905 m/s^2, which is equal to 17.658 km/hr^2. Maximum acceleration moves the vehicle from zero to 17.658 km/hr in the first second. In six seconds with maximum acceleration, the vehicle can approach a speed of 106 km/hr, which is reasonable for most vehicles. However, different accelerations are achieved by different driver habits and road and traffic conditions. These differences are stated by acceleration factor (α), which in turn is the proportion of acc_{max}. For instance, acc will approach acc_{max} when α tends to reach unity. During the normal course of operation, the value of α will be in the range $0 \leq \alpha \leq 1$.

$$dec = dec_{max} \times \beta \tag{3-2}$$

$$acc = a_{max} \times \alpha \tag{3-3}$$

3) The original CA uses one randomisation factor, (p), while DTCA uses three independent randomisation factors (α, β and p). α is acceleration factor, β is deceleration factor, and p is driver reaction factor, which mainly focuses on the time delay for making decisions. Those factors describe the driving situation on highways. α, β and p are very obvious, describing the vehicle moving from zero or no movement, such as moving up from a traffic light or normal congestion on the highway.

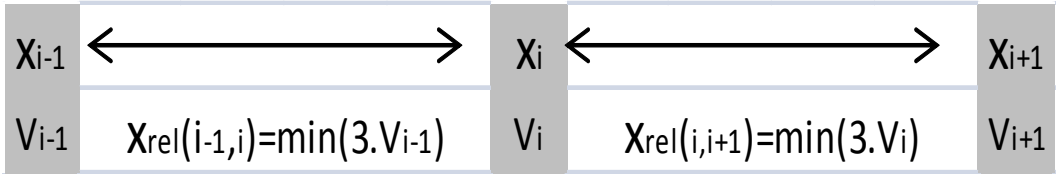

Figure 3-1: Relation between velocity and gaps between vehicles on the highway

Changes in speed due to acceleration

$$\begin{aligned} &if\ v_{i,n} < V_{max}\ \&\ \varphi \cdot x_{rel}(i, i+1) > v_{i,n} \\ &\quad then\ v_{i,n+1} = v_{i,n} + t \cdot acc \end{aligned} \tag{3-4}$$

Where i is a cell number,

n is the sequence number and

t is the fixed time. We assume it equals '1' second.

φ is the safety factor.

Deceleration

$$\begin{aligned} &if\ v_{i,n} <\ \varphi \cdot x_{rel}(i, i+1) \\ &then\ v_{i,n+1} = \begin{cases} v_{i,n} - t \cdot dec \\ or \\ \varphi \cdot x_{rel}(i, i+1)/t \end{cases} \\ &\qquad\qquad\qquad\quad v_{i,n} \end{aligned} \tag{3-5}$$

Randomisation

$$\begin{aligned} &if\ v_{i,n} > 0\ with\ probability\ \beta \\ &\quad then\ v_{i,n+1} = v_{i,n} - t \cdot dec \end{aligned} \tag{3-6}$$

Vehicle motion

$$x_{i,n+1} = x_{i,n} + t \cdot v_{i,n} \tag{3-7}$$

3.2.1. Acceleration and Deceleration Factors in Real Life

Table 3-1: Examples of acceleration and deceleration factors

Factor		Acceleration factor (α)	Deceleration factor (β)
Driver	Skill	Good	Bad
	Age	Young	Old
	Experience	More experience	No experience
	Health	Healthy	Unhealthy
	Activity	Hurried and busy	Empty
	⋮	⋮	⋮
Vehicle	Model	New	Old
	Performance	Strong	Weak
	Problems	Does not have	Has
	⋮	⋮	⋮
Weather	Fog	Clear	Unclear
	⋮	⋮	⋮
Road	Straight	Yes	No
	Crowd	No	Yes
	Asphalt	Good condition	Bad condition
	⋮	⋮	⋮

$$ADRT = 0.017\,Age + 0.159\,Gender \tag{3-8}$$

At this point, it appears to be quite important to understand the concept of acceleration α and deceleration factors β before going into the future details of the model. Acceleration and deceleration factors (α and β) are a combination of driver, vehicle, weather and road activities [116, 117]. A study conducted by Mehmood and Easa reveals that acceleration/deceleration reaction time (ADRT) is affected by the age and gender of the driver, as presented in (3-8) [118]. Where age is the driver age in years and gender is the driver gender where 0 is for males and 1 is for females. In Table 3-1, some examples of acceleration (α) and deceleration (β) factors such as driver skills, vehicle model, and road and weather conditions are mentioned. In the table above, all the factors listed under the acceleration factor are favourable to increase the speed or acceleration of the vehicle. Factors listed under the deceleration

factor are clearly in favour of restricting the vehicle's motion or deceleration. Both factors α and β are linked as one combination, but in this project, we preferred to understand the relation between them to find the proper combination between them.

This approach (as is the case in most real-life situations) requires normal distribution variables. Thus, α and β are independent bivariate normal distributions [119].

Since α and β are important factors for the dynamics of the vehicle, they therefore indirectly present the numerical description of the traffic flow. It can be observed that the impact of acceleration and deceleration on traffic flow affects the speed of each individual vehicle and hence influences the entire traffic system. There are two essential operational situations in the traffic flow:

1. Starting-up flow area.
2. Steady-state running. In both cases, the comparison between α and β decides the accelerating and deceleration action as indicated by the following equations.

$$f_{\mathrm{A,B}}(\alpha,\beta)=\begin{cases}V_n(t-\tau)=V_n(t)+\alpha(t) & if\ \alpha\geq\beta\\ V_n(t-\tau)=V_n(t)-\beta(t) & if\ \alpha<\beta\end{cases} \tag{3-9}$$

Individually, each factor, α and β, is the normal random distribution. The probability of α depends on $f_{\mathrm{A}}(\alpha)$, where most of the probability is around the mean value μ_α, and the standard deviation, σ_α, shows the extent of variation from the mean value μ_α.

$$f_{\mathrm{A}}(\alpha)=\frac{1}{\sigma_\alpha\sqrt{2\pi}}\mathrm{e}^{-(\alpha-\mu_\alpha)^2/2\sigma_\alpha^2} \tag{3-10}$$

Similarly, the probability of β depends on $f_{\mathrm{B}}(\beta)$, where most of the probability is around the mean value μ_β, and the standard deviation is represented by σ_β.

$$f_{\mathrm{B}}(\beta) = \frac{1}{\sigma_\beta \sqrt{2\pi}} e^{-(\beta-\mu_\beta)^2/2\sigma_\beta^2} \tag{3-11}$$

Figure 3-2 reveals the normal distribution around $\mu = 0.4$ and with different standard deviations, that is, $\sigma = 0.3, 0.5$ and 0.8. The joint probability density function (PDF) of the continuous random variables $f_{\mathrm{A,B}}$ is a function of $f_{\mathrm{A,B}}(\alpha, \beta)$ [120].

$$f_{A,B}(\alpha, \beta) = \int_{-\infty}^{\alpha} \int_{-\infty}^{\beta} f_{A,B}(\alpha, \beta)\, d\alpha\, d\beta \tag{3-12}$$

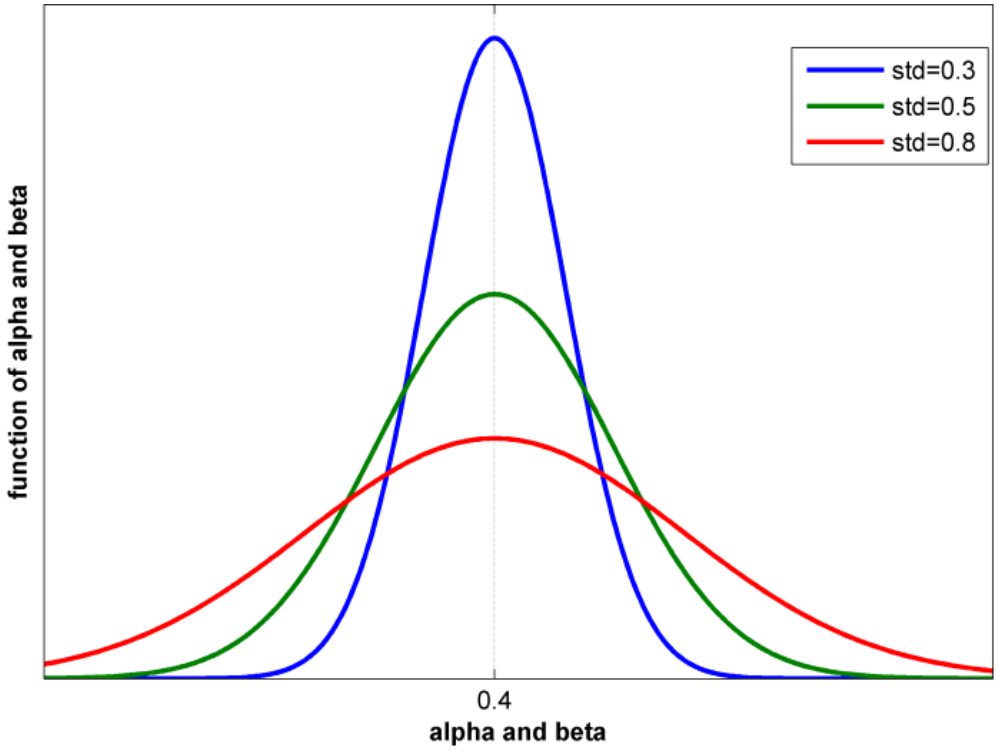

Figure 3-2: Normal distribution with $\boldsymbol{\mu = 0.4}$

The relation between α and β is affected by four variables $(\mu_\alpha, \mu_\beta, \sigma_\alpha, \sigma_\beta)$. The mean and standard deviation for both α and β respectively with zero correlation is depicted as $\rho = 0$. From equations (3-10), (3-11), (3-12) and (3-13), $f_A(\alpha)$ will be as in [120].

$$f_{A,B}(\alpha,\beta) = \frac{1}{2\pi\sigma_\alpha\sigma_\beta} e^{\left(-(\alpha-\mu_\alpha)^2/2\sigma_\alpha^2-(\beta-\mu_\beta)^2/2\sigma_\beta^2\right)} \quad (3\text{-}13)$$

Where

$$f_A(\alpha) = \int_\alpha^1 f_{A,B}(\alpha,\beta)\, d\beta \quad (3\text{-}14)$$

This equation will be equivalent to

$$f_A(\alpha) = \frac{1}{\sigma_\alpha\sqrt{2\pi}} e^{-(\alpha-\mu_\alpha)^2/2\sigma_\alpha^2} \int_\alpha^1 \frac{1}{\sigma_\beta\sqrt{2\pi}} e^{-(\beta-\mu_\beta)^2/2\sigma_\beta^2} \quad (3\text{-}15)$$

To simplify Equation 3-15,

$$f_A(\alpha) = \left(\frac{1}{\sigma_\alpha\sqrt{2\pi}} e^{-(\alpha-\mu_\alpha)^2/2\sigma_\alpha^2}\right) \times \sqrt{\frac{\pi}{4/\sigma_\beta\sqrt{2\pi}}}\left(1 - erf\left(\frac{\beta-0.5}{\sigma_\beta\sqrt{2\pi}}\right)\right) \quad (3\text{-}16)$$

To activate β

$$f_B(\beta) = 1 - f_A(\alpha) \quad (3\text{-}17)$$

Figure 3-3 illustrates the $f_{A,B}(\alpha,\beta)$, obtained from equations (3-12) and (3-13), plotted against the standard deviation of α and β. Figure 3-3A expresses the change of $f_{A,B}(\alpha,\beta)$ by changing μ_α and μ_β from 0.4, 0.5 and 0.6 and σ_β from 0.1 to 0.9 with a constant increment of 0.1, while σ_α is 0.1. μ_α clearly affects the mean of acceleration action function more than μ_β. Figure 3-3A is distributed into three groups depending on the value of μ_α. The highest group of curves has μ_α value equal to 0.6, while the lowest group has μ_α value equal to 0.4. It is quite clear from the figure that the curves plotted for similar values of μ_α and different values for μ_β tend to be identical for the scenarios having $\sigma_\beta > 0.6$. Moreover, Figure 3-3B expresses the change of $f_{A,B}(\alpha,\beta)$ with μ_α and μ_β from 0.4, 0.5 and 0.6 and for σ_α

from 0.1 to 0.9 , while $\sigma_\beta = 0.1$. The groups of curves in Figure 3-3B are commingled more compared to curves in Figure 3-3A, especially when σ_α is less than 0.5. It is interesting to note that the position of the curve depends heavily on the σ_α values. For $\sigma_\alpha > 0.5$, three distinct groups are evident, but with lower values of μ_β. Those distinct groups of curves tend to mix with one another.

Figure 3-4 shows the impact of changing σ_α and σ_β while keeping μ_α and μ_β equal to 0.5. Figure 3-4A illustrates that, when $\sigma_\alpha = 0.1$, no considerable change occurs for $f_{A,B}(\alpha, \beta)$ with the alteration of σ_β. Moreover, most output is concentrated around μ_α. Figure 3-4B indicates that, when $\sigma_\alpha = 0.4$, changes are quite evident when σ_β is altered from 0.1 to 0.9. It can be seen that the concentration of $f_{A,B}(\alpha, \beta)$ is less in Figure 3-4B as compared to Figure 3-4A and with the increase in σ_β from 0.1 to 0.9 in Figure 3-4B, the concentration of $f_{A,B}(\alpha, \beta)$ decreases.

Figure 3-5 presents the compression between equations (2-16) and (2-17). The impact of the standard deviation of acceleration and deceleration factors on the traffic system can be observed in Figure 3-5. When σ_α and σ_β are similar, $f(\alpha.\beta)$ will be around zero. The impact of $f(\alpha.\beta)$ will be clear from Figure C-2, Figure C-7, Figure C-9, Figure C-10, Figure C-12, Figure C-13 and Figure C-14. It is evident from the figures mentioned earlier that, with an increase in σ_α values, the thickness of congestion decreases. Moreover, when σ_β is more than σ_α, $f(\alpha.\beta)$ results in a negative value, a conclusion that is clear from Figure C-1, Figure C-3, Figure C-4, Figure C-5 and Figure C-8. Those figures show thick congestion. The thickness of congestion decreases as the value of σ_α increases. Moreover, increasing σ_β reduces the moving backward for congestion flux and thickness of congestion. Finally, when σ_α is greater than σ_β, $f(\alpha.\beta)$ will be positive, as is evident from Figure C-6 and Figure C-11. It is clear from Figure C-11 that the probability of alleviating congestion is higher with an increase in values for σ_α. There are common trends for all approaches, from Figure 3-5 and Figure C-1 to Figure C-14, that increasing σ_α leads to a decline in the congestion flux, while increasing σ_β leads to an increase in the thickness of congestion and eliminates congestion's backward movement.

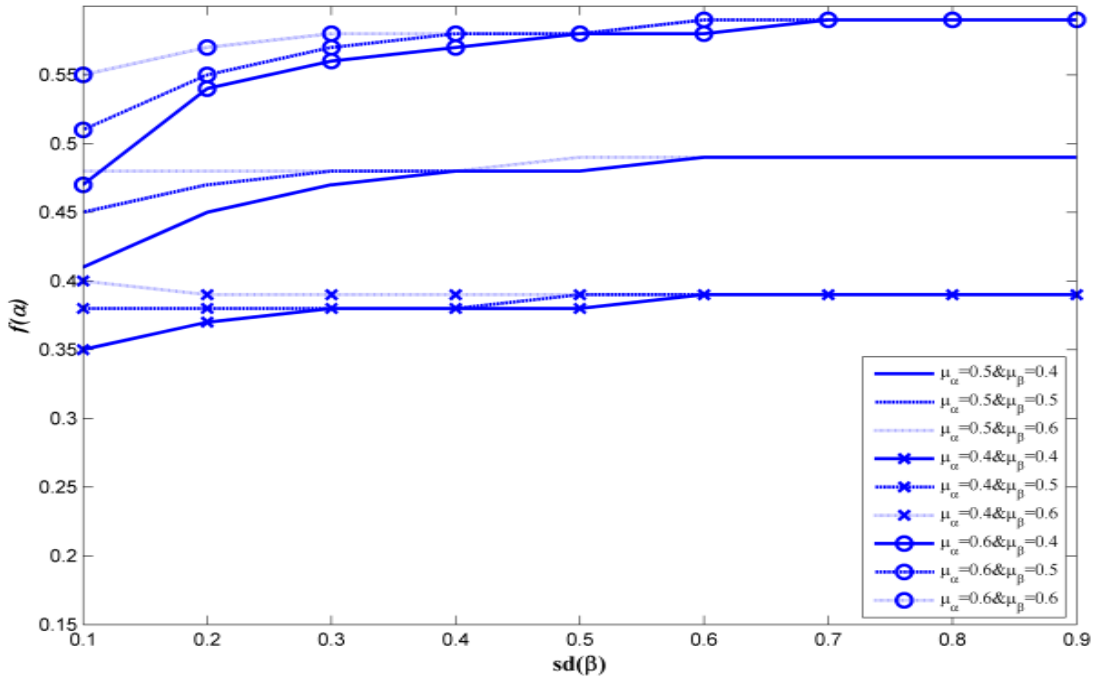

(A)

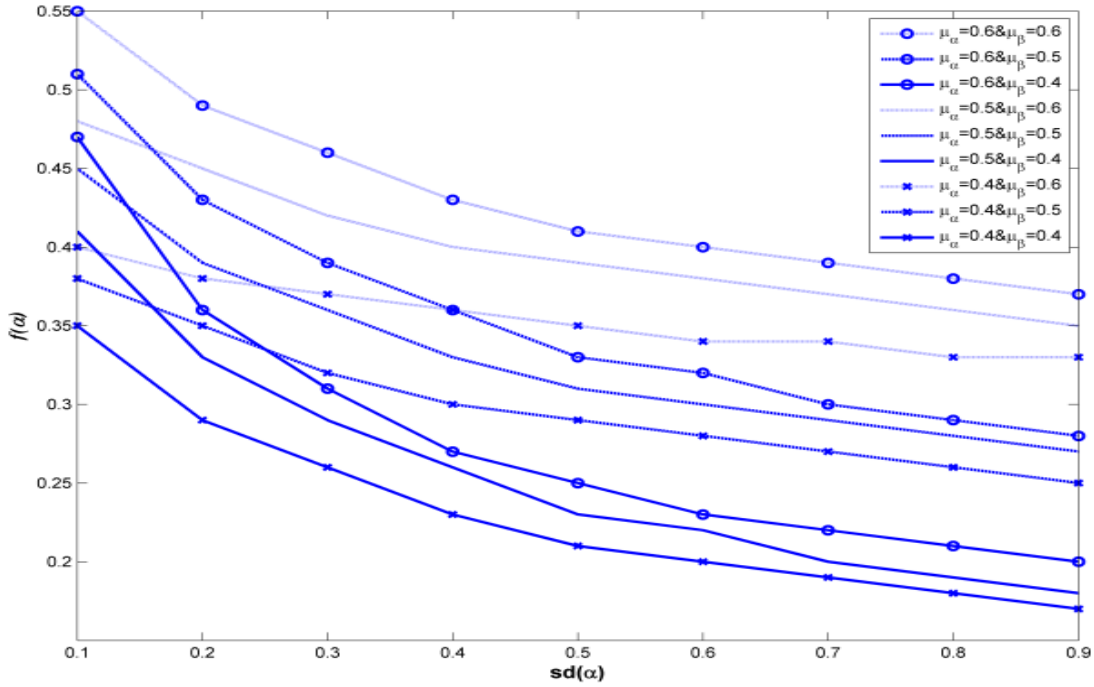

(B)

Figure 3-3: Impacts of $\boldsymbol{\mu_{\alpha\&\beta}}$ on the $\boldsymbol{f_{A,B}(\alpha,\beta)}$

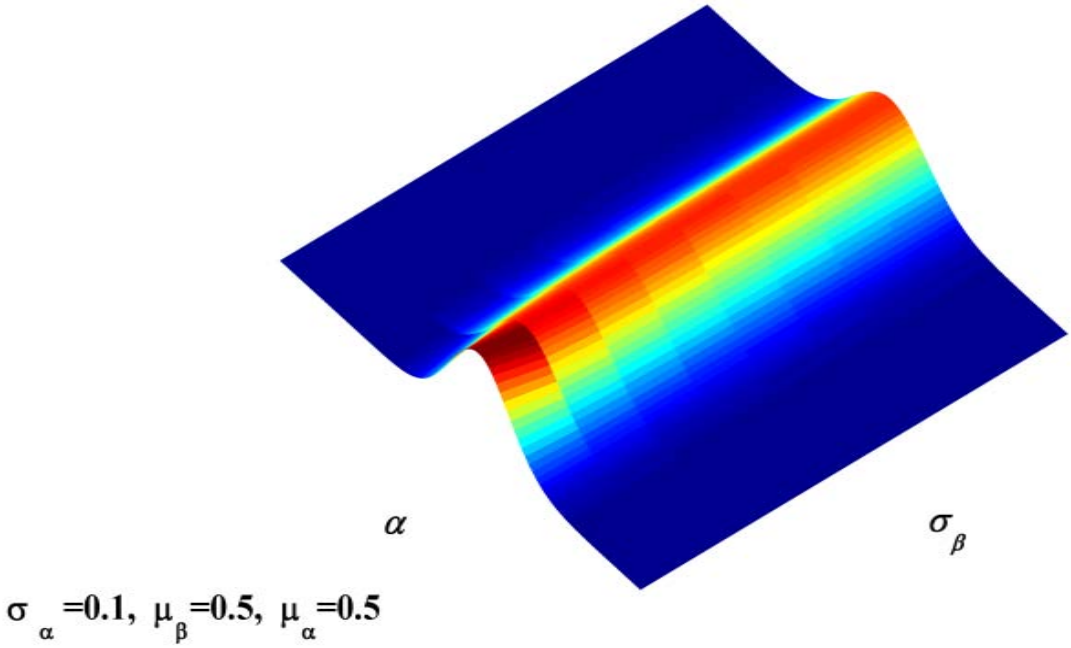

(A)

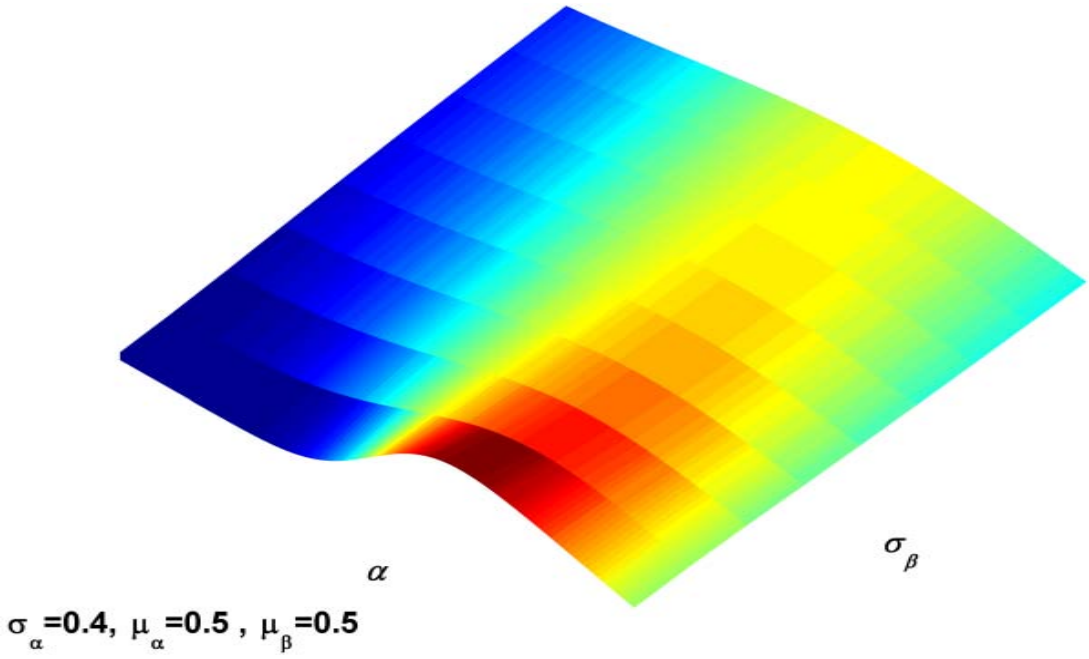

(B)

Figure 3-4: $f_{\mathrm{A}}(\alpha)$ because of the impact of standard deviation on the $f_{\mathrm{A,B}}(\alpha, \beta)$

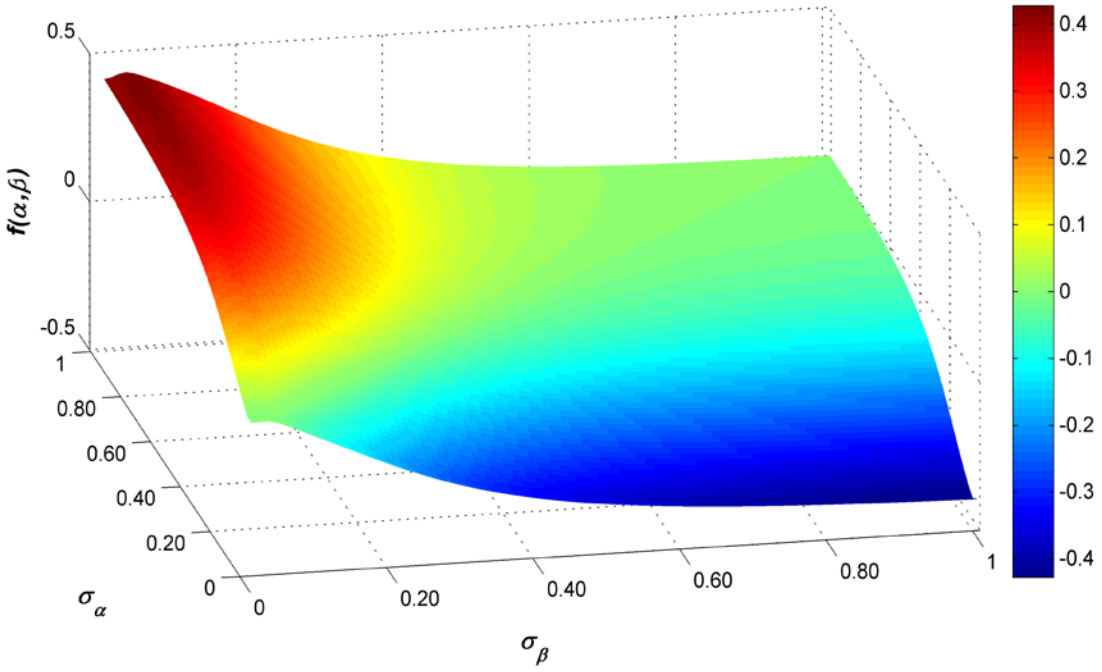

Figure 3-5: The relation between $\boldsymbol{f(\alpha,\beta)}$ and $\boldsymbol{\sigma_\alpha}$ and $\boldsymbol{\sigma_\beta}$

3.2.2. Reaction Factor

The driver's action can be regarded as an action in traffic at the physical level and represents a process that requires time and can only be determined with uncertainty [121]. The reaction factor, p, is the variance between the drivers. It is expressed as uniform random distribution, where $f_P(p)$ is equal to (1) if $0.5 \geq p \geq 1$. Otherwise, it will be (0), as shown in Equation 3-18.

$$f_P(p) = \begin{cases} 1, 0.5 \leq p \leq 1 \\ 0, otherwise \end{cases} \quad (3\text{-}18)$$

3.2.3. Speed Conflict

The vehicle following model describes the combination of the driver and vehicle dynamic as presented in Figure 3-5 [122]. In the figure, the driver of the vehicle acts as a controller, and the inputs may be relative velocity (v_{rel}) and comparison relative position (x_{rel}) to achieve the required relative position x_{rel}. Controller

output is then sent to the non-linear vehicle model as shown in the figure. The feedback is produced by relative velocity between the vehicle (v) and lead vehicle (v_{lead}), and v_{rel} is the time derivative of $x_{rel,}$ as presented in Equation 3-20.

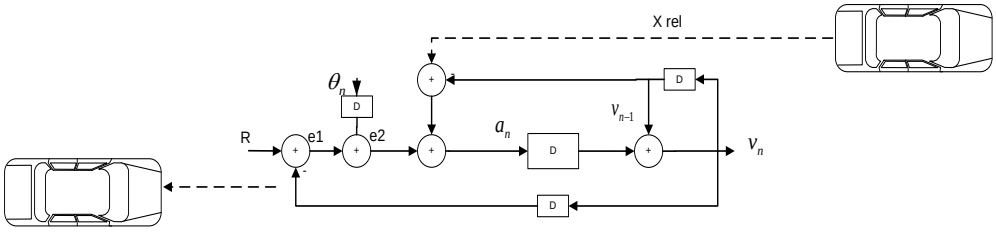

Figure 3-6: Vehicle following model

$$v_{rel} = v_{lead} - v \tag{3-19}$$

$$x_{rel} = \frac{dv_{rel}}{dt} \tag{3-20}$$

Using the vehicle following model for traffic systems allowing unlimited vehicles is one part of the DTCA model. As evident from Figure 3-7, $x_{1.}$ is impacted by x_2 directly, while x_n will have an indirect effect on x_1. For example, Figure 3-1 shows the position of vehicles on a one-lane highway. For safety reasons, the front displacement distance between the vehicles or relative position (x_{rel}) is equal to

$$x_{rel} = x_{n,n+1} \geq 3 \times v_n \times t \tag{3-21}$$

Where t is constant and assumed to be 1.

Vehicle-following behaviour has been widely studied [123, 124]. In some vehicle-following models, following drivers estimate their leaders' acceleration and velocity [123]. As evident from Figure 3-7, if x_{n+1} reduces speed immediately, the gap between the vehicles x_{n+1} and x_n will be reduced depending on the deceleration. The because of reducing the gap between them and time delay to take decision x_n

will start to decrease the velocity further to maintain the same gap. This because of reducing velocity will be translated from the leading vehicle through all the vehicles following it until the last vehicle. The consequence of decreasing x_{rel} will increase the probability of congestion. The speed conflict is the function of position, velocity, and acceleration and deceleration factors $f\ (x, v, \alpha, \beta)$.

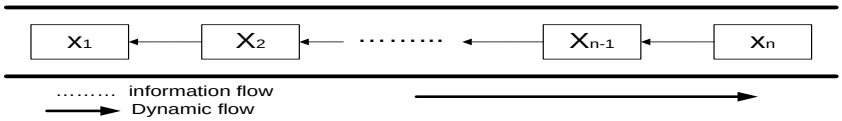

Figure 3-7: Dynamic of traffic system

The relation between the front displacement distance x_{rel} and vehicle velocity is presented in Figure 3-8. Reducing x_{rel} forces the vehicle velocity to be reduced. In Figure 3-9, the relation between the x_{rel} and vehicle velocity is shown; it follows a linear relation, as suggested by Figure 3-7 and Figure 3-8. The reaction factor, (p), of the vehicle's driver and the delayed startup can explain the nonlinear cluster in Figure 3-9.

$$f(x, v, \alpha, \beta) = \begin{cases} v_n(t-\tau) = v_n(t) - k_\beta \cdot \beta, & \text{if } x_{rel}(t) \le 3 \times v_n(t) \times t \\ v_n(t-\tau) = 0, & \text{if } x_{rel}(t) = 0 \\ v_n(t-\tau) = 0, & \text{if } v_n(t) = 0 \text{ and } \beta > \alpha \end{cases} \quad (3\text{-}22)$$

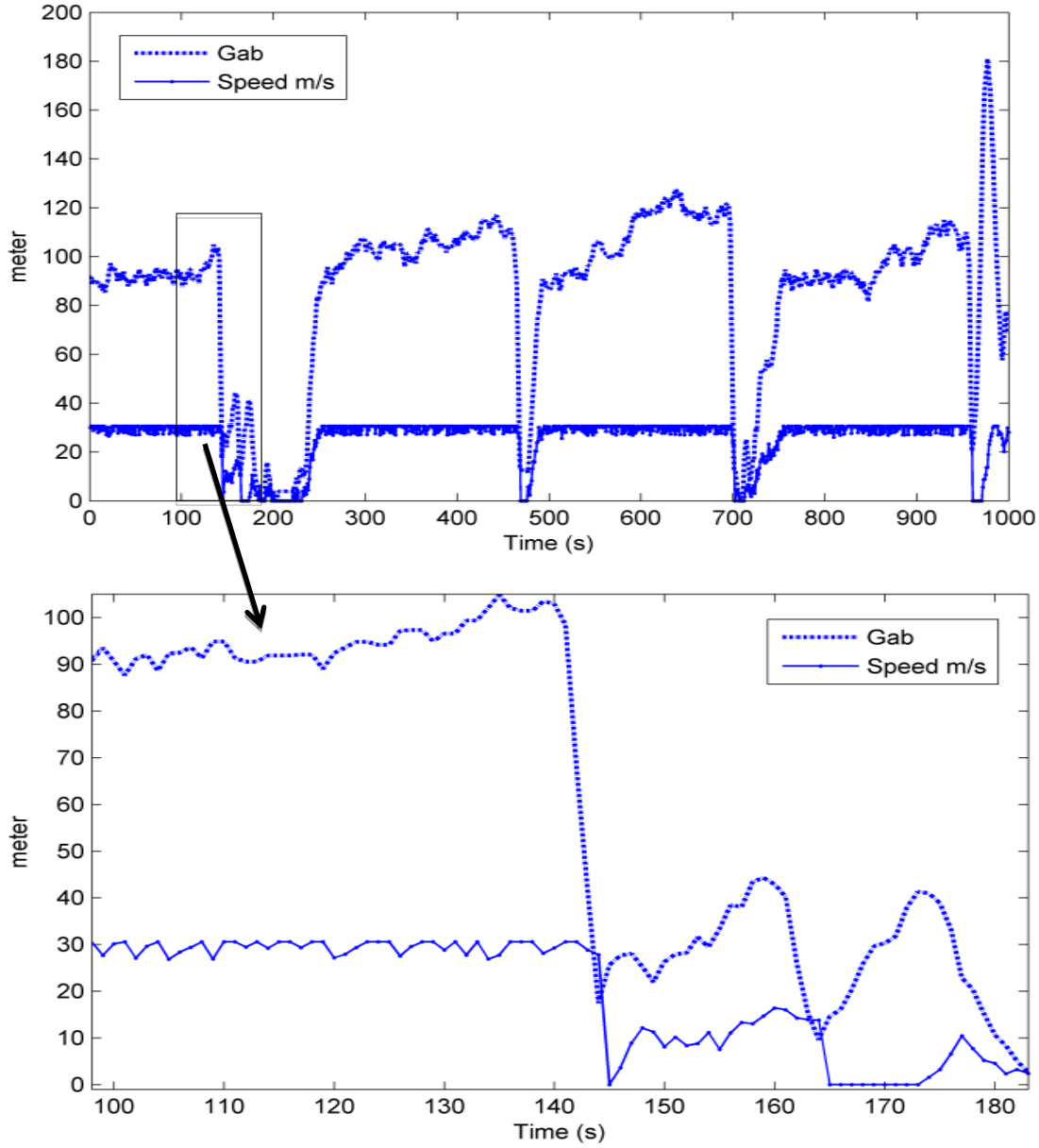

Figure 3-8: Relation between the FDD and velocity

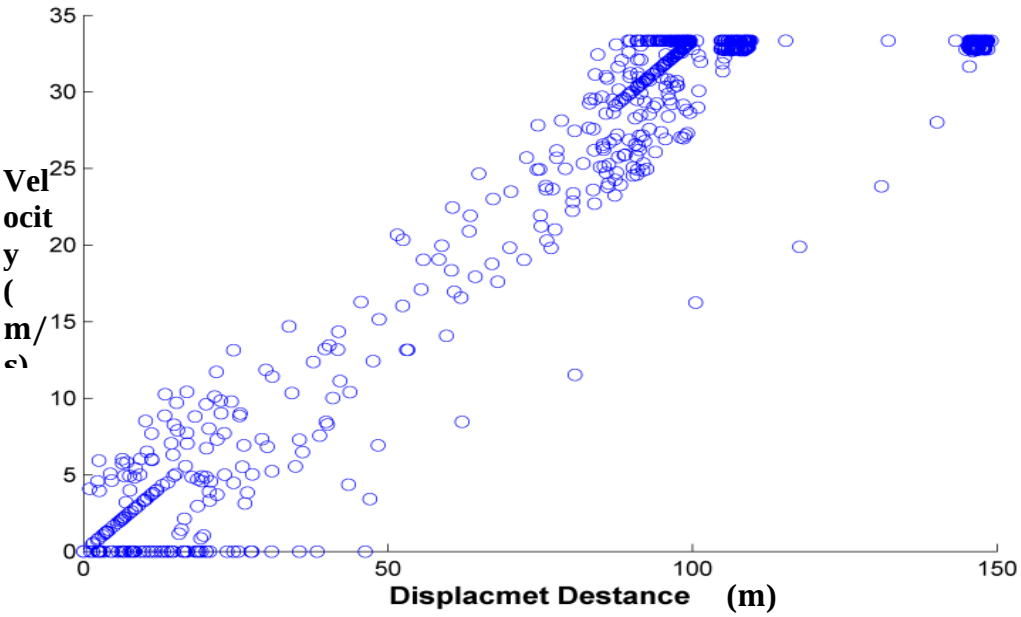

Figure 3-9: Relationship between the x_{rel} and velocity

3.2.4. Delaying the Startup

Delaying the startup is also an important factor in creating congestion. It is a function of position, acceleration factor, reaction factor and time $f(x, \alpha, p, t)$. If the front vehicle's speed is zero, the vehicles behind it will remain stationary until it starts moving. No movement time is very important in eliminating the amount of congestion. An increase in the no-movement time leads to an expansion of congestion. There are four conditions in starting up a vehicle:

1. The vehicle velocity at the time moment is zero $v_n(t) = 0$.
2. There should be enough x_{rel}. It can be accepted if $x_{rel} > 0$.
3. Reactive action (p) should be more than 0.5.
4. Acceleration factor (α) should be more than the deceleration factor (β).

The conditions of vehicle startup can be clarified in Equation (3-23).

$$f(x, \alpha, \beta, p, t) = \begin{cases} v_n(t-\tau) = v_n(t) - k_\alpha \cdot \alpha, & \text{if } x_{rel}(t) \le 3 \times v_n(t) \times t \\ & v(t) = 0, \alpha \ge \beta \\ & 0.5 \le p \le 1 \\ v_n(t-\tau) = 0, & otherwise \end{cases} \quad (3\text{-}23)$$

3.3. Traffic flow

Drawing a map of traffic flow on the highway is an essential part of this thesis. 'Traffic system' is defined as an infinite matrix according to the following relations:

$$\boldsymbol{TF} = [\boldsymbol{a} \quad \boldsymbol{v} \quad \boldsymbol{x}]^T \tag{3-24}$$

Where $\boldsymbol{a}$ is the traffic acceleration vector and

m is the number of the vehicle in the cluster queue.

$$\boldsymbol{a} = [a_1 \quad a_2 \quad \cdots \quad a_m] \tag{3-25}$$

v is the traffic velocity vector

$$\boldsymbol{v} = [v_1 \quad v_2 \quad \cdots \quad v_m] \tag{3-26}$$

and x is the traffic position vector.

$$\boldsymbol{x} = [x_1 \quad x_2 \quad \cdots \quad x_m] \tag{3-27}$$

Each traffic cluster has two types of vehicles: leader and follower vehicles. For the leader cluster (x_1), the acceleration equation will be

$$a_{1,l} = \frac{R - v_{1,n-1}}{t} + \theta_{1,n-1} \tag{3-28}$$

Where R is the desired speed,

t is the sampling time,

θ is the combination of α and β and

n is the vehicle order number on queue.

The velocity will be

$$v_{1,n} = v_{1,n-1} + t \cdot a_{1,n-1} \tag{3-29}$$

While the acceleration for the follower vehicles is given by:

$$a = \theta_{Total} + a_{Total} + R_{Total} + v_{Total} + x_{Total}\Big|_{a_{min}}^{a_{max}} \tag{3-30}$$

a_{max} and a_{min} are boundary conditions for maximum and minimum acceleration.

$$\theta_{Total} = \sum_{n=0}^{m-1} (-\gamma_1)^n \theta_{m-n,l-n-1} \tag{3-31}$$

$$a_{Total} = \sum_{n=0}^{m-1} -(-\gamma_1)^n a_{m-n+1,l-n} \tag{3-32}$$

$$R_{Total} = \frac{\gamma_1^{m-1} R}{t} \left| \sum_{n=0}^{m-1} (-\gamma_3)^n \right| \tag{3-33}$$

$$v_{Total} = \frac{\gamma_2}{T} \begin{pmatrix} \left(\sum_{n=0}^{m-2} -(-\gamma_1)^n \left(\gamma_4 v_{m-n,l-n-1} + \gamma_4 v_{m-n-1,l-n-1} \right) \right) \\ +(-\gamma_1)^{m-2} \gamma_5 v_{1,-k+1} \end{pmatrix} \tag{3-34}$$

$$x_{Total} = \frac{\gamma_2}{T^2} \left(\sum_{n=1}^{k-2} \left(-\frac{\gamma_1}{2} \right)^n \cdot \left(x_{k-n,-n} - x_{k-n-1,-n} \right) \right) + \frac{\gamma_2 \left(x_{k,0} - x_{k-1,0} \right)}{t^2} \tag{3-35}$$

Where $\gamma_1, \gamma_2, \gamma_3, \gamma_4$ and γ_5 are regression coefficients that equal 0.1666, 0.3333, 1, 5 and 0.5, respectively. While

$$v_{m,l} = v_{m,l-1} + t \cdot a_{m,l-1} \tag{3-36}$$

Figure 3-10 illustrates the correlation and coefficient determination between the vehicle simulation and the results of Equation (2-24). It can be seen from the figure that, after vehicle #4, correlations and coefficients reach a stable value except for the correlation and coefficient determination for the position that equals 1 for all the vehicles because of an increase in the data from front-queue vehicles.

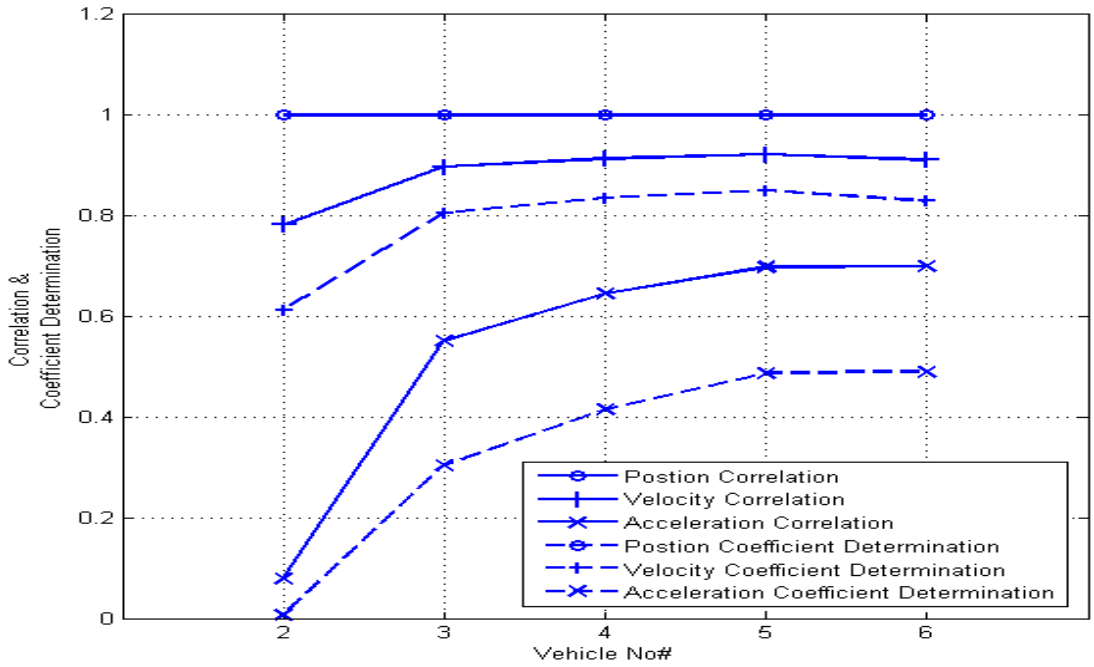

Figure 3-10: Correlation and coefficient determination of the vehicle simulation and the equation

Chapter 4

FUZZY Logic Controller Model

4.1. Introduction

Vehicle and highway automation has been proven significantly successful in avoiding accidents, improving safety, increasing capacity, reducing fuel consumption and enhancing the comfort and performance of drivers[125]. Nevertheless, one of the most essential goals of a transportation system is maintaining speed not just for an individual vehicle but for the system. Congestion can be alleviated as much as possible while increasing the efficiency of energy consumption [126]. In recent years, many traffic models efforts have begun with the goal of enhancing the safety and efficiency of highway/urban traffic with the aid of wireless communication and modern control techniques [11, 127].

Traffic system modulation can be classified according to the level of detail with which traffic systems are represented by considering discrete traffic individuals and describing these individuals in the respective flow models. The models can be [11]:

I. Submicroscopic simulation models, which are high-detail descriptions of the functioning of vehicles' subunits and the interaction with their surroundings;
II. Microscopic simulation models, which are high-detail descriptions in which individual entities are distinguished and traced;

III. Mesoscopic models, which have medium detail and
IV. Macroscopic models that are low detail.

Many studies have discussed the dynamics of traffic flow by using a microscopic model such as CA and DTCA [11, 26]. Microscopic simulation models describe the characteristics of individual vehicles in the traffic stream, driving behaviour and vehicle control behaviour [11].

This chapter will express the dynamic of an individual system by using the Astrom model of ACC; a FUZZY Logic Control system (FLC) has been used for this project and for describing differences between the human-driven machine and the automatic machine.

4.2. Human Intelligence

Human intelligence is a human's ability to find a solution for a problem [123, 128]. Knowledge and experience have a large impact on human actions [128]. Vehicle controller models depend on the human driver model, and different drivers may adopt different strategies [129, 130]. It is important to understand driver behaviour systems and their interactions, such as the perception of self-motion, the usage of haptic devices and the identification of human neuromusculoskeletal properties, which is the combination of the nervous system and muscles working together to move [129]. Figure 4-1 gives the schematic interpretation of a following vehicle that was used to drive the frequency response function H_d^{out} and H_d^{in} of the driver to change the relative velocity v_{rel} and relative distance x_{rel} [131]. Vehicle following is a compensatory control task. Any deviation in v_{rel} and $x_{rel}$is minimised by H_c^{in} and H_c^{out}.

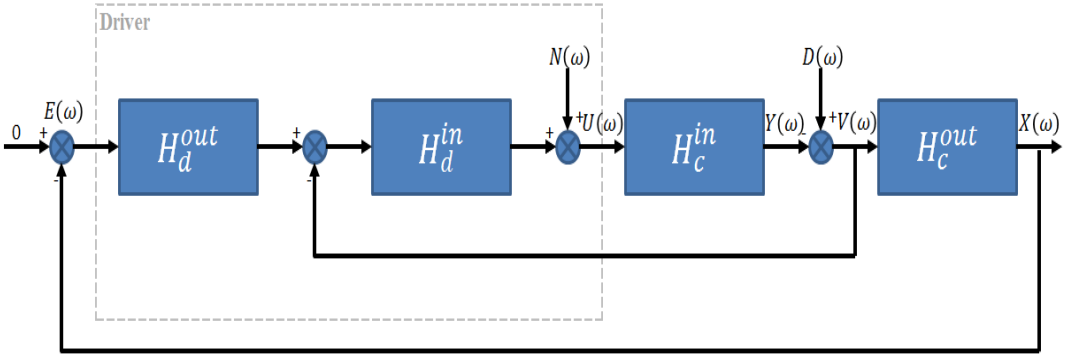

Figure 4-1: Quasi-linear, serial, multi-loop vehicle-following model [131]

Controlling individual vehicles in the traffic system through controlling the vehicle speed, brake system and cruise control has been discussed previously through such means as a PID controller [132]. Also, a modern controller can control the movement of the vehicle and can sense a system, compare it with the desired behaviour, compute corrective actions depending on a inputs and affect the system to make the desired change [133]. There are many types of modern controllers, such as the FUZZY Logic Controller (FLC). FLC is a method of intelligent control that represents human thinking and reacting by using multivalent FUZZY logic and elements of artificial intelligence, such as adaptive and lateral controlling [125, 134-136]. FLC is utilised to design the controller because driving conditions often are nonlinear, FLC does not need complete knowledge of the controlled system, and it is easy for experienced designers and experts to implement the control algorithm in the FLC.

4.3. Model

In this chapter, we will deal with three models, applying the following:

I. Traffic system model,
II. Individual vehicle model and
III. Controller of the vehicles.

4.3.1. Traffic System Model.

The traffic model has closed boundary conditions, that is, traffic running in a one-lane loop. In this case, 69 vehicles are driven 7.5 km. This model used the initial congestion in Figure 4-2.

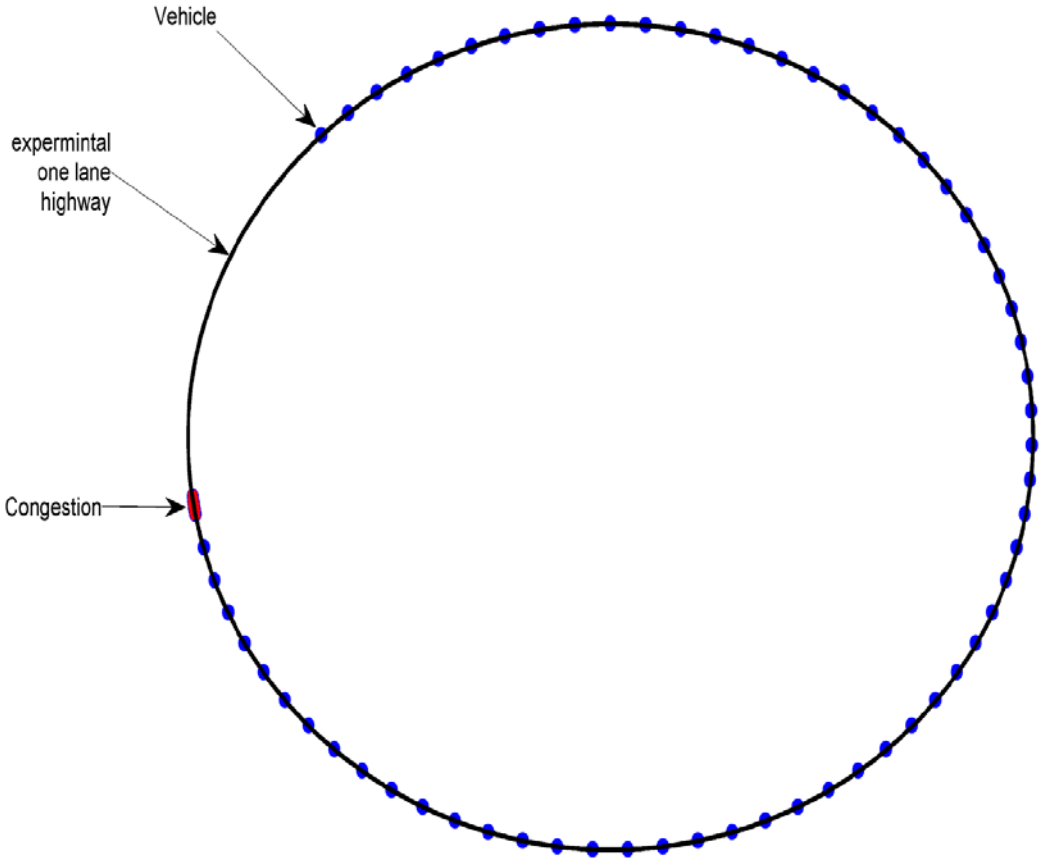

Figure 4-2: One-lane initial vehicle distribution

There are four types of simulations:

I. Human Driver Behaviour,
II. Asymmetric Auto Driving,
III. Symmetric Auto Driving and
IV. Human Driver Behaviour utilising ITS.

4.3.2. Individual Vehicle Model

According to Astrom's first-order model [133], designing the dynamics of individual vehicle systems depends on

$$Ma + cv = F \tag{4-1}$$

While M is mass of the vehicle,

a is the acceleration,

c is the resistance constant,

v is the velocity and

F is the force.

It is known $a = \frac{dv}{dt}$ and F is the input equal to u.

$$m\frac{dv}{dt} + cv = u \tag{4-2}$$

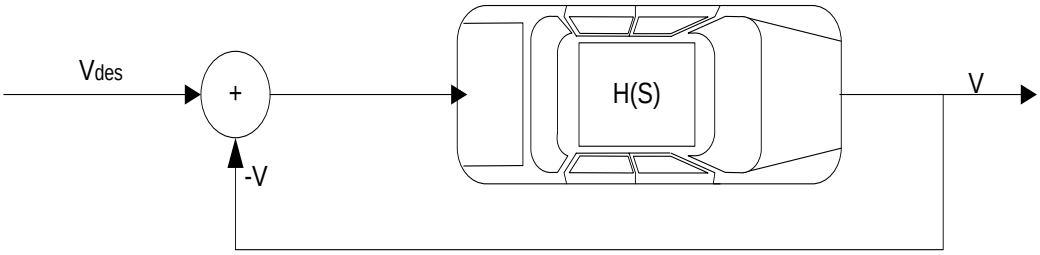

Figure 4-3: The Astrom model, which is used in this paper

For the maximum input, (u) is normalised to be in the interval $0 \leq u \leq 1$. In the velocity approach, the maximum with stability of speed makes $\frac{dv}{dt} = 0$. Then c will be equal to

$$c = \frac{1}{v} \tag{4-3}$$

If we assumed the maximum speed for a vehicle is 180 km/hr (50 m/s), then c equals 0.02. The equation will be

$$\frac{dv}{dt} + 0.02v = u \tag{4-4}$$

The Laplace transfer for (4-4) is

$$H(s) = \frac{V(s)}{U(s)} = \frac{1}{s + 0.02} \tag{4-5}.$$

Creating an adaptive cruise control (ACC) system, as an example of a vehicle controller, can enhance the performance of the vehicle speed control, actively track and follow a target vehicle, and continue to maintain a following distance. This following distance is proportional to the time headway between the following vehicle and the leader vehicle and is controlled by applying acceleration force to the vehicle over a range spanning positive and negative accelerations [7, 137, 138].

The ACC system will have two modes of steady-state operation: 1) speed control and 2) vehicle following [138]. Figure 4-4 is a block diagram of ACC, which makes the decision for Human Driver Behaviour to control both the speed and the following vehicle.

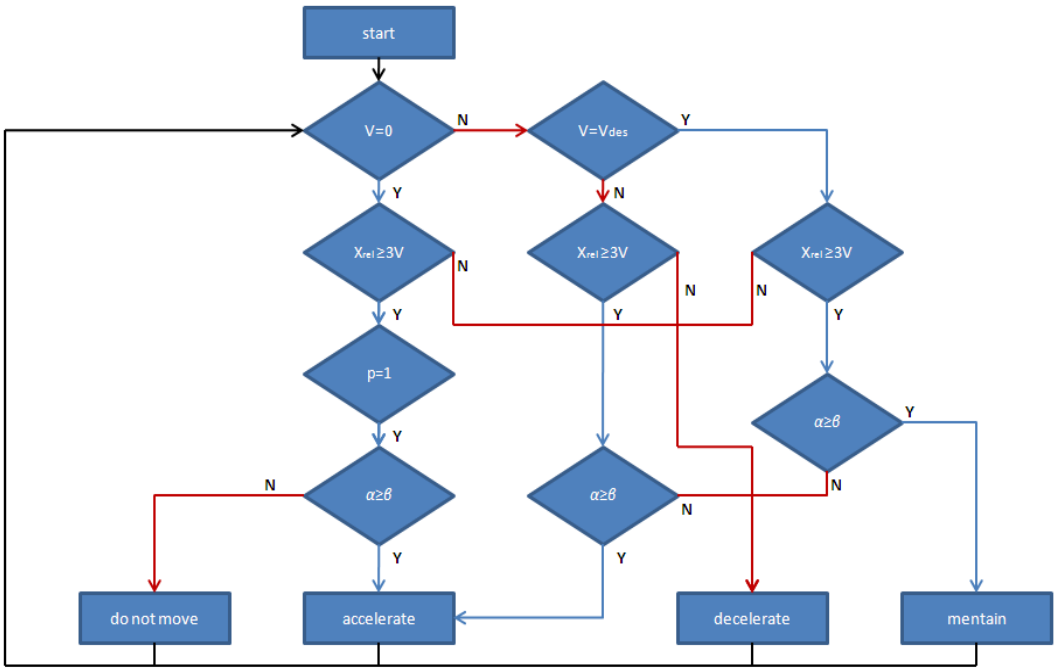

Figure 4-4: The flow diagram of ACC

The following model for the human driver modeler or human machine model is nonlinear [122, 139]. One of the easiest ways to simulate the human driver model is by using the FUZZY Logic Controller (FLC) [140]. According to Casciati, Faravelli and Yao [141], the reasons for using an FLC, mentioned briefly in the introduction, include the following points:

- Attention is focused on nonlinear systems by changing the action gradually, adaptive control and expert control.
- It is difficult to find an accurate form and robust control schemes for mathematical models. Therefore, the FUZZY control approach represents the only robust scheme within expert control.
- The control forces must be of limited intensity. The FUZZY controller implicitly allows this, while classical control schemes are more restricted.

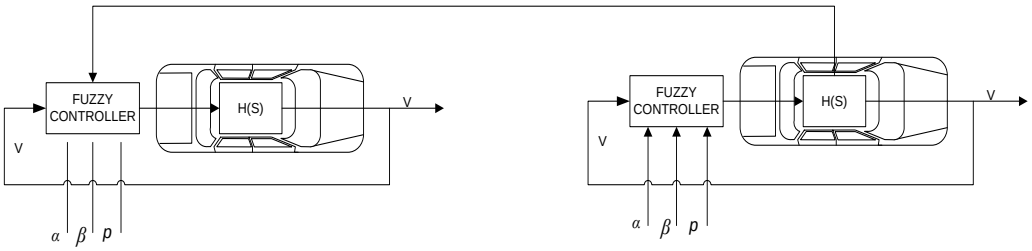

Figure 4-5: Vehicle flowing system with using a FUZZY controller. Disturbances $\boldsymbol{\alpha}, \boldsymbol{\beta}$ and $\boldsymbol{p}$ are added to the control system with no desired velocity as reference.

The vehicle system contains the vehicle dynamic system $H(s)$ and FLC, in which the FLC receives five signals:

1) Vehicle velocity (V), which is the main system output,
2) x_{rel}, the result of the relation between the vehicle and a head vehicle,
3) Acceleration factor α,
4) Reaction factor p and
5) Deceleration factor β.

FLC output ($\mathrm{FLC_{out}}$) is a result of the relation of v, x_{rel} and enteraction factors α, β and p, as in Figure 4-5 and Equation (4-6).

$$FLC_{out} = f(v, x_{rel}, \alpha, \beta, p) \quad (4\text{-}6)$$

Human Driving Behaviour differs from automated driving in the probability of a delay interaction or reaction factor (p). Human Driving Behaviour has acceleration and deceleration factors ($\alpha\&\beta$) as the result of combining multivariable factors such as driver, vehicle, road and weather (Table 3-1). The interaction factor is simulated by uniform distribution with a probability of 0.5. Acceleration and deceleration factors are simulated by normal distribution with $f(\alpha) = N\,(0.5,0.1)$ and $f(\beta) = N\,(0.5,0.1)$. Conversely, Asymmetric Auto Driving doesn't include interaction factor (p), but it includes acceleration and deceleration factors ($\alpha\&\beta$). The purpose of acceleration and deceleration factors is studying the impacts of the differences of vehicles, roads and weather. Finally, Symmetric Auto Driving doesn't include the interaction factor (p) and acceleration and deceleration factors ($\alpha\&\beta$) [116, 117].

4.3.3. Controller of the Vehicles (FUZZY Logic Controller Model)

In this project, there are four types of scenarios:

I. Human Driver Behaviour,
II. Asymmetric Auto Driving,
III. Symmetric Auto Driving and
IV. Human Driver Behaviour utilising ITS.

The difference between them is the controller specification itself. The Human Driver Behaviour contains 5 inputs and 1 output (5×1). Asymmetric Auto Driving contains 4 inputs and 1 output (4×1). Symmetric Auto Driving contains 2 inputs and 1 output (2×1), and Human Driver Behaviour utilising the ITS have 5 inputs and 1 output (5×1) by replacing x_{rel} input to be the ITS controller output. The number of inputs is changed in each scenario. The Human Driver Behaviour scenario has velocity and a head gap (x_{rel}) as the external data. This data comes from the dynamic movement of vehicles. The Human Driver Behaviour scenario also has acceleration, deceleration and reaction factors, as discussed in detail in Sections 3.2.1 and 3.2.2. Contrastingly, the Asymmetric Auto Driving scenario has four

fuzzification inputs. This model is similar to the human driver behaviour model, except that it disregards the reaction factor. The reaction factor is disregarded because Asymmetric Auto Driving does not consider time to react. Finally, the symmetric auto driving scenario has external data, and all acceleration and deceleration factors are disregarded.

4.3.3.1. Human Driver Behaviour.

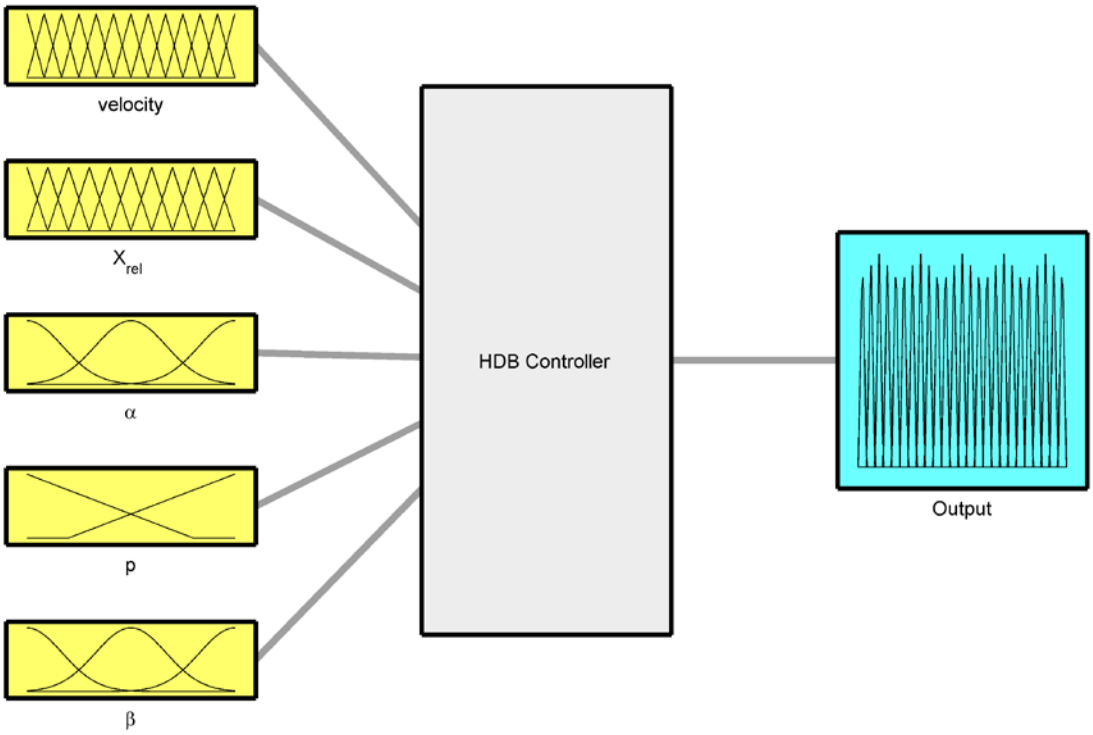

Figure 4-6: Human Driver Behaviour controller block diagram

Figure 4-6 shows the parts of the controller of Human Driver Behaviour Model, which contains elements of fuzzification, controller rules and defuzzification.

4.3.3.1.1. Fuzzification

The fuzzification of the Human Driver Behaviour Model contains five parts. The first is

a) Velocity.

The velocity parameter, which expresses the vehicle's velocity, contains 13 membership functions. The high number of velocity members helps control to increase and decrease in velocity, depending on the traffic demand. Individually,

each membership expresses a small component of speed—for example, (V1) expresses the velocity in that particular velocity boundaries, as shown in Figure 4-7 and Equation 4-7.

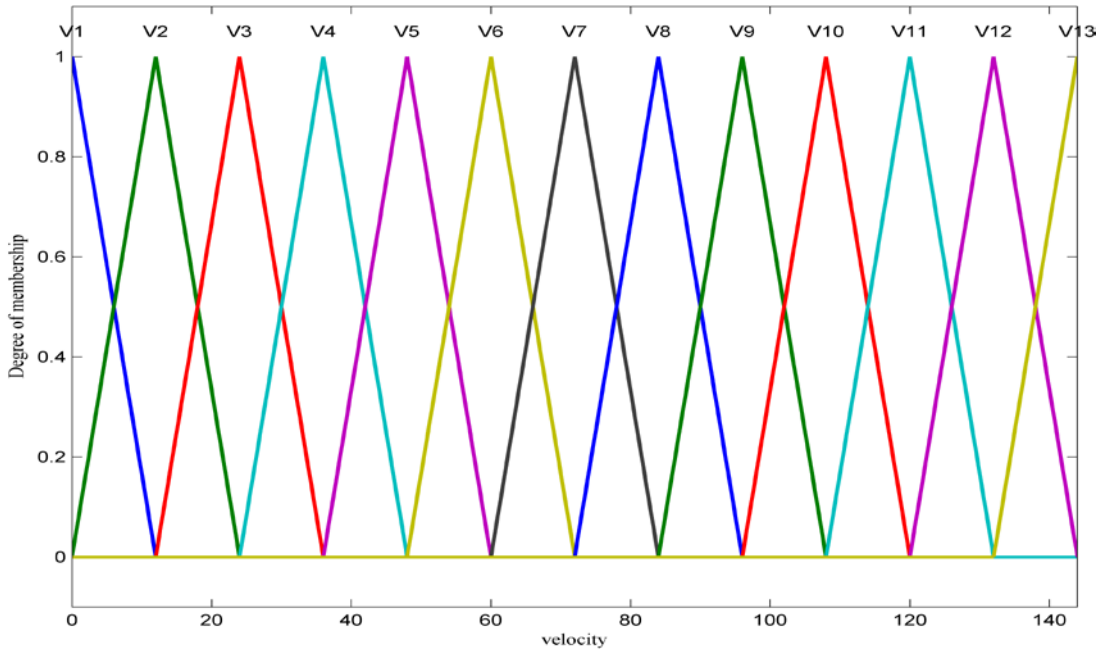

Figure 4-7: Velocity membership functions

$$v = \begin{cases} V_1 & if\ velocity \le V_2 \\ V_2 & if\ V_1 \le velocity \le V_3 \\ V_3 & if\ V_2 \le velocity \le V_4 \\ V_4 & if\ V_3 \le velocity \le V_5 \\ V_5 & if\ V_4 \le velocity \le V_6 \\ V_6 & if\ V_5 \le velocity \le V_7 \\ V_7 & if\ V_6 \le velocity \le V_8 \\ V_8 & if\ V_7 \le velocity \le V_9 \\ V_9 & if\ V_8 \le velocity \le V_{10} \\ V_{10} & if\ V_9 \le velocity \le V_{11} \\ V_{11} & if\ V_{10} \le velocity \le V_{12} \\ V_{12} & if\ V_{11} \le velocity \le V_{13} \\ V_{13} & if\ V_{12} \le velocity \end{cases} \quad (4\text{-}7)$$

b) A head gap (x_{rel})

A head gap (x_{rel}) parameter indicates the gap between a vehicle and the lead vehicle. x_{rel} contains 11 membership functions. The high number of x_{rel} members helps increase the sensitivity of the controller to change the gap between the nth vehicle and the lead vehicle ($n-1$). Each curve of the membership reveals a small part of x_{rel}, such as (X_1) expresses the gap in that particular distance with a lead vehicle, as shown in Figure 4-8 and Equation 4-8.

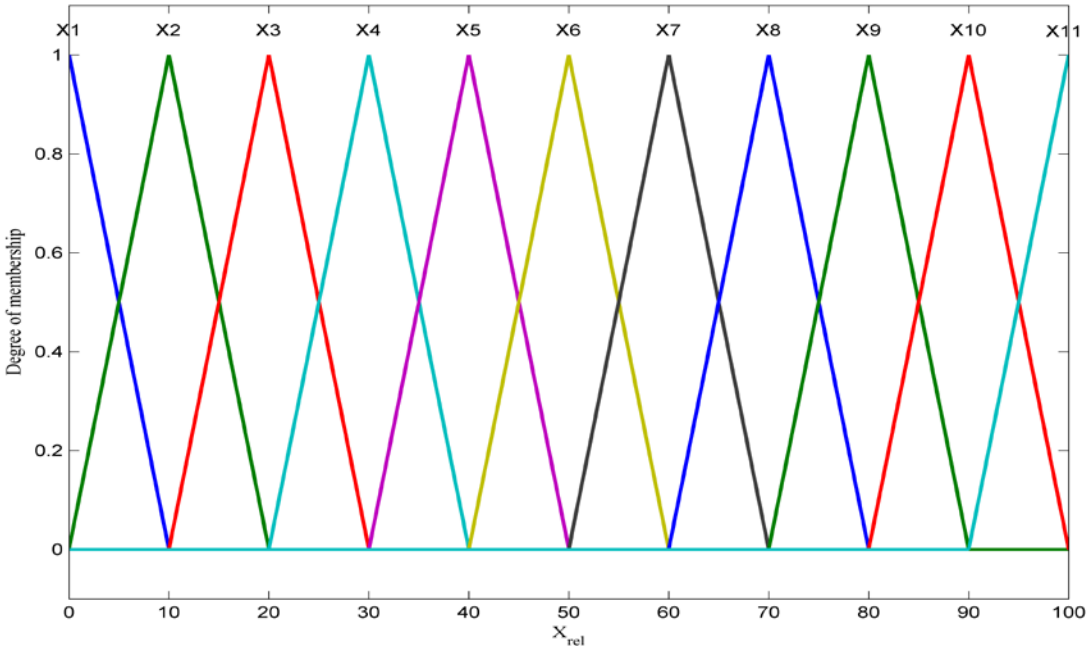

Figure 4-8: $\boldsymbol{x_{rel}}$ membership functions

$$x_{rel} = \begin{cases} X_1 & if\ velocity \leq X_2 \\ X_2 & if\ X_1 \leq velocity \leq X_3 \\ X_3 & if\ X_2 \leq velocity \leq X_4 \\ X_4 & if\ X_3 \leq velocity \leq X_5 \\ X_5 & if\ X_4 \leq velocity \leq X_6 \\ X_6 & if\ X_5 \leq velocity \leq X_7 \\ X_7 & if\ X_6 \leq velocity \leq X_8 \\ X_8 & if\ X_7 \leq velocity \leq X_9 \\ X_9 & if\ X_8 \leq velocity \leq X_{10} \\ X_{10} & if\ X_9 \leq velocity \leq X_{11} \\ X_{11} & if\ X_{10} \leq velocity \end{cases} \quad (4\text{-}8)$$

c) Acceleration factor (α)

Referring to the discussion on the acceleration factor (α) in Section 3.2.1, it is important to apply α in this simulation. It contains three membership functions and presents the intensity of acceleration. Each membership expresses a part of α, as shown in Figure 4-9 and Equation 4-9.

$$\alpha = \begin{cases} \alpha_1 & if\ \alpha \le \alpha_2 \\ \alpha_2 & if\ \alpha_1 \le \alpha \le \alpha_3 \\ \alpha_3 & if\ \alpha_2 \le \alpha \end{cases} \quad (4\text{-}9)$$

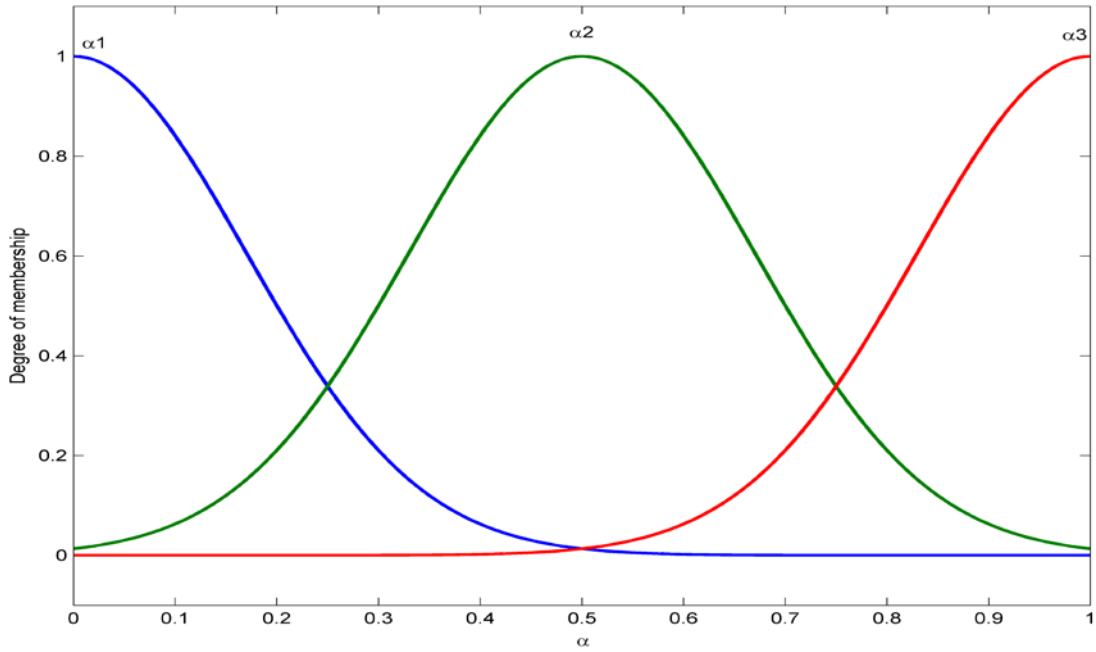

Figure 4-9: Acceleration factor ($\boldsymbol{\alpha}$) membership functions

d) Reactive action factor (p)

Referring to the discussion of the reactive action factor (p) in Section 3.2.2, it is important to apply p in this model. It contains two membership functions. Each membership expresses a part of p, which is displayed in Figure 4-10 and Equation 4-

10. The importance of p can be observed on the delay time of starting up of the vehicle from 0 km/hr.

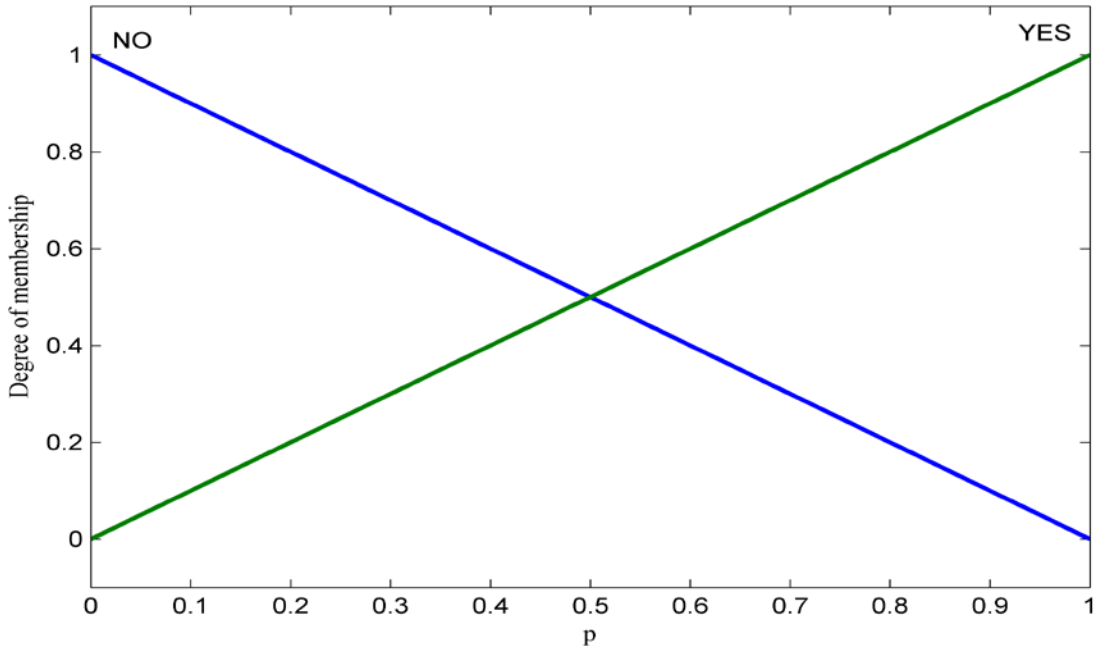

Figure 4-10: Reaction ($\boldsymbol{p}$) membership functions

$$p = \begin{cases} NO & if\ p < YES \\ YES & else \end{cases} \quad (4\text{-}10)$$

e) Deceleration factor (β)

Referring to the discussion of the deceleration factor (β) in Section 3.2.1, it is important to apply β in our model. It consists of three membership functions and presents the degree of deceleration. Each membership reveals a part of β, as depicted in Figure 4-11 and Equation 4-11.

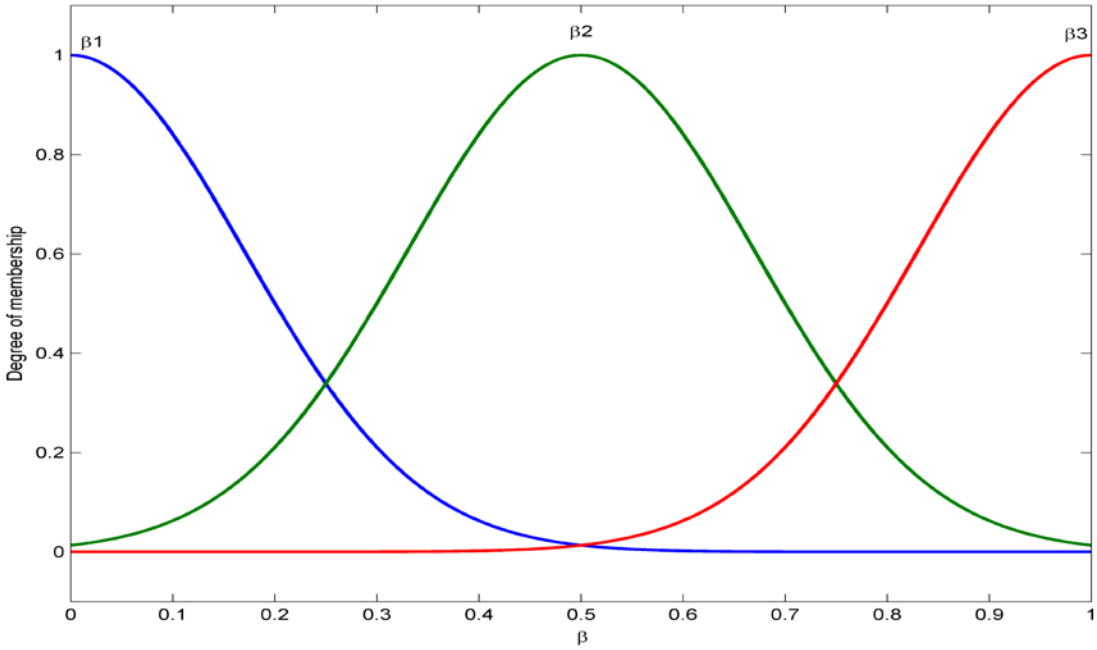

Figure 4-11: Acceleration factor ($\boldsymbol{\beta}$) membership functions

$$\beta = \begin{cases} \beta_1 & if\ \beta \leq \beta_2 \\ \beta_2 & if\ \beta_1 \leq \beta \leq \beta_3 \\ \beta_3 & if\ \beta_2 \leq \beta \end{cases} \tag{4-11}$$

If Velocity and X_{rel} are in the safe mode or they don't impact the output of FLC, the comparison between α and β have the right to impact the output of the controller, which expresses a combination of driver, vehicle, weather and road activities. The impacts of α and β is more obvious during the matching of Velocity and x_{rel} [116] [117].

4.3.3.1.2. Controller Rules

Each membership of FLC output results from a combination of inputs. Table 4-1 expresses the FLC base rules. Some relation between first and second (Velocity and x_{rel}) inputs is clear, such as ($V_1 \otimes X_1 = Z$), and some other relations will be expressed in Appendix (D). Moreover, the relation between first and second inputs and the output of FLC is revealed in Figure 4. Most of the output is around zero and starts dropping by increasing the Velocity or decreasing the x_{rel}. The FLC output

approaches the minimum when x_{rel} is low, especially when the Velocity is more than 60 km/hr. Increasing the gap between the vehicles and decreasing the Velocity leads to an increase in the FLC output. The FLC output maximum is approached when x_{rel} is the maximum, and Velocity is the minimum. As revealed in Figure 4-12, the controller is biasing to the negative side to support the brake system.

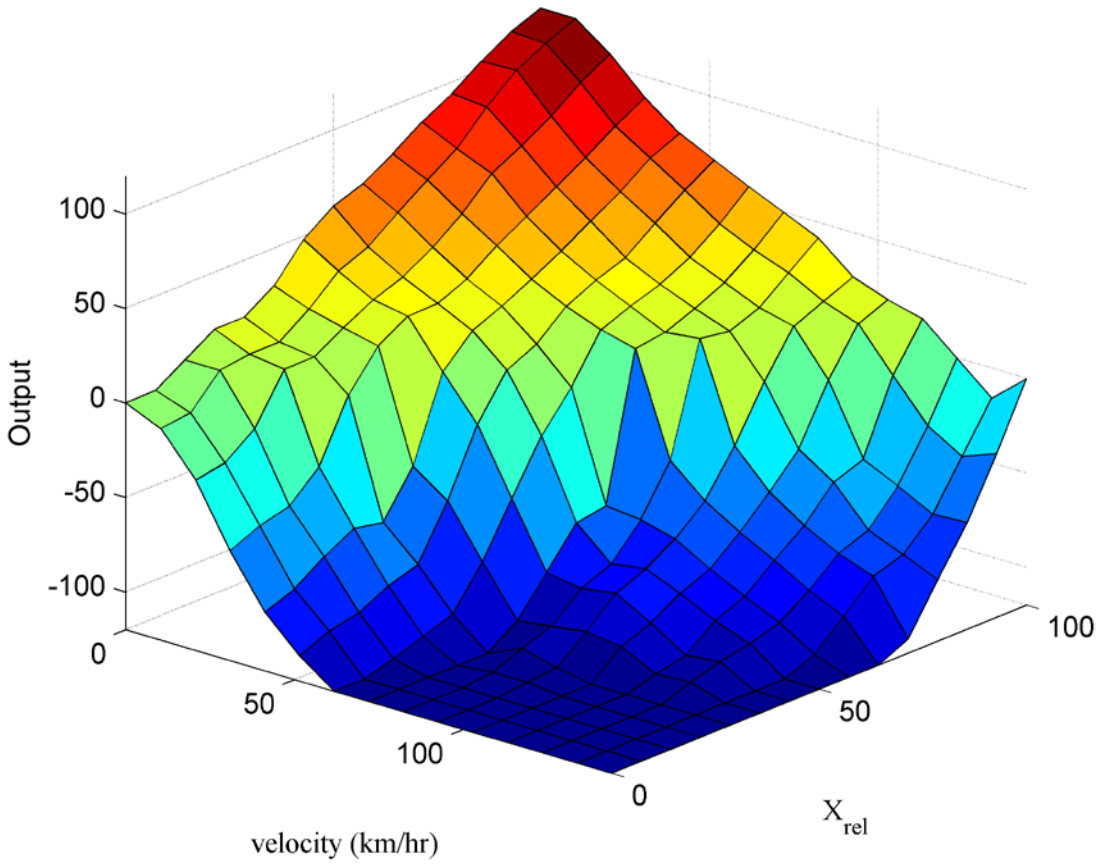

Figure 4-12: FUZZY controller relation between Velocity, x_{rel} and the output

Table 4-1: FUZZY rule base of FUZZY controller

	V1	V2	V3	V4	V5	V6	V7	V8	V9	V10	V11	V12	V13
X1	Z	NO1	NO4	NO8	NO10	NO12	NO12	NO12	NO12	NO12	NO12	NO12	NO12
X2	E1	Z	NO3	NO7	NO9	NO12	NO12	NO12	NO12	NO12	NO12	NO12	NO12
X3	E2	E11	E17	NO5	NO9	NO12	NO12	NO12	NO12	NO12	NO12	NO12	NO12
X4	E3	E12	E11	E17	NO8	NO11	NO12	NO12	NO12	NO12	NO12	NO12	NO12
X5	E4	E13	E18	E11	E26	NO10	NO12	NO11	NO9	NO12	NO11	NO12	NO12
X6	E5	E14	E19	E18	E11	E26	NO8	NO10	NO8	NO10	NO11	NO12	NO12
X7	E6	E15	E20	E19	E18	E11	E17	NO7	NO8	NO9	NO10	NO11	NO12
X8	E7	E16	E21	E20	E13	E18	E11	E17	NO5	NO7	NO8	NO8	NO12
X9	E8	E8	E22	E21	E20	E19	E18	E11	E17	NO3	NO7	NO8	NO8
X10	E9	E9	E23	E22	E21	E20	E19	E18	E11	E17	NO4	NO6	NO5
X11	E10	E10	E24	E25	E27	E28	E29	E30	E31	E31	E11	E32	Z

4.3.3.1.3. Defuzzification

The defuzzification of the Human Driver Behaviour Model contains only one part, which is FLC output. It contains 25 membership functions, from negative output 12 (NO12) to positive output 12 (O12). Each membership of the FLC output results from the combination of five inputs, which is visible in Figure 4-12, Table 4-1 and Equation (4-12).

$$FLC_{out} = f(v, x_{rel}, \alpha, p, \beta) \tag{4-12}$$

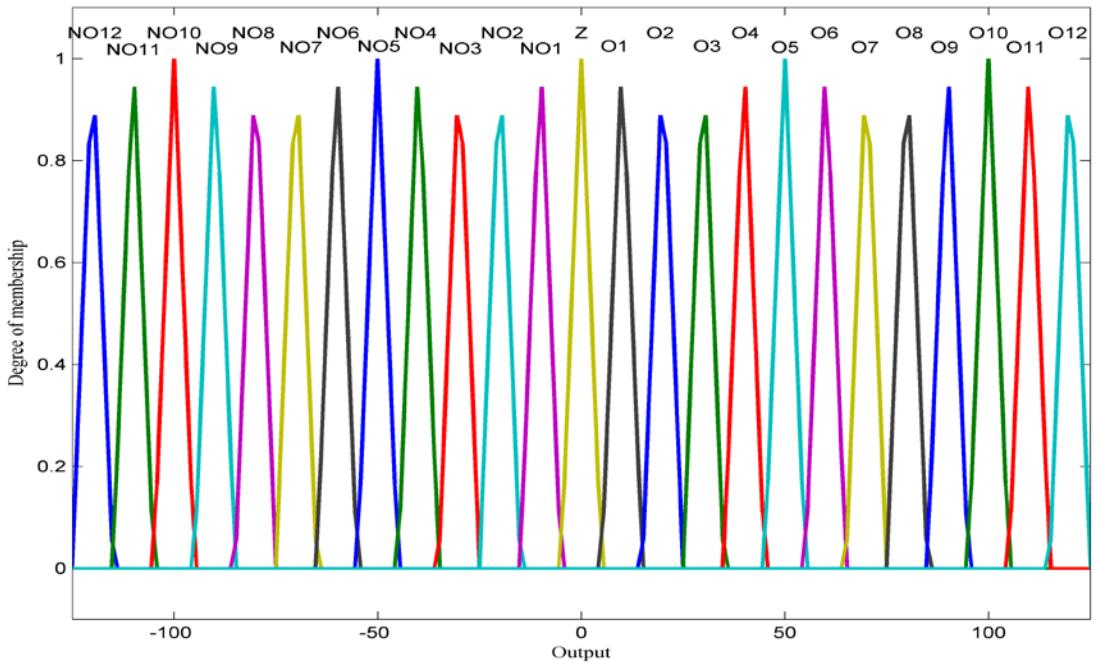

Figure 4-13: FLC output memberships

4.3.3.2. Asymmetric Auto Driving

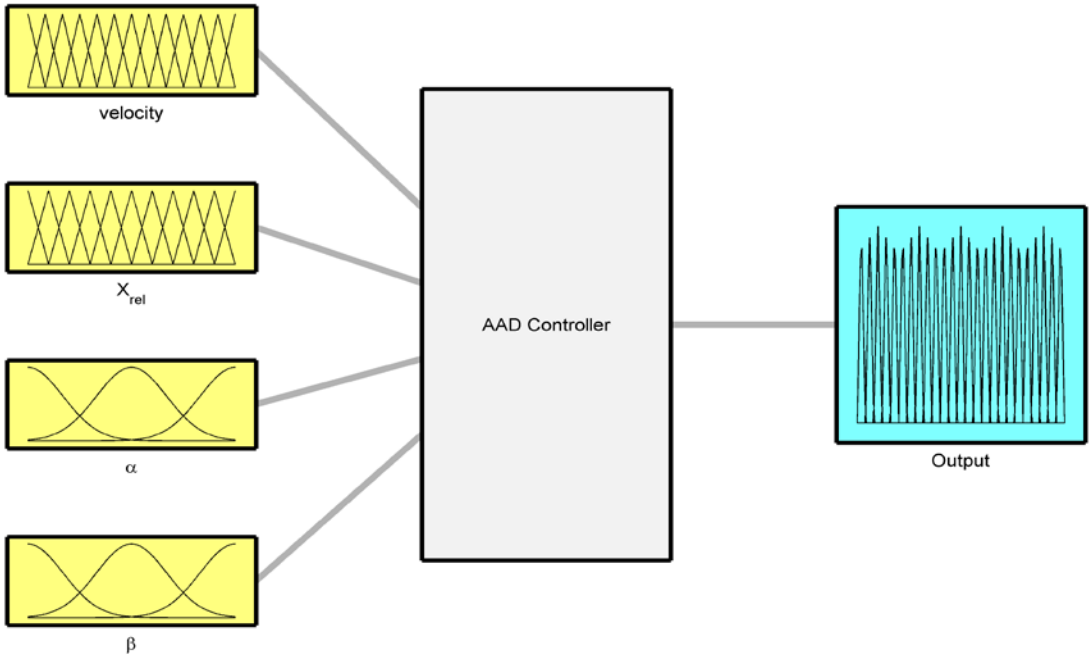

Figure 4-14: Asymmetric Auto Driving controller

Figure 4-14 shows the parts of the controller of the Asymmetric Auto Driving Model, which contains fuzzification, controller rules and defuzzification.

The fuzzification of Asymmetric Auto Driving controller Model contains four parts (Figure 4-14) similar to Human Driver Behaviour Model, except for disregarding the reactive action factor (p).

The disregarding of p especially eliminates differences in the output of the controller. The eliminated startup delays the vehicle from $0\ \mathrm{km/hr}$. The relation between Velocity, x_{rel} and Defuzzification will be similar to the HDB controller.

There are two reasons to utilise this model:

1. Recognise the impacts of reactive action factor (p) and
2. Simulate traffic system with automatic vehicle with different brands, models, situation, controller model …etc.

4.3.3.3. Symmetric Auto Driving

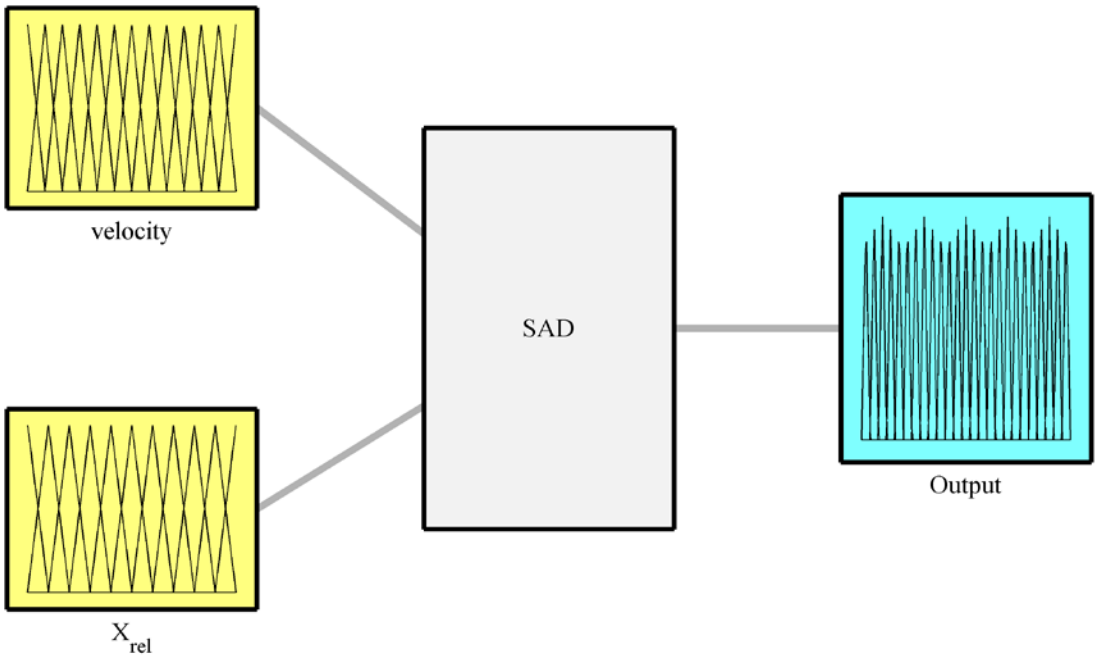

Figure 4-15: Symmetric Auto Driving controller

Fuzzification, controller rules and the defuzzification of the Symmetric Auto Driving Model is shown in Figure 4-15.

The fuzzification of Symmetric Auto Driving controller Model contains two parts (Figure 4-15). They are similar to HDB except they the reactive action factor (p), acceleration factor (α) and deceleration factor (β).

The relation between Velocity, x_{rel} and Output will be similar to other controllers.

There are two reasons to utilise this model:

1. Recognise the impacts of acceleration, deceleration and reaction factor and
2. Simulate traffic system with automatic vehicle with similar specific vehicles.

4.3.3.4. Human Driver Behaviour utilising ITS.

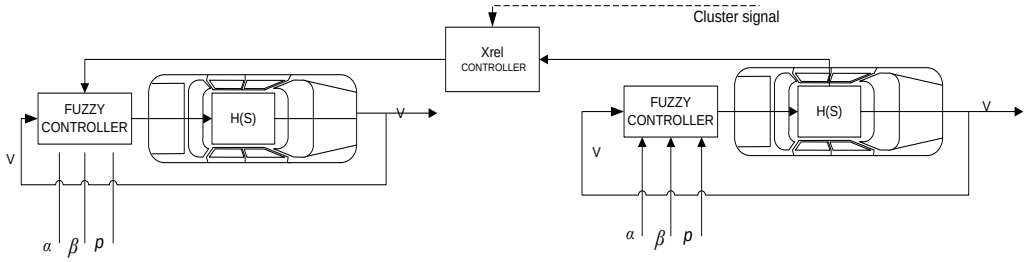

Figure 4-16: Flowing system with using FUZZY controller, acceleration, deceleration and reaction factors ($\boldsymbol{\alpha}$, $\boldsymbol{\beta}$ and $\boldsymbol{p}$) to be added to the control system. $\boldsymbol{x_{rel}}$ is created by the $\boldsymbol{x_{rel}}$ FUZZY controller, and there is no desired velocity as reference.

From Figure 4-16, we see the Human Driver Behaviour with utilising ITS Model is similar to the Human Driver Behaviour Model with controlling the x_{rel} signal when required by utilising cluster signal, which comes from other vehicles through the ITS system. The purpose of controlling the x_{rel} is to increase the gap among the vehicles to decrease the vehicles' speed to decrease the number of vehicles going into a congestion zone.

As been observed in Figure 4-17, the x_{rel} controller is in three parts:

1. A detection part, where the x_{rel} controller detects congestion by receiving the ITS signal (from neighbouring vehicles or infrastructures).
   The ITS signal contains two essential messages:
   - Minimum x_{rel} in the cluster among the vehicles.
   - Minimum v for all the vehicles in the cluster.
2. A decision part. If congestion has detected, the controller will change from normal mode to congestion mode. After solving to congestion, the controller will go back to normal mode.
3. An action part. The signal from the sensor of vehicle x_{rel} will not change during normal mode, but during the congestion mode, x_{rel} sensor's signal will modify by x_{rel} FUZZY controller.

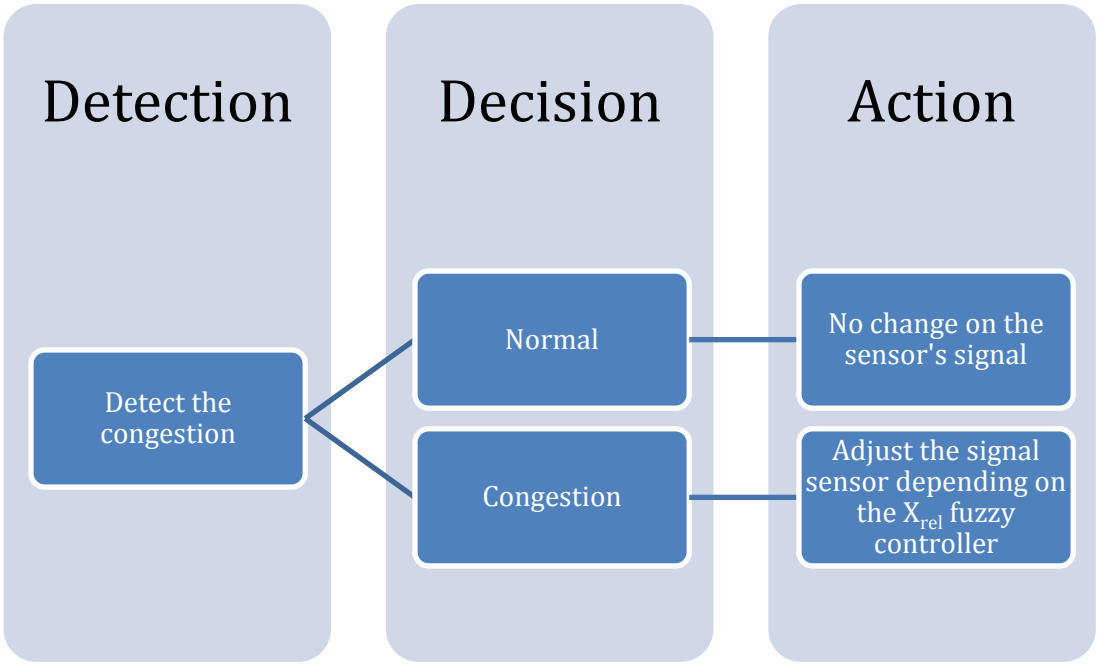

Figure 4-17: $\boldsymbol{x_{rel}}$ controller

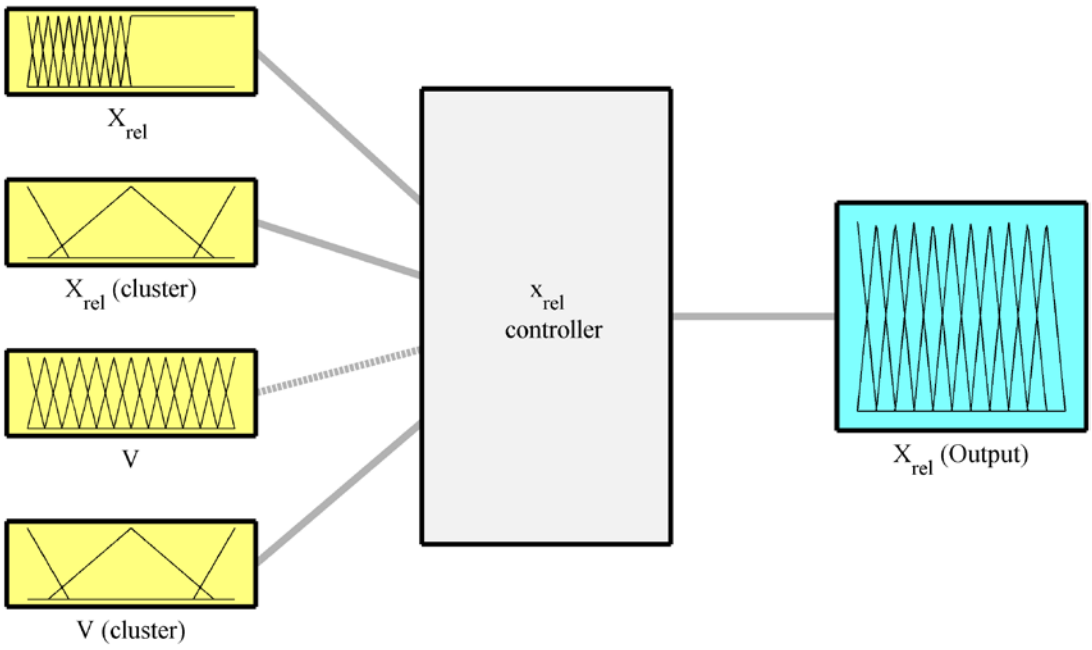

Figure 4-18: $\boldsymbol{x_{rel}}$ fuzzy controller

According to Figure 4-18, x_{rel} FUZZY controller fuzzification contains four inputs. Two of them come from the vehicle itself (x_{rel} and v), and others come through the ITS system (x_{rel}(cluster) and v(cluster)). The purpose of utilising x_{rel} for both the

individual and cluster is comparing between v and x_{rel} from one side and x_{rel} and the x_{rel}(cluster) from the other side. The v(cluster) importance is indicating whether there are any breakdowns on the highway traffic system.

The relation between x_{rel}, v and $x_{rel}(o)$ is illustrated in Figure 4-19. The most change happened in the high x_{rel} with eliminating the maximum less than 100 m to reduce the vehicle velocity indirectly to a certain amount through reducing x_{rel}. Conversely, low x_{rel} does not have any change from the other origin signal.

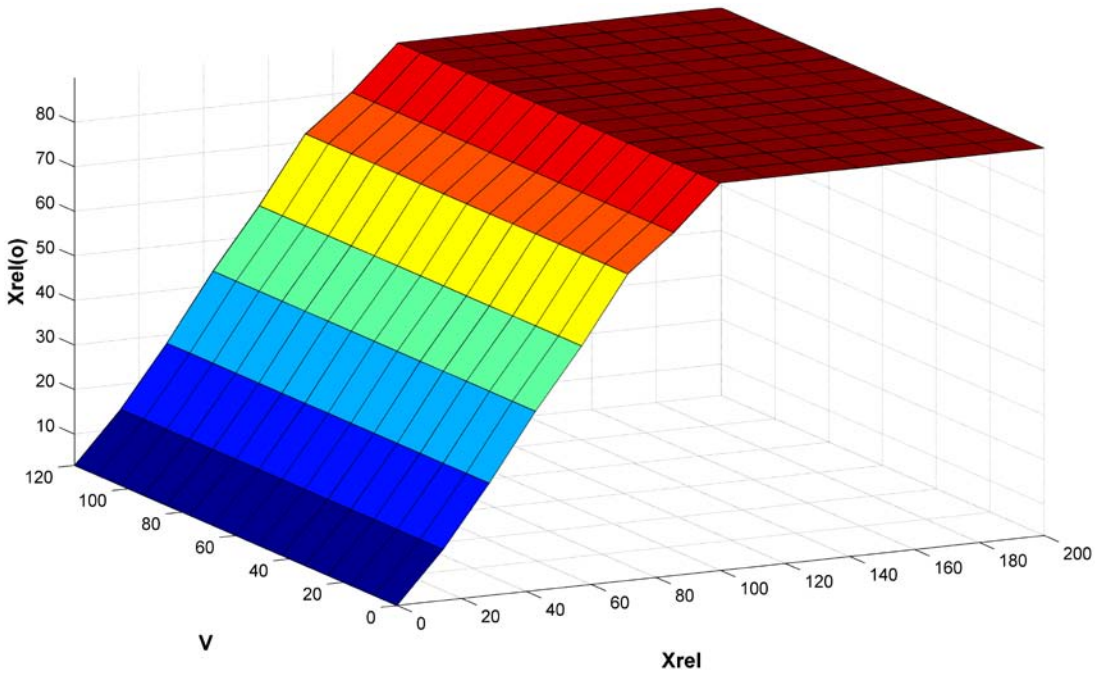

Figure 4-19: The relation between $\boldsymbol{v}$, $\boldsymbol{x_{rel}}$ and $\boldsymbol{x_{rel}(o)}$

Chapter 5

Results of Simulated Traffic Flow by Using FUZZY Logic Controller Models

5.1. Introduction

Chapter 4 has expressed the traffic system model, individual vehicle model and vehicle FUZZY controller model that have been used in the project. As expressed, the traffic system model and individual vehicle model are fixed, and the vehicle FUZZY controller model is changeable between the four main approach scenarios. Moreover, Human Driver Behaviour, Asymmetric Auto Driving and Symmetric Auto Driving that was changing in the FUZZY controller were limited in the fuzzification membership. Human Driver Behaviour utilising the ITS Model changing is not in a fuzzification membership but in the x_{rel} input signal the of vehicle controller. According to Figure 4-16, the x_{rel} input signal is the x_{rel} controller output, which is the result of utilising the ITS system and vehicle direct sensing and managing by x_{rel} controller. The differences between those scenarios will be expressed through the results. In this chapter, we are going to illustrate the results of the approaches.

This chapter will be distributed into four sections: Section 5.2 will express Human Driver Behaviour at different speeds (20, 40, 60, 80, 100, 120 and 140 km/hr). Asymmetric Auto Driving will be presented in section 5.3. Symmetric Auto Driving and Human Driver Behaviour with utilising ITS will be presented in section 5.4 and section 5.5, respectively.

5.2. Human Driver Behaviour Model

5.2.1. V_{des} is 20 km/hr

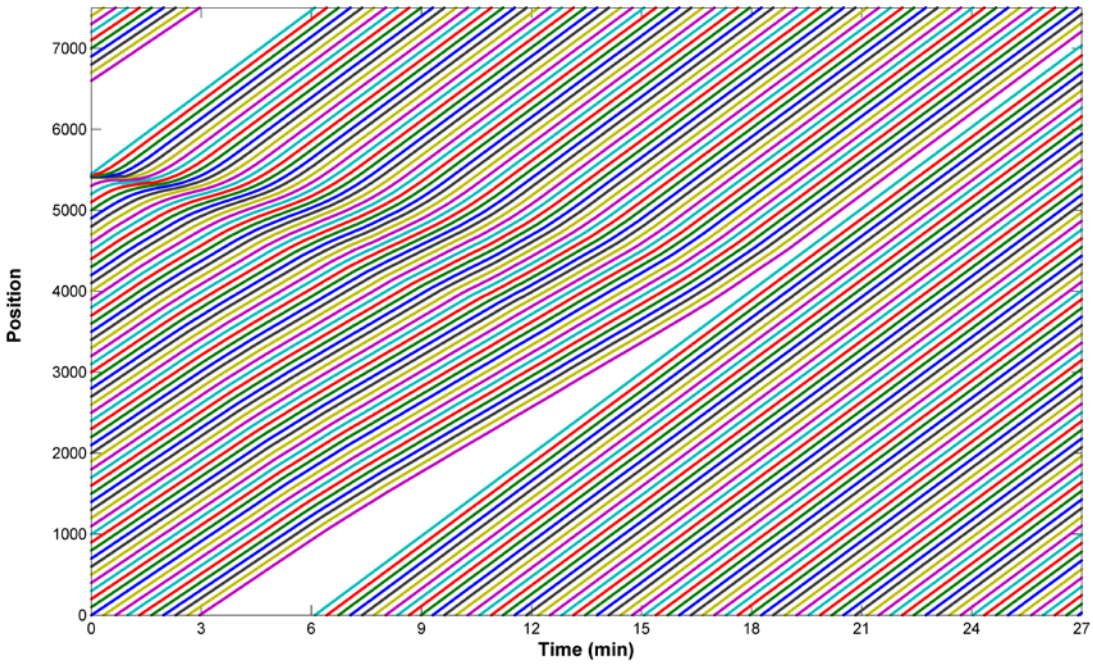

Figure 5-1: Traffic flow of Human Driver Behaviour Model with 20 Km/hr desired velocity scenario

From my observation of the approaches in this project, I found three essential factors that can impact congestion either by reducing or expanding:

1. Velocity of the vehicles coming into the congestion zone.
2. Acceleration and reaction time delay for the vehicle going out of the congestion zone. At this point in acceleration, deceleration and reaction factors play a serious impact on congestion.
3. The relation between the capacity and velocity over the cluster.

Figure 5-1 shows the traffic flow for the Human Driver Behaviour Model with a 20 Km/hr desired velocity scenario. In a general overview, it is clear that the congestion is solved in the 19th minute of the approach. The congestion, which is created in the initial approach, is sharp and clear in the first three minutes, but after the 3rd minute, the congestion starts to solve as a because of the difference between congestion's input and the output of traffic flow. For example, the first vehicle impacted by the congestion during the initial model took more than 15 seconds. But, simultaneously, 50% of the vehicles held in the congestion during the initial time, are left the

congestion zone. Moreover, in 54 seconds, all the vehicles held in congestion during the initial time are left in the congestion zone, and only two vehicles enter the congestion zone.

Figure 5-1 illustrates human driver behaviour at 20 km/hr desired velocity. At position 5,400 m and zero time, we can see that the positions of the vehicles following each other (each represented by an approximately 45-degree line) either do not shift or shift very little. The continuum of each line indicates a steady shift in the position of each vehicle. Hence, the dark shaded area represents congestion, since practically all the vehicles are stuck in their positions for some period of time. This congestion is dissolved after time by the continuum of each line. For example, a vehicle starting at three minutes point makes a steady shift in its position without delay. The darker and longer patches indicate the severity of the congestion.

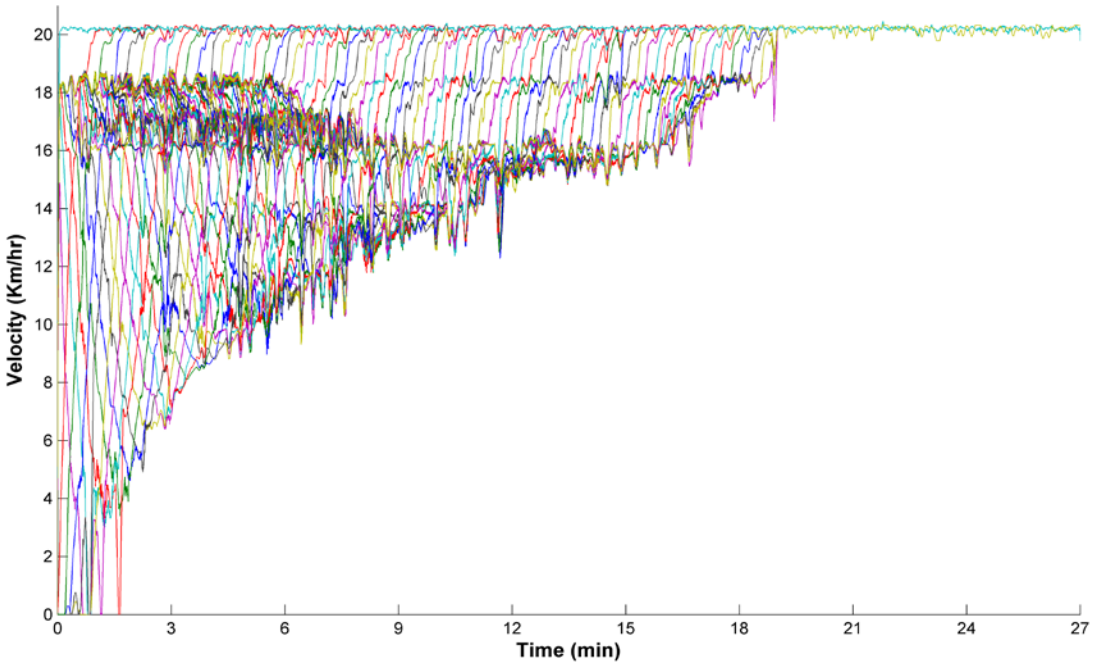

Figure 5-2: Velocity of human driver behaviour model with 20 Km/hr desired velocity scenario

Moreover, Figure 5-2 illustrates the velocity of the Human Driver Behaviour Model with a 20 Km/hr desired velocity scenario and displays the vehicles' velocity envelope. It is clear that, in the first two minutes, there are few vehicles its velocity going to zero as because of the vehicles following in the stopover situation in the congestion zone. The number of vehicles is held in the station situation in the congestion zone that is reducing dramatically. After the 2nd minute, the down limit of

the vehicle velocity limit is increased up to the 19th minute, where it matches the upper limit. Also, Figure 5-4 expresses the velocity average over the cluster, where the average of the cluster velocity after the initial time jumps to 17 km/hr because of the initiation of the model. After 6 minutes, the cluster's velocity increased to approach the desired velocity in 19th minute.

Figure 5-2 shows that the velocity of each vehicle in the line is relatively steady up to 16 km/hr. Between 16 km/h and 18 km/h, there are erratic attempts to attain a steady speed (as evidenced by the heavy lines). Thereafter, the 18 km/h speed increases steadily to 20 km/h. At 20 km/h. Some minor adjustments in the speeds of each vehicle can be seen. Similar attempts to attain steady speeds can be observed between 5 minutes and 9 minutes points at speeds of 9 km/h to 14 km/h.

$$\dot{v}_{free}(v) = a[1 - (v/V_{des})^{\delta}] \quad (5\text{-}1)$$

Furthermore, Figure 5-3 shows the acceleration when the Human Driver Behaviour Model applied at 20 km/h desired velocity scenario. In this simulation, continuous accelerations and decelerations are taking place to achieve the desired speed. In many cases, these accelerations and decelerations are severe, as evidenced by the spikes on both sides of the 0 acceleration values in the middle of the graph. This figure illustrates that the acceleration curves started at the highest acceleration level because of the desire to reach required velocity as soon as possible, as in Equation 5-1. After the initial erratic time, the acceleration decreases gradually due to increase of the velocity. At the 19th minute, the acceleration curve is in its lowest range, confirmed by Figures 5-1, 5-2 and 5-3.

The main reason of solving is the capacity, where the rate of the approach capacity to maximum capacity is 0.21 and where the congestion has time to be absorbed through unoccupied areas in the highway. Regarding (Table E-1), the traffic flow rate and approach capacity to maximum capacity rate are almost similar. Moreover, a common vehicle low velocity reduces the number of vehicles to approach the congestion zone and accumulate on it. Conversely, regarding Equation (2-8), during no stationary startup (+0 Km/hr), the acceleration will be low, and that will cause the

delay of congestion fully solving until the 19th minute, as seen in Figure 5-2, Figure 5-3 and Figure 5-4.

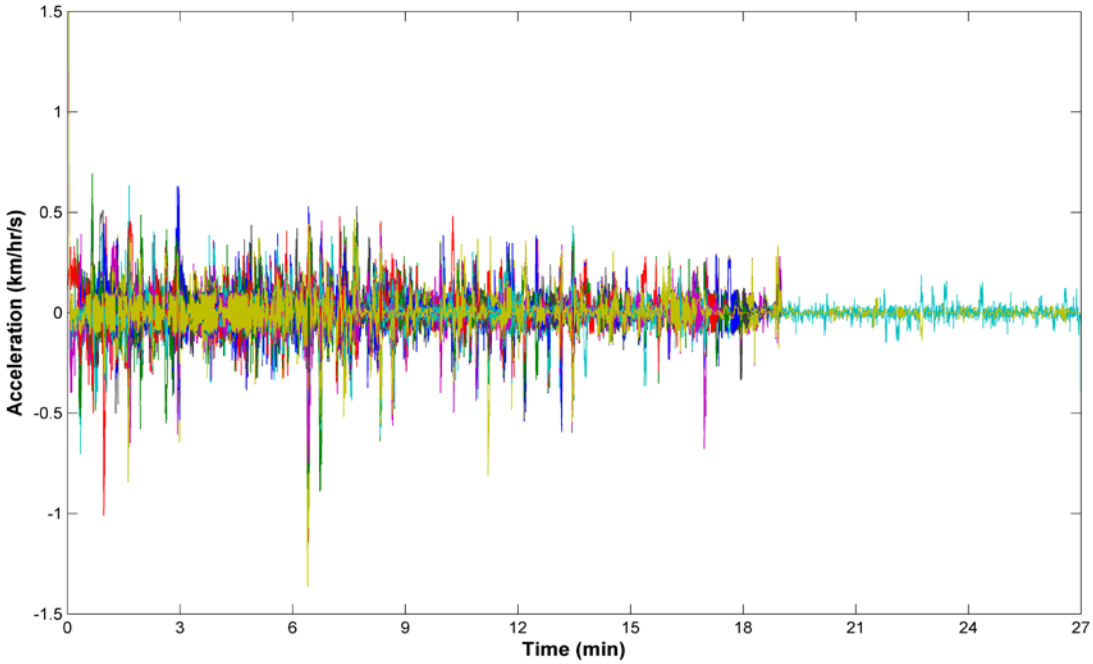

Figure 5-3: Acceleration of Human Driver Behaviour Model with 20 Km/hr desired velocity scenario

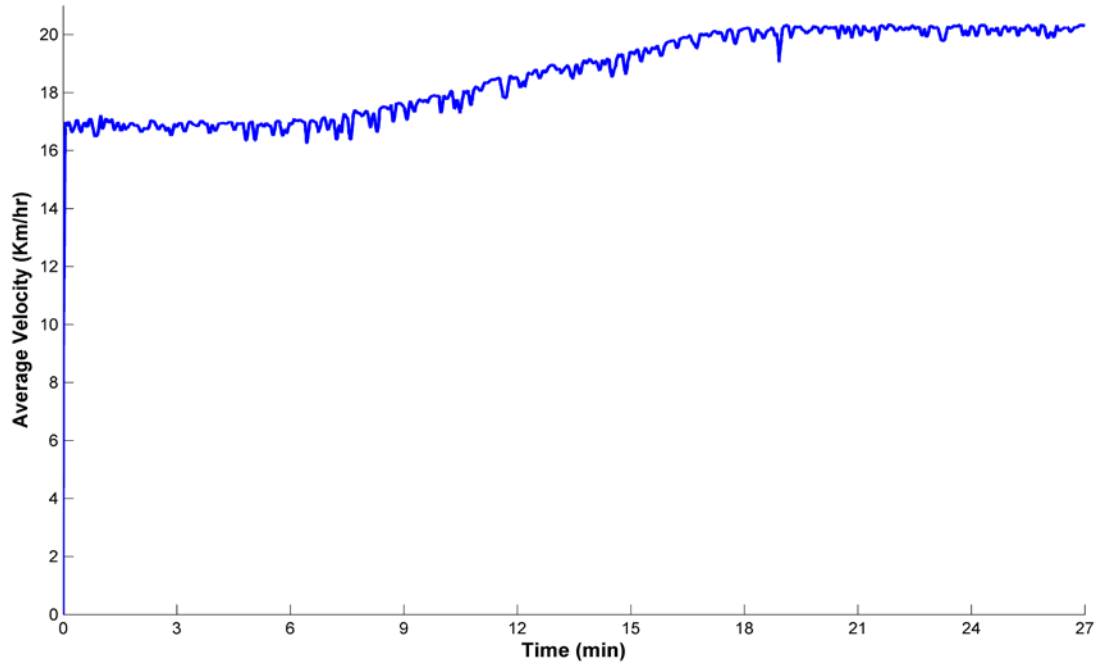

Figure 5-4: Average velocity of Human Driver Behaviour Model with 20 Km/hr desired velocity scenario

5.2.2. V_{des} is 40 km/hr

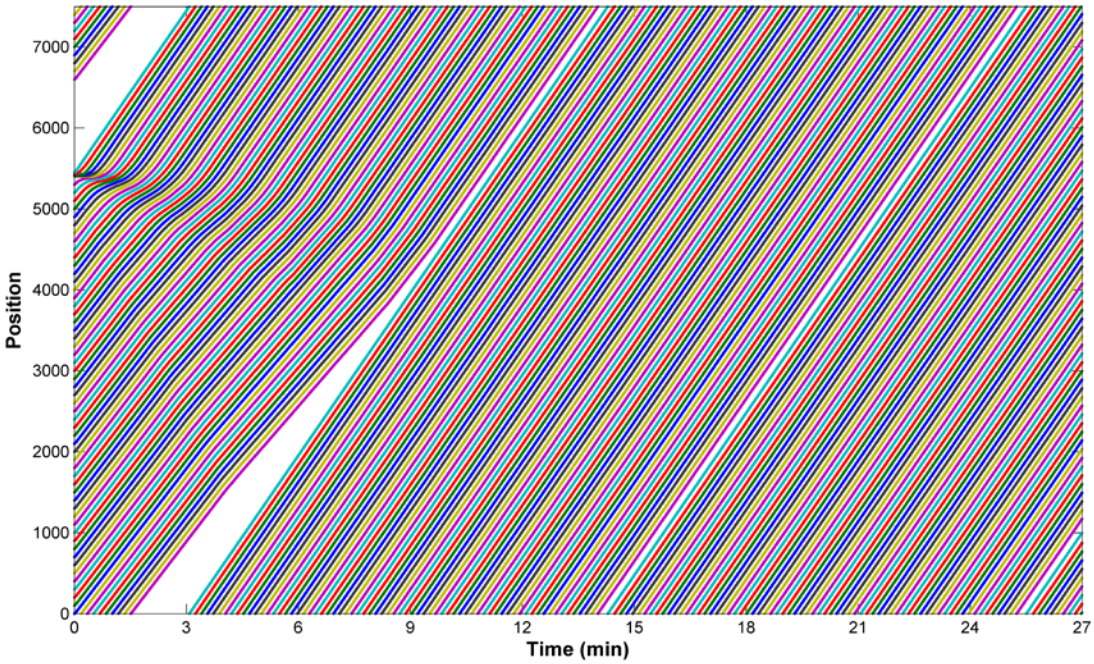

Figure 5-5: Traffic flow of Human Driver Behaviour Model with 40 Km/hr desired velocity scenario

Figure 5-5 illustrates the traffic flow for the Human Driver Behaviour Model with a 40 Km/hr desired velocity scenario. In a general overview, it is clear that the congestion is solved in minute 9.6 of the approach. Similar to the scenario of the 20 Km/hr desired velocity, the congestion is sharp and clear in the first 1.5 minutes, but after that, the congestion starts to solve as a because of the difference between congestion's input and output's traffic flow. For example, the first vehicle impacted by the congestion that during the initial model took more than 6 seconds. But, at the same time, 33% of the vehicles are left in the congestion zone. Moreover, in 24 seconds, all the vehicles held in congestion during the initial time are left in the congestion zone, and no vehicles enter the congestion zone.

Figure 5-5 shows Human Driver Behaviour model at 40 km/h desired velocity. The congestion is short-lived as in the case of Figure 5.1. It can be see that the positions of the vehicles following each other (each represented by an approximately 45-degree line) do not change or change very little. Each line indicates a steady shift in the position of each vehicle. A vehicle starting at two minutes shifts its position

steadily and without any delays. This indicates that darker and longer patches show the severity of the congestion.

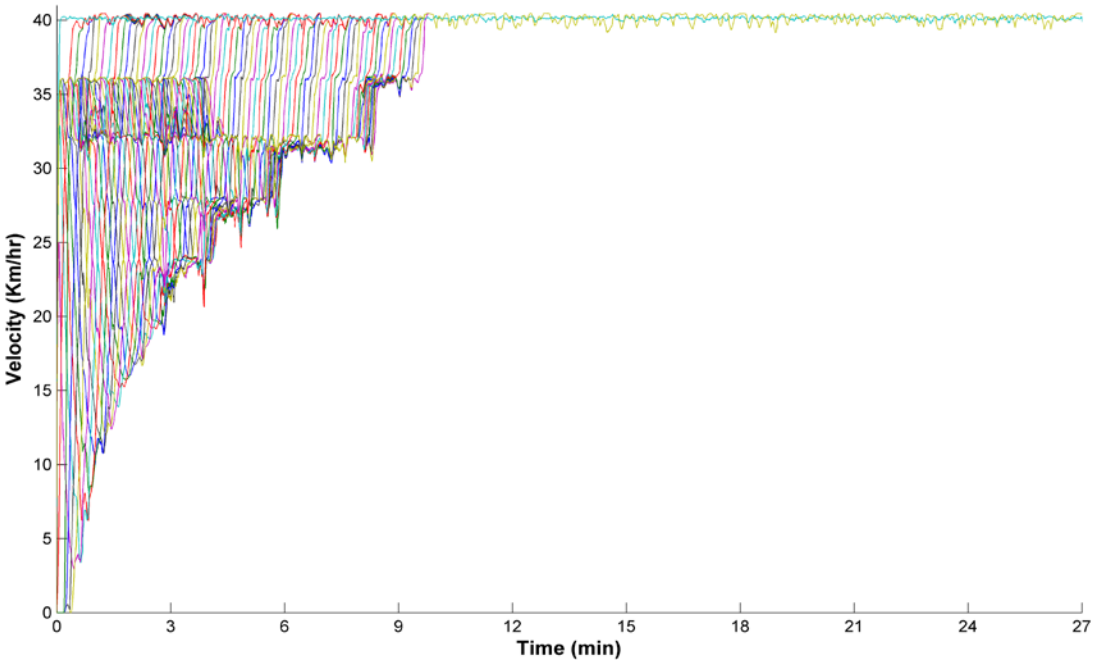

Figure 5-6: Velocity of the Human Driver Behaviour Model with 40 Km/hr desired velocity scenario

Moreover, Figure 5-6 shows the velocity when the Human Driver Behaviour Model is applied at 40 Km/h desired velocity level. It displays the velocity envelope of each vehicle. It is clear that in the first 24 seconds, there are vehicles with reduced velocities because they are approaching to the congestion zone. Moreover, this figure shows that the velocity of each vehicle is relatively steady up to 28 km/h. Between 28, 33 and 36 km, there is erratic attempts to get steady speed (as evidenced by the heavy lines). However, after 36 km/h, there is a sudden jump to 40 km/h. At 40 km/h minor adjustments in the speeds of each vehicle can be seen. Also, Figure 5-8 displays the average velocity of the vehicles in the cluster. The velocity of the cluster of vehicles jumps to 33 Km/h after the initial acceleration. The cluster velocity increased gradually over time until it approached the desired velocity in 9.6 minutes.

Furthermore, Similar to Figure 5-3, Figure 5-7 shows vehicle acceleration profile when the human model is used. It can be seen that continuous acceleration and decelerations are taking place to reach the desired speed. In many cases, these accelerations and decelerations are intense, as evidenced by spikes on both sides at 0

acceleration values in the middle of the graph. This figure shows the acceleration of the Human Driver Behaviour Model with the 40 Km/h desired velocities. The acceleration curves started at the highest levels because vehicles try to reach the desired velocity quickly as described by the Equation 5.1. Later, the acceleration decreases because of the rise in the velocity. When the velocity reaches the desired velocity, the accelerations become low to automatically maintain the speed.

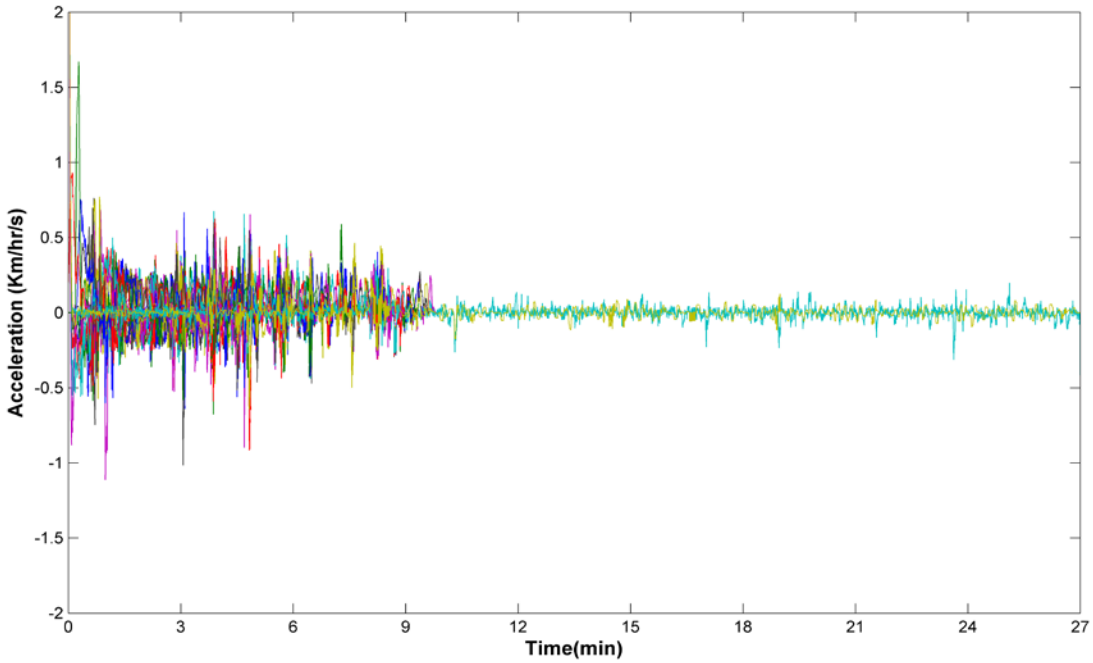

Figure 5-7: Acceleration of the Human Driver Behaviour Model with 40 Km/hr desired velocity scenario

The main reason for solving is the capacity, where the rate of the approach capacity to maximum capacity is 0.369 and where the congestion has time to be absorbed through the unoccupied area of the highway. Regarding (Table E-1), the traffic flow rate and approach capacity to maximum capacity rate are almost similar. A common vehicle velocity is higher than the desired velocity 20 km/hr scenario, but is still in the low vehicle common velocity. That leads to a reduction of the number of vehicles approaching and accumulating in the congestion zone. During no stationary startup (+0 Km/hr) and regarding Equation (5-1), that acceleration will be low, and that will cause the delay of congestion fully solving until minute 9.6 minute, as can be seen in Figure 5-6, Figure 5-7 and Figure 5-8.

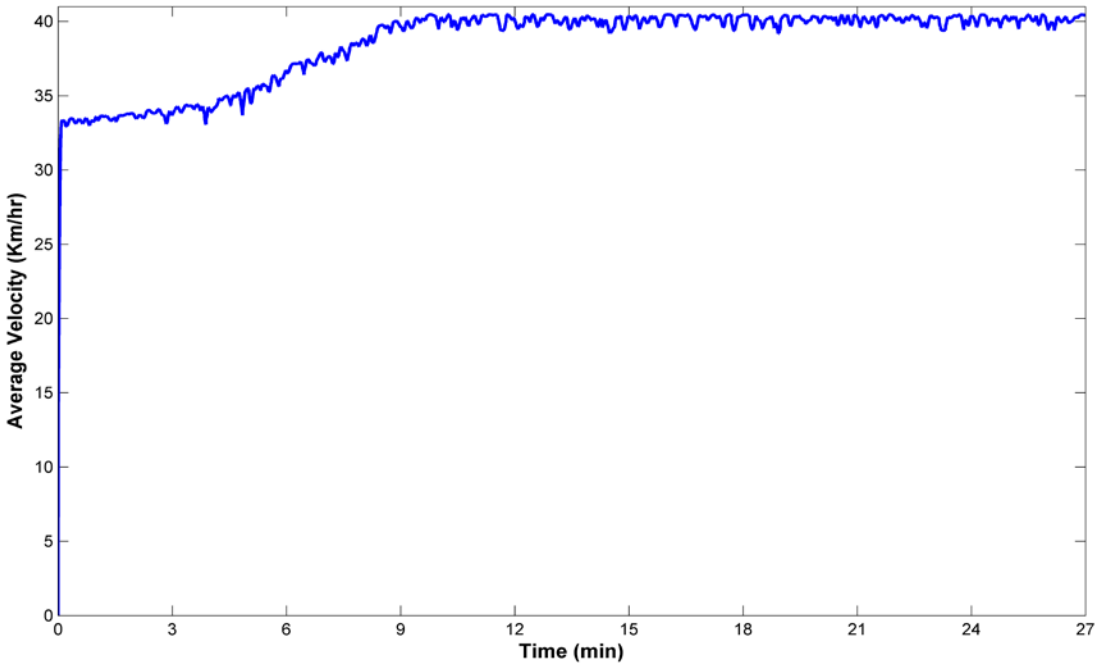

Figure 5-8: Average velocity of human driver behaviour model with 40 Km/hr desired velocity scenario

5.2.3. V_{des} is 60 km/hr

Figure 5-9 shows the traffic flow for the Human Driver Behaviour Model with the 60 Km/hr desired velocity scenario. In general, it is clear that the congestion is solved in the 5.8th minute of the approach. Similar to the scenarios of the 20 Km/hr and 40 Km/hr desired velocity, the congestion is sharp and clear in the first minute, but after that time, the congestion starts to solve as a because of the difference between congestion's input and output traffic flow. For example, the first vehicle going in is impacted by the congestion that, during the initial phase, took more than 3.6 seconds in the model. But, at the same time, there are 33% of the vehicles left in the congestion zone. Moreover, similar to the 40 Km/hr desired velocity, in 24 seconds, all the vehicles in the congestion during the initial time are left the congestion zone, and no vehicles enter the congestion zone.

Figure 5-9 illustrates human driver behaviour at 60 km/h desired velocity. As explained in Figures 5-1 and 5-5, the congestion here is short-lived. At position 5,400 m and zero time, we can see that the positions of the vehicles (each represented by an approximately 45-degree line) do not change or change very little.

The continuum of each line indicates a steady shift in the position of each vehicle. The dark area represents congestion since practically the velocity of vehicles unchanged for a period of time. It can be seen that congestion is dissolved after a period of time. The lead vehicle makes a steady shift in its position without delay to be followed by others. The severity of the congestion is represented by the magnitudes of dark areas. This explanation is valid for the similar remaining figures in this chapter.

$$\dot{v}_n(X_{rel}, v_n, \Delta v_n) = a\left[1 - \left(\frac{v_n}{v_{des}}\right)^{\delta} - \left(\frac{\mathrm{X}_{des}(v_n, v_{rel})}{X_{rel}}\right)^2\right] \qquad (5\text{-}2)$$

Figure 5-10 illustrates the velocity of the Human Driver Behaviour Model with the 60 Km/h desired velocities. It is clear that in the first 24 seconds, the congestion is taking place. The number of vehicles stuck in the congestion zone is reduced, similar to the 40 Km/h desired velocity scenario. The difference between 40 Km/h and 60 Km/h desired velocity scenarios is the relation between the velocity (v), desired velocity (V_{des}), bumper-to-bumper gab (x_{rel}) and desired bumper-to-bumper gab (x_{des}) as described in Equation (5-2). This figure shows that velocity of each vehicle is relatively steady up to 35 km/h. Between 35 and 48 km velocity profiles change erratically to attain steady velocity. However, after 48 km/h, the speed smoothly increases to 60 km/h. At 60km/h, minor adjustments in the velocity of each vehicle can be seen. Figure 5-12 shows the average velocity of vehicle cluster. The cluster velocity increases over time until it reaches the desired velocity in 5.8 minutes.

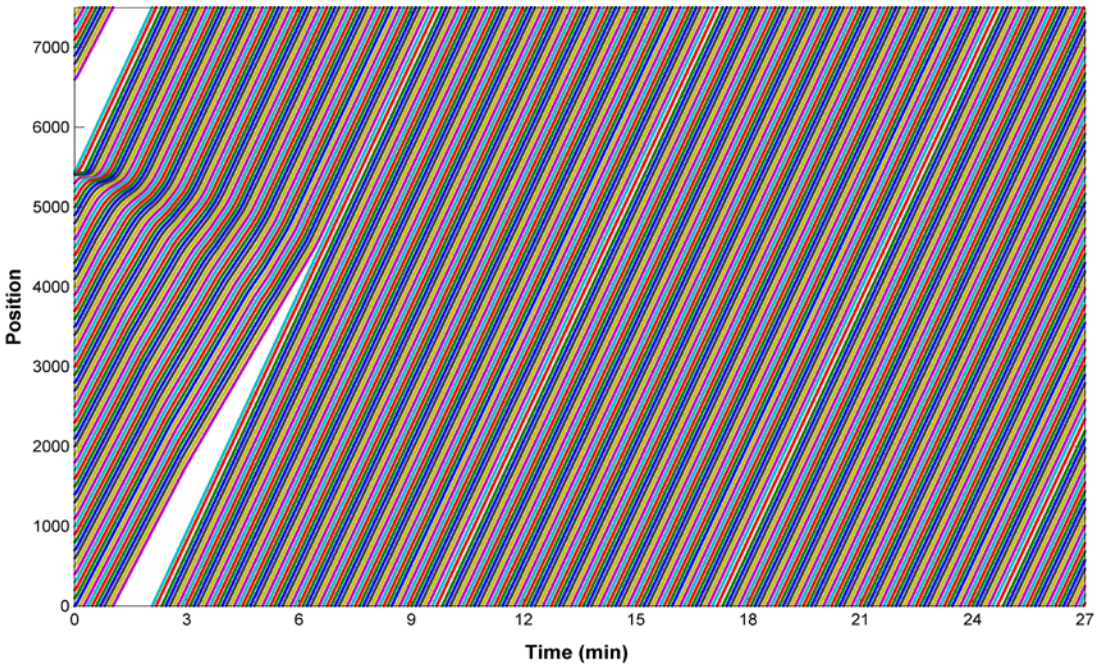

Figure 5-9: Traffic flow of Human Driver Behaviour Model with 60 Km/hr desired velocity scenario

Similar to Figure 5-3 and Figure 5-7, Figure 5-11 shows acceleration profile when human model is used at 60 Km/h desired velocities. Continuous accelerations and decelerations are taking place to achieve the desired speed. In many cases, these accelerations and decelerations are severe, as evidenced by spikes on both sides at 0 acceleration levels that can be seen in the middle of the graph. It can be seen that acceleration curves starts at the highest rate to reach the desired velocity as in Equation (5-1) and (5-2). Later, the acceleration decreases because of a rise in the velocity. The deceleration is lower than acceleration because v_{des} and x_{rel} are normally more than v and x_{des}. After the vehicle velocity reaches the desired velocity, the acceleration profile is at its lowest level.

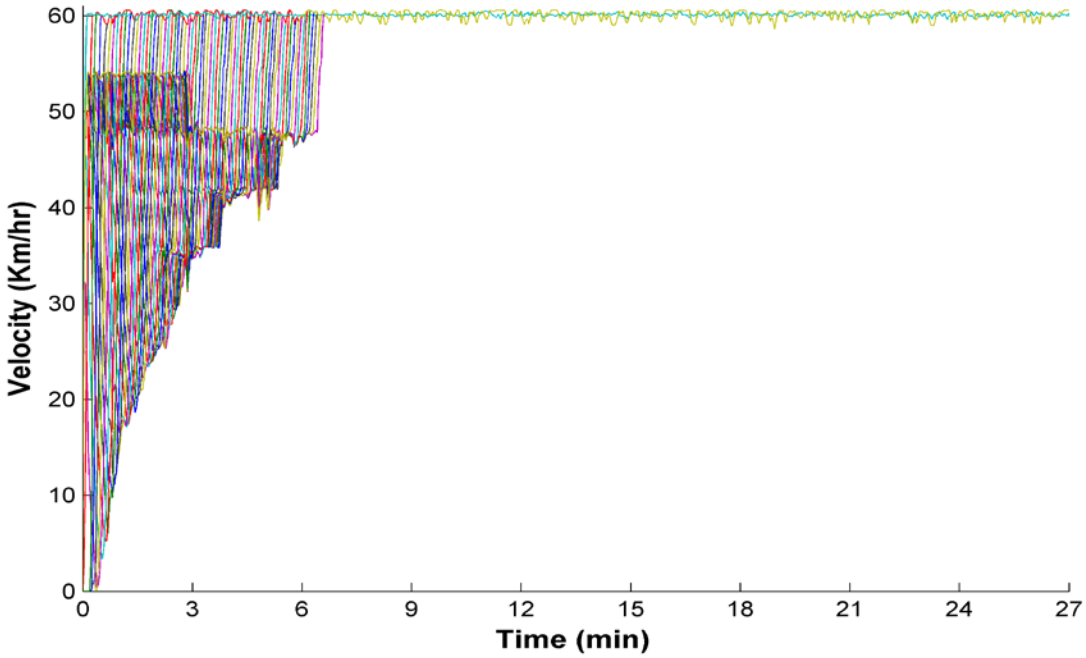

Figure 5-10: Velocity of Human Driver Behaviour Model with 60 Km/hr desired velocity scenario

There are many reasons to alleviate congestion, has been initiated, faster than 20 Km/hr and 40 Km/hr desired velocity scenarios. Capacity is one of the reasons, where the rate of the approach capacity to maximum capacity is 0.52. Similar to previous scenarios the congestion has time to be absorbed throughout the unoccupied area in the highway. In this scenario and according to (Table E-1), the traffic flow rate and approach capacity to maximum capacity rate are almost similar. In this scenario, a common vehicle velocity is higher than previous scenarios; still vehicle common velocity is accepted to reduce the number of vehicles that approach the congestion zone and accumulate on it. During no stationary startup (+0 Km/hr) and regarding Equation (2-8), the acceleration will be accepted, and that makes the congestion fully solve earlier than previous scenario's 10th minute, as be seen in Figure 5-10, Figure 5-11and Figure 5-12.

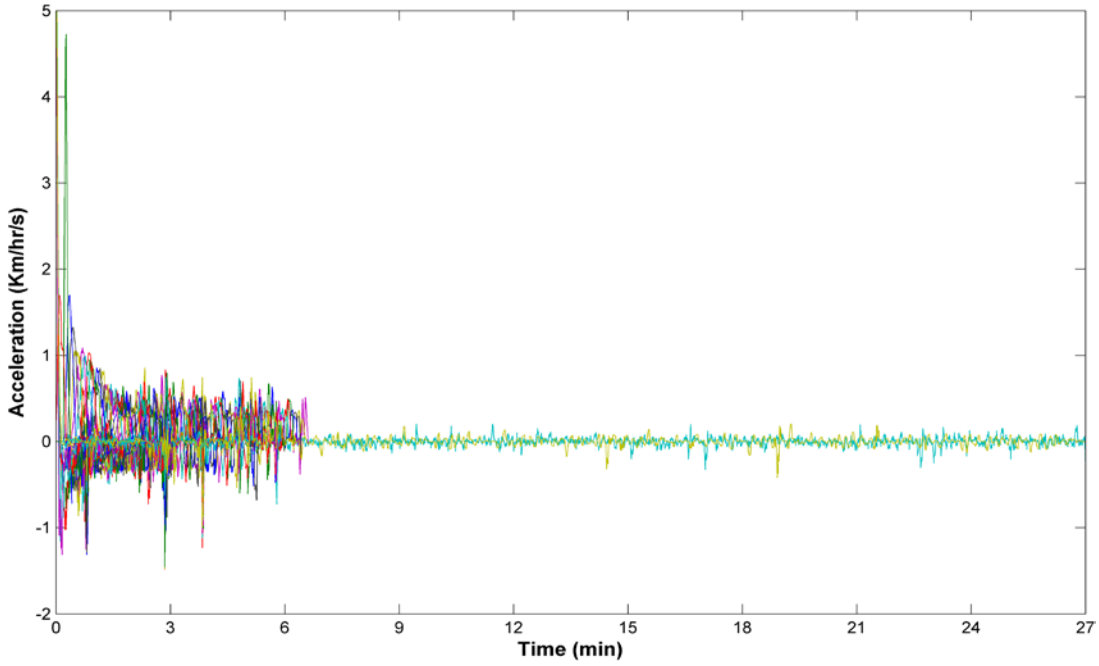

Figure 5-11: Acceleration of Human Driver Behaviour Model with 60 Km/hr desired velocity scenario

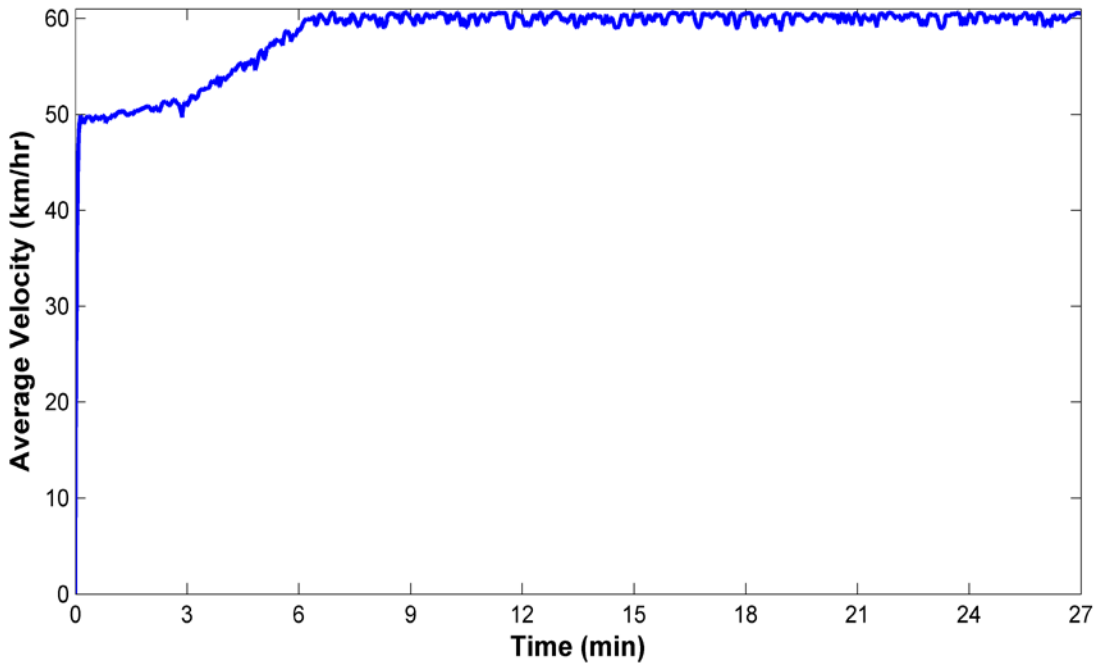

Figure 5-12: Average velocity of Human Driver Behaviour Model with 60 Km/hr desired velocity scenario

5.2.4. V_{des} is 80 km/hr

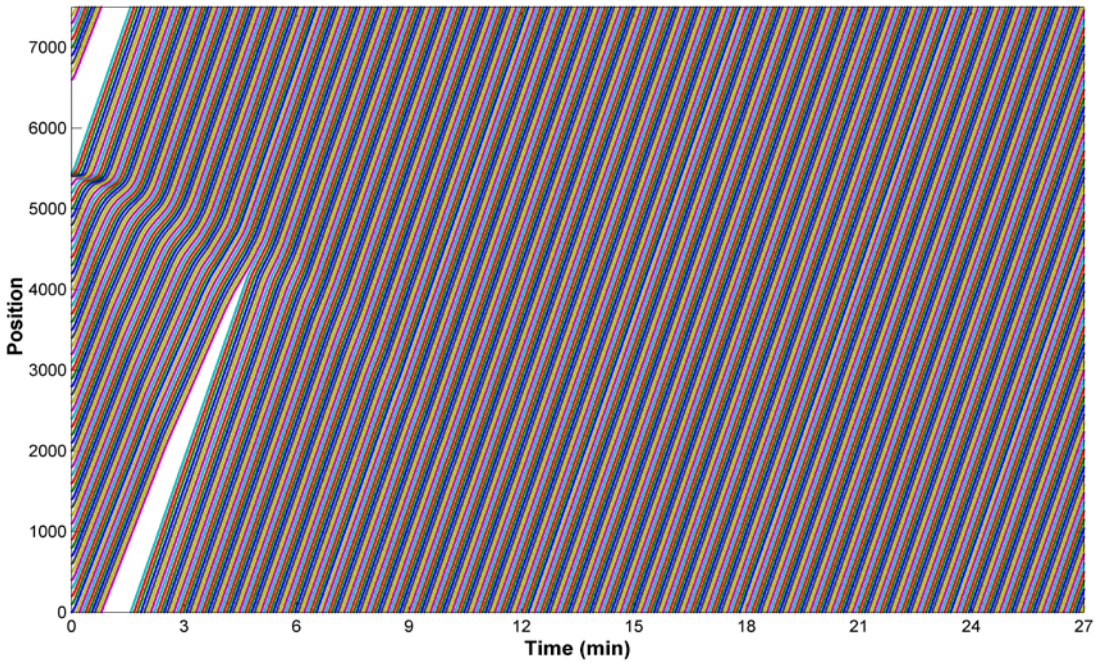

Figure 5-13: Traffic flow of Human Driver Behaviour Model with 80 Km/hr desired velocity scenario

Figure 5-13 shows the traffic flow for the Human Driver Behaviour Model with the 80 Km/hr desired velocity scenario. In general, it is clear that the congestion is solved to in the 10.73rd minute of the approach. Similar to previous scenarios, the congestion is sharp and clear in the first minute, but after that time, the congestion starts to solve as a because of the difference between congestion's input and output's traffic flow. For example, similar to 60 Km/hr desired velocity scenario, the first vehicle going in is impacted by the congestion that during the initial phase of the model took more than 3.6 seconds. But simultaneously, there are 33% of the vehicles left the congestion zone. Moreover, similar to the 40 Km/hr and 60 Km/hr desired velocity scenarios, in 24 seconds, all the vehicles held in congestion during the initial time are left the congestion zone. Only one vehicle enters the congestion zone.

Figure 5-13 shows human driver behaviour in the 80 km/h desired velocity. Similar to Figure 5-1, the congestion in Figure 5-13 is short-lived. At position 5,400 m and zero time, we can see that the positions of the vehicles following each other (each represented by an approximately 45-degree line) do not change or change very little. The continuum of each line indicates a steady shift in the position of each vehicle.

Congestion is overcome after a period of time. The vehicles starting at the second minute makes a steady shift in their position without delaying the vehicles following them.

Figure 5-14 illustrates the velocity of the Human Driver Behaviour Model at 80 Km/h desired velocities. Similar to the 40 Km/h and 60 Km/h desired velocity scenarios, it is clear that in 24 seconds, there are a few vehicles at 0 Km/h. The number of vehicles stuck in the congestion zone is gradually reduced as in the case of 60 Km/h desired velocity scenario. The similarity between the 60 Km/h and the 80 Km/h desired velocity scenarios can explained in the Equation (5-2). Around 73 km/h, the congestion starts dissolving. This figure shows that velocities of each vehicle are relatively steady up to 48 km/hr. Between 48 and 72 km, there is an erratic attempt to attain a steady speed. However, after 72 km/h, the speed increases gradually to 80 km/h. At 80 km/h, minor adjustments in the speed of each vehicle can be seen. Figure 5-16 shows the average velocities of the cluster. The cluster velocity after the initial phase jumps to 67 Km/h, and the cluster velocity increases over time until it approached the desired velocity at 10.73 minutes

Figure 5-15 shows acceleration attempts when human model is used at 80 Km/h desired velocities. It can be seen that continuous accelerations and decelerations are taking place to achieve the desired speed. These accelerations and decelerations are severe, as evidenced by spikes on both sides at 0 acceleration values in the middle of the graph. Figure shows that the acceleration stars with the highest rate in order to reach the desired velocity described by in equations (5-1) and (5-2). Later, the intensity of acceleration decreases because of the increase in the velocity. The negative acceleration (deceleration) is lower than positive acceleration because V_{des} and x_{rel} are normally more than v and x_{des}. When the desired velocity is reached the acceleration profile assumes low acceleration range.

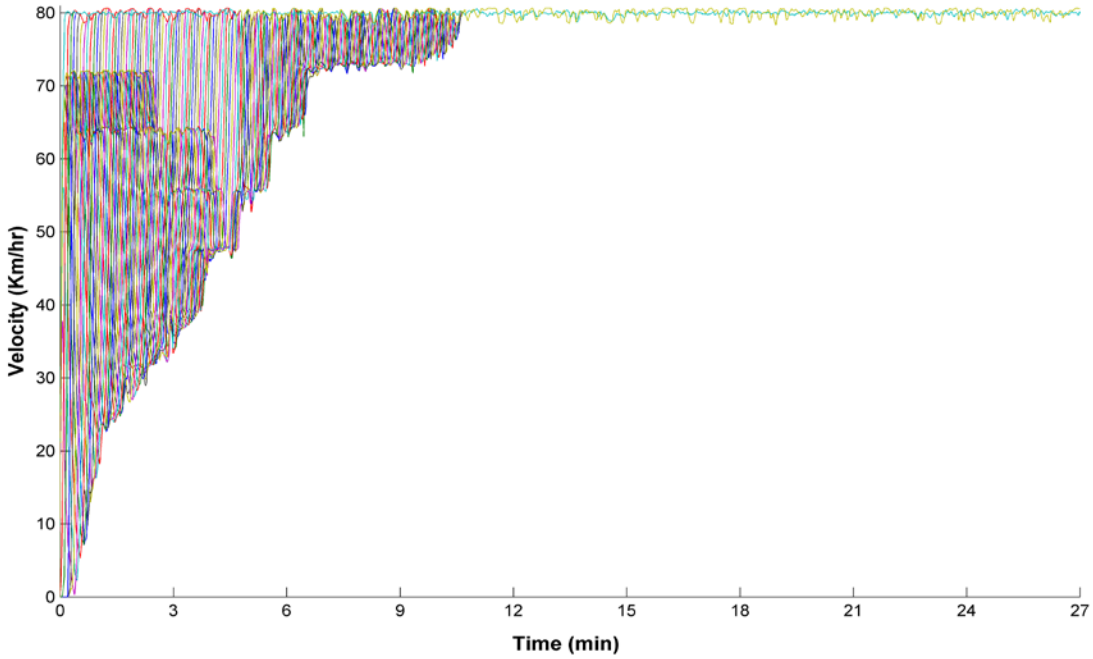

Figure 5-14: Velocity of Human Driver Behaviour Model with 80 Km/hr desired velocity scenario

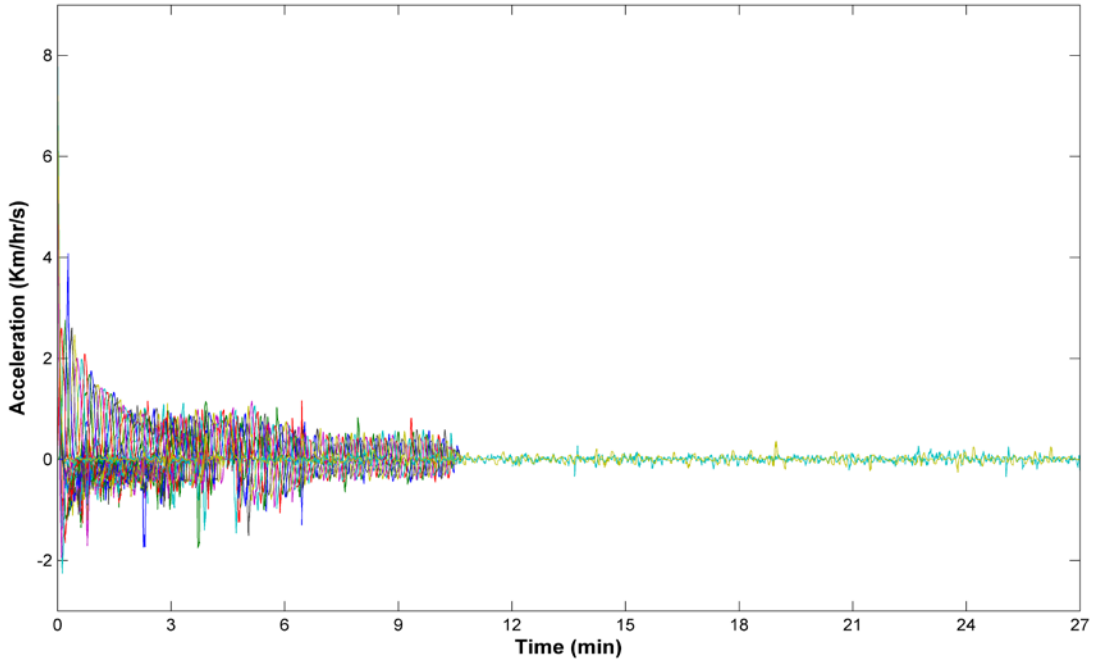

Figure 5-15: Acceleration of Human Driver Behaviour Model with 80 Km/hr desired velocity scenario

The congestion in this scenario need more time to solve than the 40 Km/hr and 60 Km/hr desired velocity scenarios. The delay of solving congestion is because the common vehicle velocity in this scenario is higher than previous scenarios, which

makes the vehicles approach the congestion earlier than in previous scenarios. During no stationary startup (+0 Km/hr) and regarding Equation (2-8), the acceleration is sufficient to make the congestion fully solve early in the 11th minute, as seen in Figure 5-14, Figure 5-15 and Figure 5-16. In this scenario, the rate of the approach capacity to maximum capacity is 0.66, where the congestion has time to be absorbed through an unoccupied area in the highway. In this scenario and according to (Table E-1), the traffic flow rate and approach capacity to maximum capacity rate are almost similar.

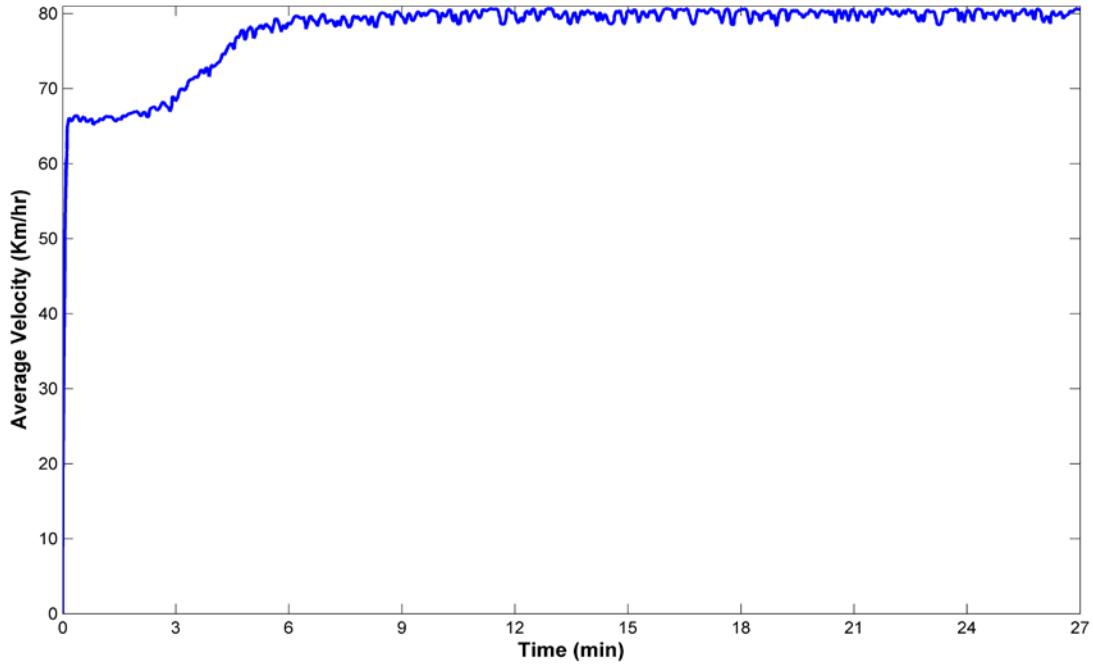

Figure 5-16: Average velocity of Human Driver Behaviour Model with 80 Km/hr desired velocity scenario

5.2.5. V_{des} is 100 km/hr

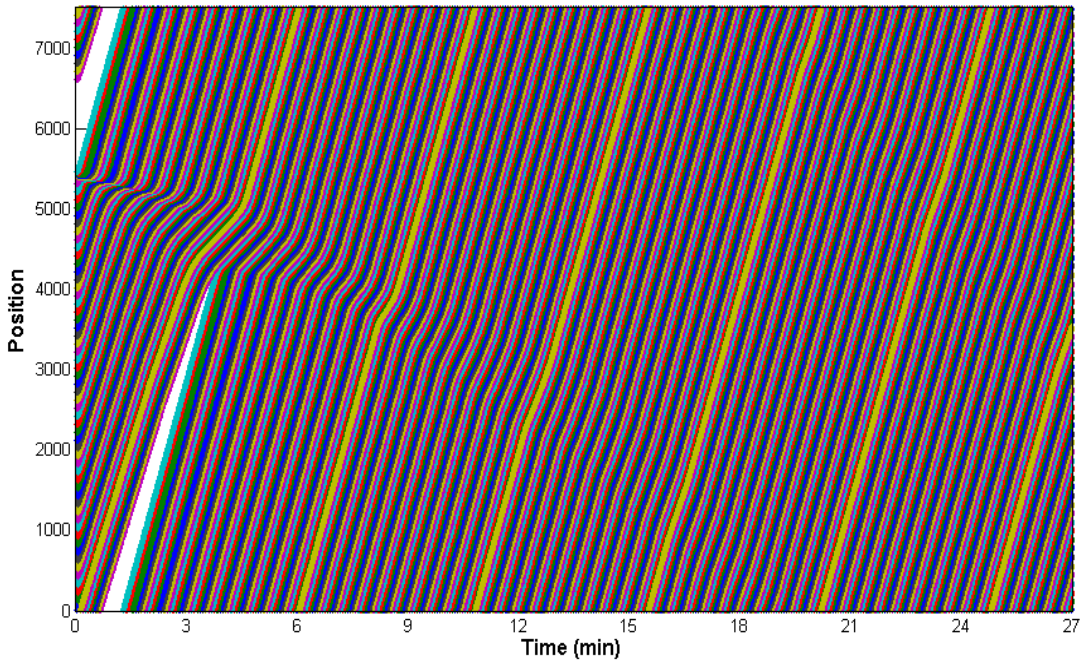

Figure 5-17: Traffic flow of Human Driver Behaviour model with 100 Km/hr desired velocity scenario

Figure 5-17 shows the traffic flow for the Human Driver Behaviour Model with 100 Km/h desired velocities. In this figure it appears that the congestion is dissolved but the congestion is persistent. Similar to the previous scenarios, the congestion is sharp and strong at 1.5th minute, but after that time, the congestion starts to dissolve when the number of vehicles arriving the congestion zone is less that those leaving. For example, it takes more than 2.4 seconds for the first vehicle going affected by the congestion at the initial phase. About 33% of the vehicles are still the congestion zone. At position 5,400 m and zero time, we can see that the positions of the vehicles (each represented by approximately 45-degree line) do not change or change very little. The continuum of each line indicates steady shift in position of each vehicle. It is clear to see that the congestion is not overcome totally during the allowed time frame.

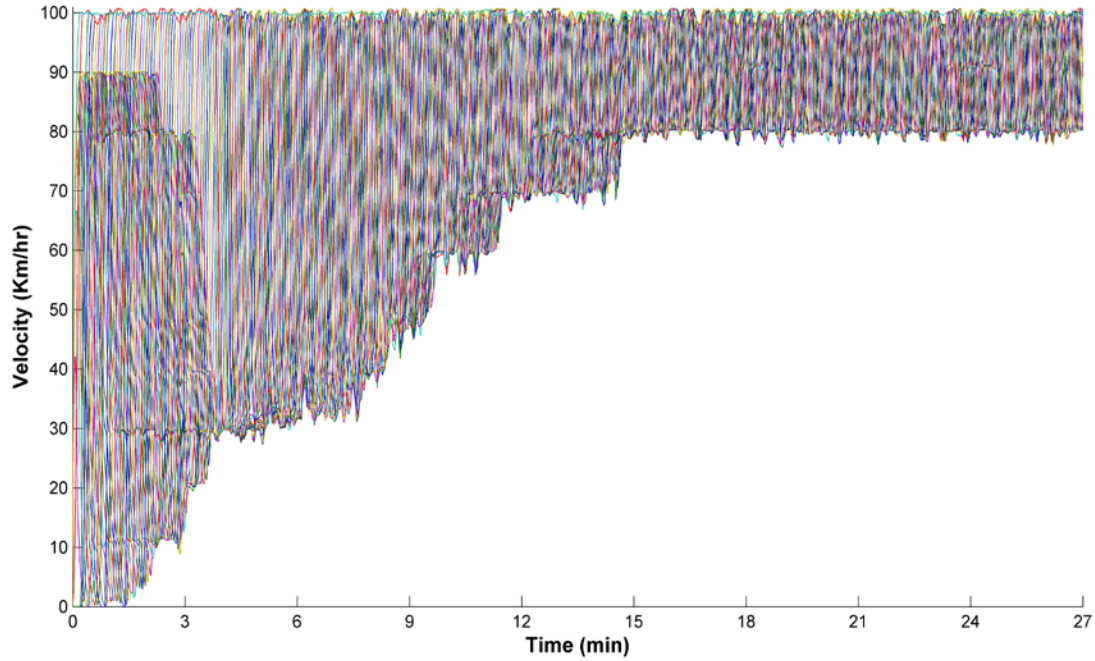

Figure 5-18: Velocity of Human Driver Behaviour Model with 100 Km/hr desired velocity scenario

Figure 5-18 illustrates the velocity of the Human Driver Behaviour Model with a 100 Km/h desired velocities. It is clear that up to the 1.5-minute mark, there are few vehicles with velocity approaching to zero as they approach to the congestion zone. After 1.5 minutes, the velocity increases up to 4th minute holding steady at 40 Km/h for about three and half minutes. Figure 5-18 shows that velocity of each vehicle relatively steady up to 30 km/h. Between 30 km/h and 80 km/h speeds, erratic attempts takes place to attain a steady speed. However, at a steady speed of 80 km/h, there is congestion, and minor adjustments in the speeds of each vehicle can be seen. Figure 5-20 displays the average velocity of the cluster. After the initial phase, the velocity jumps to about 82 Km/h, and the cluster velocity decreased until the 3rd minute, when the average velocity reaches 72 Km/h. After the 3rd minute, the average velocity increases dramatically as evidenced in Figure 5-17. Average velocity does not approach the desired velocity as a because of the flux created from the initial congestion.

Similar to previous acceleration's figures, Figure 5-19 shows the acceleration of the Human Driver Behaviour Model with the 100 Km/h desired velocities scenario. During the first 4- minutes, the acceleration curves for most of the vehicles tend to

be on the positive side. From the 4th minute to the 12th minute, the cluster profiles tend to shift more towards the negative side. The 12th minute is the beginning of when most vehicles start accelerating, showing more balance on both positive and negative sides.

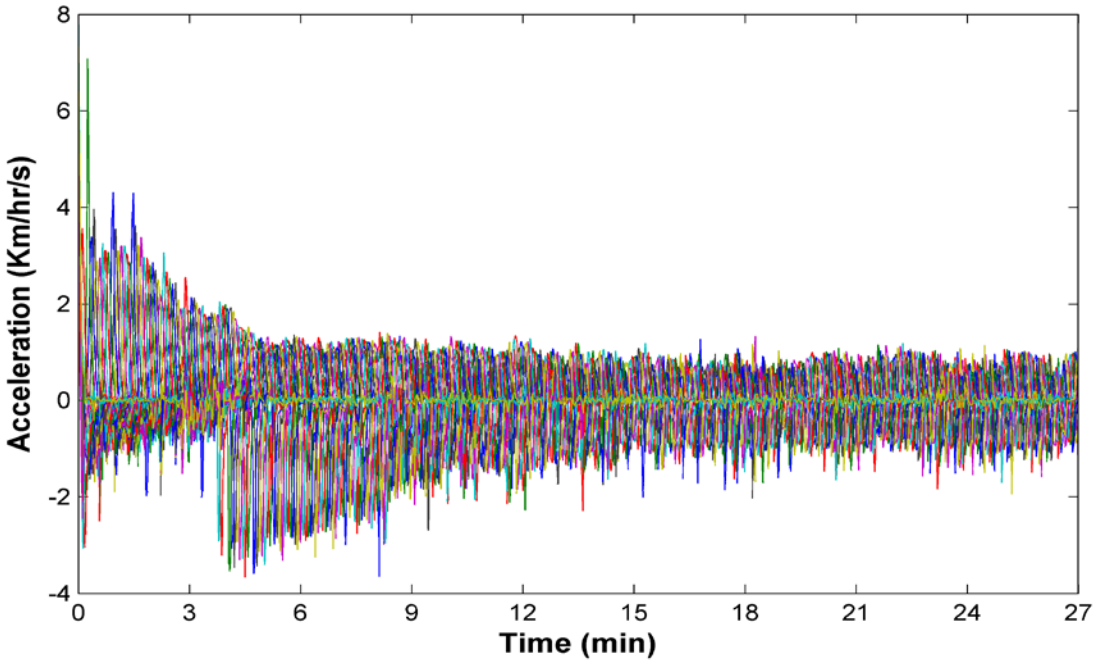

Figure 5-19: Acceleration of Human Driver Behaviour Model with 100 Km/hr desired velocity scenario

In the Human Driver Behaviour Model with 100 Km/hr desired velocity scenario, the congestion is not fully solved to because of the vehicle velocity where the vehicle can approach the congestion zone faster than in previous scenarios. The rate of the approach capacity to maximum capacity is 0.84, and the traffic flow rate to the maximum traffic flow is 0.77, according to (Table E-1). In this scenario, a common vehicle velocity is higher than in previous scenarios; a still vehicle common velocity is accepted to reduce the number of vehicles that approach the congestion zone and accumulate on it. During no stationary startup (+0 Km/hr) and regarding Equations (5-1) and (5-2), the acceleration will be accepted to solve or may be eliminated, as the congestion can be seen in Figure 5-18, Figure 5-19 and Figure 5-20. In this scenario, one may need more time to approach the fully solving congestion.

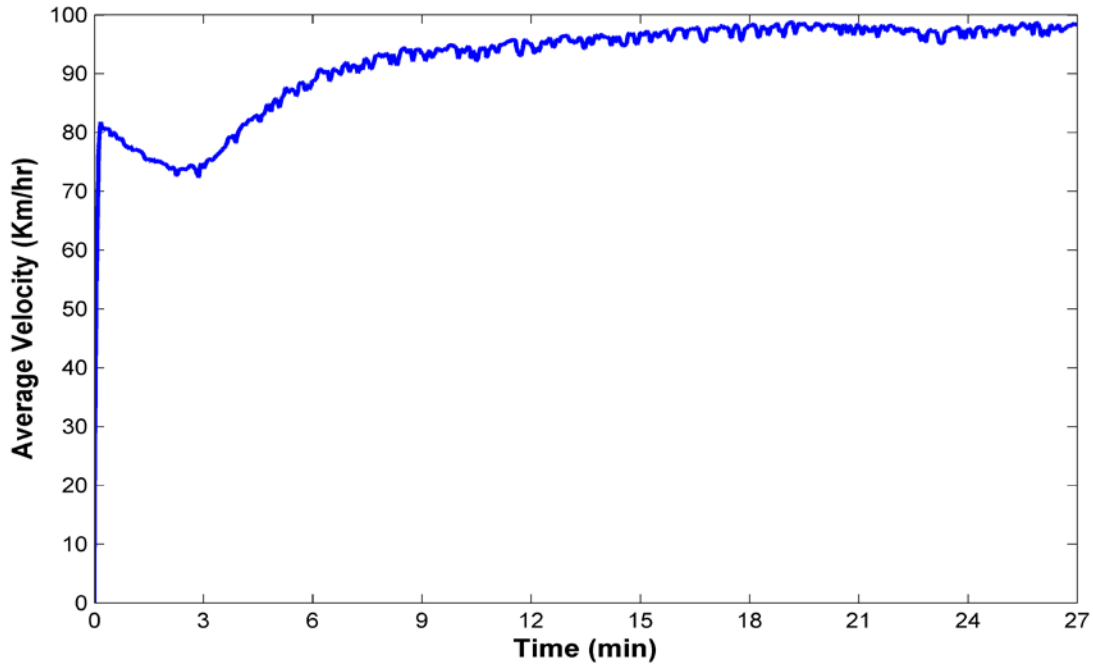

Figure 5-20: Average velocity of the Human Driver Behaviour Model with 100 Km/hr desired velocity scenario

5.2.6. V_{des} is 120 km/hr

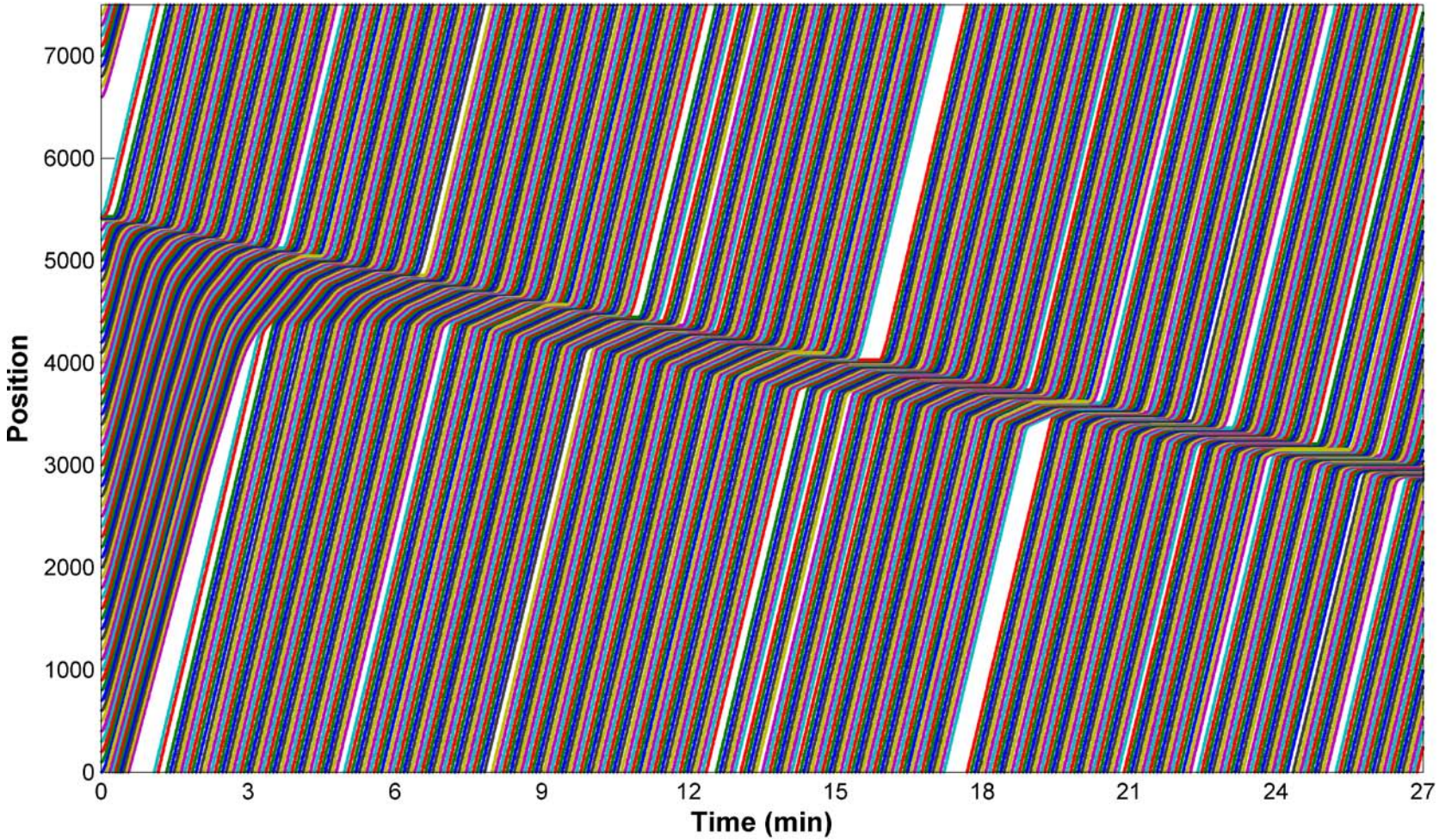

Figure 5-21: Traffic flow of Human Driver Behaviour Model with 120 Km/hr desired velocity scenario

Figure 5-21 shows the traffic flow for the Human Driver Behaviour Model with 120 Km/hr desired velocity scenario. The congestion in this scenario is different than previous scenarios (Figure 5-21) because it is not solved and the congestion is harder and thicker over time. It can be seen that, in the beginning of the approach, there is an area at the pre-congestion zone; over time, that zone reduces dramatically to disappear later on because of the difference between congestion's input and output traffic flow. For example, the first vehicle going in is impacted by the congestion that during the initial phase of the model took more than one second. But simultaneously, 33% of the vehicles are left in the congestion zone. Moreover, in 24 seconds, all the vehicles in the congestion during the initial time are left in the congestion zone, and three vehicles enter the congestion zone. With more time, the number of vehicles that left the congestion will be less than the number of vehicles going into the congestion zone.

The congestion in Figure 5-21 is much greater than the previous speed scenarios and it has not been resolved. We can see this at position 5,400 m and zero time. However, the congestion shows signs of being resolved at 27th minute, position 4,000 m. The dark area in the middle of the graph shows the duration of delays of the vehicles.

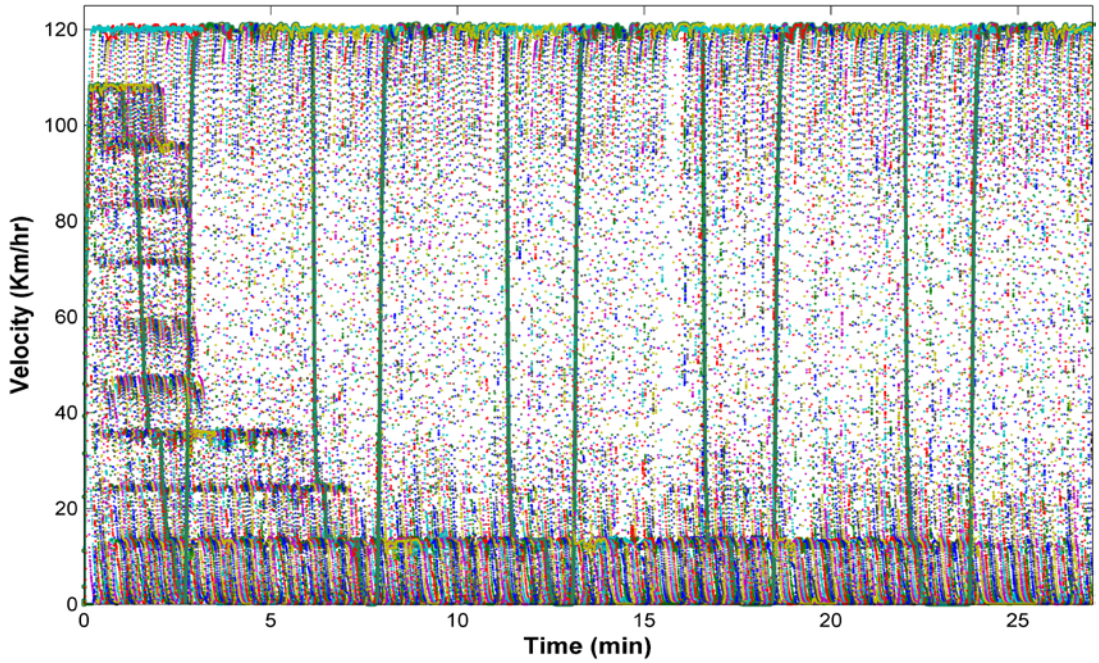

Figure 5-22: Velocity of the Human Driver Behaviour Model with 120 Km/hr desired velocity scenario

The difference is clearer in the next figures, where Figure 5-22 illustrates the velocity of the Human Driver Behaviour Model with the 120 Km/hr desired velocity scenario and shows that the vehicles velocity envelope is not changed. Nor is the upper and lower limit gap fixed and unchanging during the approach. Velocity is concentrated in this scenario, which is different than previous scenarios in which speed is reduced over time. After the initial time, the concentration of overall vehicles' velocity is distributed from the low speed (around zero Km/hr) to the desired velocity. After the 3rd minute, the velocity is separated into two parts: desired velocity and low velocity. Moreover, focusing on the green curve in Figure 5-22, the velocity curve indicates that the pre-congestion zone is reduced during the passing time. Moreover, Figure 5-24 shows that the velocity average over the cluster that the clusters' velocity after the initial phase jumped to around 97 Km/hr, and the cluster velocity decreased to be around 80 Km/hr for the remaining time of the approach. Conversely, Figure 5-23 shows the acceleration of the Human Driver Behaviour Model with a 120 Km/hr desired velocity scenario. Disregarding the peaks clarifies that the acceleration curve is the first 3-minute curve that is higher on the positive side. From the 3rd minute to the end of the approach, cluster acceleration curves biased to the negative side. During all the approaches, positive acceleration is mostly stable around 4 Km/hr/s, but the deceleration side is separated into two parts: first from the initial acceleration to the 3rd minute, when the deceleration part starts from -4 km/hr/s and declined to almost 0 Km/hr/s. The second part starts from the 3rd minute; the deceleration shows less stability around -6Km/hr/s.

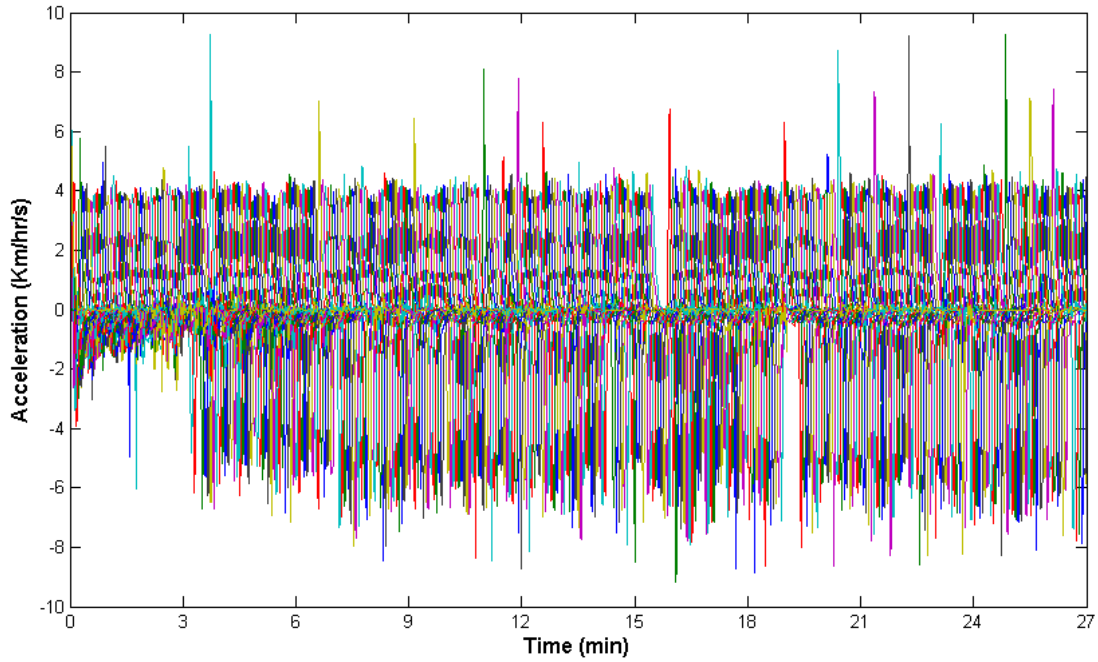

Figure 5-23: Acceleration of the Human Driver Behaviour Model with 120 Km/hr desired velocity scenario

In the Human Driver Behaviour Model with 120 Km/hr desired velocity scenario, the congestion is not solved because the vehicle velocity where the vehicle can approach the congestion zone is fast. The rate of the approach capacity to maximum capacity is 1, and the traffic flow rate to the maximum traffic flow is 0.69 according to (Table E-1). There is a serious comparison between the common vehicles' velocity scenario, which is higher than previous scenarios, that leads to an approach of the congestion zone earlier than before previous scenarios. Starting up from stationary, (+0 Km/hr) is regarded in equations (5-1) and (5-2) to observe the congestion situation, solved or not. Acceleration of starting up from congestion zone is not able to solve or eliminate the congestion. See Figure 5-21 to Figure 5-25.

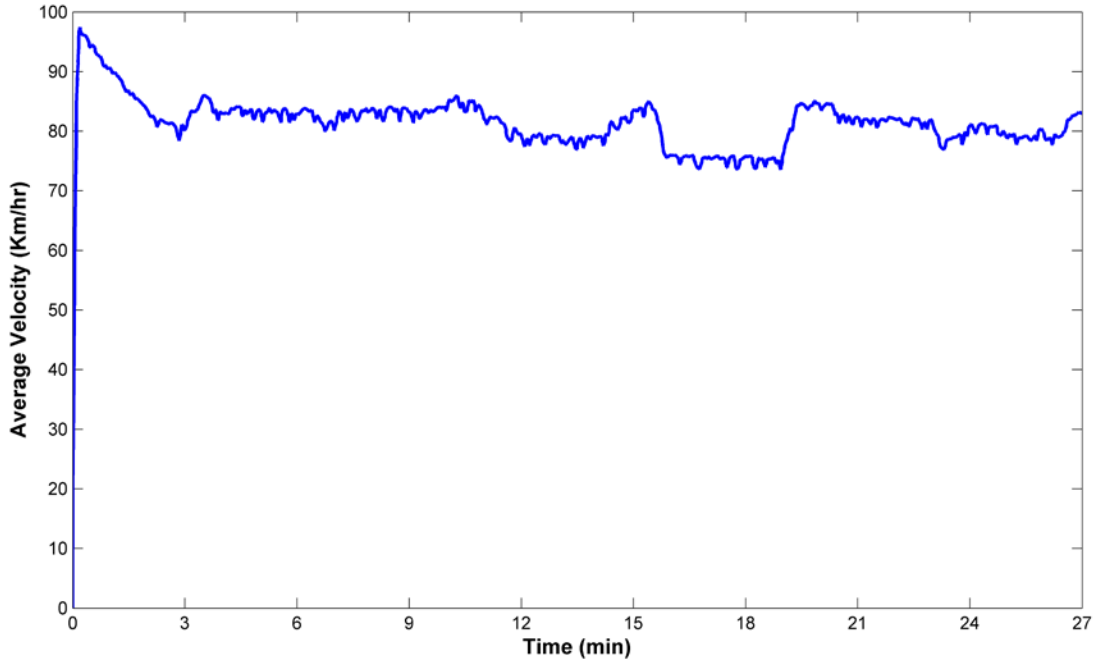

Figure 5-24: Average velocity of Human Driver Behaviour Model with 120 Km/hr desired velocity scenario

Figure 5-25 expresses vehicles' velocities available in the congestion zone. It can be seen during the initial time that up to 20% of the total vehicles in the congestion zone are less than or equal to 40 km/hr. After that, congestion vehicle velocities decrease to be less than 20 km/hr and 10 km/hr. Last, 30% of the total vehicles available in the congestion zone are travelling at less than 10 km/hr. It is obvious the vehicles with a velocity of less than 120 km/hr are increasing and that is related to the disappearance of pre-congestion zone. Over time, the member vehicles keep frozen in the congestion while other velocities start disappearing, except for the highest speed caused by the disappearing of pre-congestion.

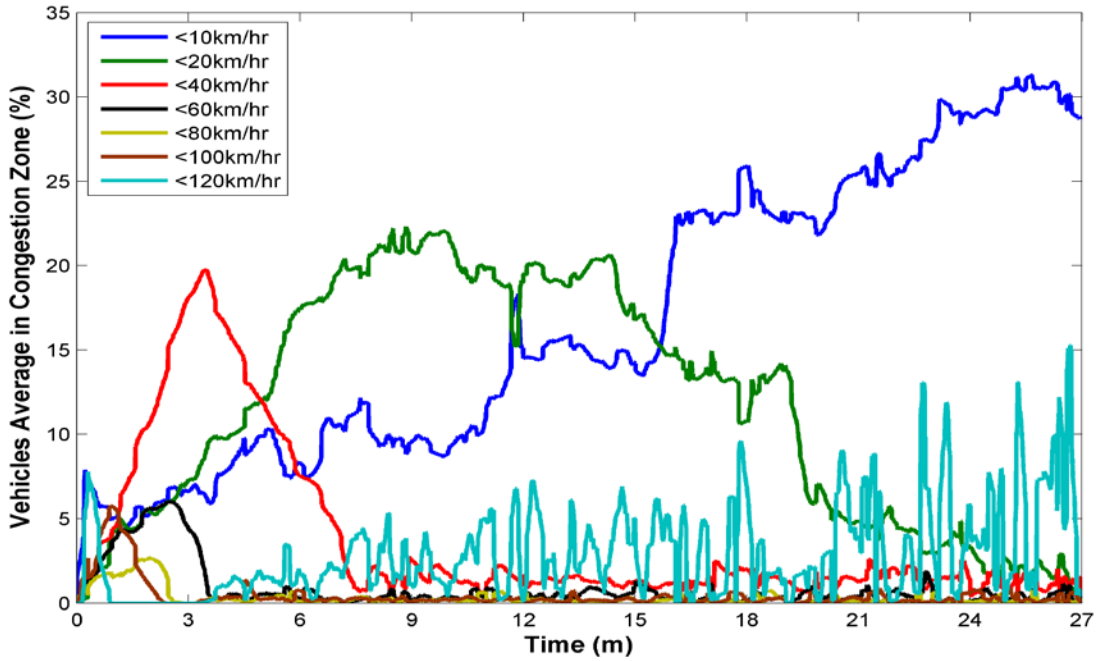

Figure 5-25: Velocity of Human Driver Behaviour Model with 120 Km/hr desired velocity scenario during the congestion zone

Figure 5-6 reveals the impact of density on velocity and traffic flow in the Human Driver Behaviour Model with 120 Km/hr desired velocity scenario. For the contraction curve of traffic flow where the density and traffic flow relationship is shown in Figure 5-26A, traffic flow is exceeding the critical point of density (ρ), where the density critical point is (0.069767, 0.31). Although the traffic flow is increasing dramatically between 0.1 and 0.2 vehicle/sec, the velocity has fallen to around 40 Km/hr, as shown in the relation between the density and velocity, as expressed in Figure 5-26B. When the density is between 0.2 and 0.4 vehicle/m, the traffic flow is matching the density critical line because of the elimination of velocity in the same period of density. However, after 0.4 vehicle/m to the critical jam point, the traffic flow contraction curve matches the density critical line with high dispersion. However, that expansion curve of traffic flow is matching 0 from 0.3 vehicle/m density to the critical jam point. From 0.1 and 0.2 vehicle/sec density, the expansion curve of traffic flow is rising gradually as a result of density pressure that eliminates velocity. Finally, the traffic flow is vividly increasing as a result of the dramatic increase of velocity with the declining of density.

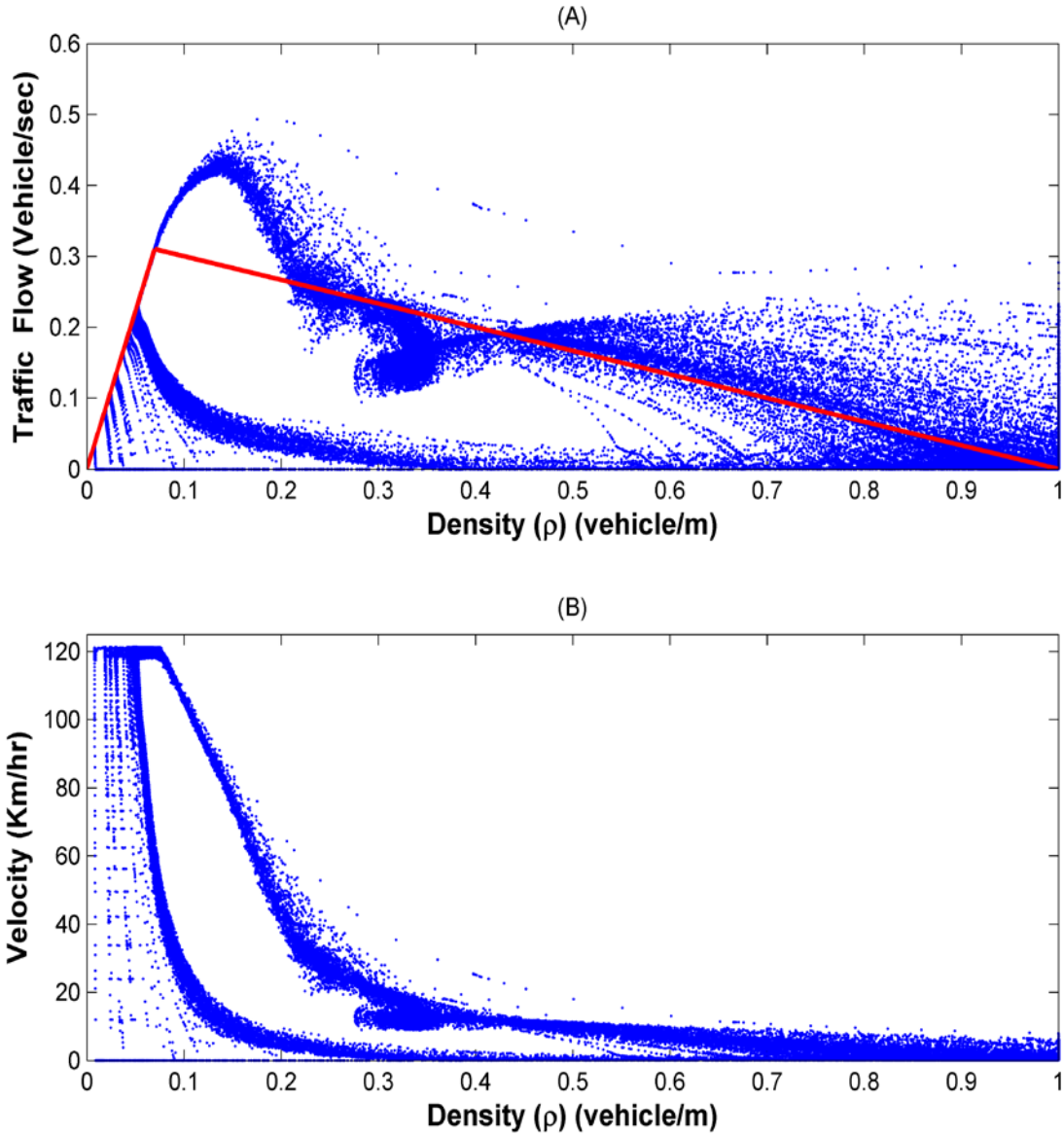

Figure 5-26: Velocity, Density and Traffic flow in Human Driver Behaviour Model with 120 Km/hr desired velocity scenario

5.2.7. V_{des} is 140km/hr

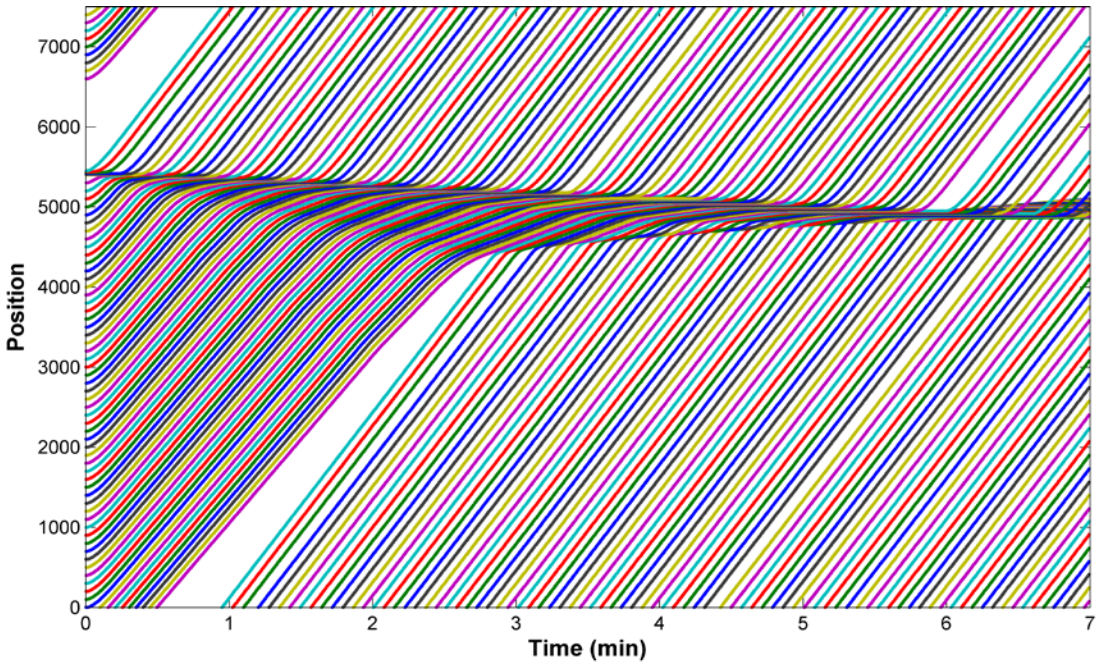

Figure 5-27: Traffic flow of Human Driver Behaviour Model with 140 Km/hr desired velocity scenario

Figure 5-27 shows the traffic flow for the Human Driver Behaviour Model with the 140 Km/hr desired velocity scenario. Regarding congestion, this scenario is unlike previous scenarios because there is a crash between vehicles. For that reason, the approach is finished in the 7th minute after the crash occurred around the 4th minute. In the initial phase, the motivation to approach the desired speed makes the vehicles accelerate more than required, but unfortunately, most of the vehicles were forced to decelerate because of the safety gap (x_{rel}). During the approach, some vehicles approached the desired velocity (V_{des}) and after some time found themselves forced to decelerate dramatically. The sudden deceleration makes the following vehicles obliged to decelerate more than the front ones. After some vehicles in the queue, one vehicle finds its deceleration insufficient to avoid an accident.

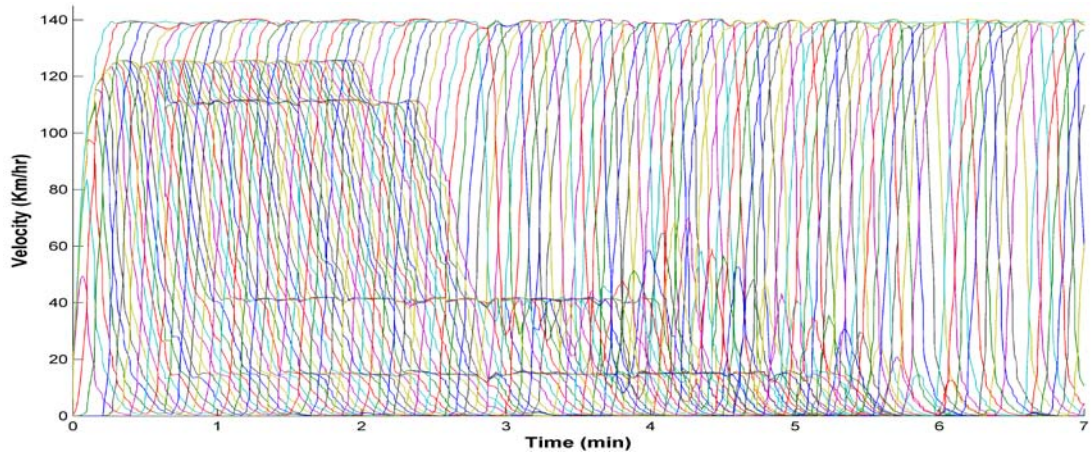

Figure 5-28: Velocity of Human Driver Behaviour Model with 140 Km/hr desired velocity scenario

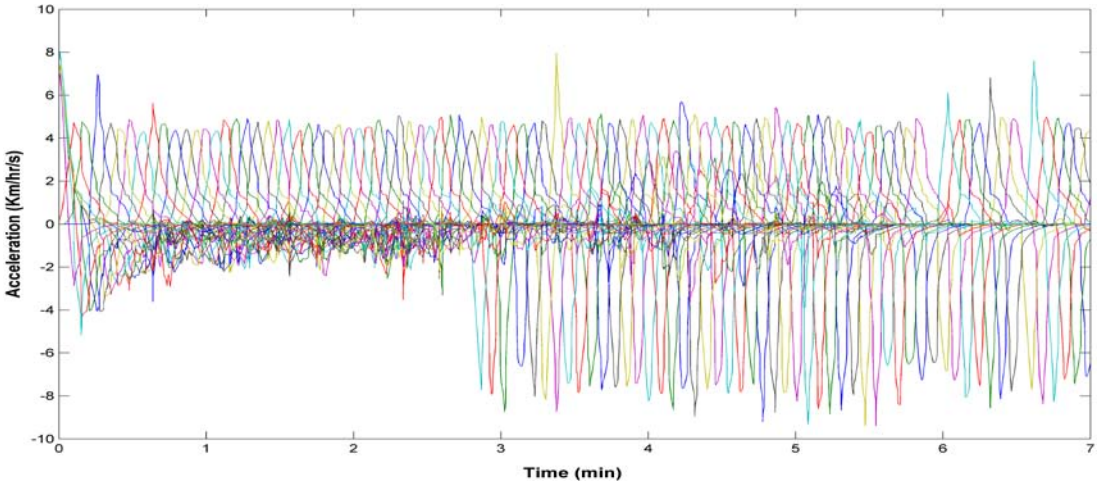

Figure 5-29: Acceleration of Human Driver Behaviour Model with 140 Km/hr desired velocity scenario

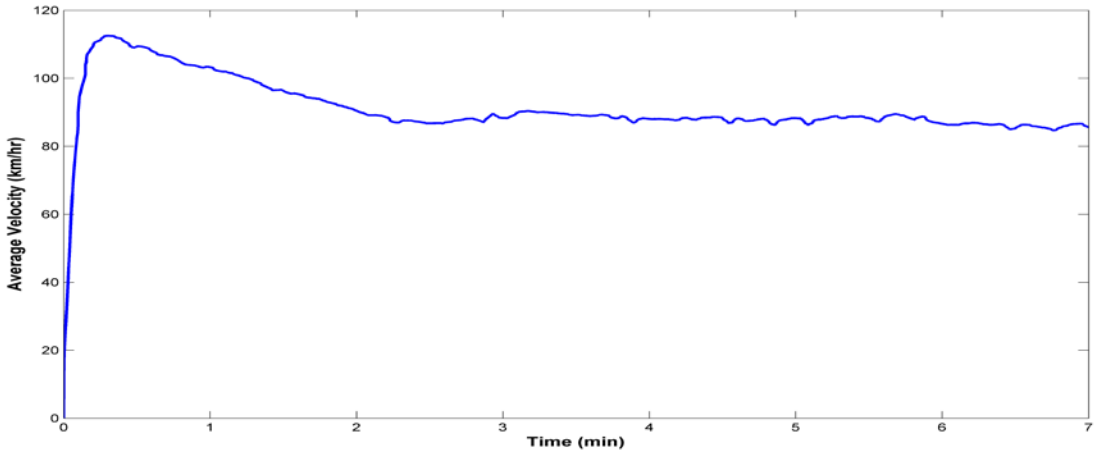

Figure 5-30: Average velocity of Human Driver Behaviour Model with 140 Km/hr desired velocity scenario

5.3. Asymmetric Auto Driving

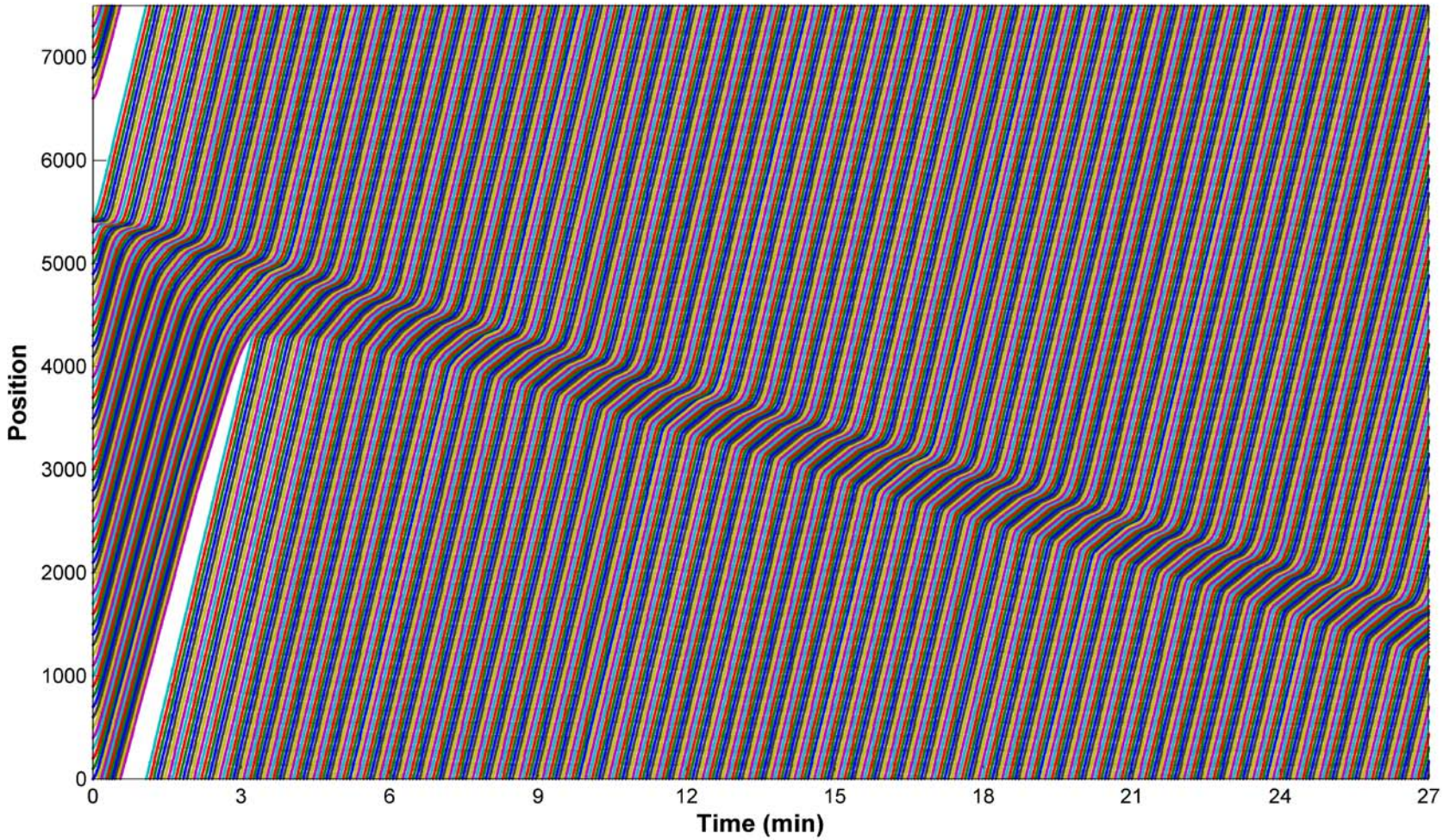

Figure 5-31: Traffic flow of Asymmetric Auto Driving Model with 120 Km/hr desired velocity scenario

Figure 5-31 shows the Asymmetric Auto Driving Model with 120 Km/hr desired velocity scenario. The congestion shape in this approach has similar thickness over time. Similar to the traffic flow of the Human Driver Behaviour Model with 120 Km/hr desired velocity scenario (Figure 5-21), it can be seen that the congestion zone position goes backward over time. The difference between both scenarios is the congestion zone moves backward more than the congestion in the Human Driver Behaviour Model with 120 Km/hr desired velocity scenario in the Figure 5-21 and Figure 5-31. However, the congestion in this scenario is different than the Human Driver Behaviour Model with 120 Km/hr desired velocity scenario in that, after the initial time, no vehicles' velocity approaches 0 in the congestion. Therefore, the congestion is not sharp, and traffic flow for all approaching member vehicles in and out of the congestion is smooth. But the congestion is not solving.

The difference is clearer in the next figures, where Figure 5-32 illustrates the velocity of the Asymmetric Auto Driving Model with 120 Km/hr desired velocity scenario and displays the vehicles' velocity envelope. After the initial time, the upper and lower limit in the vehicles' velocity envelope is fixed and unchanged during the approach where the upper limit is V_{des} and lower limit is around 10 Km/hr. Velocity concentrated in this scenario declines over time. After the initial time, the concentration of overall vehicle velocity is distributed from the low speed (around 0 Km/hr) to the desired velocity. After the 3rd minute, the velocity is separated into four parts: desired velocity, around 35 Km/hr, which disappears after 8 minutes of the experience, around 25 Km/hr and around 10 Km/hr. Moreover, Figure 5-34 displays the velocity average over the cluster; the cluster's velocity after the initial phase jumped to around 97 Km/hr, and the cluster velocity decreased to less than 90 Km/hr up to 3rd minute. For the remaining approach, the velocity is stable, around 96 Km/hr.

Conversely, Figure 5-33 shows the acceleration of the Asymmetric Auto Driving Model with 120 Km/hr desired velocity scenario. Disregarding the peaks, what clarifies the acceleration curves is that the first 3-minutes curves are higher to the positive side. From the 3rd minute to the end of the approach, the cluster acceleration curves are biased to the negative side. During the entirety of the approach, positive acceleration starts with 4 Km/hr/sand decreases to be mostly stable around 2 Km/hr/s. The deceleration side is separated into two parts. The first part is from the

initial approach to the 3rd minute, when the deceleration parts start from -4 km/hr/s and declines to almost 0 Km/hr/s. The second part starts from the 3rd minute; the deceleration, around -5 Km/hr/s.

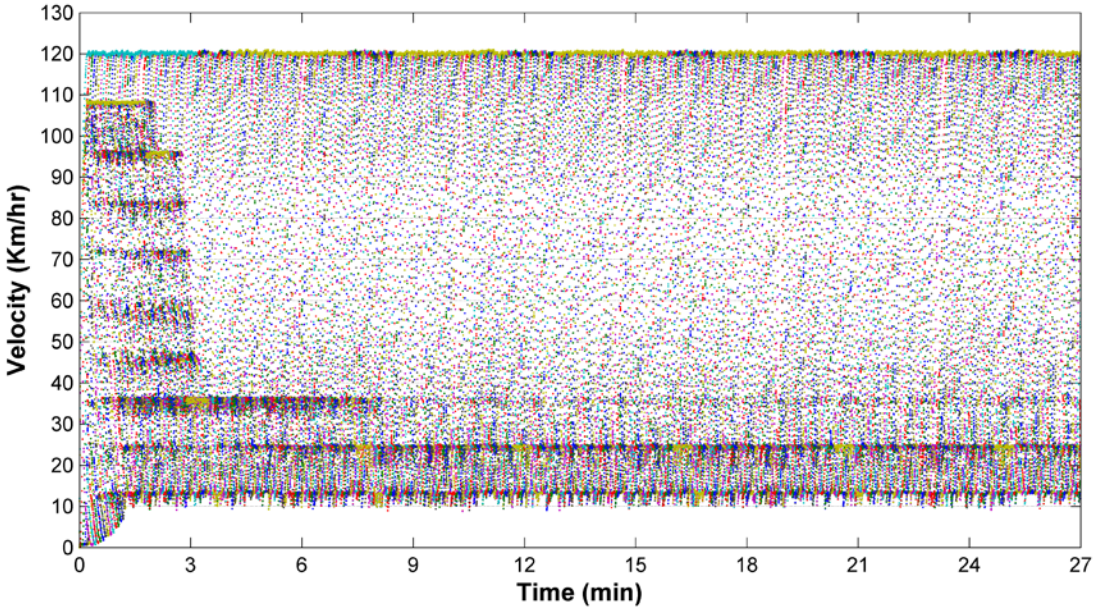

Figure 5-32: Velocity of Asymmetric Auto Driving Model with 120 Km/hr desired velocity scenario

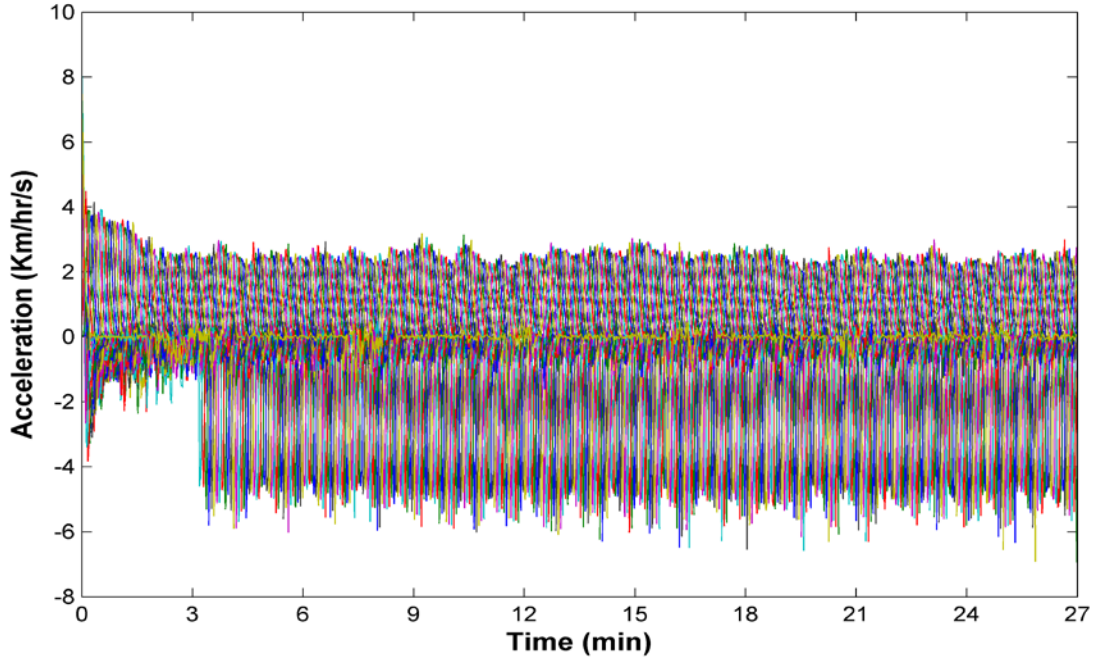

Figure 5-33: Acceleration of Asymmetric Auto Driving Model with 120 Km/hr desired velocity scenario

From Figure 5-31 and Figure 5-35, we express vehicles' velocities available in the congestion zone in the Asymmetric Auto Driving Model with the 120 Km/hr desired velocity scenario. During the initial time that almost 20% of the total vehicles, which are in the congestion zone, are less or equal to 40 km/hr, after the initial time, the congestion vehicle velocities' concentration is mostly kept as is. Almost 15% of vehicles are travelling at less than 40 km/hr, and about 6% of vehicles are moving at less than 20 km/hr. Similar to Figure 5-25, it is clear that there are vehicles that have a velocity less than 120 km/hr and are increasing over time, but less than in Figure 5-25.

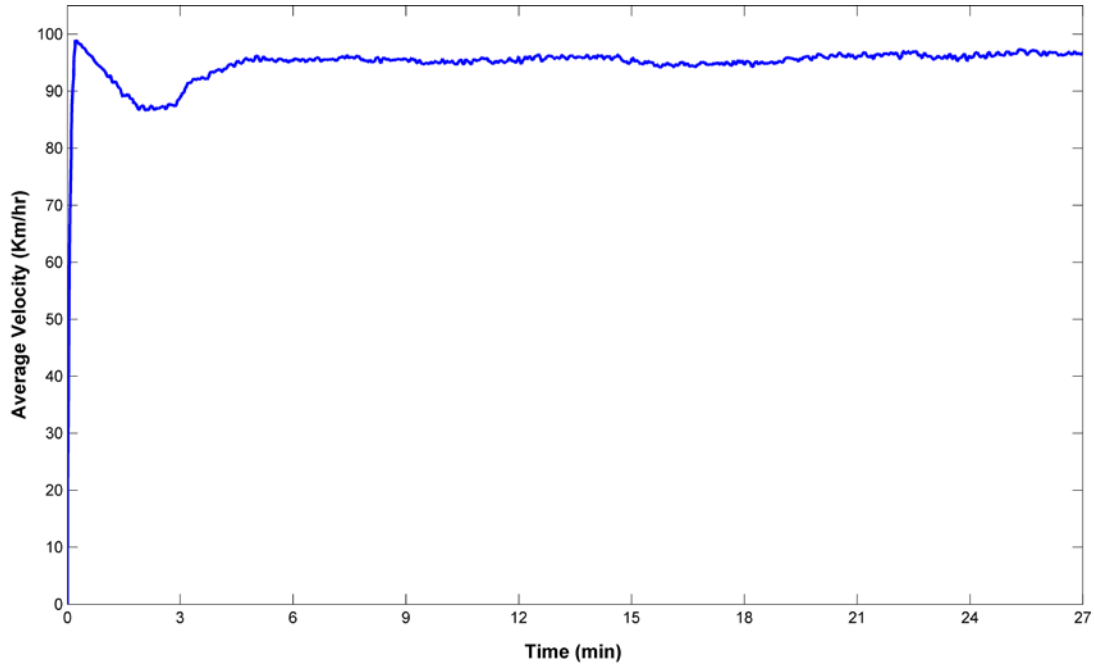

Figure 5-34: Average Velocity of Asymmetric Auto Driving Model with 120 Km/hr desired velocity scenario

The impact of density on velocity and traffic flow in the Asymmetric Auto Driving Model with 120 Km/hr desired velocity scenario has been shown in Figure 5-36. The density and traffic flow contraction curve of the traffic flow is shown in Figure 5-36A in that traffic flow is exceeding the critical point of density (ρ), where the density critical point is (0.069767, 0.31). Although the traffic flow is increasing dramatically between 0.1 and 0.2 vehicle/m, the velocity has fallen to less than 40 Km/hr, as shown in relation between the density and velocity, as expressed in Figure 5-36B. Moreover, during the range of density between 0.2 and 0.35

vehicle/m, the traffic flow is matching the density critical line because of the elimination of velocity in the same period of density.

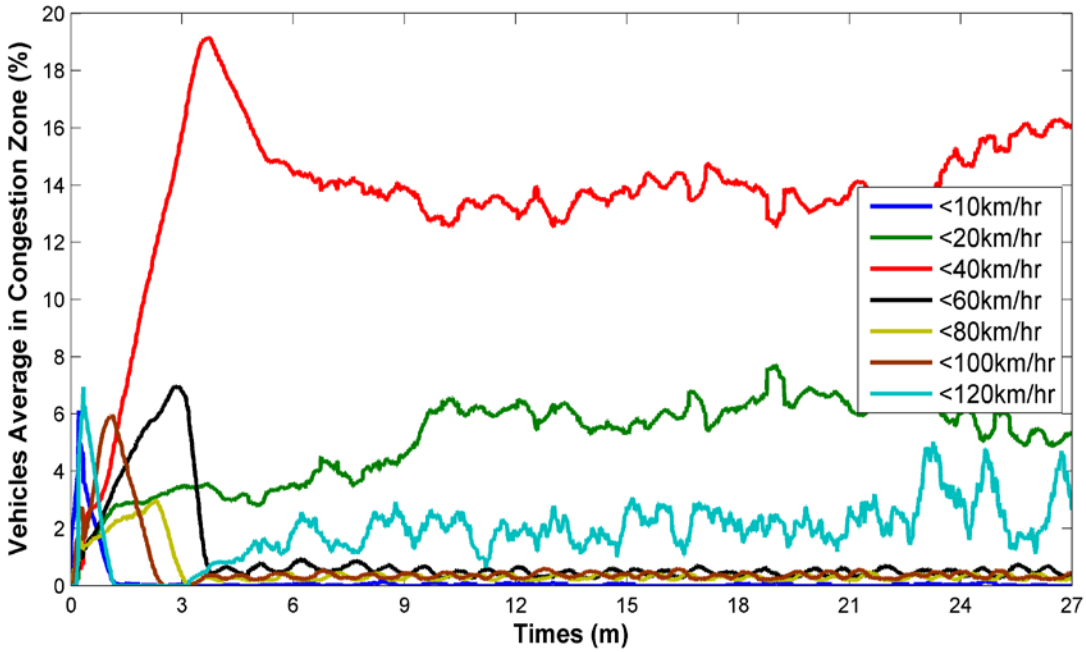

Figure 5-35: Velocity of Asymmetric Auto Driving Model with 120 Km/hr desired velocity scenario during the congestion zone

However, that expansion curve of traffic flow is starting from 0.075 vehicle/m density to 0.35 vehicle/m, which is rising gradually as the result of the pressure of the density that eliminates velocity. The traffic flow is vividly increasing because of the dramatic increase of velocity with the declining of density. The gap between contraction and expansion curves in the Asymmetric Auto Driving Model with 120 Km/hr desired velocity scenario is less than in the Human Driver Behaviour Model with 120 Km/hr desired velocity scenario.

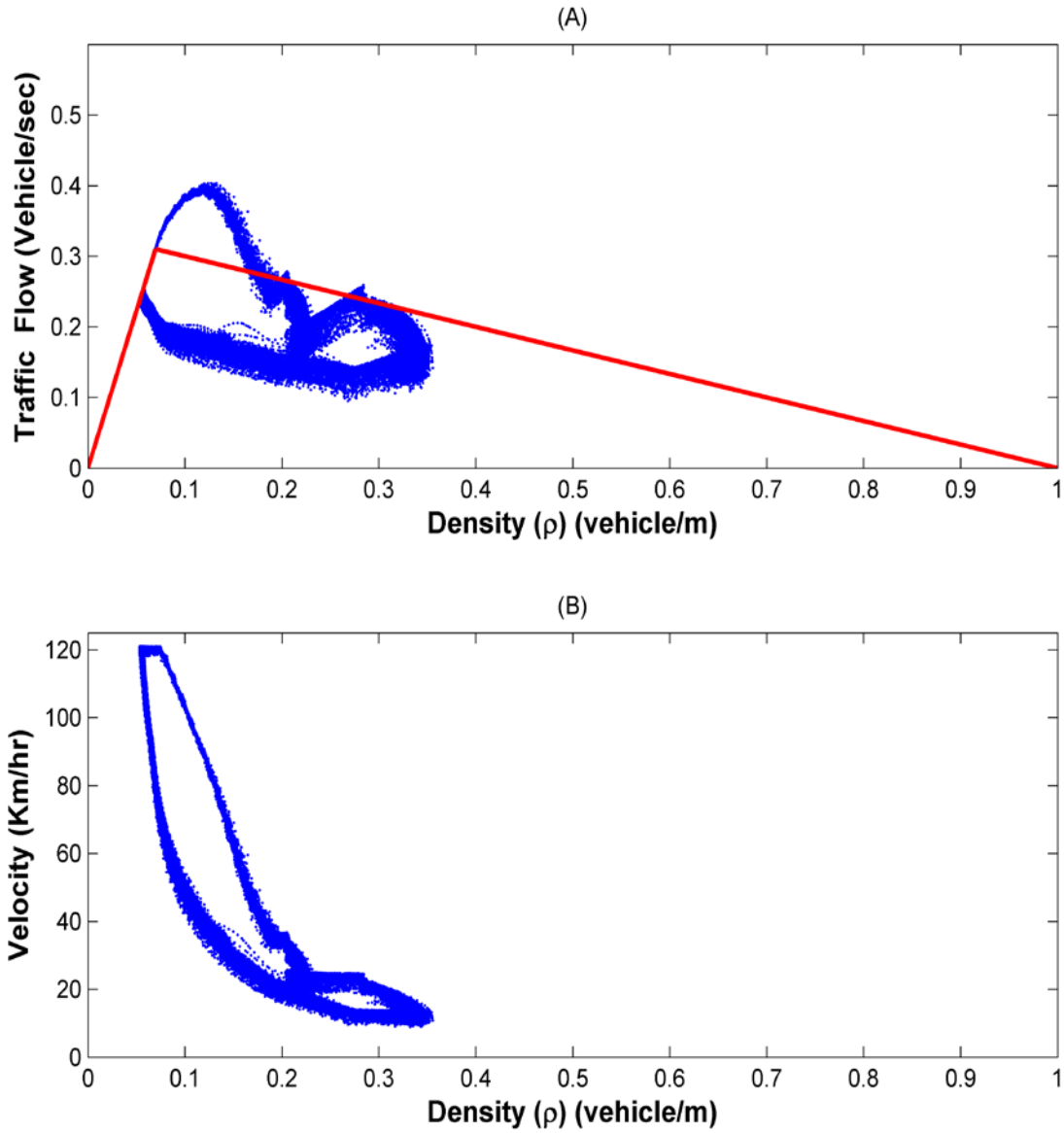

Figure 5-36: Velocity, Density and Traffic flow in Asymmetric Auto Driving Model with 120 Km/hr desired velocity scenario

5.4. Symmetric Auto Driving

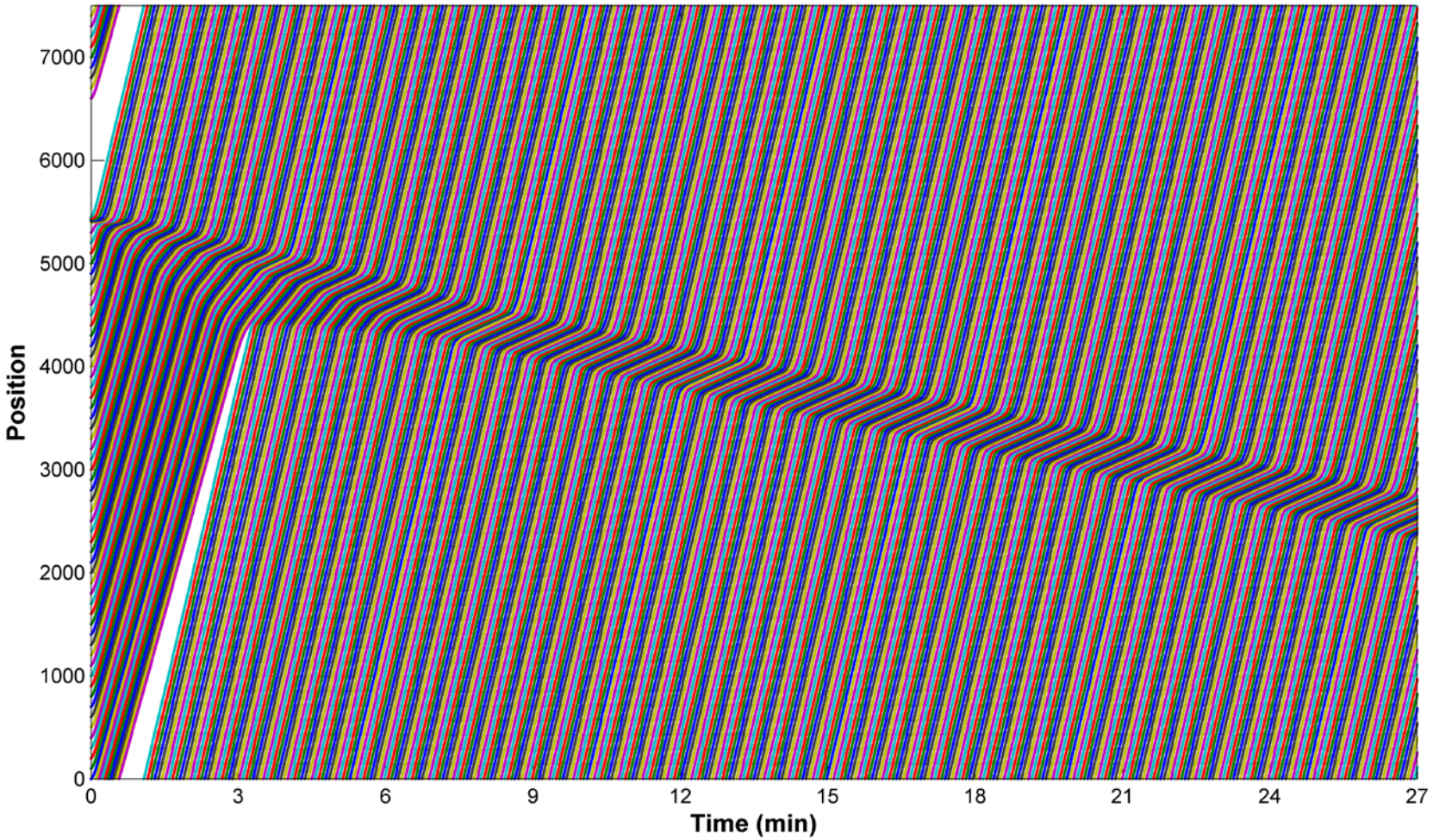

Figure 5-37: Traffic flow of Symmetric Auto Driving Model with 120 Km/hr desired velocity scenario

Figure 5-37 shows the Symmetric Auto Driving Model with 120 Km/hr desired velocity scenario. Congestion shape in this approach has similar thickness over time. Similar to the traffic flow of the Human Driver Behaviour Model with 120 Km/hr desired velocity scenario in Figure 5-21 and Asymmetric Auto Driving Model with 120 Km/hr desired velocity scenario in Figure 5-31, it can be seen that the congestion zone position goes backward over time. The difference between both scenarios, the Human Driver Behaviour Model with 120 Km/hr desired velocity scenario and the Asymmetric Auto Driving Model with 120 Km/hr desired velocity scenario, and the Symmetric Auto Driving Model with 120 Km/hr desired velocity scenario is that the congestion zone in the Symmetric Auto Driving Model with 120 Km/hr desired velocity scenario moves backward more than the congestion in the Human Driver Behaviour Model with 120 Km/hr desired velocity scenario in Figure 5-21 and less than the Asymmetric Auto Driving Model with 120 Km/hr desired velocity scenario in Figure 5-31. However, the congestion in this scenario is different than the Human Driver Behaviour Model with 120 Km/hr desired velocity scenario in that, after the initial time, no vehicles' velocity approaches 0 in the congestion. Therefore, the congestion is not sharp. The traffic flow for all approaching member vehicles in and out of the congestion is smooth, but the congestion is not solving.

Figure 5-38 illustrates the difference of the velocity of the Symmetric Auto Driving Model with the 120 Km/hr desired velocity scenario and displays the vehicles' velocity envelope. After the initial time, the upper and lower limit in vehicles' velocity envelope is fixed and unchanged during the approach where the upper limit is V_{des} and the lower limit is more than 10 Km/hr. Velocity concentrated, in this scenario, declines over time. After the initial phase, the concentration of the overall vehicle velocity is distributed from low speed (around 0 Km/hr) to the desired velocity. After the 3rd minute, the velocity is separated into three parts: 1) desired velocity, 2) around 35 Km/hr, which disappears after the 7th minute of the experience and 3) around 12 Km/hr. Moreover, Figure 5-40 shows in the velocity average over the cluster that the cluster's velocity after the initial phase jumped to around 95 Km/hr, and the cluster velocity decreased to less than 90 Km/hr up to the 3rd minute. For the remaining time of the approach, the velocity is stable, around 90 Km/hr.

Conversely, Figure 5-39 shows the acceleration of the Symmetric Auto Driving Model with the 120 Km/hr desired velocity scenario. Positive acceleration peaks are very limited, but negative acceleration peaks are similar to the acceleration of the Asymmetric Auto Driving Model with the 120 Km/hr desired velocity scenario in Figure 5-33. Acceleration curves show the first 3-minute curve is higher on the positive side, similar to the Asymmetric Auto Driving Model with the 120 Km/hr desired velocity scenario. From the 3rd minute to the end of the approach, the cluster acceleration curves are biased to the negative side. During all of the approach, positive acceleration starts with 4 Km/hr/s and decreases to be mostly stable around 3 Km/hr/s. The deceleration side is separated into two parts. The first part is from the initial phase to the 3rd minute, when the deceleration part starts from -4 km/hr/s and declines to almost 0 Km/hr/s. The second part starts from the 3rd minute; the deceleration, around -5 Km/hr/s.

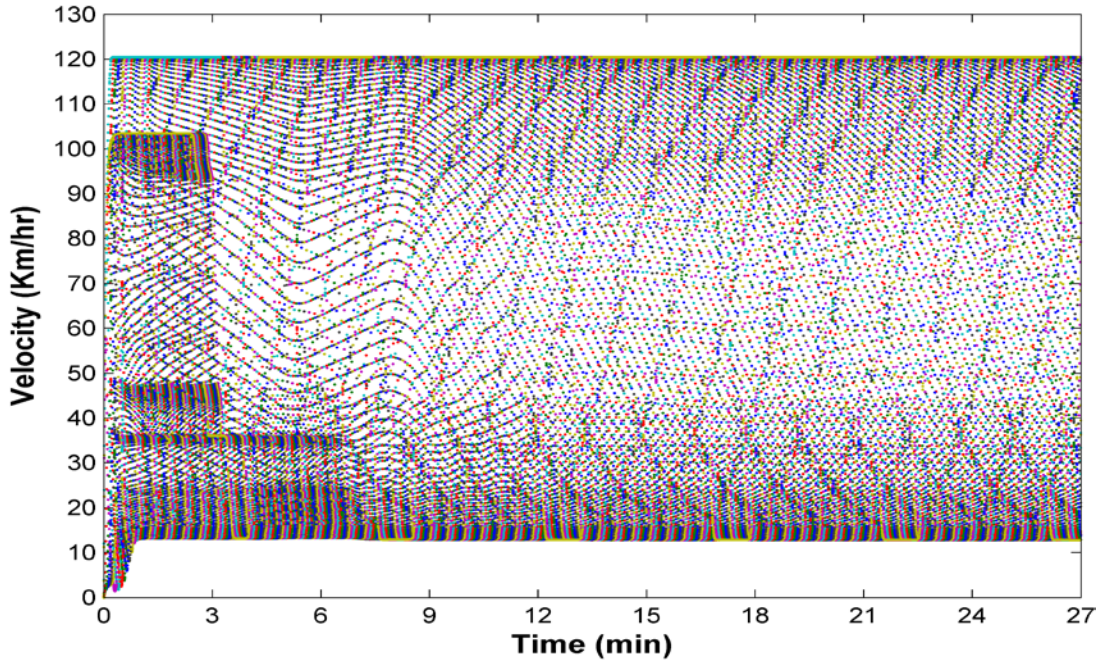

Figure 5-38: Velocity of Symmetric Auto Driving Model with 120 Km/hr desired velocity scenario

Figure 5-37 and Figure 5-41 express vehicles' velocities available in the congestion zone in the Symmetric Auto Driving Model with the 120 Km/hr desired velocity scenario. During the initial time, almost 17% of the total vehicles in the congestion zone are travelling at less than or equal to 40km/hr. After the 3rd minute, the

congestion vehicle velocities' concentration changes to be more or less equal to 20 km/hr. Almost 24% of the vehicles are travelling at less than 20 km/hr. It is clear that the other vehicles' velocity rates are very low and not similar to Figure 5-25 and Figure 5-35.

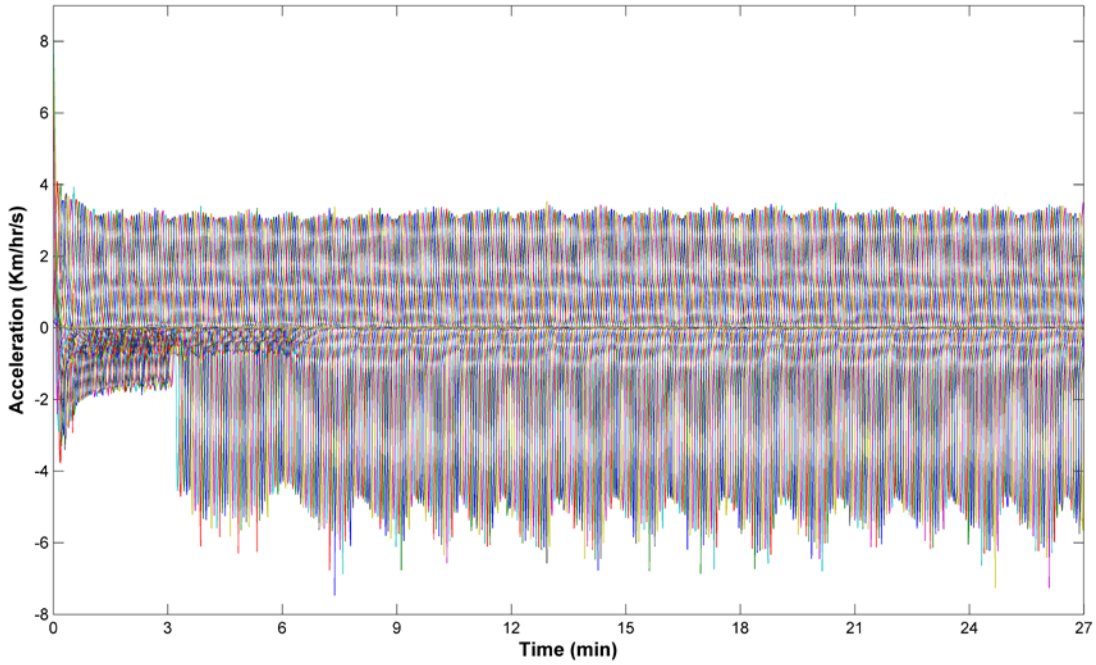

Figure 5-39: Acceleration of Symmetric Auto Driving Model with 120 Km/hr desired velocity scenario

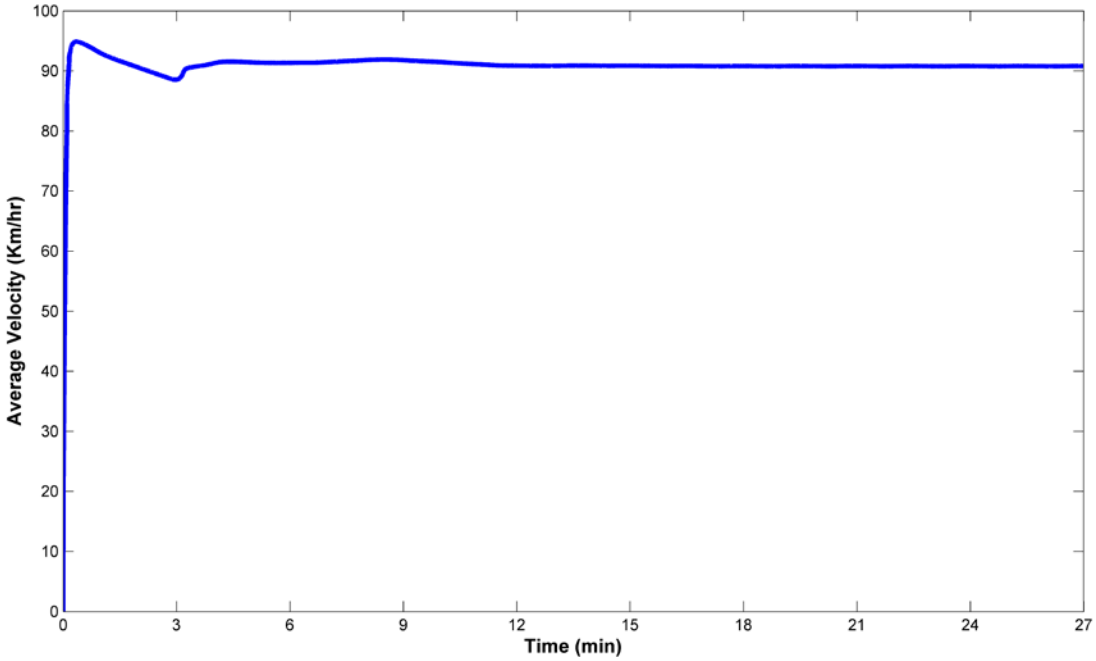

Figure 5-40: Average Velocity of Symmetric Auto Driving Model with 120 Km/hr desired velocity scenario

The impact of density on velocity and traffic flow in the Symmetric Auto Driving Model with 120 Km/hr desired velocity scenario has been shown in Figure 5-42. The density and traffic flow contraction curve of traffic flow is shown in Figure 5-42A. Traffic flow is exceeding the critical point of density (ρ), where the density critical point is (0.069767, 0.31). Although the traffic flow is increasing dramatically between 0.1 and 0.2 vehicle/m, the velocity has fallen to less than 40 Km/hr as shown in relation to the density and velocity, as expressed in Figure 5-42B. Moreover, during the range of density between 0.2 and 0.37 vehicle/m, the traffic flow is matching the critical density line because of the elimination of velocity in the same period of density.

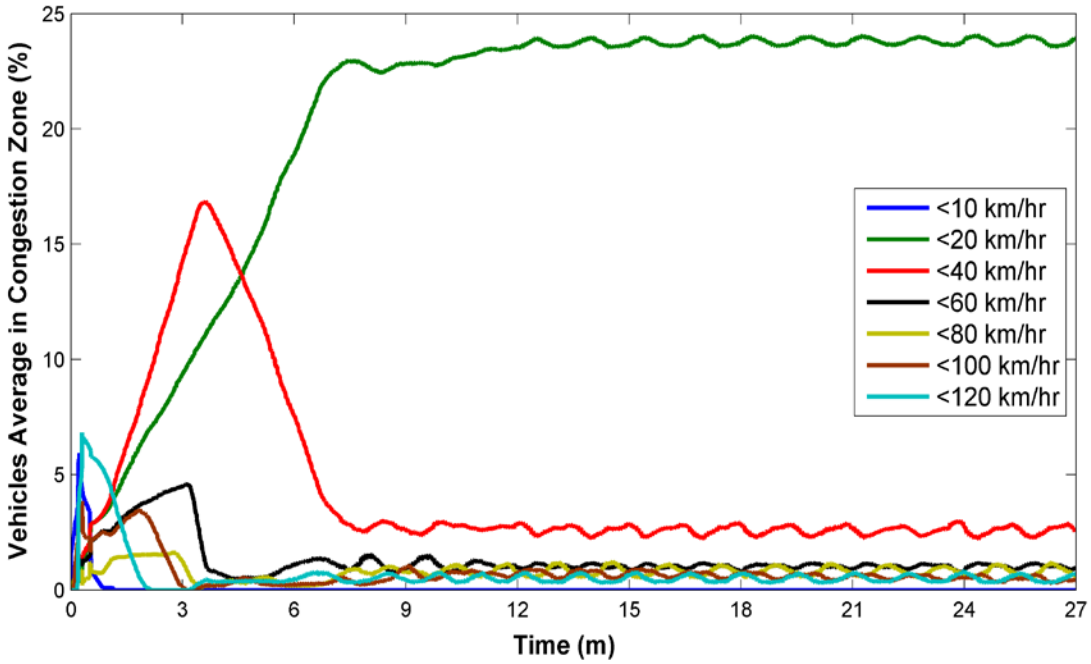

Figure 5-41: Velocity of Symmetric Auto Driving Model with 120 Km/hr desired velocity scenario during the congestion zone

Conversely, the expansion curve of traffic flow is starting from 0.175 vehicle/m density to 0.37 vehicle/m. Traffic flow is dropped gradually as a result of the pressure of the density with stability of velocity. Between 0.08 and 0.2 vehicle/m, the traffic flow rises gradually as a result of the pressure of the density, which eliminates velocity. The traffic flow is increasing dramatically as a result of the dramatic increase of velocity with the declining of density between 0.07 and 0.08 vehicle/m. The gap between contraction and expansion curves in the Symmetric Auto Driving Model with 120 Km/hr desired velocity scenario is less than the

Human Driver Behaviour Model with 120 Km/hr desired velocity scenario and more than the Asymmetric Auto Driving Model with 120 Km/hr desired velocity scenario.

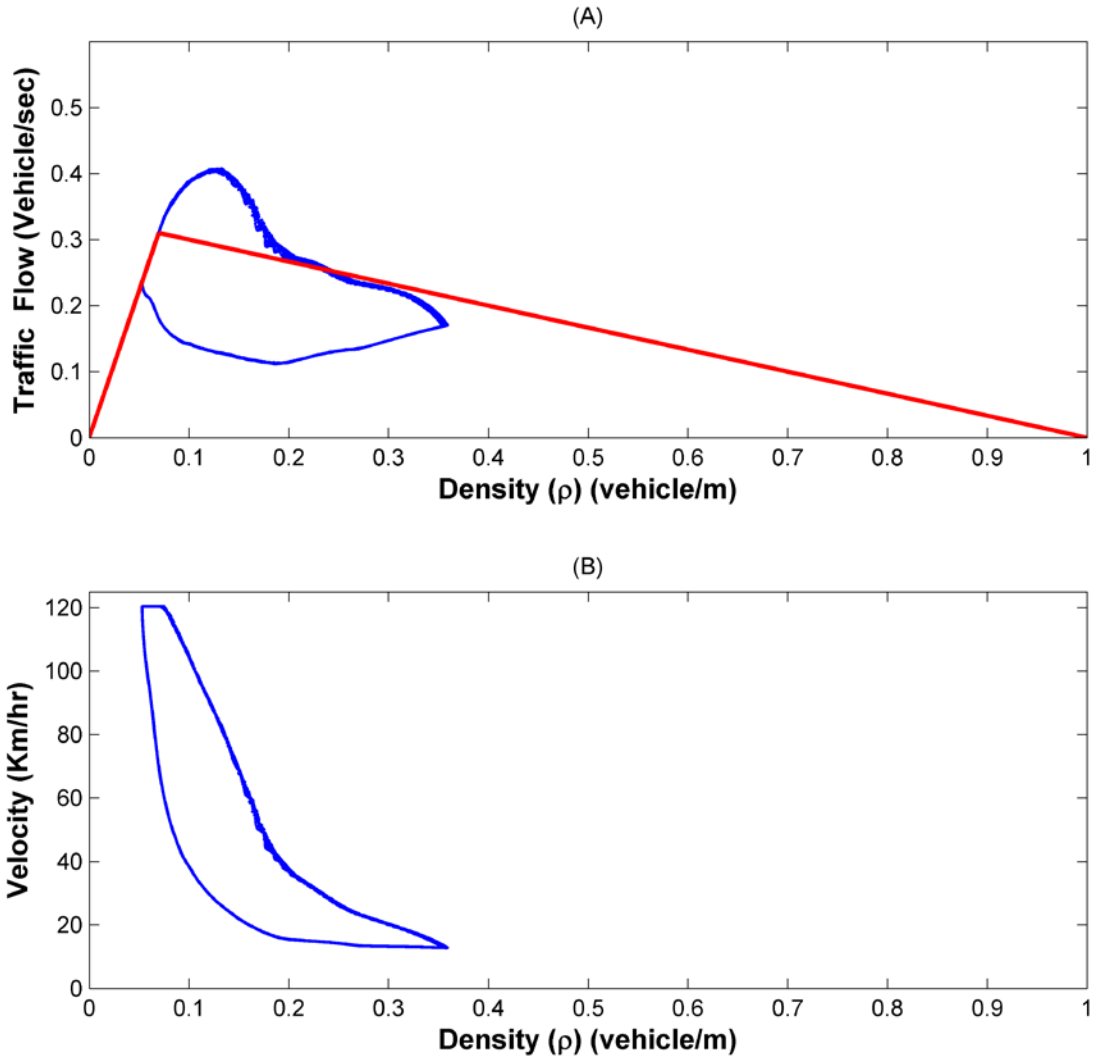

Figure 5-42: Velocity, Density and Traffic flow in Symmetric Auto Driving Model with 120 Km/hr desired velocity scenario

Chapter 6

Human Driver Behaviour with utilising ITS

6.1. Introduction

In Chapter 4, the model used in this thesis was explained. Conversely, Chapter 5 has expressed that the results of approaches should either be:

1) Human Driver Behaviour,
2) Asymmetric Auto Driving or
3) Symmetric Auto Driving.

From this approach, the Traffic Congestion Thickness Change Rate (TCTCR) is the difference between the traffic flow going to the congestion zone (TF_{in}) and the traffic flow leaving the congestion zone (TF_{out})

$$TCTCR = TF_{in} - TF_{out} \tag{6-1}$$

Where the traffic flow results from the multiplication of Velocity (V) by traffic density (ρ),

$$TCTCR = (V_{in} \times \rho_{in}) - (V_{out} \times \rho_{out}) \tag{6-2}$$

Normally, V_{in} is equal to the desired Velocity (V_{des})

$$TCTCR = (V_{des} \times \rho_{in}) - (V_{out} \times \rho_{out}) \quad (6\text{-}3)$$

While V_{out} is either in the stationary mode ($V = 0$) or very low velocity. Therefore, using acceleration (a_{out}) will be better than using velocity.

$$TCTCR = (V_{des} \times \rho_{in}) - ((a_{out} \times t) \times \rho_{out}) \quad (6\text{-}4)$$

With regards to $f(\alpha, \beta, p)$, which is the function of acceleration, deceleration and reaction factors respectively and from a basic physics equation, we can find that $a_{out} = \frac{V_{des} - V_0 / f(\alpha,\beta,p)}{t}$ where V_0 is the initial velocity at leaving point

$$TCTCR = (V_{des} \times \rho_{in}) - ((V_{des} - V_0) \times \rho_{out}) \quad (6\text{-}5)$$

However, density (ρ) is the number of vehicles in a defined distance. Because the congestion is changing its position to calculate the number of vehicles in a distance, we replace the number of vehicles by one vehicle because in one lane there is one vehicle that leaves each time and makes the distance equal to the length of vehicle (L) with front gap (x_{rel}). Therefore, $\rho_{out} = \frac{L}{L_{out} + x_{rel-out}}$

$$TCTCR = V_{des}\left(\rho_{in} - \left(\left(1 - {}^{v_0}/_{V_{des}}\right) \times \rho_{out}\right)\right) \quad (6\text{-}6)$$

$$TCTCR = V_{des}\left(\rho_{in} - \left(\rho_{out} - \rho_{out}\, {}^{v_0}/_{V_{des}}\right)\right) \quad (6\text{-}7)$$

$$TCTCR = V_{des}\left(\rho_{in} + \rho_{out}\, {}^{V_0}/_{V_{des}} - \rho_{out}\right) \quad (6\text{-}8)$$

From the equation, we can see there are three ways to control $CTCR$:

1) Increase ρ_{out}. In this part, ρ_{out} is limited by velocity v, where $\rho_{out} = \frac{L}{L + x_{rel}}$ and where $x_{rel} = 3 \times v$.

2) Increase V_{des} to reduce the positive side. The impacts of increasing of V_{des} is a decrease by decreasing v_0 until it disappears when $v_0 = 0$ is the equation.

$$TCTCR = V_{des}(\rho_{in} - \rho_{out}) \tag{6-9}$$

3) Decreasing ρ_{in} will lead to a decrease in the number of vehicles going to the congestion zone.

Conversely, according to Maerivoet and De More [29], the capacity flow near the critical density will move with a constant speed of V_{des} m/s. The critical density is defined as the vehicle length, single-cell length (L), divided by the safety time gap (T) and the vehicle cell length.

$$\rho = \frac{L}{(T \cdot v) + L} \tag{6-10}$$

The desired traffic flow can be computed by means of the fundamental relation

$$TF = \rho \cdot v \tag{6-11}$$

Because the $Max(TF) = 1/T$, TF has been normalised by multiplication by 'c'.

$$TF = T \cdot \rho \cdot v \tag{6-12}$$

The basic mathematical idea has been utilised in Human Driver Behaviour with utilising the ITS scenario approach. This scenario is distributed into three parts:

1. Congestion initial part,
2. Solving congestion by using ITS part and
3. After solving congestion part.

6.2. Congestion Initiation

This part of the Human Driver Behaviour with utilising ITS scenario approach is similar to the Human Driver Behaviour Scenario. Figure 6-1 expresses the traffic flow for the Human Driver Behaviour Model with utilising ITS with a 120 Km/hr desired velocity scenario. Between the initial time to the 9th minute in this approach, it is similar to the same time period of the Human Driver Behaviour Model with the 120 Km/hr desired velocity scenario in Figure 5-21. Moreover, Figure 6-2, Figure 6-4 and Figure 6-3 show similar action in the velocity, acceleration and average velocity, respectively, to Figure 5-22, Figure 5-23 and Figure 5-24.

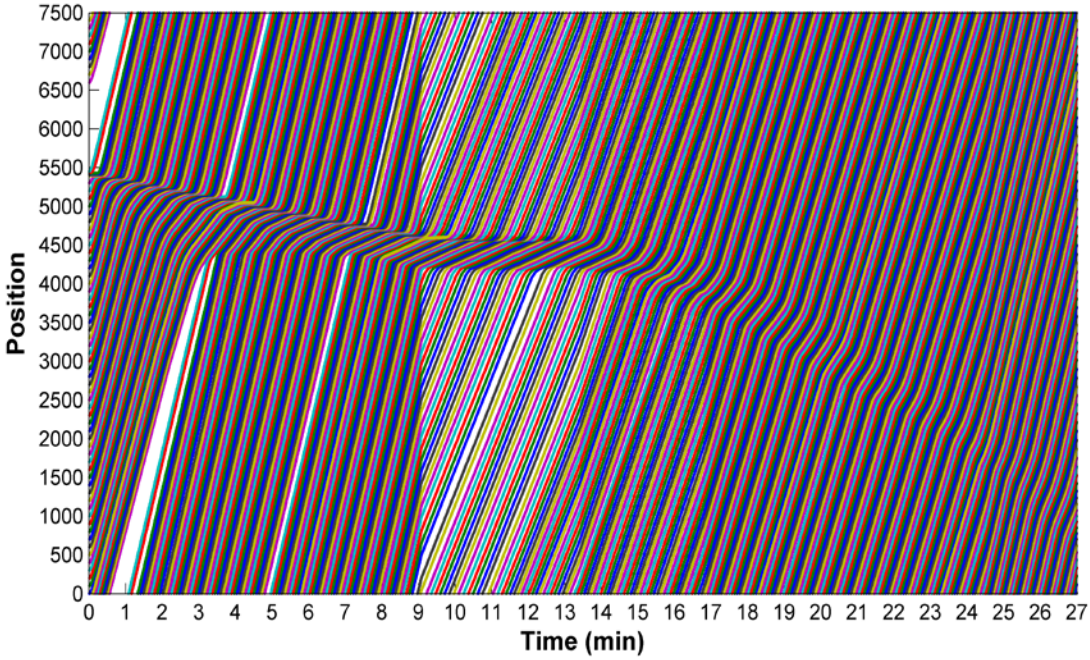

Figure 6-1: Traffic flow of Human Driver Behaviour with utilising ITS Model with 120 Km/hr desired velocity scenario

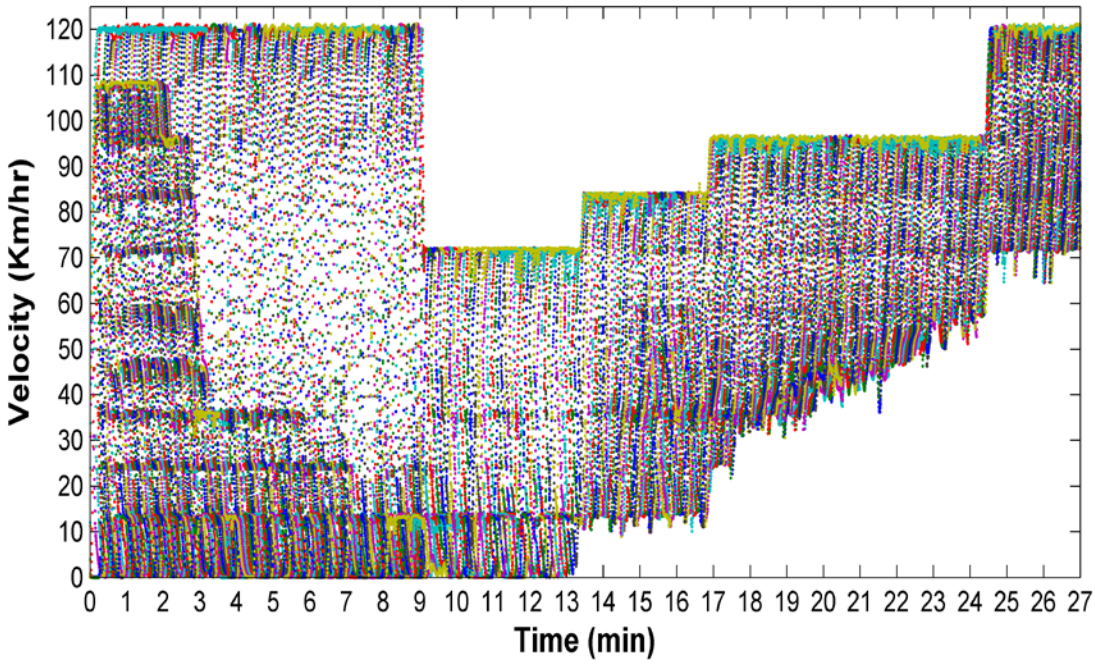

Figure 6-2: Velocity of Human Driver Behaviour utilising ITS Model with 120 Km/hr desired velocity scenario

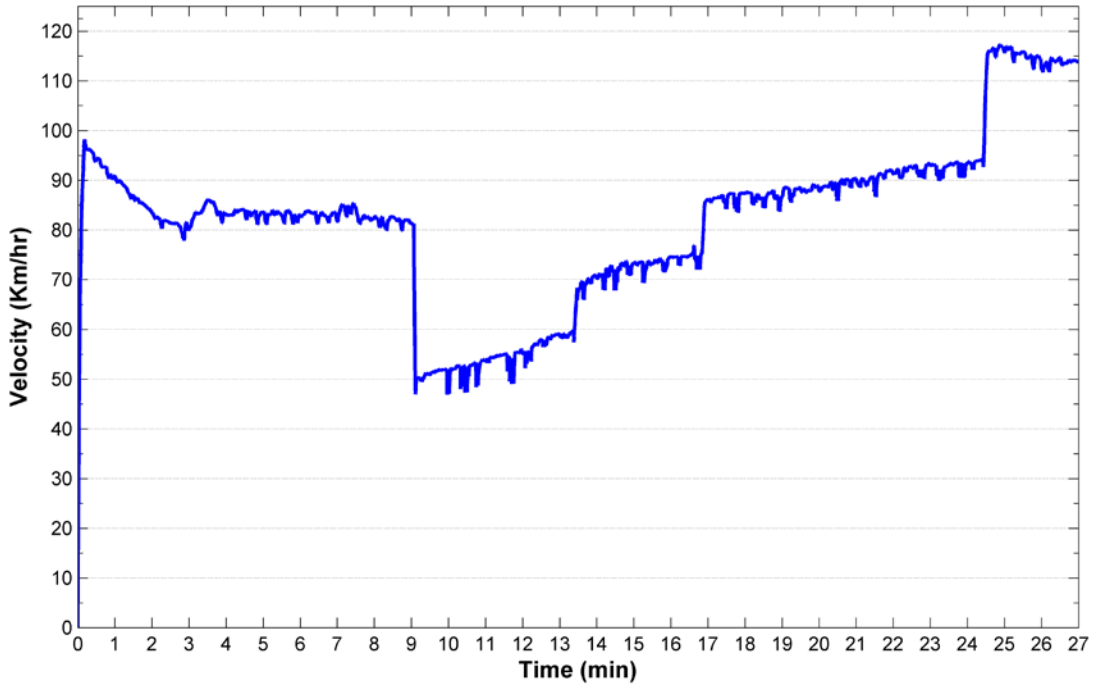

Figure 6-3: Average Velocity of Human Driver Behaviour utilising ITS Model with 120 Km/hr desired velocity scenario

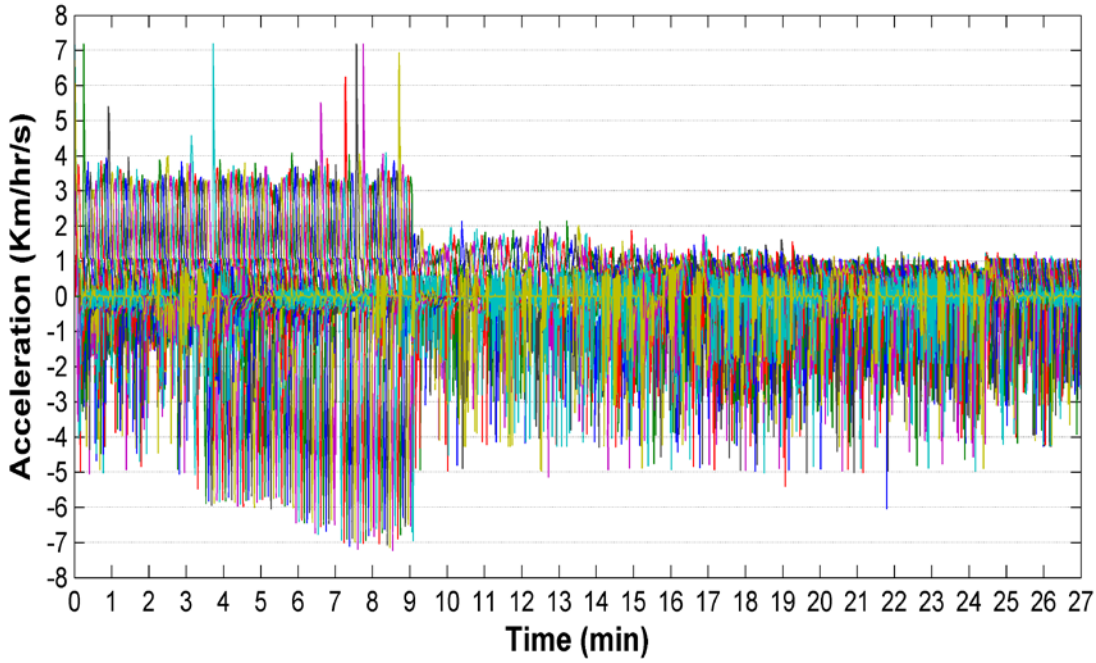

Figure 6-4: Acceleration of Human Driver Behaviour utilising ITS Model with 120 Km/hr desired velocity scenario

6.3. Solving Congestion by using ITS Part

Here, we try to solve to congestion by utilising the ITS system. There are three different ITS systems that have been used:

1. Adaptive Cruise Control (ACC),
2. x_{rel} sensors and
3. The VANET system.

Those ITS systems need to support adapting to the congestion. Also, from (6-8) and (6-9), we can see there are three ways to control Traffic Congestion Thickness Change Rate (TCTCR):

1. Desired Velocity (V_{des}),
2. Output Density (ρ_{out}) and
3. Input Density (ρ_{in}).

It is preferred to utilise input density ρ_{in} because, as revealed in (6-9), the $TCTCR$ is a result of the compression between ρ_{out} and ρ_{in}, but V_{des} is a

proportional factor that could help to solve the congestion or may make it worse.

Therefore, x_{rel} sensors' signals play an essential part as the input signal for ACC, which is the FUZZY Logic Controller (FLC) in the project, to make a decision about whether to accelerate or decelerate. x_{rel} Sensors and ACC have been used in previous scenarios:

1. Human Driver Behaviour. scenario,
2. The Asymmetric Auto Driving scenario and
3. The Symmetric Auto Driving scenario.

In this part, the VANET system has been added to the system to broadcast the velocity (v_i) and x_{rel}between the vehicle members. During a normal situation, the FLC receives the original signal from x_{rel} sensors (Figure 6-5). Conversely, during traffic congestion, the original signal from x_{rel} sensors will be modified by x_{rel}controller (Figure 6-5).

Table 6-1 shows the density control logarithm where one can control the cluster density and velocity. The VANET message contains the minimum velocity of the cluster (v_{min}) and the minimum head gap in the cluster ($x_{\min\ \_rel}$). That signal will compare with the vehicle velocity (v_i) and (x_{i_rel}). FLS will adjust the x_{rel} signal depending on its fuzzification inputs.

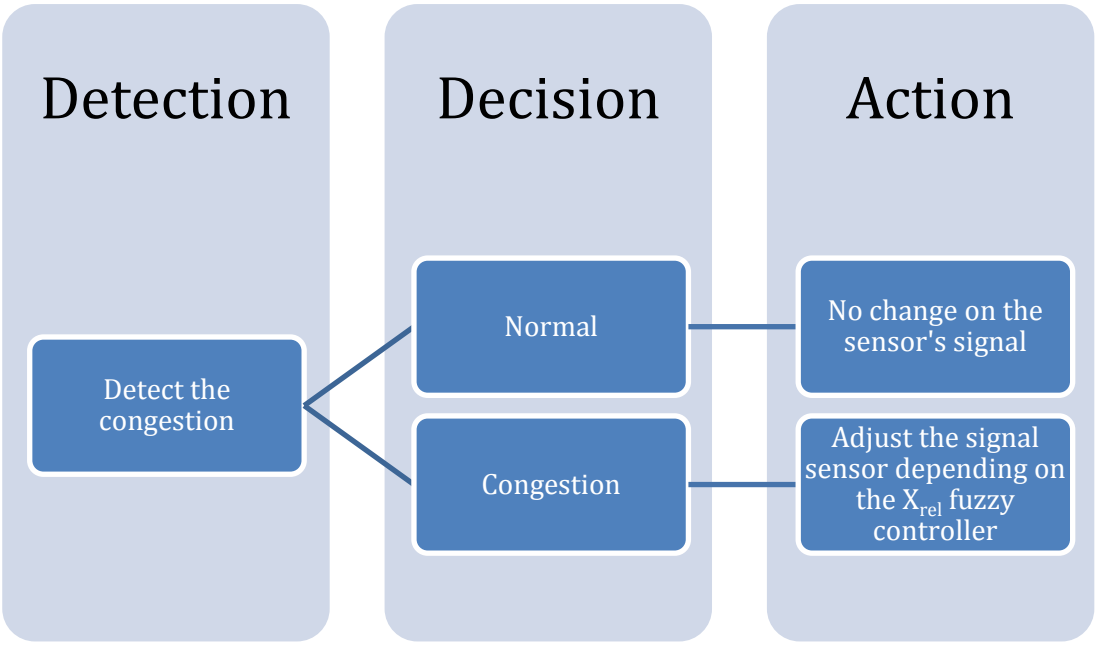

Figure 6-5: $\boldsymbol{x_{rel}}$ controller

Figure 6-6 shows the traffic flow of Human Driver Behaviour with utilising ITS Model with the 120 Km/hr desired velocity scenario during solving the congestion by using the ITS part. This figure reveals two areas:

a. The congestion zone
b. Off-congestion zone.

The congestion zone expresses the area where the vehicle is congested. It can be observed that the darkness of the congestion changes over time. In the beginning of this part of the scenario approach, the congestion zone gets darker, and over time, that darkness is reduced. But the congestion angle is more horizontal and stationary, and after the 13th minute, the congestion starts moving. That movement started after the 17th minute.

Table 6-1: Density control logarithm

$start$

$receive\ VANET\ signal$

$apply\ in\ normal\ situation$

$Keep\ original\ x_{rel}$

$if\ the\ congestion\ is\ applied$

$start\ using\ x_{rel}\ controller\ model$

$adjust\ individual\ x_{rel}\ signal$

$transfer\ the\ signal\ to\ vehicle\ controller$

$adjusted\ the\ velocity$

$if\ congested\ adapted$

$break$

end

Off the congestion zone is the area not congested or the free area. In the general overview, Figure 6-6 expresses the darkness of the off-congestion zone. In the beginning of this part of the scenario approach, the off-congestion zone is brighter because of density reduction. After the 13th minute, the darkness is increased and increased more after the 17th minute. At the end of this part, the darkness is merged between the congestion and off-congestion zone.

Figure 6-7 reveals the Velocity of Human Driver Behaviour with utilising ITS Model with the 120 Km/hr desired velocity scenario during the solving to congestion by using the ITS part. In Figure 6-7, it can be seen that this part is distributed into three parts. The first part's velocity envelope starts from 0 to 70 Km/hr. This section starts from the 9th minute and extends to the 13th minute. The second section has curves with an amplitude between 12 to 85 Km/hr. This section starts from the 13th minute and goes to the 17th minute. The last section is started at the 17th minute and goes until the end of this part. The last section envelope at the beginning of this section was between 25 and 95 Km/hr. Over time, the lower limit of the velocity envelope rose until it reached 60 Km/hr.

Figure 6-8 reveals the single vehicle velocity of Human Driver Behaviour with utilising ITS Model with 120 Km/hr desired velocity scenario during solving congestion by using the ITS part. Figure 6-8 expresses the congestion strength during solving the congestion period time. The first dropped peak in the velocity for the vehicle was dropped to 0 speed with a hold for almost 2 minutes. The 2nd dropped peak in the vehicle velocity was dropped to 10 Km/hr and held for 1 minute. The 3rd drop peak in the vehicle velocity was dropped to 40 Km/hr and does not hold. The 4th drop peak in the vehicle velocity was dropped to 60 Km/hr and does not hold. Generally, like Figure 6-7, there is a rise in velocity during the solving congestion period time.

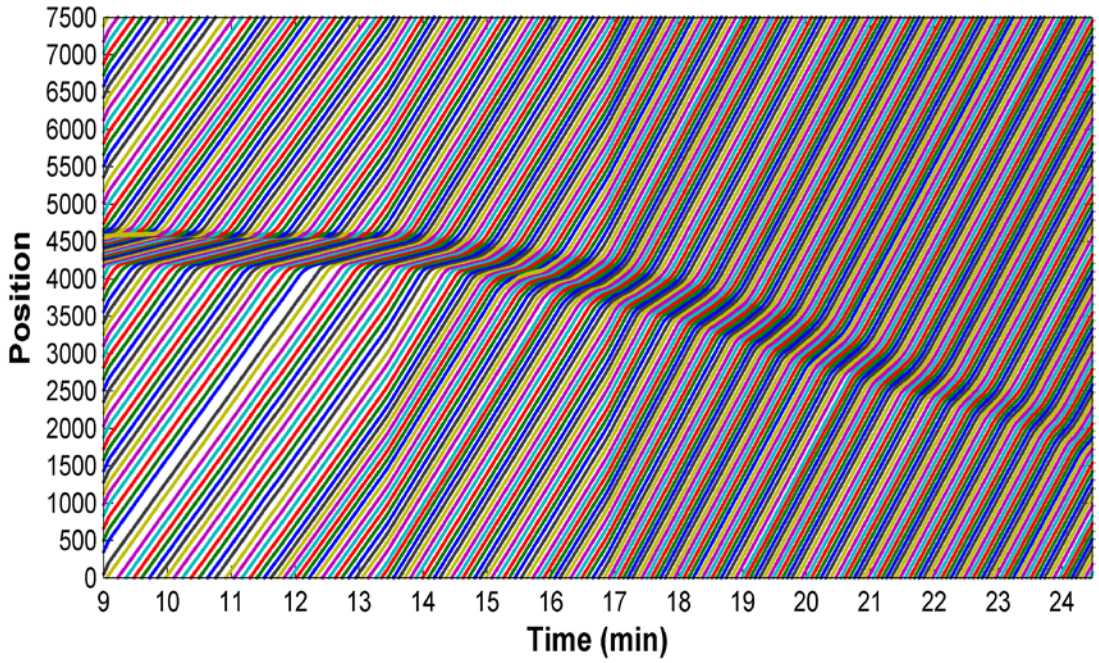

Figure 6-6: Traffic flow of Human Driver Behaviour with utilising ITS Model with 120 Km/hr desired velocity scenario during solving congestion by using ITS

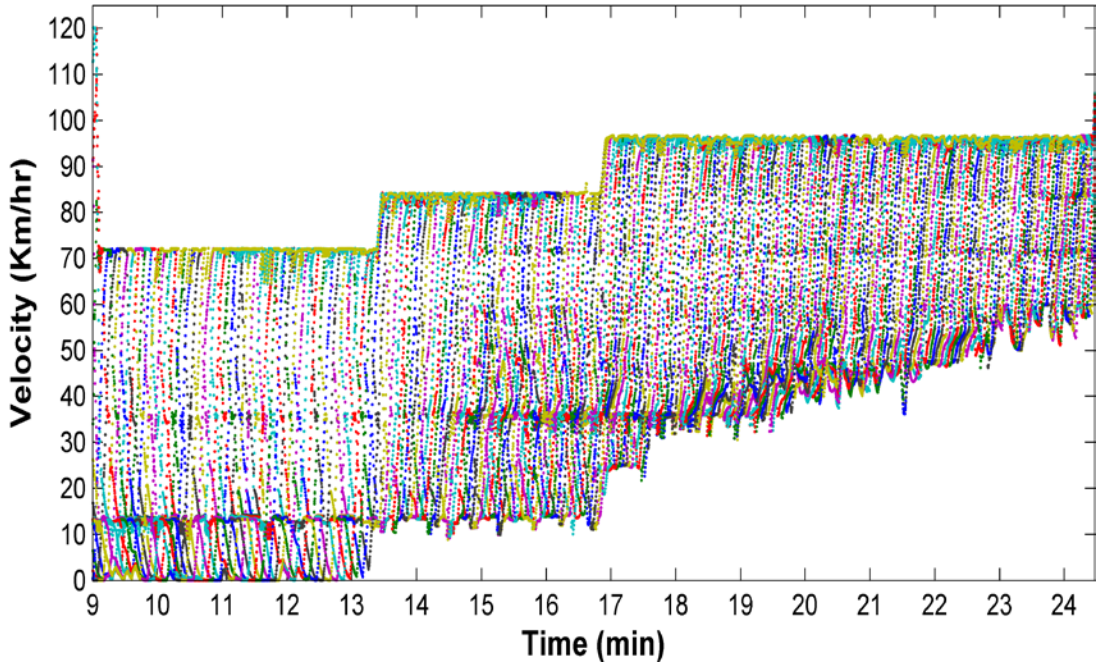

Figure 6-7: Velocity of Human Driver Behaviour with Utilising ITS Model with 120 Km/hr desired velocity scenario during solving congestion by using ITS

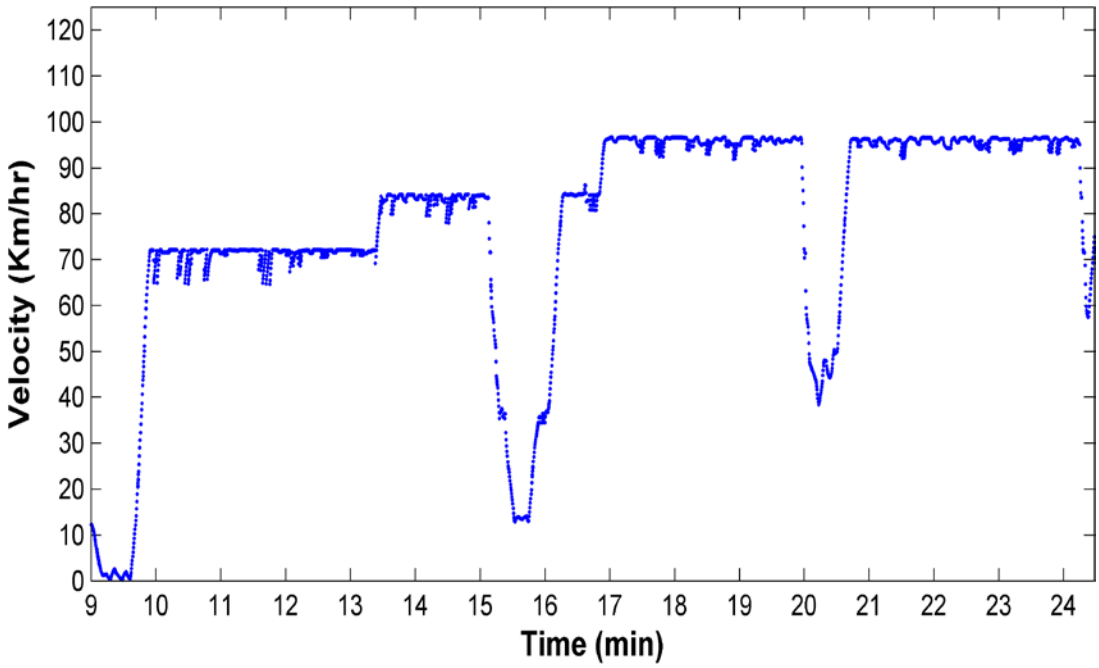

Figure 6-8: Velocity of single vehicle of Human Driver Behaviour with utilising ITS Model with 120 Km/hr desired velocity scenario during solving congestion by using ITS

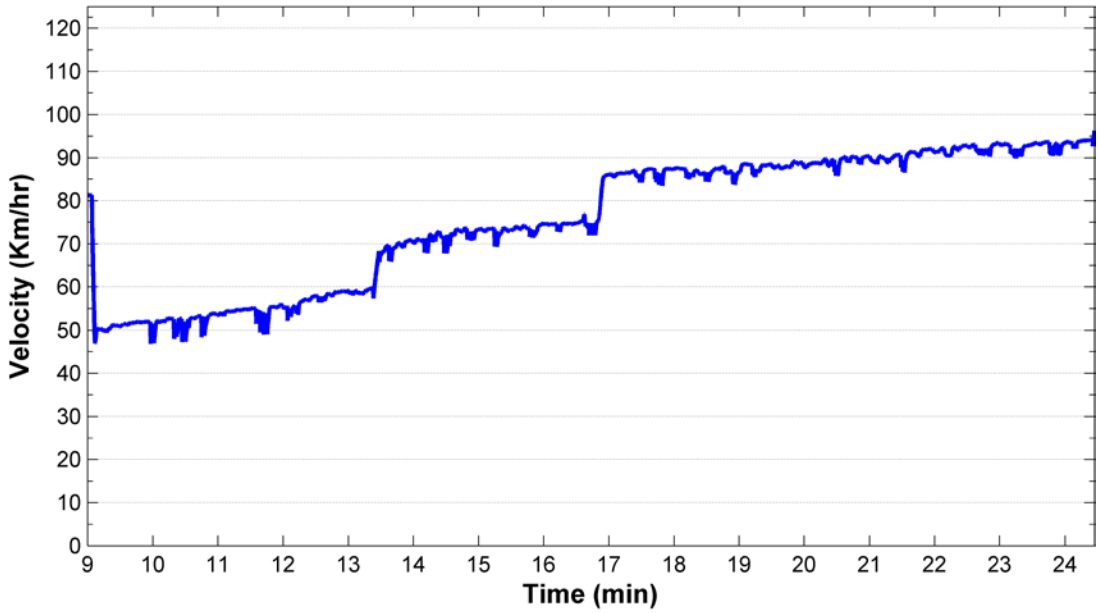

Figure 6-9: Average velocity of Human Driver Behaviour with utilising ITS Model with 120 Km/hr desired velocity scenario during solving congestion by using ITS

Figure 6-9 illustrates the cluster average Velocity of Human Driver Behaviour with utilising ITS Model with 120 Km/hr desired velocity scenario during solving congestion by using the ITS part. Regarding Figure 6-7 and Figure 6-8, Figure 6-9 reveals how the cluster improves over time during the solving to congestion part. After just dropping the average velocity from 80 Km/hr to 50 Km/hr, which is in the beginning of this part the result of solving congestion and adjusting vehicle gaps (x_{rel}), there is a gradual increasing in the average speed. Overall, there is a gradual rising in the average speed, and there are two sudden jumps at the same time of changing the upper limit in the overall vehicles' velocity. See Figure 6-7 and Figure 6-8. Moreover, the average velocity gradual rising in Figure 6-9 is because of the reduction of station period time and the reduction of the drop peak, as shown in Figure 6-8. The last part of the average velocity gradual rise is because of increasing the lowest limit of the overall velocity envelope in Figure 6-7.

Figure 6-10 shows the Acceleration of Human Driver Behaviour with utilising ITS Model with 120 Km/hr desired velocity scenario during the solving to congestion by using the ITS part. The positive acceleration in the beginning of this part was more than 3 Km/hr/s, but the acceleration was dropped to less than 2 Km/hr/s because of dropping the velocity high limit in Figure 6-7. After first minute of solving the congestion part, the positive acceleration was increased to 2 Km/hr/s because of the

station speed for the vehicle in the congestion. Because of the change of the lowest limit of the velocity envelope from 0 Km/hr to around 10 Km/hr (Figure 6-7), the acceleration curves dropped slowly to be around 1 Km/hr/s. Conversely, negative acceleration peaks are almost around -4 and -5 Km/hr/s because of the drop in speed during congestion.

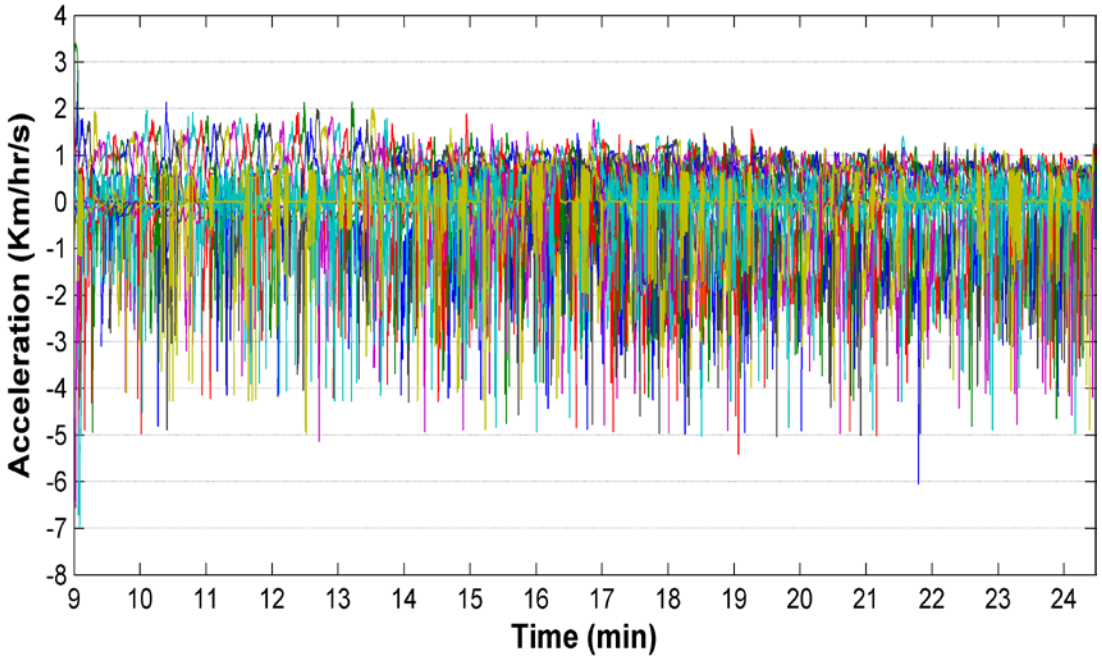

Figure 6-10: Acceleration of Human Driver Behaviour with utilising ITS Model with 120 Km/hr desired velocity scenario during solving congestion by using the ITS

For more acceleration detail, Figure 6-11 shows the Acceleration of Single Vehicle of Human Driver Behaviour with utilising ITS Model with the 120 Km/hr desired velocity scenario during solving congestion by using the ITS part. The acceleration range is between -3.5 Km/hr/s and 1.5 Km/hr/s. Figure 6-11 has 4 positive acceleration peaks. Because of this increase, the velocity rises dramatically after the congestion zone. The highest peak was the first, at 1.5 Km/hr/s, because the vehicle was at the station. The other acceleration peaks are lower than 1 Km/hr/s. For example, the last acceleration peak is the lowest peak at 0.75 Km/hr/s. Conversely, the negative acceleration has four dropped peaks. The first peaks have happened between the 10th and 11th minute to eliminate density because of adjusting the X_{rel} signal. The other three peaks match the velocity drop peaks as a result of approaching the vehicle-to-congestion zone.

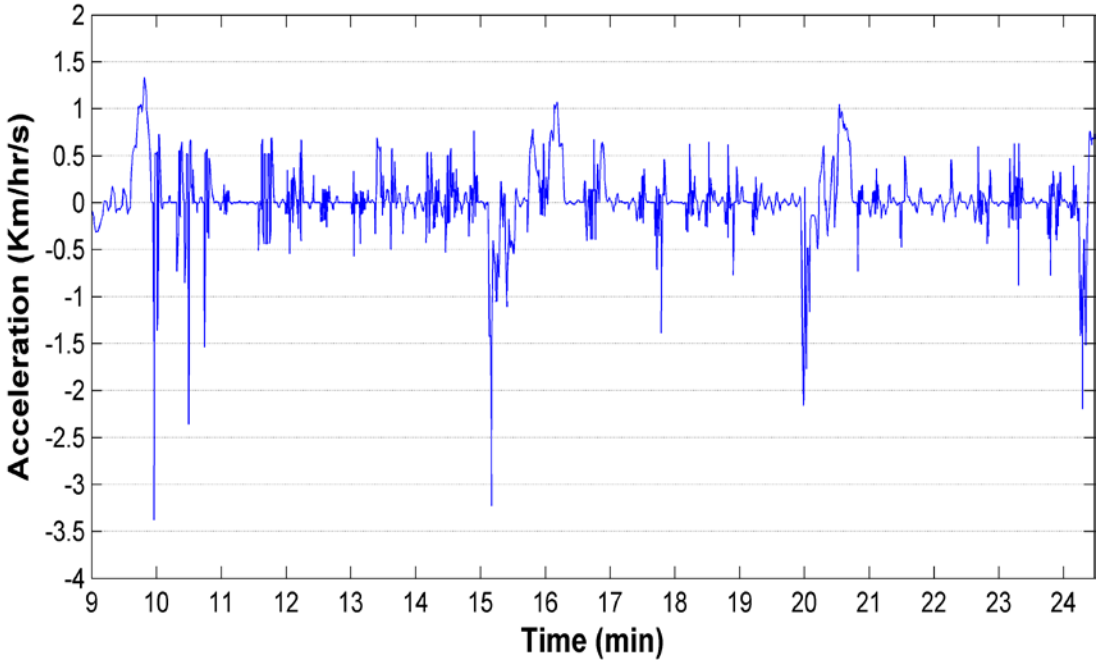

Figure 6-11: Acceleration of Single Vehicle of Human Driver Behaviour with utilising ITS Model with 120 Km/hr desired velocity scenario during solving congestion by using ITS

6.4. After Solving Congestion

This section of the Human Driver Behaviour with utilising ITS illustrates what happens after solving congestion by utilising the ITS system part. Also, during the solving congestion by utilising the ITS system part, $x_{rel}$was adjusted and modified to solving the congestion. Moreover, in this part of the arrangement and after solving to congestion, the X_{rel}signal reverted back to the original signal.

Figure 6-12 expresses the Traffic Flow of Human Driver Behaviour with utilising ITS Model with a 120 Km/hr desired velocity scenario after solving congestion by using the ITS part. It has been illustrated that the congestion has not fully solved. A flux has been initiated because of the vehicles' speed conflict, which is because of some vehicles exceeding the desired velocity (V_{des}): for example, if the vehicle (M_i) exceeded V_{des} and found the head gap (x_{rel-i}) is less than the safety gap ($x_{rel-i} < 3 \times v_i$). Therefore, the vehicle has to maintain x_{rel-i} by reducing $vehicle_i$. Also, the following vehicle ($vehicle_{i+1}$) faces the same issue of the safety gap. Therefore, $vehicle_{i+1}$ will execute the same action of $vehicle_i$ with more force. That action will transfer from one vehicle to another.

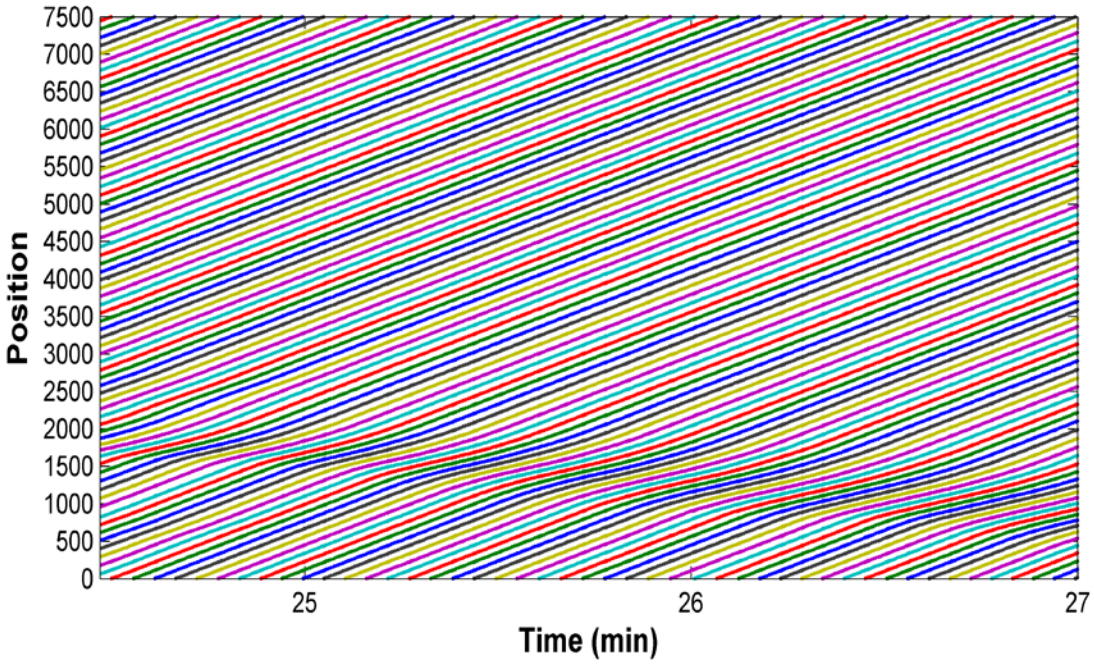

Figure 6-12: Traffic flow of Human Driver Behaviour with utilising ITS Model with 120 Km/hr desired velocity scenario after solving congestion by using ITS

Figure 6-13 shows the Velocity of Human Driver Behaviour with utilising ITS Model with the 120 Km/hr desired velocity scenario after solving congestion by using the ITS part. The velocity, as shown in Figure 6-13, is more stable than the initial congestion part and solving congestion part. The velocity envelope is between 70 and 120 Km/hr. Most vehicle velocities didn't drop less than 70 Km/hr.

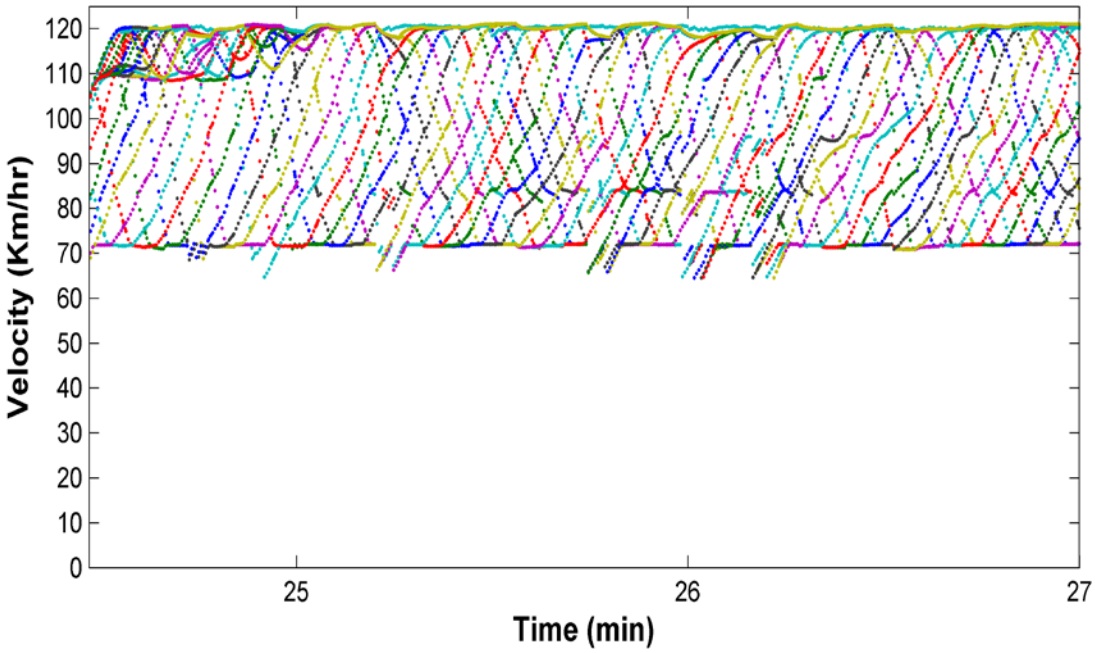

Figure 6-13: Velocity of Human Driver Behaviour with utilising ITS Model with 120 Km/hr desired velocity scenario after solving congestion by using the ITS

Moreover, Figure 6-14 illustrates the velocity of a single vehicle of Human Driver Behaviour with utilising the ITS Model with the 120 Km/hr desired velocity scenario after solving congestion by using the ITS part. A vehicle velocity curve in Figure 6-14 reveals that, after finish the solving congestion part and x_{rel} reverting to the original signal, the vehicle velocity increased directly to approach the V_{des}. The sudden increment in the velocity faced a limited head gap, x_{rel}, that forced the vehicle to reduce velocity to 110 Km/hr. The vehicle velocity drop and increase in the velocity of the head vehicle helped to increase the x_{rel}. Increasing the (x_{rel}) leads the vehicle to increase its velocity to V_{des}. After the vehicle approached V_{des}, it maintained the velocity until the end of the arrangement.

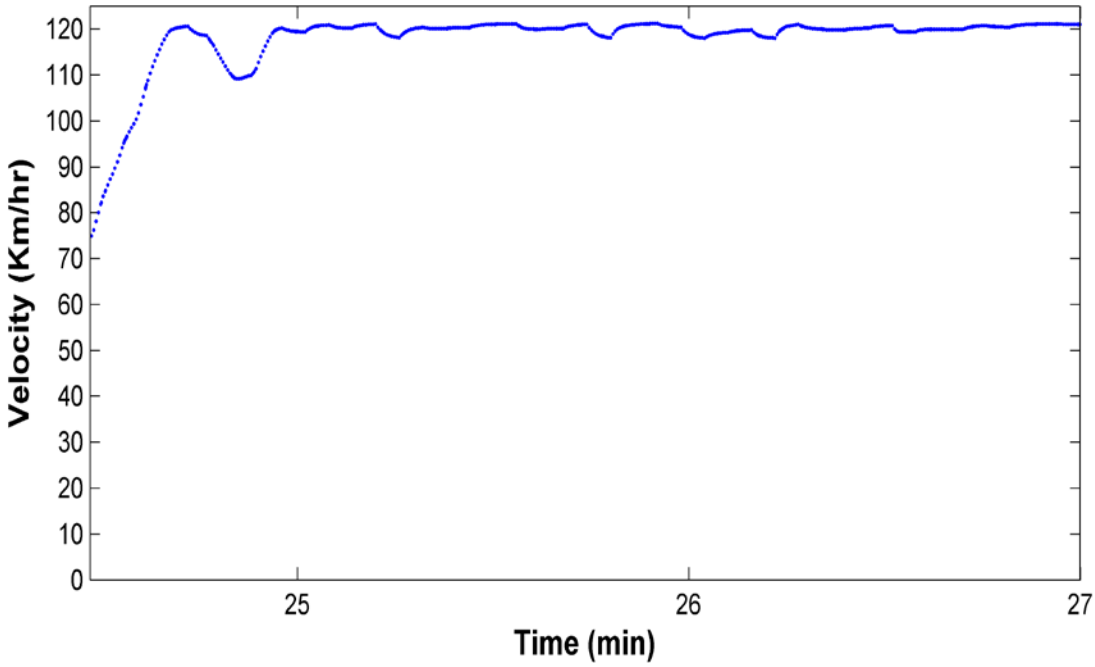

Figure 6-14: Velocity of single vehicle of Human Driver Behaviour with utilising ITS Model with 120 Km/hr desired velocity scenario after solving congestion by using ITS

According to Figure 6-12 and Figure 6-13, there is a flux because of the velocity fluctuation between the vehicles that eliminates the x_{rel}. Moreover, Figure 6-15 reveals the Average Velocity of Human Driver Behaviour with utilising ITS Model with the 120 Km/hr desired velocity scenario after solving congestion by using the ITS part. In Figure 6-15, the cluster average velocity jumped from less than 100 Km/hr to more than 116 Km/hr. Because of velocity fractionation between the vehicles and the elimination of x_{rel}, the cluster average velocity gradually dropped

to around 114 Km/hr. The cluster average velocity varies because of cluster vehicles' velocity and the number of vehicles impacted by the created flux.

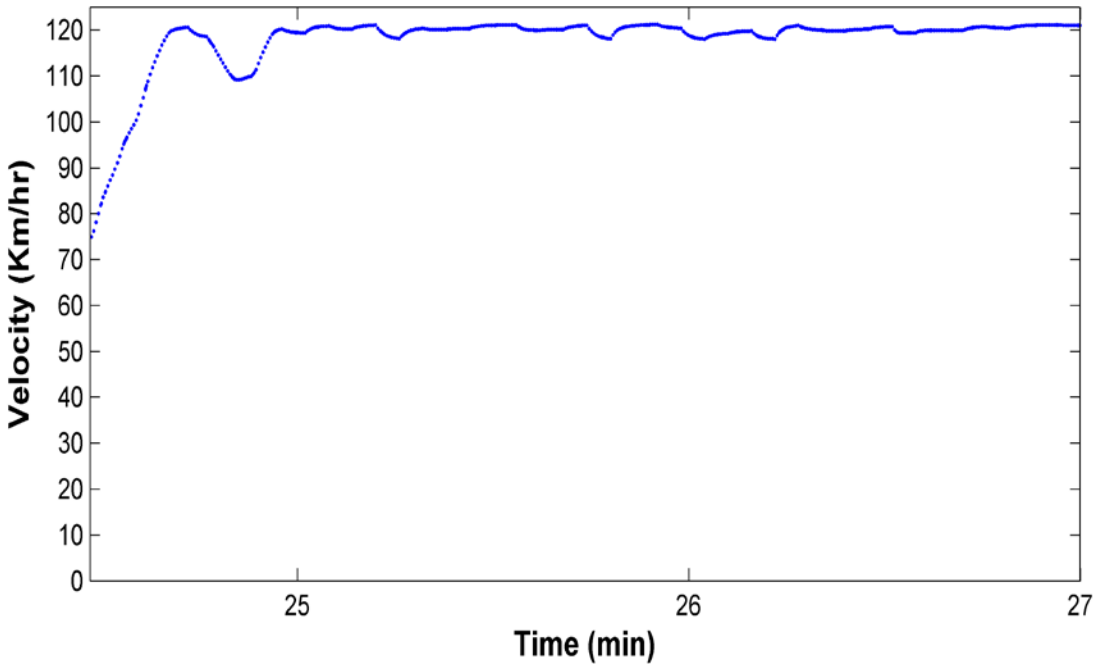

Figure 6-15: Average velocity of Human Driver Behaviour with utilising ITS Model with 120 Km/hr desired velocity scenario after solving congestion by using ITS

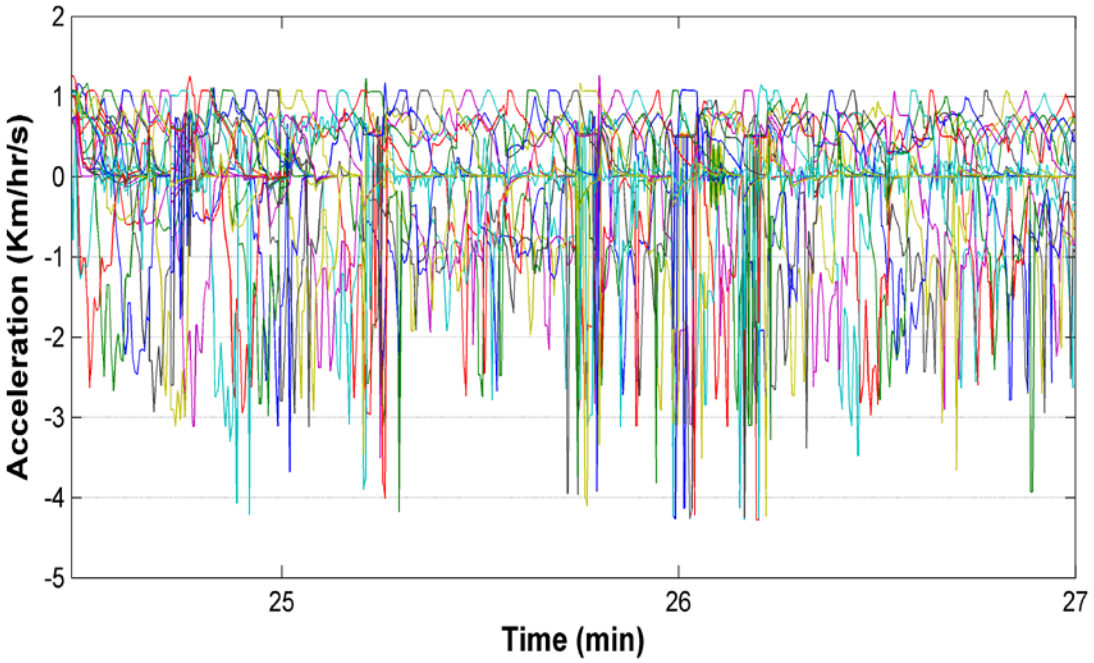

Figure 6-16: Acceleration of Human Driver Behaviour with utilising ITS Model with 120 Km/hr desired velocity scenario after solving congestion by using ITS

Conversely, Figure 6-16 displays the Acceleration of Human Driver Behaviour with utilising ITS Model with the 120 Km/hr desired velocity scenario after solving congestion by using ITS part. It can be observed that the positive acceleration does not exceed 1.2 Km/hr/s, which is essential to eliminate fuel consumption and emissions. While maximum negative acceleration is around -4 Km/hr/s, after solving congestion, this part has a lower negative side than the initial congestion and solving congestion parts. Moreover, Figure 6-17 shows the acceleration of a single vehicle of Human Driver Behaviour with utilising ITS Model with the 120 Km/hr desired velocity scenario after solving congestion by using ITS part. The maximum positive acceleration is in the beginning of this part because of searching of the vehicle to approach V_{des}. See Figure 6-14. After approaching V_{des}, the limited head gap x_{rel} forces the vehicle to reduce velocity by negative acceleration (-0.5 Km/hr/s). The vehicle velocity drop increases the velocity of the head vehicle to help increase the x_{rel}. Increasing the (x_{rel}) leads the vehicle to positive acceleration. After the vehicle approached V_{des}, it maintained the velocity until the end of the arrangement. Acceleration peaks are reducing gradually over time in this part of the arrangement, caused by the stability of this particular vehicle.

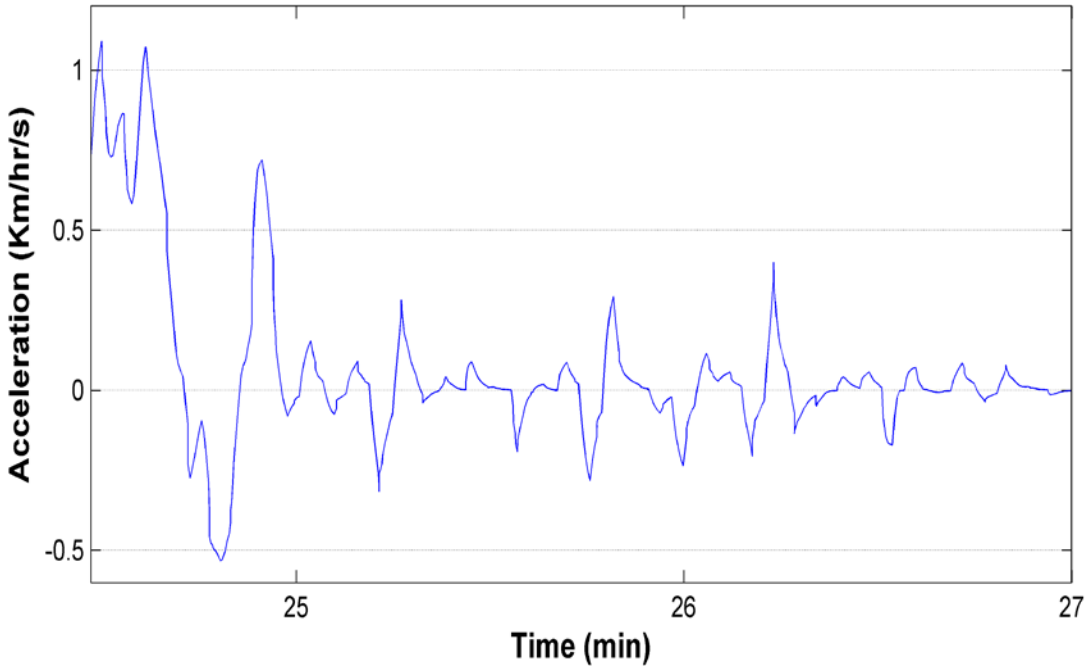

Figure 6-17: Acceleration of a single vehicle of Human Driver Behaviour with utilising ITS Model with 120 Km/hr desired velocity scenario after solving congestion by using ITS

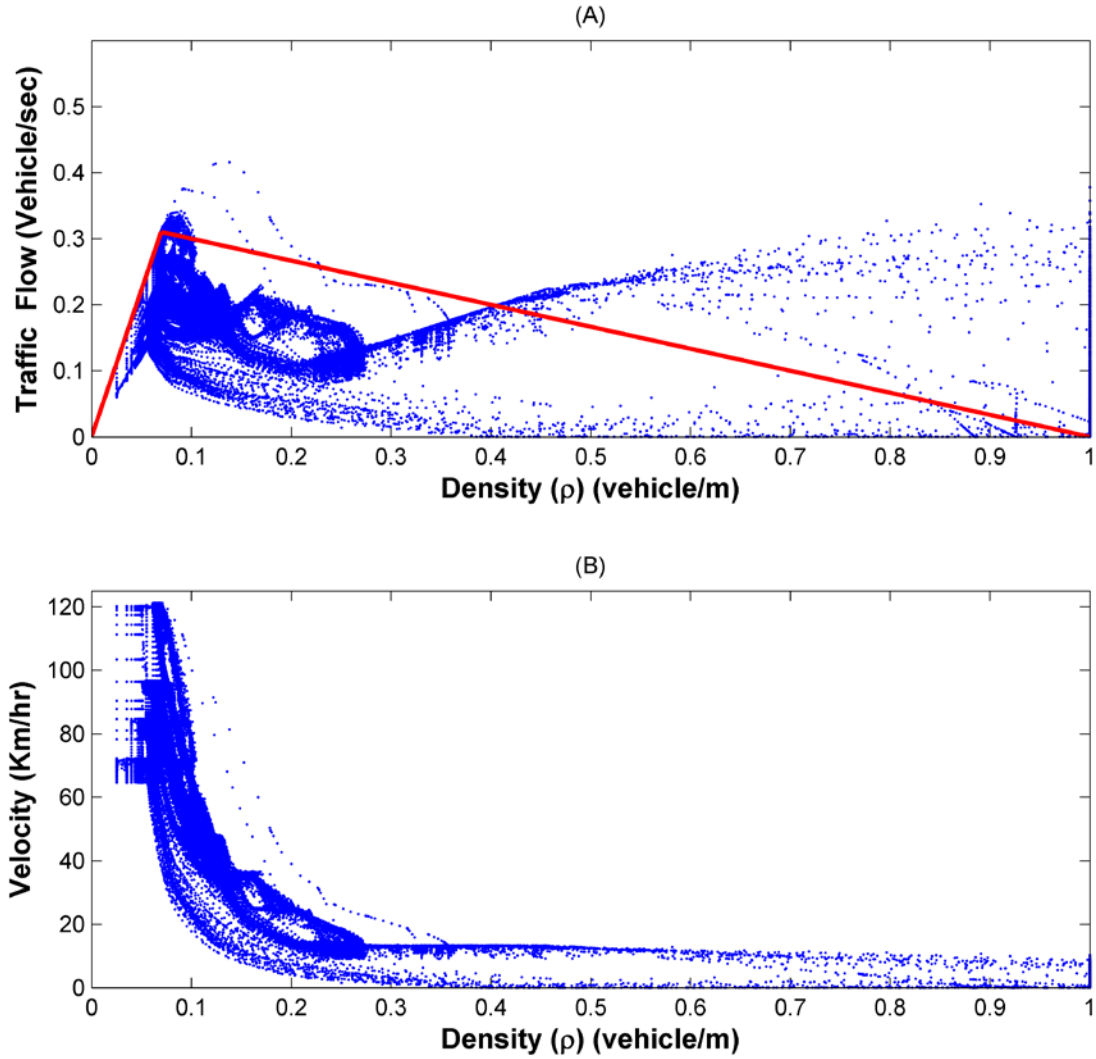

Figure 6-18: Velocity, Density and Traffic flow in Human Driver Behaviour Model with utilising ITS Model with 120 Km/hr desired velocity scenario

The impact of density on velocity, and traffic flow in Human Driver Behaviour with utilising ITS Model with 120 Km/hr desired velocity scenario has been revealed in Figure 6-18. For the contraction curve of traffic flow, the density and traffic flow relationship is shown in Figure 6-18A. Traffic flow is concentrated on the critical point of density (ρ), where the density critical point is (0.069767, 0.31). From the critical density point until 0.45 vehicle/m, the traffic flow is under critical line. After 0.45 vehicle/m with high dispersion, the traffic flow is above the critical line because of the velocity in the same period of density, which happened during the congestion-solving period. Figure 6-18B expressed the relation between the density and velocity. The velocity curves, contraction and expansion, are almost matching. Moreover, Figure 6-19 shows the impact of density on velocity, and traffic flow in

Human Driver Behaviour with utilising ITS Model with 120 Km/hr desired velocity scenario after solving time. Figure 6-19A shows the concentration of traffic flow around the density critical point. Figure 6-19B also shows a mostly similar curve for both contraction and expansion.

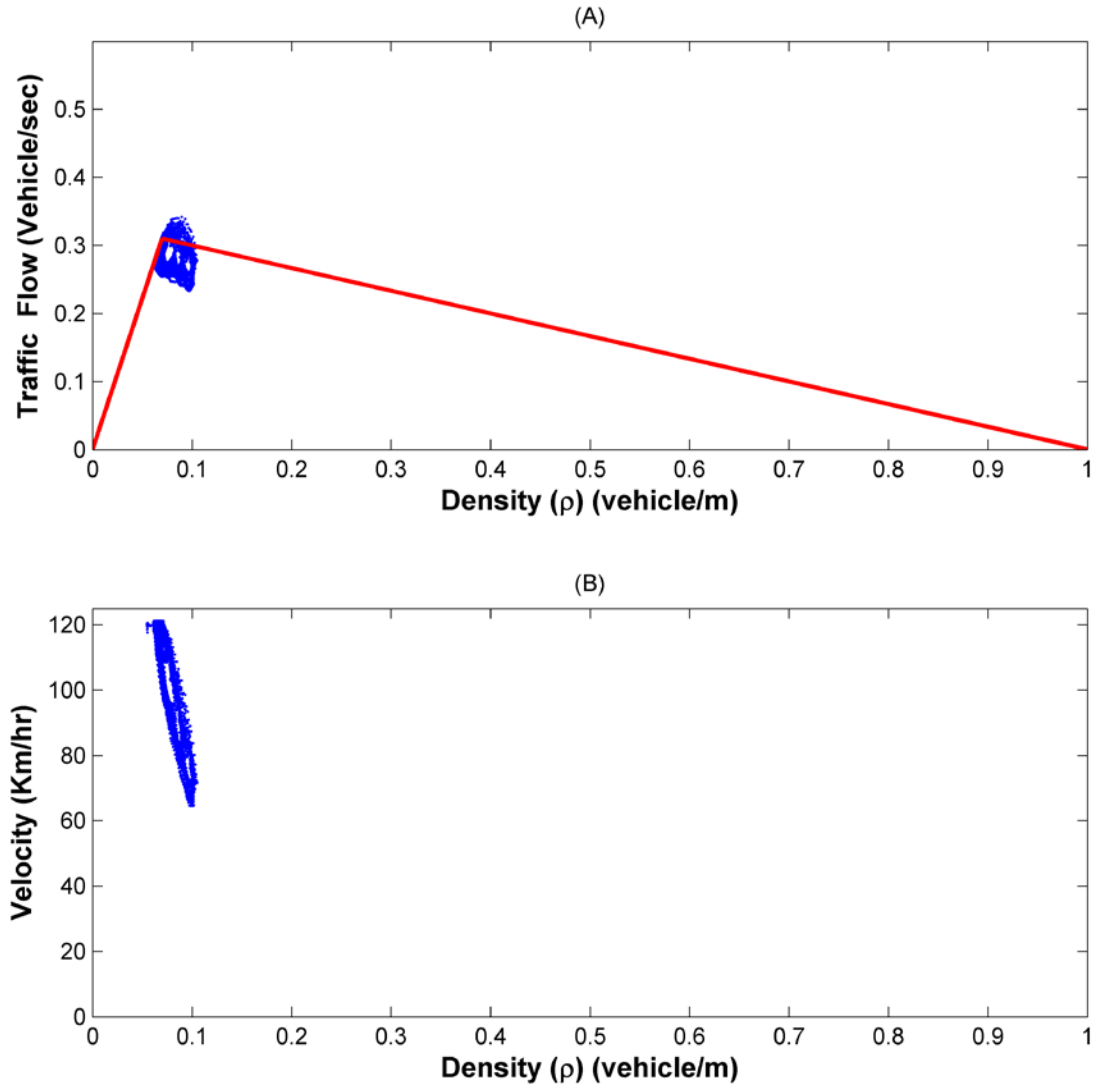

Figure 6-19: Velocity, Density and Traffic flow in Human Driver Behaviour Model with utilising ITS Model with 120 Km/hr desired velocity scenario after solving congestion time

Chapter 7

Comparison among the Models at Passing Distance, Fuel Consumption and Emissions

7.1. Introduction

There are many significant advantages to solving the traffic congestion problem either on urban or highway roads. Time consumed, fuel consumption and environmental issues have been discussed in many ways and with different strategies. This project focuses on similar issues in four scenarios:

I. Human Driver Behaviour,
II. Asymmetric Auto Driving,
III. Symmetric Auto Driving and
IV. Human Driver Behaviour with utilising ITS.

There are four main points we will discuss in this chapter: distance passed by simulation-attended vehicles, simulated traffic flow, simulated fuel consumption and emissions.

7.2. Vehicles' Passing Distance

The basic contrast between the simulation scenarios is vehicles' pass distance during scenarios' simulations, which is observed in Figure 7-1. The Human Driver Behaviour scenario model curve shows the distance passed for vehicles were in the simulation scenarios. The vehicles in the Human Driver Behaviour Scenario Model passed between 25.369 Km and 22.058 Km. The mean of the Human Driver Behaviour Scenario Model is 24.008 Km. The vehicles in this scenario have the

lowest passed distance average. Moreover, the Asymmetric Auto Driving Scenario Model shows the distance passed for vehicles were in the simulation scenarios. The vehicles in the Asymmetric Auto Driving Scenario Model passed between 29.09 Km and 27.77 Km. The mean of the Asymmetric Auto Driving Scenario Model is 28.71 Km. Vehicles in this scenario have the most passed distance average. Also, the Symmetric Auto Driving Scenario Model shows the distances passed for the vehicle were in the simulation scenarios. The vehicles in the Symmetric Auto Driving Scenario Model passed between 28.06 Km and 26.93 Km. The mean of the Human Driver Behaviour Scenario Model is 27.25 Km. Finally, the Human Driver Behaviour with utilising ITS Scenario Model shows the distance passed for vehicles were in the simulation scenarios. The vehicles in the Human Driver Behaviour with utilising ITS Model passed between 25.6 Km and 23.31 Km. the mean of the Human Driver Behaviour Scenario Model is 24.34 Km.

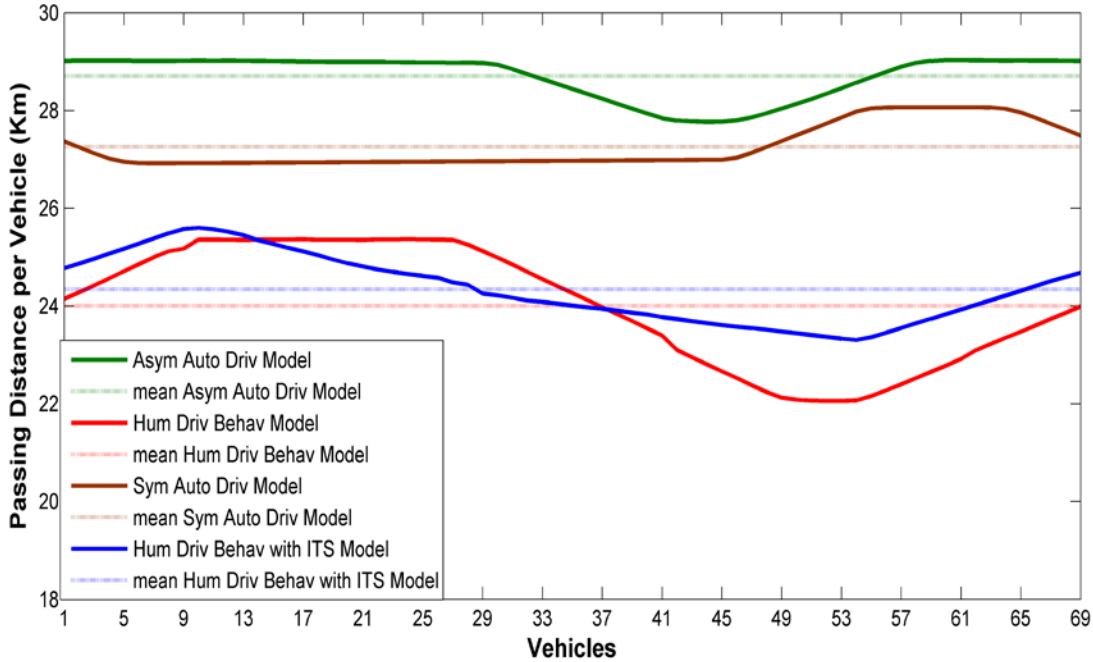

Figure 7-1: Vehicles pass distance during scenario simulation

Figure 7-1 reveals that the maximum average passed distance consists of vehicles in the Asymmetric Auto Driving Scenario Model because of the vehicles' velocity on the congestion zone see Figure 5-35. The second average passed distance belongs to

vehicles in the Symmetric Auto Driving Scenario Model because of the vehicles' velocity on the congestion zone; see Figure 5-41. Conversely, the lowest average passed distance belongs to vehicles in the Human Driver Behaviour Scenario Model because of the vehicles' velocity in the congestion zone. See Figure 5-25. Finally, the average of Human Driver Behaviour with utilising ITS Model is lower than Symmetric Auto Driving Scenario model and Asymmetric Auto Driving Scenario model because of general speed reduction during solving congestion period time Figure 6-7. However, the average of Human Driver Behaviour with utilising ITS Model is higher than the average of Human Driver Behaviour Model because of the general high speed after solving congestion period time, as shown in Figure 6-13.

7.3. Traffic Flow

Traffic flow (TF) results from the multiplication of density (ρ) and velocity (v). See Equation (7-1).

$$TF = \rho \cdot v \tag{7-1}$$

Where the density is defined as the vehicle length, single cell length (L), divided by the safety gap (T) and the vehicle cell length [29].

$$\rho = \frac{L}{(T \cdot v) + L} \tag{7-2}$$

Regarding (**7-1**), Figure 7-2 shows the traffic flow for scenario simulation. The 18-minute Symmetric Auto Driving Scenario model and Asymmetric Auto Driving Scenario model are stable, especially the Symmetric Auto Driving Scenario Model, which is around 15.2 vehicles/second. However, generally, the Asymmetric Auto Driving Scenario Model is stable with limited fluctuation because of acceleration and deceleration factors (α, β) respectively, which is around 16 vehicles/second. Conversely, the traffic flow of the Human Driver Behaviour Scenario Model declines gradually from around 13.5 vehicles/second to 10.5 vehicles/second because of an increase in the number of vehicles that are stationary in the congestion zone, as

shown in Figure 5-25. The last model is Human Driver Behaviour with utilising ITS, where the traffic flow is increased dramatically because of solving to congestion and matching the average velocity. See Figure 6-1 and Figure 6-3.

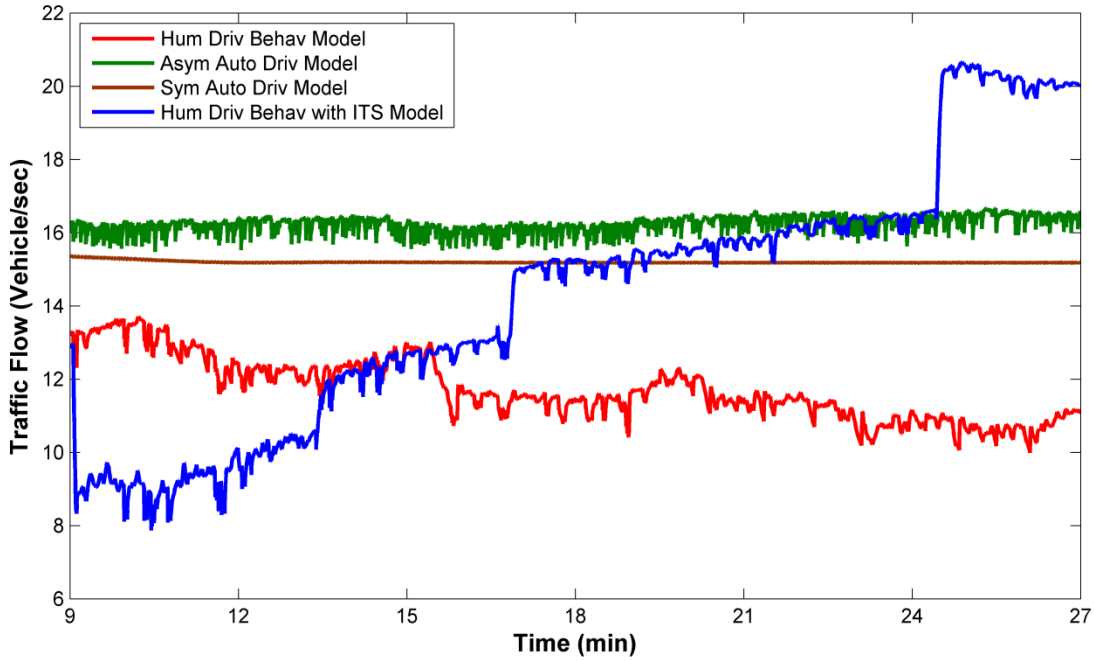

Figure 7-2: Traffic flow during scenarios simulation

7.4. Fuel Consumed

Propulsive work (W), which is the work implemented by the propulsive force as the vehicle moves along its path, will be used as proportional to fuel consumption (z) [91, 92].

$$z = W * r \tag{7-3}$$

Where r is the fuel rate and W is the total propulsive work performed by propulsive force ($P_m(x)$) in travelling from x_1 to x_2 , depicted as:

$$W = \int_{x_1}^{x_2} P_m(x)dx \tag{7-4}$$

Where P is the total resistance of the vehicle plus the acceleration force (E):

$$P_m(x) = \max(E, 0) \tag{7-5}$$

$$E = R_m + H + G_F + M\dot{v} \tag{7-6}$$

Where M is mass of the vehicle, $\dot{v}$ is the acceleration of the vehicle, R_m is inherent resistance to motion, H is any added curvature resistance and G_F is the gradient. R_m will be:

$$R_m = \Gamma U + CA(\rho_{air}/2)v^2 \tag{7-7}$$

Where Γ is the weight of the vehicle, U is the coefficient of rolling resistance for automobiles, C is the air drag coefficient, A is the frontal cross-sectional area of vehicle, ρ_{air} is the air density, and v is velocity [91]. F is:

$$F = \Gamma * \sin\alpha \tag{7-8}$$

As mentioned, propulsive work is proportional to fuel consumption. The fuel consumption has been subject of many studies such as Ahn [19],who produced many models to predict fuel consumption or emission rates, as shown in Appendix (A). Yue [93] began his model from the general format of the VT-Micro mode, which was developed at Virginia Tech to compute mode-specific fuel consumption and emission rates[94].

$$MOE_e = \begin{cases} \sum_{i=0}^{3}\sum_{j=0}^{3} e^{k_{i,j}^{e} v^i a^j} & for\ a \geq 0 \\ \sum_{i=0}^{3}\sum_{j=0}^{3} e^{l_{i,j}^{e} v^i a^j} & for\ a < 0 \end{cases} \tag{7-9}$$

Equation (7-9) is distributed into three parts:

1. **Deceleration Mode** is the instantaneous maneuver from a pre-defined cruising speed to a complete stop. Equation (7-9) is modified to be

$$MOE_e^{decel} = d_0 + d_1 v_c + d_2 v_c^2 + d_3 v_c^3 + d_4 v_c^4 + d_5 v_c^5 + d_6 v_c^6 \qquad (7\text{-}10)$$

Where MOE_e^{decel} is the fuel consumed or pollutants emitted while decelerating (L/s, or mg/s, respectively), v is the vehicle speed (km/h), and d_0, d_1, d_2, d_3, d_4, d_5 and d_6 are vehicle-specific regression coefficients.

In this project, the model that has been used is for high-emission vehicles with engine sizes of less than 5.7 litres [93] to recognise the differences in consumption between the models. Therefore, the coefficient Yue used has been utilised in Appendix (B) [93].

2. **Idling and Cruise Modes** are instantaneous speed of 0 km/h and an instantaneous acceleration rate of 0 km/h/s.

$$MOE_e^{cruise} = e^{k_{0,0}^e + k_{1,0}^e v + k_{2,0}^e v^2 + k_{3,0}^e v^3} \qquad (7\text{-}11)$$

Where MOE_e^{cruise} is the fuel consumed or pollutants emitted while cruising (L/s, or mg/s, respectively) and $k_{i,0}^e$ is vehicle-specific regression coefficients.

Similar to the deceleration model, the model that has been used is for high-emission vehicles [93]; regression coefficients are available in Appendix (B).

3. **Acceleration Mode** is the fuel consumed and pollutants emitted by a vehicle during an acceleration event.

$$MOE_e^{accel} = b_0 + b_1 v_c + b_2 v_c^2 + b_3 v_c^3 + b_4 v_c^4 + b_5 v_c^5 + b_6 v_c^6 \qquad (7\text{-}12)$$

Where MOE_e^{accel} is the fuel consumed or pollutants emitted during acceleration (L/s, or mg/s, respectively) and b_0, b_1, b_2, b_3, b_4, b_5 and b_6 are vehicle-specific regression coefficients.

The model that has been used is for a high-emission vehicle [93], and regression coefficients are available in Appendix (B).

Table 7-1: fuel consumption specification

	Human Driver Behaviour Model	Asymmetric Auto Driving Model	Symmetric Auto Driving Model	Human Driver Behaviour with ITS
Mean	10.1523	10.2897	10.0533	7.2850
Median	10.4025	10.3793	9.9611	7.2658
STD	0.6271	0.1671	0.1679	0.1654
Minimum	9.1190	9.9546	9.8816	7.0203
Maximum	11.1059	10.4824	10.3455	7.6174

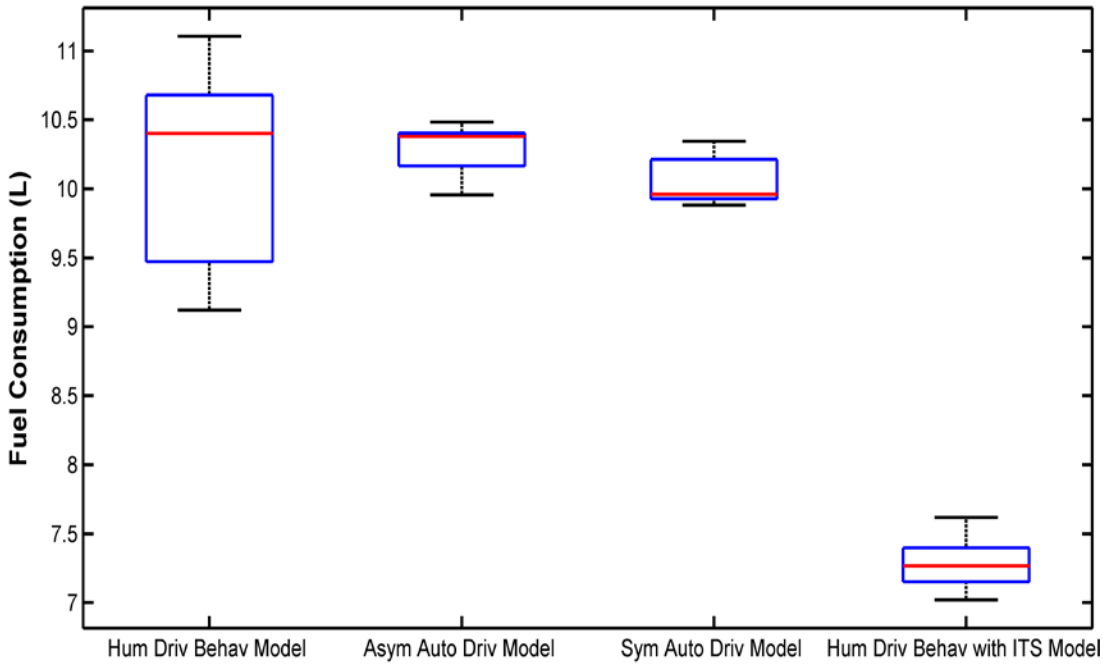

Figure 7-3: Total fuel consumption

Although the Asymmetric Auto Driving Scenario Model's mean vehicle fuel consumption is more than the Human Driver Behaviour Scenario Model's mean vehicle fuel consumption as seen in Table 7-1, Figure 7-3 illustrates that the Human Driver Behaviour Scenario Model makes the vehicles in the simulation consume fuel more than other scenarios. Also, the model has more variety of fuel consumption than approaches because of differing time in the station than in the congestion zone

and the variety of acceleration from the station. Symmetric Auto Driving Scenario model and Asymmetric Auto Driving Scenario model have consumed less fuel than the Human Driver Behaviour Scenario Model. As shown in Table 7-1, the mean of the Asymmetric Auto Driving Scenario Model is higher than the Symmetric Auto Driving Scenario Model. The final model is the Human Driver Behaviour with ITS Scenario. This scenario consumes less fuel than other scenarios because of the elimination of velocity and acceleration because of using ITS. The simulation of fuel consumption specifications is expressed in Table 7-1.

Table 7-2: Fuel consumption rate specification

	Human Driver Behaviour Model	**Asymmetric Auto Driving Model**	**Symmetric Auto Driving Model**	**Human Driver Behaviour with ITS**
Mean (L/Km)	0.4250	0.3618	0.3698	0.2993
Median (L/Km)	0.4226	0.3615	0.3698	0.2996
STD (L/Km)	0.0242	0.0010	0.0013	0.0021
Minimum (L/Km)	0.3752	0.3599	0.3675	0.2957
Maximum (L/Km)	0.4716	0.3645	0.3730	0.3032

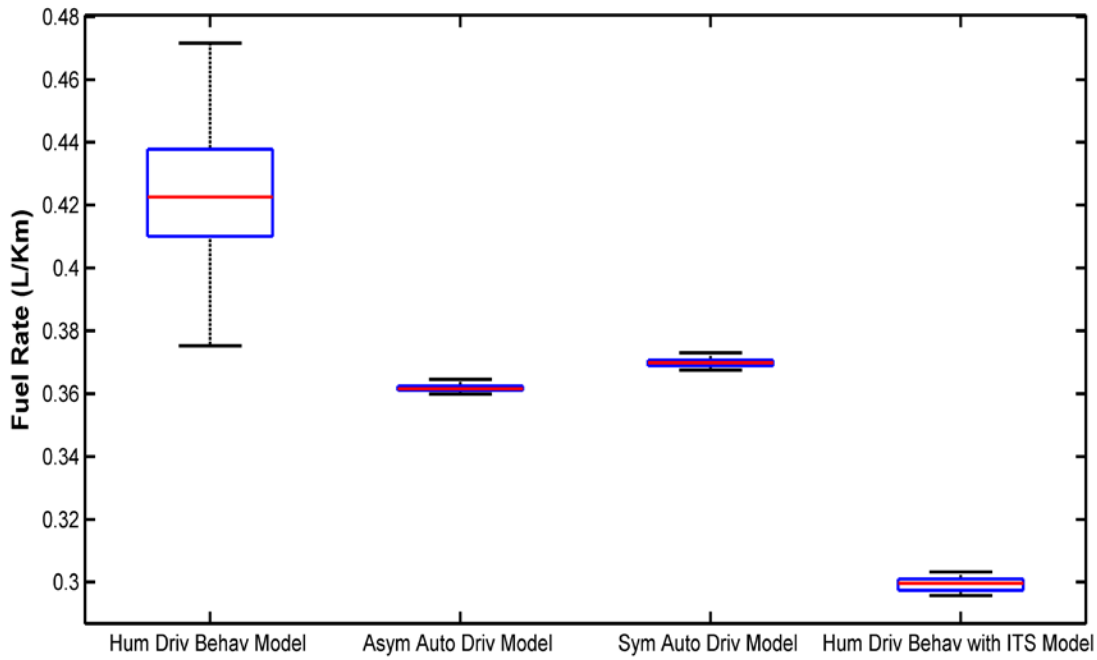

Figure 7-4: Fuel consumption rate

Figure 7-4 relates between Figure 7-1 and Figure 7-3 to reveal how much fuel the vehicle consumes to pass one Kilometer. High fuel consumed in the lowest distance for member vehicles in the Human Driver Behaviour Scenario Model expresses the impact of non-work consumption because of the station situation and the impact of high acceleration from the station situation in the congestion zone. From Figure 7-4 and Table 7-2, we see that the minimum fuel rate consumption for the Human Driver Behaviour Scenario Model vehicles is more than the maximum model consumption rate. Conversely, the vehicles in the Human Driver Behaviour with ITS Scenario Model consume the lowest rate of fuel because of the elimination of acceleration by reducing the desired velocity and solving the congestion. It is observed that the maximum fuel rate consumption for Human Driver Behaviour with ITS Scenario Model vehicles is less than the minimum model consumption rate. The difference between the mean of Human Driver Behaviour with ITS and without ITS scenario models is 0.125 L/Km. Finally, comparing Symmetric Auto Driving Scenario model and Asymmetric Auto Driving Scenario model, the Asymmetric fuel consumption rate is slightly lower than the Symmetric fuel consumption rate because it travelled more distance.

7.5. Emissions

The National Ambient Air Quality Standards (NAAQS) provide threshold concentrations for six pollutants: vehicle borne monoxide (CO), lead (pb), nitrogen dioxide (NO_2), ozone (O_3), particulate matter (PM-10) and sulfur dioxide (SO_2) [93, 103].

Vehicle fuel consumption and emission rates are the main goal of many approaches that have been developed [93]. Based on the VT-Micro mode shown in (7-9) and similar to fuel consumption, Ahn [19] produced many models to predict fuel consumption or emission rates, as depicted in Appendix (A). Furthermore, Yue [93] developed (7-9) and divided it into three parts:

1. **Deceleration Mode** is the instantaneous maneuver from a pre-defined cruising speed to a complete stop. Similar to fuel consumption, Yue created (7-10) with

different regression coefficients. It has utilised the coefficient used by Yue in Appendix (B) [93].

2. Idling and Cruise modes are an instantaneous speed of 0 km/h and an instantaneous acceleration rate of 0 km/h/s. From (7-11) and Yue [93], the regression coefficients of Idling and Cruise modes appear in Appendix (B).

3. Acceleration Mode is the fuel consumed and pollutants emitted by a vehicle during an acceleration event. From (7-12) and Yue [93], the regression coefficients of the Acceleration mode appear in Appendix (B).

7.5.1 CO Emission

CO emission for simulation models has been expressed in Figure 7-5. Regarding the mean total CO emissions in Table 7-3, the Asymmetric Auto Driving Scenario Model is the highest mean CO emission producer because of the average distance passed and the vehicles' average passed the congestion zone. There, each vehicle must produce more CO during high acceleration, so they are the highest. The second model is the Symmetric Auto Driving Scenario for reasons similar to the Asymmetric Auto Driving Scenario Model with less distance and range of vehicles passing the congestion zone. Although the Asymmetric and Symmetric Auto Driving Scenario models' mean vehicle CO emission is more than the Human Driver Behaviour Scenario Model mean vehicle CO emission as seen in Table 7-3, Figure 7-5 shows that the Human Driver Behaviour Scenario Model makes the member vehicles produce more CO emission than other scenarios. Also, that model has more of a variety of CO emissions because of different times in the station and in the congestion zone and a variety of accelerations from the station. The final model is the Human Driver Behaviour with ITS Scenario. This scenario produces the least CO emissions because of the elimination of velocity and acceleration because of the use of ITS.

Table 7-3: CO Emission specification (gram)

	Human Driver Behaviour Model	Asymmetric Auto Driving Model	Symmetric Auto Driving Model	Human Driver Behaviour with ITS
Mean	781.0087	805.6040	787.5893	471.1776
Median	790.9273	808.0065	782.5981	469.4956
STD	47.2352	12.5654	13.3005	12.6752
Minimum	692.5190	774.3534	764.1000	451.4928
Maximum	861.4603	829.8659	816.5901	496.1525

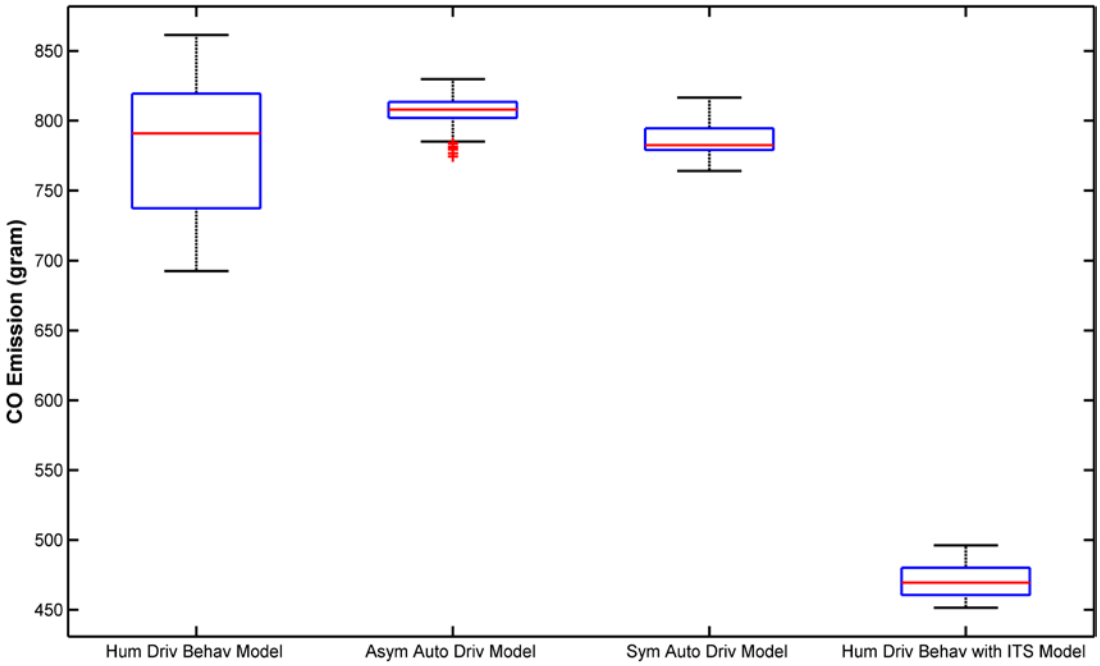

Figure 7-5: CO Emission

Table 7-4: CO emission rate specification (gram/Km)

	Human Driver Behaviour Model	Asymmetric Auto Driving Model	Symmetric Auto Driving Model	Human Driver Behaviour with ITS
Mean	31.2604	26.8853	27.5969	19.3571
Median	31.1942	26.8502	27.5938	19.3613
STD	1.9407	0.1348	0.2036	0.0858
Minimum	27.6409	26.6721	27.0769	19.1770
Maximum	35.1014	27.1974	28.0900	19.5487

Figure 7-6 shows the CO emission rate per Km. Obviously, high fuel consumption and longtime hold in the congestion zone impact the Human Driver Behaviour Scenario Model. Moreover, from Figure 7-6 and Table 7-4, the minimum CO emission rate in the Human Driver Behaviour Scenario Model is higher than the maximum Asymmetric Auto Driving Scenario Model and Human Driver Behaviour with ITS Scenario Model. Similar to fuel rate consumption in Figure 7-4 that vehicles in the Human Driver Behaviour with ITS Scenario Model is the lowest rate of CO emission caused by eliminate of acceleration and solving the congestion. Also, the maximum CO emission rates for Human Driver Behaviour with ITS Scenario Model vehicles is less than the minimum other models. The mean of Human Driver Behaviour with ITS is less than two-third of the mean of Human Driver Behaviour Scenario models. Finally, Symmetric Auto Driving is slightly higher than the Asymmetric Auto Driving Scenario Model because of the distance passed.

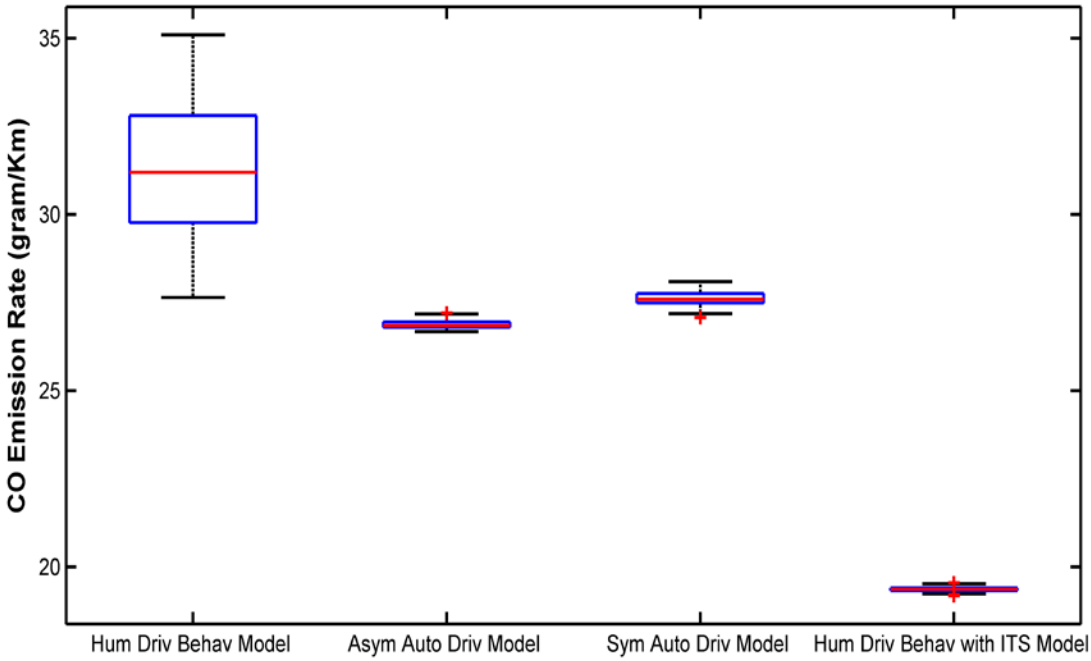

Figure 7-6: CO emission rate

7.5.2 CO_2 Emission

Table 7-5: CO_2 Emission specification (gram)

	Human Driver Behaviour Model	Asymmetric Auto Driving Model	Symmetric Auto Driving Model	Human Driver Behaviour with ITS
Mean	5734.7	5850.3	5697.8	4182.4
Median	5874.3	5899.5	5643.4	4171.6
STD	366.9453	96.6079	98.1443	110.6677
Minimum	5137.1	5658.1	5598.0	4005.0
Maximum	6294.9	5961.6	5867.3	4394.3

CO_2 emission for simulation models has been expressed in Figure 7-7. Regarding the mean total CO_2 emission in Table 7-5, the Asymmetric Auto Driving Scenario Model is the highest mean CO_2 emission producer because of the average distance passed and the vehicles' average passed the congestion zone, where each vehicle has to produce more CO_2 during the high acceleration, is the highest. The second highest model is the Human Driver Behaviour Scenario Model because of being stationary in the congestion zone with rapid acceleration and deceleration to move out of the hold station. Although the Asymmetric Auto Driving Scenario Model's mean vehicle CO_2 emission is more than Human Driver Behaviour Scenario Model mean vehicle CO_2 Emission as seen in Table 7-5, Figure 7-7 shows that the Human Driver Behaviour Scenario Model makes the member vehicles produce CO_2 emission more than other scenarios. Also, the model has more variety of CO_2 emissions because of different time in station that in congestion zone and variety of acceleration from station. The Symmetric Auto Driving Scenario is the third-highest mean CO_2 emission for the same reason as the Asymmetric Auto Driving Scenario Model with less distance and range of vehicles passing the congestion zone. The final model is the Human Driver Behaviour with ITS Scenario. This scenario is the lowest CO_2 emission producer of all scenarios because of the elimination of velocity and acceleration because of using ITS.

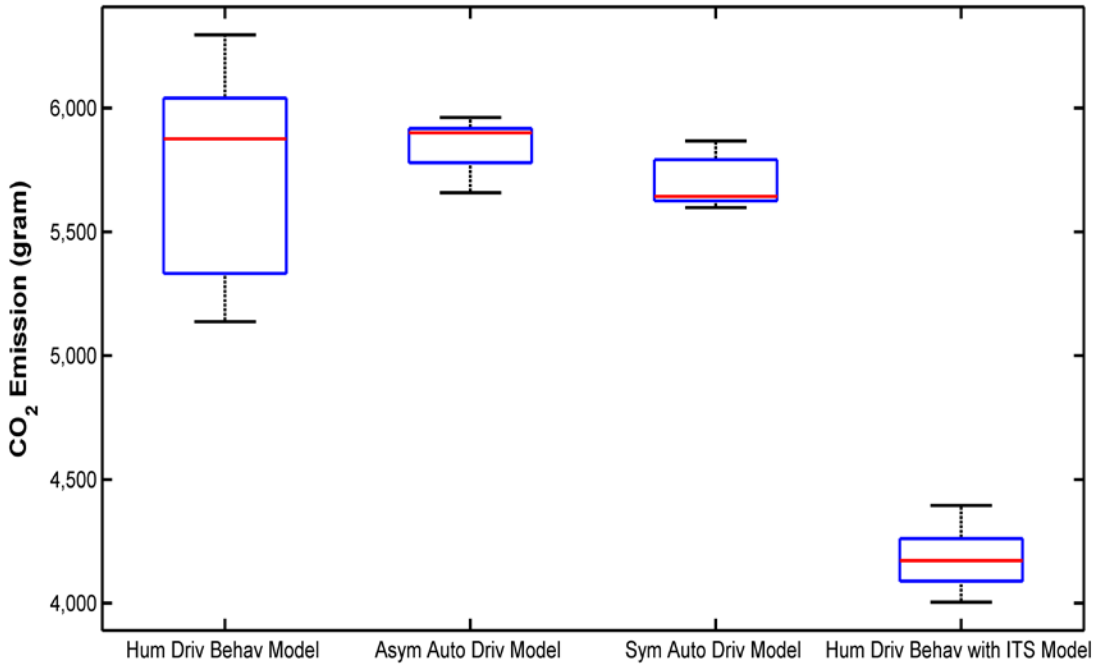

Figure 7-7: CO_2 emission

Figure 7-8 shows the CO_2 emission rate per Km. Clearly high fuel consumption and longtime hold in the congestion zone affect the Human Driver Behaviour Scenario Model. Moreover, in Figure 7-8 and Table 7-6, we see the minimum CO_2 emission rate in the Human Driver Behaviour Scenario Model is higher than the maximum of the other models. In Figure 7-8, vehicles in the Human Driver Behaviour with ITS Scenario Model have the lowest rate of CO_2 emissions caused by the elimination of acceleration and solving congestion. Also, the maximum CO_2 emission rates for Human Driver Behaviour with ITS Scenario Model vehicles is less than the minimum of other models. The mean of Human Driver Behaviour with ITS is less than three-quarters of the mean of Human Driver Behaviour Scenario models. Finally, Symmetric Auto Driving is slightly higher than Asymmetric Auto Driving Scenario Model because of the distance passed.

Table 7-6: CO2 emission rate specification (gram/Km)

	Human Driver Behaviour Model	**Asymmetric Auto Driving Model**	**Symmetric Auto Driving Model**	**Human Driver Behaviour with ITS**
Mean	240.3276	206.0089	209.9334	171.8261
Median	238.3704	205.8492	209.9386	171.7876
STD	13.9995	0.5991	0.7925	0.6494
Minimum	211.5381	204.9631	208.5417	170.6302
Maximum	266.9625	207.4860	211.9061	173.4269

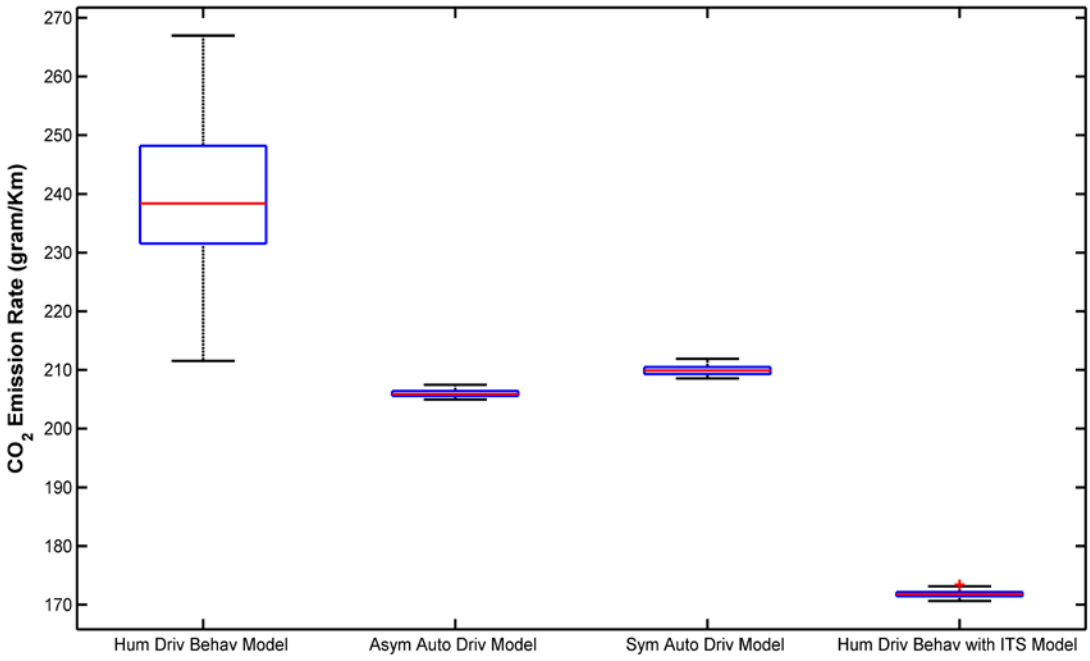

Figure 7-8: CO_2 emission rate

7.5.3 HC Emissions

Table 7-7: HC emission specification (gram)

	Human Driver Behaviour Model	Asymmetric Auto Driving Model	Symmetric Auto Driving Model	Human Driver Behaviour with ITS
Mean	26.9110	29.0844	27.1248	20.2003
Median	26.4705	29.0020	27.2620	20.2271
STD	2.1861	0.6215	0.5746	0.4354
Minimum	23.0444	27.8930	25.5016	19.4427
Maximum	33.9642	30.5963	27.9829	20.9223

The HC emission for simulation models has been expressed in Figure 7-9. Regarding the mean total HC emissions in Table 7-7, the Asymmetric Auto Driving Scenario Model is the highest mean HC emission producer because of the average distance passed and the vehicles' average passing the congestion zone, where each vehicle has to produce more HC during high acceleration. The second model is the Symmetric Auto Driving Scenario for reasons similar to the Asymmetric Auto

Driving Scenario Model with less distance and range of vehicles passing the congestion zone. Although the Asymmetric and Symmetric Auto Driving Scenario models' mean vehicle HC emissions are more than the Human Driver Behaviour Scenario Model's mean vehicle HC emission, as seen in Table 7-7, Figure 7-9 shows that the Human Driver Behaviour Scenario Model makes the member vehicles produce more HC emissions than other scenarios. Also, the model has more variety of HC emissions because of different times in station in the congestion zone and variety of acceleration from the station. The last model is the Human Driver Behaviour with ITS Scenario. This scenario is a lower HC emission producer than other scenarios because of the elimination of velocity and acceleration because of using ITS.

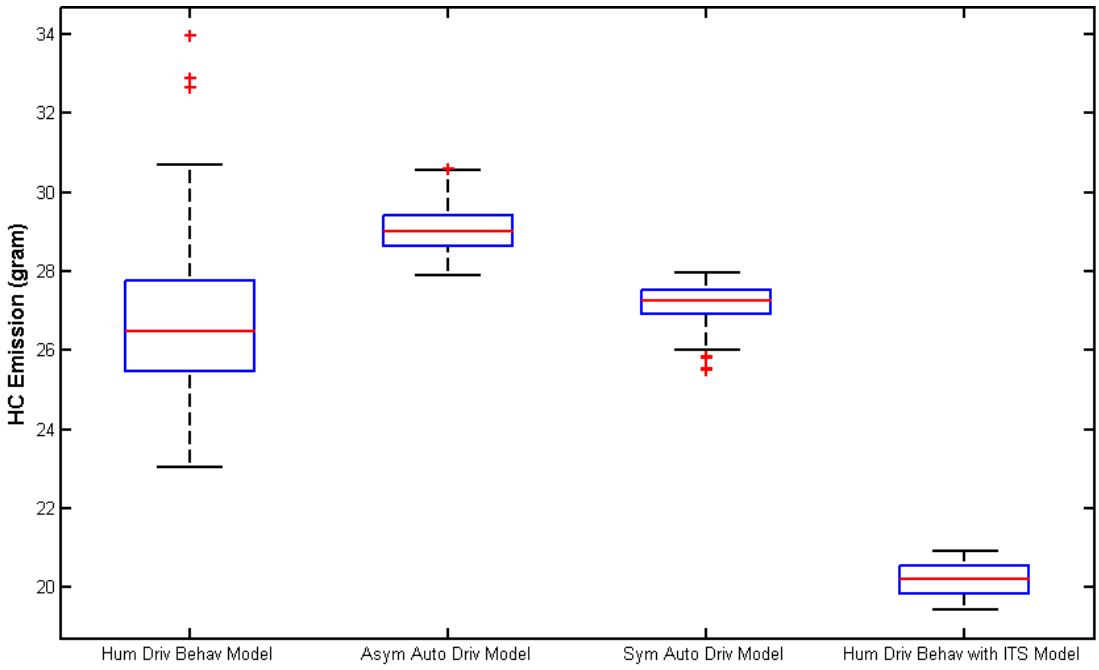

Figure 7-9: HC emission

Table 7-8: HC emission rate specification (gram/Km)

	Human Driver Behaviour Model	Asymmetric Auto Driving Model	Symmetric Auto Driving Model	Human Driver Behaviour with ITS
Mean	0.9936	0.8526	0.8602	0.8300
Median	0.9753	0.8486	0.8648	0.8325
STD	0.0679	0.0118	0.0107	0.0068
Minimum	0.8853	0.8397	0.8289	0.8174
Maximum	1.1846	0.8798	0.8752	0.8400

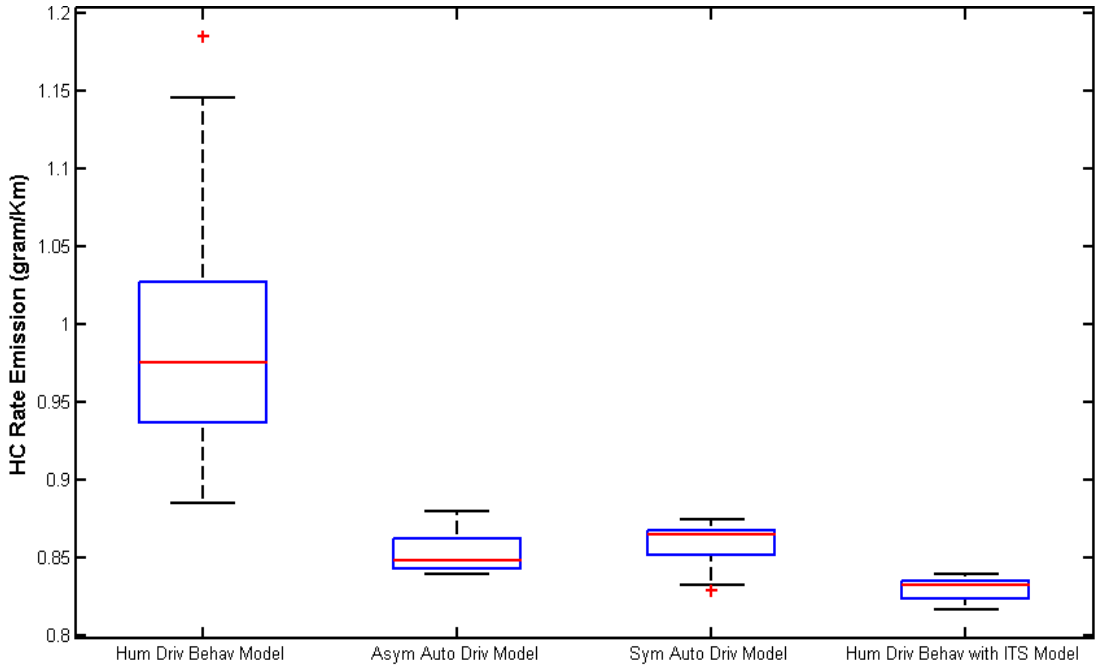

Figure 7-10: HC emission rate

Figure 7-10 shows the HC emission rate per Km. Obviously, high fuel consumption and longtime hold in the congestion zone affect the Human Driver Behaviour Scenario Model. Moreover, we can see from Figure 7-10 and Table 7-8 that the minimum HC emission rate in the Human Driver Behaviour Scenario Model is higher than the maximum of the Asymmetric Auto Driving Scenario Model and Human Driver Behaviour with ITS Scenario Model. Similar to the fuel rate consumption in Figure 7-10, vehicles in the Human Driver Behaviour with ITS Scenario Model have the lowest rate of HC emissions caused by the elimination of acceleration and solvation to congestion. Also, the maximum HC emission rates for Human Driver Behaviour with ITS Scenario Model vehicles is less than the minimum of the other models. The mean of Human Driver Behaviour with ITS is less than two-thirds of the mean of Human Driver Behaviour Scenario models.

7.5.4 NOx Emission

Table 7-9: NO_x emission specification (gram)

	Human Driver Behaviour Model	Asymmetric Auto Driving Model	Symmetric Auto Driving Model	Human Driver Behaviour with ITS
Mean	9.0982	10.0042	9.4168	3.3723
Median	9.0113	10.0339	9.4118	3.3415
STD	0.8192	0.2304	0.2173	0.1199
Minimum	7.5666	9.4455	8.8637	3.2098
Maximum	11.3660	10.5117	9.8295	3.6311

The NO_x emissions for simulation models has been expressed in Figure 7-11. Regarding the mean total NO_x emission in Table 7-9, the Asymmetric Auto Driving Scenario Model is the highest mean NO_x emission producer because of the average distance passed and the average vehicles passing the congestion zone, where each vehicle has to produce more NO_x during high acceleration. The second model is the Symmetric Auto Driving Scenario for reasons similar to the Asymmetric Auto Driving Scenario Model with less distance and range of vehicles passing the congestion zone. Although the Asymmetric and Symmetric Auto Driving Scenario models' mean vehicle NO_x emissions are more than the Human Driver Behaviour Scenario Model's mean vehicle NO_x emissions as seen in Table 7-9, Figure 7-11 shows that the Human Driver Behaviour Scenario Model makes member vehicles produce more NO_x emissions than other scenarios. Also, the model has more variety in NO_x emissions because of differerent time in station in the congestion zone and variety of acceleration from the station. The final model is the Human Driver Behaviour with ITS Scenario. This scenario is the lowest NO_x emission producer of all the scenarios because of the elimination of velocity and acceleration because of using ITS.

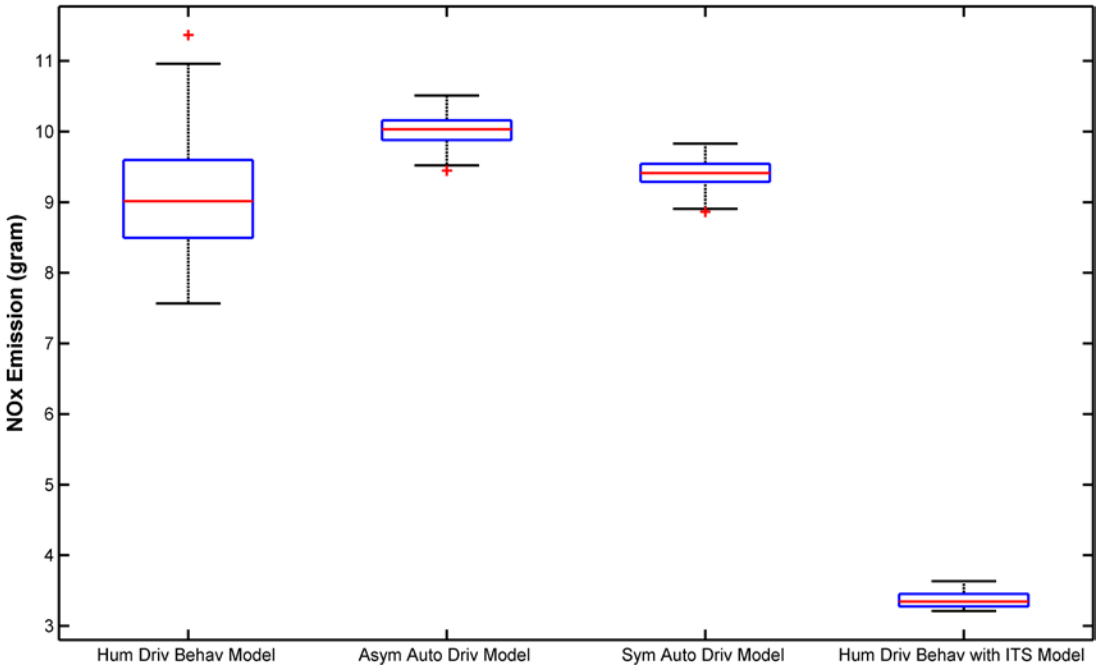

Figure 7-11: NO_x emission

NO_x emissions for simulation models have been expressed in Figure 7-12. Regarding the mean total NO_x emissions in Table 7-10, the Asymmetric Auto Driving Scenario Model is the highest mean NO_x emission producer because of the average distance passed. The vehicles' average passing the congestion zone, where each vehicle has to produce more NO_x during high acceleration, are the highest. The second model is the Symmetric Auto Driving Scenario for the same reason as the Asymmetric Auto Driving Scenario Model with less distance and range of vehicles passing the congestion zone. Although the Asymmetric and Symmetric Auto Driving Scenario models' mean vehicle NO_x emission is more than the Human Driver Behaviour Scenario Model's mean vehicle NO_x emission as seen in Table 7-10, Figure 7-12 shows that the Human Driver Behaviour Scenario Model makes the member vehicles produce NO_x emission more than other scenarios. Also, the model has more variety in NO_x emissions because of the different time in station from the congestion zone and variety of acceleration from the station. The final model is the Human Driver Behaviour with ITS Scenario. This scenario is the lowest NO_x emission producer of all the scenarios because of the elimination of velocity and acceleration because of using ITS.

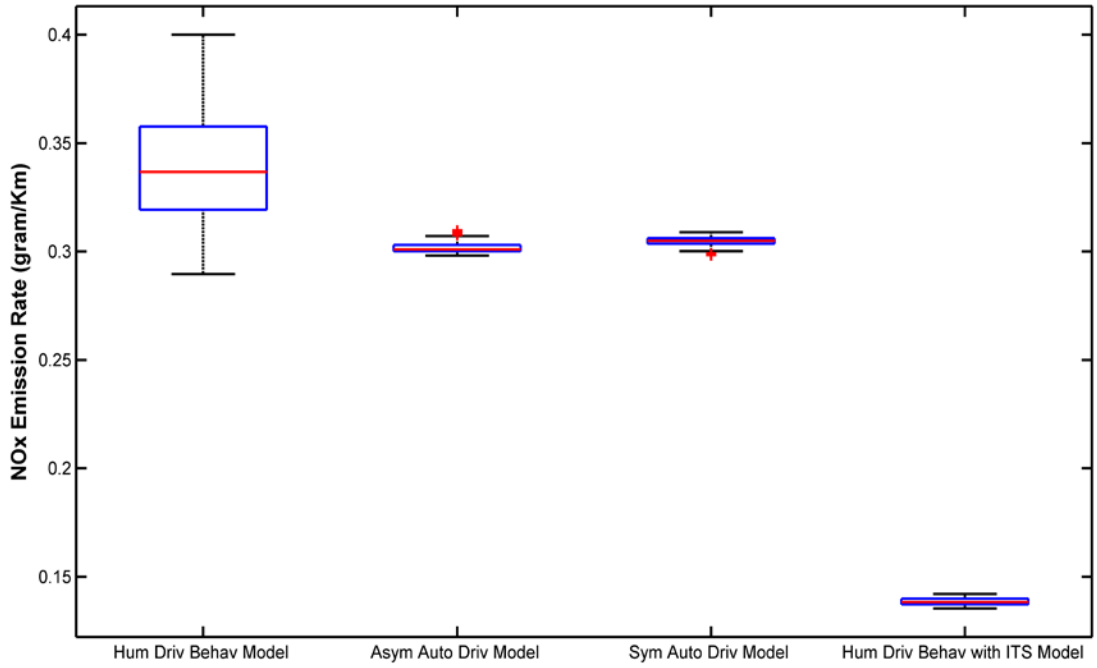

Figure 7-12: NO_x emission rate

Table 7-10: NO_x emission rate specification (gram/Km)

	Human Driver Behaviour Model	Asymmetric Auto Driving Model	Symmetric Auto Driving Model	Human Driver Behaviour with ITS
Mean	0.3375	0.2730	0.3494	0.2439
Median	0.3391	0.2731	0.3510	0.2468
STD	0.0209	0.0016	0.0045	0.0179
Minimum	0.2931	0.2694	0.3375	0.1113
Maximum	0.3780	0.2761	0.3548	0.2584

Chapter 8

Conclusion and Future Work

8.1. Summary

In the third chapter, Cellular Automata (CA) is modified to Dynamic Traffic Cellular Automata (DTCA) to avoid the lack of intuitive appeal. Cells in the DTCA are removed except for acting members' vehicles. DTCA changes the four steps for subsequent movements from discreteness to be integral. The probability of decreasing the vehicle velocity by using one variable was changed to using three variables, which are acceleration factor, deceleration factor and reaction factor, to increase the realism in the simulation approach. Compression between the acceleration factor and deceleration factor play a key role in accelerating and decelerating in DTCA. Conversely, the reaction factor expresses the delay of the vehicle to take action especially from a stationary situation. A speed conflict between the lead vehicle and the following vehicle is affecting relative velocity and relative position. Startup from stationary delay modelling has been tested and applied to the DTCA model. Because of the DTCA model, we found a traffic flow matrix with mathematical definitions of acceleration, velocity and position.

In the fourth chapter, a simulation of driver behaviour utilising a FUZZY Logic controller (FLC) has been performed in this research. Simulation traffic was running

in a one-lane loop for vehicles that have an Astrom first-order model. Four types of simulation were performed: Human Driver Behaviour for simulating a human driving, Asymmetric Auto Driving for simulating automatic vehicles in different models or brands, Symmetric Auto Driving for simulating automatic vehicles in similar models or brands and Human Driver Behaviour with utilising ITS for simulating a human driving with utilising ITS. The vehicle controller received five inputs for Human Driver Behaviour and Human Driver Behaviour with utilising ITS, four inputs for Asymmetric Auto Driving and three inputs for Symmetric Auto Driving. Adjusting the sensor signal by using the FUZZY Logic Controller depends on the signals coming from ITS, that is, the way of solving congestion in the Human Driver Behaviour with utilising ITS Model.

In the fifth chapter, a variety of Human Driver Behaviour Model approaches, from 20 Km/hr to 140 Km/h desired speeds, have been discussed. The time required to solve congestion was reduced from a 20 Km/hr to 60 Km/hr desired speed because of reduction time between moving the congestion's lead vehicle and the ability of new congestion's lead vehicle to move comparing of time arriving ability a new vehicle to the congestion queue. Conversely, more than a 60 Km/hr desired speed meant that the time required to solve congestion rose gradually because of the decreasing of the ability of a lead vehicle in congestion after moving the previous lead vehicle is less than decreasing the arriving ability of a new vehicle to the congestion queue is reduced. Moreover, more than a 100 Km/hr desired speed found that the congestion cannot solve because the ability of a new vehicle to arrive at the congestion queue is less than the ability of congestion's lead vehicle after moving previous congestion's lead vehicle. Also, the 140 Km/hr desired speed scenario found the relation of the ability of congestion's lead vehicle after moving previous lead to arriving ability a new vehicle to the congestion queue and impulsiveness of the vehicles come into congestion, which leads the scenario to vehicles accident. Conversely, Auto Driving, Asymmetric and Symmetric models haven't solved the congestion because the ability of a congestion's lead vehicle after moving the previous lead is less than the decreasing of arriving ability of a new vehicle to the congestion queue. The density impact on the traffic flow and velocity has been expressed in the models with 120 Km/hr desired speed.

In the sixth chapter, getting the benefit of using ITS on the Human Driver Behaviour Model has been expressed in this project to share the data between vehicle clusters.

Approaching member vehicles after detecting congestion started utilising the gap signal-detecting controller. Eliminating the density of traffic flow by controlling the gap among vehicles entering the congestion leads to a reduction in velocity and an increase in the time of arriving ability of a new vehicle to the congestion queue. The gap controller receives the signal from detecting sensor, converts it to suitable signal and sends it to the Human Driver Behaviour Model controller. The gap controller shows less than a real gap to the Human Driver Behaviour Model controller. The unreal signal forces the Human Driver Behaviour Model controller to reduce the vehicles' velocity. The reduction of velocity increases the time ability of new vehicles arriving to congestion. After a certain time, the congestion starts solving because the number of vehicles leaving the congestion is higher than the number of vehicles in it. After the solving time, period relation between density and traffic flow of all data are around the critical density point.

In seventh chapter, different implications have been stated in this project, such as average passed distance, the average of instantaneous traffic flow, total fuel consumption and total different emissions. The average of passed distance for a vehicle belonging to the Human Driver Behaviour with utilising ITS Model is less than Asymmetric and Symmetric auto driving models because the speed declines during solving period time, but is more than the Human Driver Behaviour Model. Asymmetric and symmetric auto driving models have stability in traffic flow during approaches. Human Driver Behaviour Model traffic flow is reduced because of an increase in the queue of the congestion. However, the Human Driver Behaviour with utilising ITS Model rises gradually with the increase of the velocity. Fuel consumption and emissions produced indicate that the Human Driver Behaviour with utilising ITS model has the lowest amount of fuel consumption and emissions producing in the total average of vehicles or per certain distance average.

8.2. Conclusion

- Cellular Automata (CA) is modified to Dynamic Traffic Cellular Automata (DTCA) to simulate traffic flow with its congestion. DTCA model has Acceleration factor, deceleration as controlling factors in the acceleration and deceleration. In addition, reaction factor is controlling the making decision.

- Traffic flow matrix has been modified to understand the relation among the vehicles to reduce the congestion.
- Modifying FUZZY Logic as a common controller to control the vehicles has Astrom first-order model. The vehicles are running in one lane loop to make traffic flow with initiated congestion. There are four scenarios has been established: Human Driver Behaviour, Asymmetric Auto Driving, Symmetric Auto Driving and Human Driver Behaviour with utilising ITS models.
- The benefit of using the communication network technology among vehicles to sense the distance and speed of others on the road has been investigated. There are many benefits has been done: solving the congestion, reducing the fuel consumption and reducing the emissions.

8.3. Suggestion for Future Work

In future, I would like to extend on my present work to cover diverse range traffic flow situations. There are many ways to improve this research by comprehensive descriptions of mathematical modelling of vehicles, drivers, as well as different road conditions.

- In this study, the sizes of vehicles are assumed to be the same. Vehicle size are taken to be equal to cell length, which is 7.5 meters. In reality, the vehicle sizes are not fixed; their sizes range from small cars to an articulated road truck. Therefore, the vehicle model can be improved in terms of the sizes of the member vehicles in a queue rather than being fixed.
- The mathematical description of vehicles can be made more realistic by considering different automotive gears that the vehicles are in. Then driving in each gear can be described by different equations. Changing the gears during driving will make the mathematical model more complex and but much more realistic.
- The model used to indicate emissions and fuel consumption need further improvement to enable differentiation between small and large vehicles. For example, a small vehicle, which has four cylinders, consumes less fuel than a large vehicle, which might have six or eight cylinders

- In the model, the standard deviation of drivers' reaction is limited. In real life, the mathematical modelling of drivers could be different; for example, some drivers are in a hurry, or nervous or intoxicated while others are not.
- In this project, the highway is single lane and there is no attempt to change lanes. Therefore, the road model can be improved by considering multiple lanes, emerging lanes and exits.

REFERENCES

[1] I. E. Schneider, *et al.*, "Quality of Life: Assessment for Transportation Performance Measures," St. Paul, MN: MN DOT2013.

[2] M. D. Meyer, "Demand management as an element of transportation policy: using carrots and sticks to influence travel behavior," *Transportation Research Part A: Policy and Practice,* vol. 33, pp. 575-599, 1999.

[3] A. Kesting, "Microscopic Modeling of Human and Automated Driving: Towards Traffic-Adaptive Cruise Control," Doctoral thesis, Faculty of Traffic Sciences, Dresden University of Technology, Germany, 2008.

[4] C. J. G. van Driel, *et al.*, "Impacts of a Congestion Assistant on driving behaviour and acceptance using a driving simulator," *Transportation Research Part F: Traffic Psychology and Behaviour,* vol. 10, pp. 139-152, 2007.

[5] S. Thrun, "Toward robotic cars," *Communications of the ACM,* vol. 53, pp. 99-106, 2010.

[6] A. Kesting, *et al.*, "Adaptive cruise control design for active congestion avoidance," *Transportation Research Part C: Emerging Technologies,* vol. 16, pp. 668-683, 2008.

[7] G. H. Engelman, *et al.*, "Adaptive vehicle cruise control system and methodology," ed: Google Patents, 2001.

[8] R. Holve, *et al.*, "Adaptive fuzzy control for driver assistance in car-following," *Proc. 3rd EUFIT,* pp. 1149-1153, 1995.

[9] M. McDonald, *et al.*, "Development of a fuzzy logic based microscopic motorway simulation model," in *Intelligent Transportation System, 1997. ITSC'97., IEEE Conference on*, 1997, pp. 82-87.

[10] M. Plöchl and J. Edelmann, "Driver models in automobile dynamics application," *Vehicle System Dynamics,* vol. 45, pp. 699-741, 2007/07/01 2007.

[11] S. P. Hoogendoorn and P. H. L. Bovy, "State-of-the-art of vehicular traffic flow modelling," *Proceedings of the Institution of Mechanical Engineers, Part I: Journal of Systems and Control Engineering,* vol. 215, pp. 283-303, 2001.

[12] A. Kesting, *et al.*, "Agents for traffic simulation," *arXiv preprint arXiv:0805.0300,* 2008.

[13] D. Helbing, "Theoretical foundation of macroscopic traffic models," *Physica A: Statistical Mechanics and its Applications,* vol. 219, pp. 375-390, 1995.

[14] D. Helbing, "Traffic and related self-driven many-particle systems," *Reviews of modern physics,* vol. 73, p. 1067, 2001.

[15] X. Yan, *et al.*, "An inexact transportation planning model for supporting vehicle emissions management," *Journal of Environmental Informatics,* vol. 15, pp. 87-98, 2010.

[16] F.-Y. Wang, "Parallel control and management for intelligent transportation systems: Concepts, architectures, and applications," *Intelligent Transportation Systems, IEEE Transactions on,* vol. 11, pp. 630-638, 2010.

[17] J. M. Cooper, *et al.*, "An investigation of driver distraction near the tipping point of traffic flow stability," *Human Factors: The Journal of the Human Factors and Ergonomics Society,* vol. 51, pp. 261-268, 2009.

[18] M. Moussaïd, *et al.*, "How simple rules determine pedestrian behavior and crowd disasters," *Proceedings of the National Academy of Sciences,* vol. 108, pp. 6884-6888, 2011.

[19] K. Ahn, "Microscopic fuel consumption and emission modeling," Virginia Polytechnic Institute and State University, 1998.

[20] B. Chen and H. H. Cheng, "A review of the applications of agent technology in traffic and transportation systems," *Intelligent Transportation Systems, IEEE Transactions on,* vol. 11, pp. 485-497, 2010.

[21] B. S. Kerner, *The physics of traffic: empirical freeway pattern features, engineering applications, and theory*. New York: Springer, 2004.

[22] M. J. Cassidy and R. L. Bertini, "Some traffic features at freeway bottlenecks," *Transportation Research Part B: Methodological,* vol. 33, pp. 25-42, 1999.

[23] D. Chowdhury, *et al.*, "Statistical physics of vehicular traffic and some related systems," *Physics Reports,* vol. 329, pp. 199-329, 2000.

[24] Y. Sugiyama, *et al.*, "Traffic jams without bottlenecks—experimental evidence for the physical mechanism of the formation of a jam," *New Journal of Physics,* vol. 10, p. 033001, 2008.

[25] T. Nagatani, "The physics of traffic jams," *Reports on Progress in Physics,* vol. 65, p. 1331, 2002.

[26] K. Nagel and M. Schreckenberg, "A cellular automaton model for freeway traffic," *Journal de Physique I,* vol. 2, pp. 2221-2229, 1992.

[27] S. C. Benjamin, *et al.*, "Cellular automata models of traffic flow along a highway containing a junction " *Journal of Physics A: Mathematical and General,* vol. 29, pp. 3119-3127, 1996.

[28] N. Wu and W. Brilon, "Cellular Automata for Highway Traffic Flow Simulation," in *Proceedings 14th International Symposium on Transportation and Traffic Theory,* A. Ceder, Ed., ed Jerusalem, 1999, pp. 1-18.

[29] S. Maerivoet and B. De Moor, "Cellular automata models of road traffic," *Physics Reports,* vol. 419, pp. 1-64, 2005.

[30] R. Omrani and L. Kattan, "Demand and Supply Calibration of Dynamic Traffic Assignment Models," *Transportation Research Record: Journal of the Transportation Research Board,* vol. 2283, pp. 100-112, 2012.

[31] T. Luspay, *et al.*, "On acceleration of traffic flow," in *Proceedings of the 13th International IEEE Conference on Intelligent Transportation Systems (ITSC 2010)*, 2010, pp. 741-746.

[32] R. Jiang, *et al.*, "Full velocity difference model for a car-following theory," *Physical Review E,* vol. 64, p. 017101, 2001.

[33] M. Treiber, *et al.*, "Congested traffic states in empirical observations and microscopic simulations," *Physical Review E,* vol. 62, pp. 1805-1824, 2000.

[34] A. Kesting, *et al.*, "Enhanced intelligent driver model to access the impact of driving strategies on traffic capacity," *Philosophical Transactions of the Royal Society A: Mathematical, Physical and Engineering Sciences,* vol. 368, pp. 4585-4605, October 13, 2010 2010.

[35] G. Giacomin, *et al.*, "Deterministic and stochastic hydrodynamic equations arising from simple microscopic model systems," *Mathematical Surveys and Monographs,* vol. 64, pp. 107-152, 1998.

[36] C. E. Seah and H. Inseok, "Stochastic Linear Hybrid Systems: Modeling, Estimation, and Application in Air Traffic Control," *Control Systems Technology, IEEE Transactions on,* vol. 17, pp. 563-575, 2009.

[37] H. K. Lee, *et al.*, "Mechanical restriction versus human overreaction triggering congested traffic states," *Physical Review Letters,* vol. 92, p. 238702, 2004.

[38] W. Knospe, *et al.*, "Human behavior as origin of traffic phases," *Physical Review E,* vol. 65, p. 015101, 2001.

[39] M. Schreckenberg, "Neue Perspektiven des Verkehrsmanagements," *e & i Elektrotechnik und Informationstechnik,* vol. 124, pp. 90-95, 2007.

[40] P. G. Gipps, "A behavioural car-following model for computer simulation," *Transportation Research Part B: Methodological,* vol. 15, pp. 105-111, 1981.

[41] G. F. Newell, "Nonlinear effects in the dynamics of car following," *Operations Research,* vol. 9, pp. 209-229, 1961.

[42] K. Rickert, *et al.*, "Two lane traffic simulation using cellular automata," *Physica A,* vol. 231, pp. 534-550, 1996.

[43] X.-s. Li, *et al.*, "Traffic Accident Propagation Properties and Control Measures for Urban Links Based on Cellular Automata," *Advances in Mechanical Engineering,* vol. 2013, 2013.

[44] M. Treiber and A. Kesting, "Cellular Automata," in *Traffic Flow Dynamics*, ed: Springer Berlin Heidelberg, 2013, pp. 225-238.

[45] R. Feldberg, *et al.*, "Recursive definition of global cellular-automata mappings," *Physical Review E,* vol. 49, pp. 1699-1711, 1994.

[46] J. Esser, *et al.*, "Microscopic online simulations of urban traffic," in *14th International Symposium on Transportation and Traffic Theory*, 1999.

[47] K. Nagel, *et al.*, "Iterated transportation simulations for Dallas and Portland," Los Alamos National Lab., NM (United States)1998.

[48] R. J. Weiland and L. B. Purser, "Intelligent transportation systems," *Transportation in the New Millennium,* 2000.

[49] G. S. Tewolde, "Sensor and network technology for intelligent transportation systems," in *Electro/Information Technology (EIT), 2012 IEEE International Conference on*, 2012, pp. 1-7.

[50] Y. Wan, *et al.*, "Urban road congestion, capacity expansion and port competition: empirical analysis of US container ports," *Maritime Policy & Management,* vol. 40, pp. 417-438, 2013/09/01 2013.

[51] V. R. Tom, *et al.*, "A cooperative multiagent system for traffic management and control," presented at the Proceedings of the fourth international joint conference on Autonomous agents and multiagent systems, The Netherlands, 2005.

[52] X. Gang, *et al.*, "Parallel Traffic Management for the 2010 Asian Games," *Intelligent Systems, IEEE*, vol. 25, pp. 81-85, 2010.

[53] S. Y. Aye, "Design and construction of LAN based car traffic control system," *Word Academy of Science, Engineering and Technology*, vol. 46, 2008.

[54] USDT and FHWA. (2013). *The Congestion Problem*. Available: http://ops.fhwa.dot.gov/publications/congestionpricing/sec1.htm

[55] D. L. Schrank and T. J. Lomax, *The 2007 urban mobility report*: Texas Transportation Institute, Texas A & M University, 2007.

[56] C. K. Toh, *et al.*, "Highlights: IEEE ITS Society Technical Committee on Mobile Communications Networks for ITS [Technical Committees]," *Intelligent Transportation Systems Magazine, IEEE*, vol. 4, pp. 33-35, 2012.

[57] J. Blum and A. Eskandarian, "The threat of intelligent collisions," *IT professional*, vol. 6, pp. 24-29, 2004.

[58] Z. Fang, *et al.*, "A sensitive indicator of regional space–time accessibility," *Annals of GIS*, vol. 16, pp. 155-164, 2010.

[59] L. Tijerina, *et al.*, "Effects of adaptive lane departure warning system on driver response to a surprise event," *Transportation Research Record: Journal of the Transportation Research Board*, vol. 2185, pp. 1-7, 2010.

[60] Y. Dong, *et al.*, "Driver inattention monitoring system for intelligent vehicles: A review," *Intelligent Transportation Systems, IEEE Transactions on*, vol. 12, pp. 596-614, 2011.

[61] S. G. Hoek and M. W. Newton, "Blind spot detection system and method using preexisting vehicular imaging devices," ed: Google Patents, 2011.

[62] A. Ruta, *et al.*, "In-vehicle camera traffic sign detection and recognition," *Machine Vision and Applications*, vol. 22, pp. 359-375, 2011.

[63] M. Mosley. (2011). *The future of Intelligent Transport Systems (ITS)*. Available: http://mubbisherahmed.wordpress.com/2011/11/29/the-future-of-intelligent-transport-systems-its/

[64] B. D. Greenshields, "A study of traffic capacity," 1935, pp. 448-477.

[65] J. VanderWerf, *et al.*, "Modeling effects of driver control assistance systems on traffic," *Transportation Research Record: Journal of the Transportation Research Board*, vol. 1748, pp. 167-174, 2001.

[66] R. Gurulingesh, "Adaptive Cruise Control," Kanwal Rekhi School of Information Technology, Indian Institute of Technology Bombay, 2005.

[67] J. Piao and M. McDonald, "Advanced driver assistance systems from autonomous to cooperative approach," *Transport Reviews*, vol. 28, pp. 659-684, 2008.

[68] U. Palmquist, "Intelligent cruise control and roadside information," *Micro, IEEE*, vol. 13, pp. 20-28, 1993.

[69] J. Bohren, *et al.*, "Little Ben: the Ben Franklin racing team's entry in the 2007 DARPA urban challenge," *Journal of Field Robotics*, vol. 25, pp. 598-614, 2008.

[70] A. Polychronopoulos, *et al.*, "Centralized data fusion for obstacle and road borders tracking in a collision warning system," Mountain View, CA, USA, 2004, pp. 760-7.

[71] G. P. Stein, *et al.*, "A Computer Vision System on a Chip: a case study from the automotive domain," in *Computer Vision and Pattern Recognition - Workshops, 2005. CVPR Workshops. IEEE Computer Society Conference on*, 2005, pp. 130-130.

[72] K. Eghbal-Azar and T. Widlok, "Potentials and Limitations of Mobile Eye Tracking in Visitor Studies Evidence From Field Research at Two Museum Exhibitions in Germany," *Social Science Computer Review*, vol. 31, pp. 103-118, 2013.

[73] K. Bilstrup, "A survey regarding wireless communication standards intended for a high-speed vehicle environment," 2007.

[74] IEEE, "Wireless LAN medium access control (MAC) and physical layer (PHY) specifications," in *IEEE Standard* vol. 802, ed, 1999, p. 999.

[75] S. Taneja and A. Kush, "A Survey of routing protocols in mobile ad hoc networks," *International Journal of innovation, Management and technology*, vol. 1, pp. 2010-0248, 2010.

[76] H. Gossain, *et al.*, "Supporting MAC layer multicast in IEEE 802.11 based MANETs: issues and solutions," in *Local Computer Networks, 2004. 29th Annual IEEE International Conference on*, 2004, pp. 172-179.

[77] B. Mustafa and U. W. Raja, "Issues of Routing in VANET," *School of Computing at Blekinge Institute of Technology*, 2010.

[78] Y. W. Lin, *et al.*, "Routing protocols in vehicular ad hoc networks: A survey and future perspectives," *Journal of Information Science and Engineering*, vol. 26, pp. 913-932, 2010.

[79] F. Kaisser, *et al.*, "Simulations of VANET Scenarios with OPNET and SUMO," *Communication Technologies for Vehicles*, pp. 103-112, 2012.

[80] M. B. Gurjar, "Detection of Failure Node and Safety to Vehicle using V2V Communication," in *National Conference on Recent Trends in Engineering & Technology*, Gujarat,India, 2011.

[81] A. Festag, *et al.*, "Car-2-x communication for safety and infotainment in europe," *NEC Technical Journal*, vol. 3, pp. 21-26, 2008.

[82] T. Taleb, *et al.*, "A stable routing protocol to support ITS services in VANET networks," *Vehicular Technology, IEEE Transactions on*, vol. 56, pp. 3337-3347, 2007.

[83] L. Long, *et al.*, "Vehicular wireless short-range communication for improving intersection safety," *Communications Magazine, IEEE*, vol. 47, pp. 104-110, 2009.

[84] L. Reznik, *Fuzzy controllers handbook: how to design them, how they work*: Access Online via Elsevier, 1997.

[85] H. Ali, "Fuzzy controller design of servo system," *Asian Journal of Applied Science*, pp. 403-413, 2011.

[86] A. Kentli, "Studies on fuzzy logic control of electrical machines in Turkish Universities: An Overview," *Mathematical and Computational Applications*, vol. 16, p. 236, 2011.

[87] R. Sakthi, *et al.*, "Congestion Control in Differentiated Services using Fuzzy Logic Controller," *Journal of Computer and Mathematical Sciences Vol*, vol. 5, pp. 1-122, 2014.

[88] S. Hirulkar, *et al.*, "Design of Automatic Car Breaking System Using Fuzzy Logic and PID Controller," in *Electronic Systems, Signal Processing and Computing Technologies (ICESC), 2014 International Conference on*, 2014, pp. 413-418.

[89] K. M. Passino and S. Yurkovich, *Fuzzy control* vol. 42: Citeseer, 1998.

[90] A. N. Udupa, *et al.*, "An expert fuzzy control approach to voltage stability enhancement," *International Journal of Electrical Power & Energy Systems*, vol. 21, pp. 279-287, 1999.

[91] D. J. Chang and E. K. Morlok, "Vehicle speed profiles to minimize work and fuel consumption," *Journal of transportation engineering*, vol. 131, pp. 173-182, 2005.

[92] Robert Bosch GmbH., *Automotive handbook*, 4th ed. Stuttgart, [Germany]: Bosch, 1996.

[93] H. Yue, "Mesoscopic fuel consumption and emission modeling," Virginia Polytechnic Institute and State University, 2008.

[94] M. Alsabaan, *et al.*, "Applying Vehicular Ad Hoc Networks for Reduced Vehicle Fuel Consumption," in *Recent Trends in Wireless and Mobile Networks*. vol. 84, A. Özcan, *et al.*, Eds., ed: Springer Berlin Heidelberg, 2010, pp. 217-228.

[95] S. Yasunobu, *et al.*, "A fuzzy control for train automatic stop control," *Trans. of the Society of Instrument and Control Engineers*, vol. 2, pp. 1-9, 2002.

[96] K. Ahn, *et al.*, "Estimating vehicle fuel consumption and emissions based on instantaneous speed and acceleration levels," *Journal of transportation engineering*, vol. 128, pp. 182-190, 2002.

[97] D. Vallero, *Fundamentals of air pollution*: Academic press, 2007.

[98] B. Sharma, *Environmental chemistry*: Krishna Prakashan, 2001.

[99] A. Gore, *An inconvenient truth: The planetary emergency of global warming and what we can do about it*: Rodale, 2006.

[100] H. Eren, *et al.*, "Application of zigbee for pollution monitoring caused by automobile exhaust gases," in *Sensors Applications Symposium, 2009. SAS 2009. IEEE*, 2009, pp. 164-168.

[101] J. Cable. (2006). *Nitrogen: The Silent Killer*. Available: http://ehstoday.com/safety/confined-spaces/ehs_imp_38471

[102] H. a. S. National Occupational, Commission, "Guidance Note for the Completion of a Material Safety Data Sheet," 2nd ed: AGPS, Canberra, 1990.

[103] NRC, "Expanding metropolitan highways : Implications for Air Quality and Energy Use," *Transportation Research Board. National Academy Press: Washington, DC*, 1995.

[104] G. P. Roberts, *et al.*, "CO-sensing mechanisms," *Microbiol Mol Biol Rev,* vol. 68, pp. 453-73, table of contents, Sep 2004.

[105] W. Stanton, *et al.*, "Predictors of smoking cessation processes among secondary school students," *Substance use & misuse,* vol. 41, pp. 1683-1694, 2006.

[106] P. J. Warren, *Hazardous gases and fumes*: Butterworth-Heinemann, 1997.

[107] A. C. Thomas, *et al.*, "Community study of the causes of" natural" sudden death," *British Medical Journal,* vol. 297, pp. 1453-1456, 1988.

[108] S. Ramasamy, *et al.*, "Sulfide-detoxifying enzymes in the human colon are decreased in cancer and upregulated in differentiation," *American Journal of Physiology-Gastrointestinal and Liver Physiology,* vol. 291, pp. G288-G296, 2006.

[109] J. Lacy, *et al.*, "Discovery of interstellar methane-Observations of gaseous and solid CH4 absorption toward young stars in molecular clouds," *The Astrophysical Journal,* vol. 376, pp. 556-560, 1991.

[110] M. Namekawa, *et al.*, "General purpose road traffic simulation system with a cell automaton model," Melbourne, VIC, Australia, 2005, pp. 3002-3008.

[111] A. Awazu, "Dynamics of two equivalent lanes traffic flow model: self orgnization of the slow lane and fast lane," *Journal of Physical Society of Japn* vol. 64, pp. 1071-1074, 1998.

[112] K. Rawat, *et al.*, "Two-lane traffic flow simulation model via cellular automaton," *International Journal of vehicular technology,* vol. 2012, 2012.

[113] A. Daoudia and N. Moussa, "Numerical simulations of three-lane traffic model using celluler automata," *Chinese journal of physics,* vol. 41, pp. 671-681, 2003.

[114] L. Ke-Ping, "Car deceleration considering its own velocity in cellular automata model," *Commun. Theor. Phys.,* vol. 45, pp. 113-116, 2006.

[115] R. K. Bansal and J. S. Brar, *A text book of theory of machines (in S.I. units)*: Laxmi Publications, 2004.

[116] A. Zander and U. Wiesner, "Method and arrangement for avoiding and/or minimizing vehicle collisions in road traffic," ed: Google Patents, 2000.

[117] M. Hatakka, *et al.*, "From control of the vehicle to personal self-control; broadening the perspectives to driver education," *Transportation Research Part F: Traffic Psychology and Behaviour,* vol. 5, pp. 201-215, 2002.

[118] A. Mehmood and S. M. Easa, "Modeling reaction time in car-following behaviour based on human factors," *International Journal of Applied Science, Engineering and Technology,* vol. 5, pp. 93-101, 2009.

[119] T. Kagan, *et al.*, "Traffic Congestion Management as a Learning Agent Coordination Problem," in *Multi-Agent Systems for Traffic and Transportation Engineering*, A. Bazzan and F. Klügl, Eds., ed New York: Information science reference, 2009, pp. 261-279.

[120] R. D. Yates and D. J. Goodman, *Probability and stochastic processes : a friendly introduction for electrical and computer Engineers*, 2nd ed. Hoboken, NJ: John Wiley & Sons, 2005.

[121] I. Dagli, *et al.*, "Action recognition and prediction for driver assistance systems using dynamic belief networks," in *Agent Technologies, Infrastructures, Tools, and Applications for E-Services*, ed: Springer, 2003, pp. 179-194.

[122] M. Mulder, *et al.*, "Active deceleration support in car following," *Systems, Man and Cybernetics, Part A: Systems and Humans, IEEE Transactions on*, vol. 40, pp. 1271-1284, 2010.

[123] H. Deng and H. M. Zhang, "Driver Anticipation in Car Following," *Transportation Research Record: Journal of the Transportation Research Board*, vol. 2316, pp. 31-37, 2012.

[124] M. Brackstone and M. McDonald, "Car-following: a historical review," *Transportation Research Part F: Traffic Psychology and Behaviour*, vol. 2, pp. 181-196, 1999.

[125] Y. Jing and Z. Nanning, "An Expert Fuzzy Controller for Vehicle Lateral Control," in *Industrial Electronics Society, 2007. IECON 2007. 33rd Annual Conference of the IEEE*, 2007, pp. 880-885.

[126] J. Gonder, *et al.*, "Analyzing Vehicle Fuel Saving Opportunities through Intelligent Driver Feedback," presented at the SAE World Congress Detroit, Michigan, 2012.

[127] B. G. Ros, *et al.*, "Empirical analysis of the causes of stop-and-go waves at sags," 2014.

[128] Z. Kovacic and S. Bogdan, *Fuzzy controller design: theory and applications*: CRC, 2006.

[129] M. Mulder, *et al.*, "Identification of driver car-following behaviour," in *Systems, Man and Cybernetics, 2005 IEEE International Conference on*, 2005, pp. 2905-2910.

[130] M. Mulder, *et al.*, "Effects of lead vehicle speed and separation distance on driver car-following behavior," in *Systems, Man and Cybernetics, 2005 IEEE International Conference on*, 2005, pp. 399-404.

[131] D. T. McRuer and E. S. Krendel, "Mathematical models of human pilot behavior," DTIC Document1974.

[132] K. J. Astrom, "Simple Control Systems," in *Control System Design*, ed, 2002, pp. 144-176.

[133] K. J. Astrom and R. M. Murray, *Feedback systems: an introduction for scientists and engineers*: Princeton university press, 2008.

[134] S. S. L. Chang and L. A. Zadeh, "On fuzzy mapping and control," *Systems, Man and Cybernetics, IEEE Transactions on*, pp. 30-34, 1972.

[135] A. Mazeika, *et al.*, "A new approach for computing with fuzzy sets using interval analysis," Quebec, QC, Canada, 2007.

[136] T. Hessburg and M. Tomizuka, "An adaptation method for fuzzy logic controllers in lateral vehicle guidance," *Mechatronics*, vol. 5, pp. 873-898, 1995.

[137] D. Hulsebusch, *et al.*, "Adaptive Cruise Control: A Behavioral Assessment of Following Traffic Participants Due to Energy Efficient Driving Strategies," in *Proceedings of the FISITA 2012 World Automotive Congress*. vol. 200, ed: Springer Berlin Heidelberg, 2012, pp. 209-220.

[138] R. Rajamani, "Adaptive Cruise Control," in *Vehicle Dynamics and Control*, R. Rajamani, Ed., ed. New York: Springer, 2012, pp. 141-170.

[139] X. Ma and I. Andreasson, "Behavior measurement, analysis, and regime classification in car following," *Intelligent Transportation Systems, IEEE Transactions on*, vol. 8, pp. 144-156, 2007.

[140] H. Rong-wen and L. Chia-hui, "Development of Fuzzy-based Automatic Vehicle Control System in a Virtual Reality Environment," in *Emerging Technologies, 2007. ICET 2007. International Conference on*, 2007, pp. 184-189.

[141] F. Casciati, *et al.*, "Control of nonlinear structures using the fuzzy control approach," *Nonlinear Dynamics*, vol. 11, pp. 171-187, 1996/10/01 1996.

Appendix (A)

Model (A)

$$F_A = a_s + b_s Acc + c_s Acc^2 \quad \text{(A-1)}$$

F_A : Fuel consumption or emission rates (gal/hr or milligram/s)

a_s **:** entercept

b_s, c_s **:** Coefficients of the regression equation

Acc **: A**cceleration

Model (B)

$$F_B = a_s + b_s Acc + c_s Acc^2 + d_s Acc^3 \quad \text{(A-2)}$$

Model (C)

$$F_C = a_s + b_s Acc + c_s Acc^2 \quad \text{(A-3)}$$

Where

$$a_s = a_1 + b_1 S + c_1 S^2$$
$$b_s = a_2 + b_2 S + c_2 S^2$$
$$c_s = a_3 + b_3 S + c_3 S^2$$

Model (D)

$$F_D = a_s + b_s Acc + c_s Acc^2 + d_s Acc^3 \quad \text{(A-4)}$$

Where

$$a_s = a_1 + b_1 S + c_1 S^2$$
$$b_s = a_2 + b_2 S + c_2 S^2$$
$$c_s = a_3 + b_3 S + c_3 S^2$$
$$d_s = a_4 + b_4 S + c_4 S^2$$

Model (E)

$$F_E = a_s + b_s Acc + c_s Acc^2 \quad \text{(A-5)}$$

Where

$$a_s = a_1 + b_1 S + c_1 S^2 + d_1 S^3$$
$$b_s = a_2 + b_2 S + c_2 S^2 + d_2 S^3$$
$$c_s = a_3 + b_3 S + c_3 S^2 + d_3 S^3$$

Model (F)

$$F_F = a_s + b_s Acc + c_s Acc^2 + d_s Acc^3 \quad \text{(A-6)}$$

Where

$$a_s = a_1 + b_1 S + c_1 S^2 + d_1 S^3$$
$$b_s = a_2 + b_2 S + c_2 S^2 + d_2 S^3$$
$$c_s = a_3 + b_3 S + c_3 S^2 + d_3 S^3$$
$$d_s = a_4 + b_4 S + c_4 S^2 + d_4 S^3$$

Model (G)

$$F_G = a_a + b_a S + c_a S^2 \quad \text{(A-7)}$$

F_G : Fuel consumption or emission rates (gal/hr or milligram/s) for certain speed per one second

a_s **:** entercept

b_s, c_s **:** Coefficients of equation

S **:** Speed

Model (H)

$$F_H = a_a + b_a S + c_a S^2 + d_a S^3 \quad \text{(A-8)}$$

Model (I)

$$F_I = a_a + b_a S + c_a S^2 \quad \text{(A-9)}$$

Where

$$a_a = a_1 + b_1 Acc + c_1 Acc^2$$
$$b_a = a_2 + b_2 Acc + c_2 Acc^2$$
$$c_a = a_3 + b_3 Acc + c_3 Acc^2$$

Model (J)

$$F_J = a_a + b_a S + c_a S^2 + d_a S^3 \quad \text{(A-10)}$$

Where

$$a_a = a_1 + b_1 Acc + c_1 Acc^2$$
$$b_a = a_2 + b_2 Acc + c_2 Acc^2$$
$$c_a = a_3 + b_3 Acc + c_3 Acc^2$$
$$d_a = a_4 + b_4 Acc + c_4 Acc^2$$

Model (K)

$$F_K = a_a + b_a S + c_a S^2 \quad \text{(A-11)}$$

Where

$$a_a = a_1 + b_1 Acc + c_1 Acc^2 + d_1 Acc^3$$
$$b_a = a_2 + b_2 Acc + c_2 Acc^2 + d_2 Acc^3$$
$$c_a = a_3 + b_3 Acc + c_3 Acc^2 + d_3 Acc^3$$

Model (L)

$$F_L = a_a + b_a S + c_a S^2 + d_a S^3 \quad \text{(A-12)}$$

Where

$$a_a = a_1 + b_1 Acc + c_1 Acc^2 + d_1 Acc^3$$
$$b_a = a_2 + b_2 Acc + c_2 Acc^2 + d_2 Acc^3$$
$$c_a = a_3 + b_3 Acc + c_3 Acc^2 + d_3 Acc^3$$
$$d_a = a_4 + b_4 Acc + c_4 Acc^2 + d_4 Acc^3$$

Appendix (B)

Regression Coefficients for $Dec = -0.5m/s^2$

	d_0	d_1	d_2	d_3	d_4	d_5	d_6
HC	6.88E-01	3.55E-01	1.97E-02	-6.32E-04	1.13E-05	-9.85E-08	3.48E-10
CO	1.54E+01	-8.75E-01	5.12E-01	-1.98E-02	3.65E-04	-3.17E-06	1.07E-08
NO_x	1.67E-01	1.56E-01	3.95E-03	-4.08E-05	1.13E-06	-5.9E-10	-3E-11
CO_2	3.13E-01	5.31E-01	6.20E-04	5.71E-05	-4.02E-07	6.65E-09	-3.03E-11
fuel	1.40E-04	2.44E-04	3.01E-07	2.70E-08	-2.14E-10	3.04E-12	-1.18E-14

Regression Coefficients for $Dec = -0.75m/s^2$

	d_0	d_1	d_2	d_3	d_4	d_5	d_6
HC	7.15E-01	2.11E-01	1.21E-02	-4.38E-04	8.20E-06	-7.23E-08	2.57E-10
CO	1.02E+01	5.23E-01	2.33E-01	-9.64E-03	1.84E-04	-1.64E-06	5.68E-09
NO_x	1.74E-01	1.00E-01	1.17E-03	5.12E-06	4.05E-08	4.60E-09	-3.00E-11
CO_2	5.16E-01	3.47E-01	-5.23E-05	3.90E-05	-2.95E-07	4.41E-09	-1.96E-11
fuel	2.35E-04	1.60E-04	-7.49E-08	1.97E-08	-1.74E-10	2.25E-12	-8.72E-15

Regression Coefficients for $Dec = -0.1m/s^2$

	d_0	d_1	d_2	d_3	d_4	d_5	d_6
HC	7.69E-01	1.43E-01	1.00E-02	-3.94E-04	7.52E-06	-6.68E-08	2.36E-10
CO	8.58E+00	1.27E+00	9.58E-02	-4.50E-03	9.13E-05	-8.37E-07	3.04E-09
NO_x	1.87E-01	7.75E-02	1.50E-04	1.79E-05	-2.45E-07	4.67E-09	-2.21E-11
CO_2	6.25E-01	2.60E-01	-3.33E-04	2.90E-05	-2.17E-07	2.98E-09	-1.31E-11
fuel	2.87E-04	1.20E-04	-2.22E-07	1.53E-08	-1.36E-10	1.65E-12	-6.37E-15

Regression Coefficients for $Dec = -1.25m/s^2$

	d_0	d_1	d_2	d_3	d_4	d_5	d_6
HC	6.86E-01	6.59E-02	1.21E-02	-4.68E-04	8.65E-06	-7.51E-08	2.58E-10
CO	5.46E+00	1.48E+00	3.34E-02	-1.98E-03	4.34E-05	-4.11E-07	1.59E-09
NO_x	9.29E-02	6.59E-02	-2.48E-04	1.89E-05	-2.68E-07	3.55E-09	-1.45E-11
CO_2	3.18E-01	2.12E-01	-4.34E-04	2.22E-05	-1.56E-07	1.96E-09	-8.53E-12
fuel	1.46E-04	9.82E-05	-2.77E-07	1.22E-08	-1.05E-10	1.18E-12	-4.47E-15

Regression Coefficients for $Dec = -1.5m/s^2$

	d_0	d_1	d_2	d_3	d_4	d_5	d_6
HC	9.53E-01	7.66E-02	1.04E-02	-4.41E-04	8.49E-06	-7.55E-08	2.62E-10
CO	9.87E+00	1.85E+00	-1.72E-02	-1.40E-04	1.05E-05	-1.30E-07	6.43E-10
NO_x	2.43E-01	5.84E-02	-3.55E-04	1.54E-05	-2.04E-07	2.33E-09	-8.69E-12
CO_2	7.63E-01	1.79E-01	-4.16E-04	1.68E-05	-1.08E-07	1.22E-09	-5.21E-12
fuel	3.54E-04	8.34E-05	-2.53E-07	9.10E-09	-7.15E-11	7.53E-13	-2.82E-15

Regression Coefficients for Dec $= -1.75 m/s^2$

	d_0	d_1	d_2	d_3	d_4	d_5	d_6
HC	1.03E+00	7.88E-02	8.38E-03	-3.73E-04	7.36E-06	-6.65E-08	2.33E-10
CO	1.22E+01	1.62E+00	-1.81E-02	3.25E-06	6.93E-06	-9.45E-08	5.01E-10
NO_x	3.04E-01	5.01E-02	-2.94E-04	1.27E-05	-1.67E-07	1.91E-09	-7.12E-12
CO_2	9.38E-01	1.54E-01	-3.38E-04	1.40E-05	-8.75E-08	9.90E-10	-4.26E-12
fuel	4.36E-04	7.14E-05	-2.06E-07	7.55E-09	-5.80E-11	6.15E-13	-2.32E-15

Regression Coefficients for Dec $= -2 m/s^2$

	d_0	d_1	d_2	d_3	d_4	d_5	d_6
HC	8.59E-01	-2.12E-02	1.29E-02	-4.84E-04	8.64E-06	-7.32E-08	2.44E-10
CO	4.55E+00	1.27E+00	-7.49E-03	-2.15E-04	8.99E-06	-1.02E-07	4.91E-10
NO_x	1.00E-01	4.43E-02	-2.88E-04	1.21E-05	-1.59E-07	1.76E-09	-6.51E-12
CO_2	3.25E-01	1.34E-01	-2.73E-04	1.19E-05	-7.22E-08	8.39E-10	-3.69E-12
fuel	1.50E-04	6.25E-05	-1.79E-07	6.73E-09	-5.2E-11	-5.5E-13	-2.1E-15

Regression Coefficients for Acc $= 25\%$

	d_0	d_1	d_2	d_3	d_4	d_5	d_6
HC	1.93E+00	2.77E-01	5.71E-02	-1.18E-03	1.71E-05	-1.66E-07	7.16E-10
CO	5.07E+00	5.67E+00	2.06E-01	-1.23E-02	3.94E-04	-5.16E-06	2.37E-08
NO_x	-1.115E+00	2.36E+00	-1.56E-01	7.34E-03	-1.09E-04	7.76E-07	-2.21E-09
CO_2	5.93E-01	1.09E+00	-4.32E-02	2.94E-03	-5.22E-05	4.03E-07	-1.12E-09
fuel	1.38E-04	5.56E-04	-2.59E-05	1.59E-06	-2.82E-08	2.18E-10	-6.00E-13

Regression Coefficients for Acc $= 33\%$

	d_0	d_1	d_2	d_3	d_4	d_5	d_6
HC	1.78E+00	4.39E-01	2.48E-02	-5.34E-05	-1.67E-06	-9.47E-09	1.92E-10
CO	-1.428E+00	1.20E+01	-7.30E-01	2.88E-02	-4.06E-04	2.09E-06	-9.37E-10
NO_x	1.17E+00	1.30E+00	-6.06E-02	3.77E-03	-4.95E-05	3.48E-07	-1.11E-09
CO_2	1.10E+00	8.33E-01	3.06E-02	2.40E-03	-4.29E-05	3.35E-07	-9.59E-10
fuel	3.90E-04	4.44E-04	-2.10E-05	1.38E-06	-2.47E-08	1.94E-10	-5.54E-13

Regression Coefficients for Acc $= 40\%$

	d_0	d_1	d_2	d_3	d_4	d_5	d_6
HC	2.01E+00	4.01E-01	2.13E-02	-1.05E-04	1.52E-06	-4.12E-08	2.73E-10
CO	8.51E+00	6.38E+00	-2.35E-01	9.81E-03	-7.17E-05	-3.68E-07	5.03E-09
NO_x	3.25E+00	-1.56E-01	9.01E-02	-2.31E-03	5.56E-05	-4.68E-07	1.22E-09
CO_2	1.59E+00	5.18E-01	-3.25E-03	1.15E-03	-2.00E-05	1.52E-07	-4.29E-10
fuel	6.56E-04	2.79E-04	-6.30E-06	7.20E-07	-1.23E-08	9.33E-11	-2.62E-13

Regression Coefficients for Acc = 50%

	d_0	d_1	d_2	d_3	d_4	d_5	d_6
HC	2.19E+00	5.54E-01	-4.79E-03	7.41E-04	-1.06E-05	3.94E-08	5.51E-11
CO	6.50E+00	1.01E+01	-7.77E-01	3.07E-02	-3.74E-04	1.56E-06	1.25E-10
NO_x	2.99E+00	-2.15E-01	9.47E-02	-2.98E-03	6.87E-05	-5.89E-07	1.64E-09
CO_2	1.65E+00	4.94E-01	-7.25E-03	1.03E-03	-1.59E-05	1.08E-07	-2.78E-10
fuel	6.90E-04	2.86E-04	-1.04E-05	7.55E-07	-1.17E-08	7.95E-11	-2.04E-13

Regression Coefficients for Acc = 55%

	d_0	d_1	d_2	d_3	d_4	d_5	d_6
HC	2.47E+00	4.88E-01	-3.10E-03	7.04E-04	-1.08E-05	4.81E-08	1.20E-11
CO	1.18E+01	6.90E+00	5.52E-01	2.62E-02	-3.47E-04	1.60E-06	-5.73E-10
NO_x	2.75E+00	-8.89E-02	7.67E-02	-2.41E-03	5.82E-05	-5.08E-07	1.43E-09
CO_2	1.72E+00	4.66E-01	-8.20E-03	9.90E-04	-1.53E-05	1.04E-07	-2.66E-10
fuel	7.52E-04	2.57E-04	-9.57E-06	7.09E-07	-1.11E-08	7.66E-11	-1.97E-13

Regression Coefficients for Acc = 60%

	d_0	d_1	d_2	d_3	d_4	d_5	d_6
HC	2.69E+00	4.41E-01	-1.36E-03	6.28E-04	-1.02E-05	4.87E-08	-6.99E-12
CO	1.42E+01	4.66E+00	-3.51E-01	2.08E-02	-2.92E-04	1.41E-06	-6.31E-10
NO_x	2.60E+00	-1.41E-02	6.31E-02	-1.93E-03	4.89E-05	-4.34E-07	1.22E-09
CO_2	1.77E+00	4.52E-01	1.04E-02	1.02E-03	-1.60E-05	1.10E-07	-2.87E-10
fuel	7.93E-04	2.39E-04	-9.38E-06	6.86E-07	-1.10E-08	7.67E-11	-2.00E-13

Regression Coefficients for Acc = 66%

	d_0	d_1	d_2	d_3	d_4	d_5	d_6
HC	2.89E+00	4.14E-01	-1.01E-03	5.71E-04	-9.46E-06	4.70E-08	-1.61E-11
CO	1.47E+01	3.62E+00	-2.21E-01	1.61E-02	-2.33E-04	1.11E-06	-2.26E-10
NO_x	2.45E+00	5.39E-02	5.08E-02	-1.50E-03	4.03E-05	-3.66E-07	1.04E-09
CO_2	1.81E+00	4.32E-01	-1.21E-02	1.04E-03	-1.64E-05	1.14E-07	-2.99E-10
fuel	8.23E-04	2.24E-04	-9.30E-06	6.62E-07	-1.07E-08	7.54E-11	-1.98E-13

Regression Coefficients for Acc = 75%

	d_0	d_1	d_2	d_3	d_4	d_5	d_6
HC	3.08E+00	4.10E-01	-3.96E-03	6.24E-04	-1.06E-05	5.99E-08	-6.95E-11
CO	1.43E+01	4.68E+00	-3.26E-01	1.94E-02	-2.99E-04	1.74E-06	-2.49E-09
NO_x	2.30E+00	1.39E-01	3.75E-02	-1.02E-03	3.06E-05	-2.88E-07	8.32E-10
CO_2	1.83E+00	4.10E-01	-1.33E-02	1.04E-03	-1.68E-05	1.19E-07	-3.18E-10
fuel	8.45E-04	2.11E-04	-9.51E-06	6.46E-07	-1.06E-08	7.63E-11	-2.04E-13

Regression Coefficients for Acc $= 100\%$

	d_0	d_1	d_2	d_3	d_4	d_5	d_6
HC	3.12E+00	3.07E-01	-1.84E-03	4.67E-04	-8.51E-06	5.22E-08	-7.71E-11
CO	1.54E+01	3.19E+00	-2.00E-01	1.37E-02	-2.21E-04	1.32E-06	-1.96E-09
NO_x	2.19E+00	2.69E-01	1.11E-02	-2.06E-06	9.59E-06	-1.18E-07	3.61E-10
CO_2	1.84E+00	3.44E-01	-1.29E-02	9.41E-04	-1.59E-05	1.16E-07	-3.17E-10
fuel	8.66E-04	1.73E-04	-8.34E-06	5.59E-07	-9.53E-09	7.03E-11	-1.91E-13

Regression Coefficients for Cruise Mode

	$K^e_{0,0}$	$K^e_{1,0}$	$K^e_{2,0}$	$K^e_{3,0}$
HC	-6.565E+00	3.884E-02	-8.547E-04	5.620E-06
CO	-4.744E+00	3.677E-02	-9.238E-04	7.000E-06
NO_x	-7.412E+00	3.596E-02	-1.123E-04	-3.806E-07
CO_2	1.214E-01	9.530E-03	1.189E-04	-7.158E-07
fuel	-1.443E-03	1.732E-05	6.040E-08	-2.832E-10

Appendix (C)

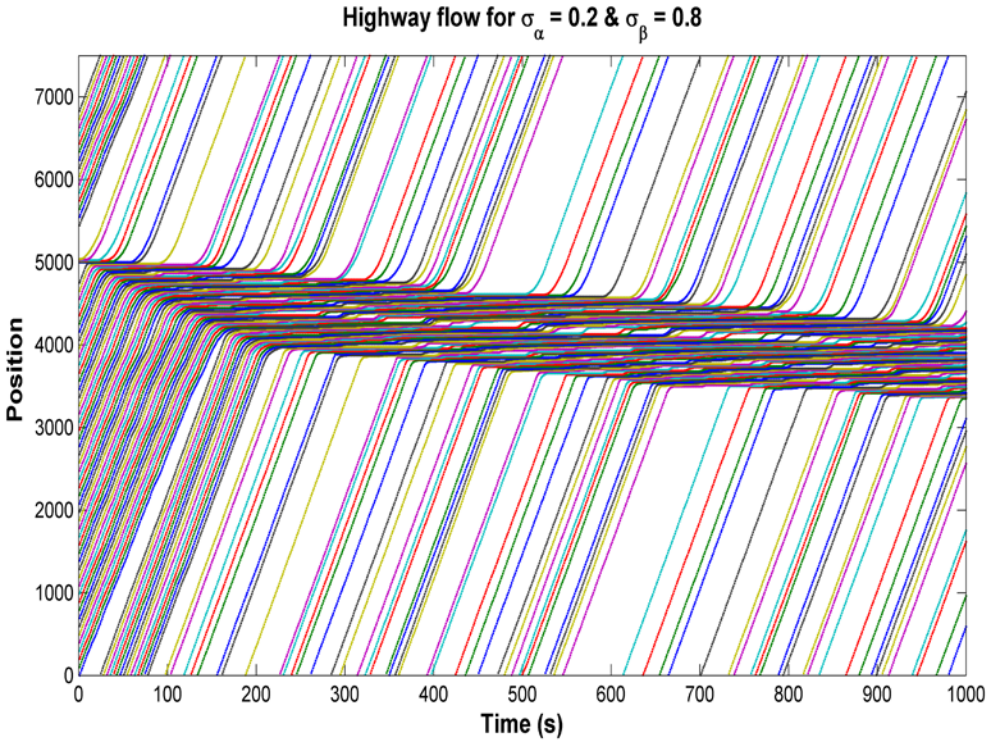

Figure C-1: Congestion shape caused by α = N (0.4, 0.2) and β = N (0.4, 0.8)

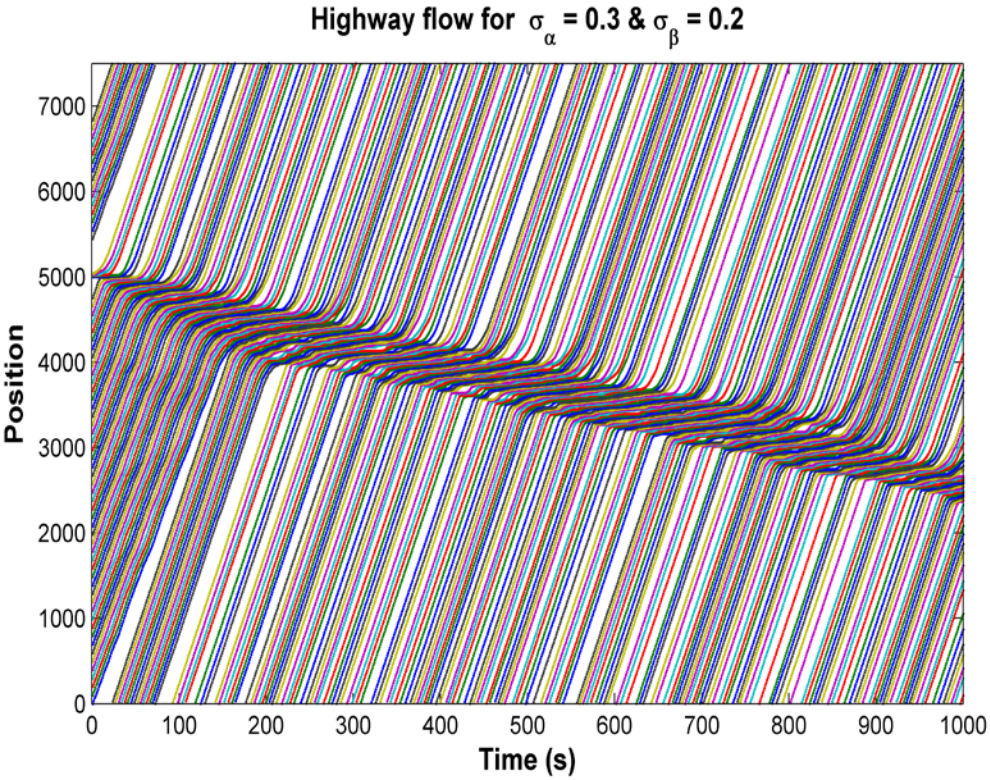

Figure C-2: Congestion shape caused by α = N (0.4, 0.3) and β = N (0.4, 0.2)

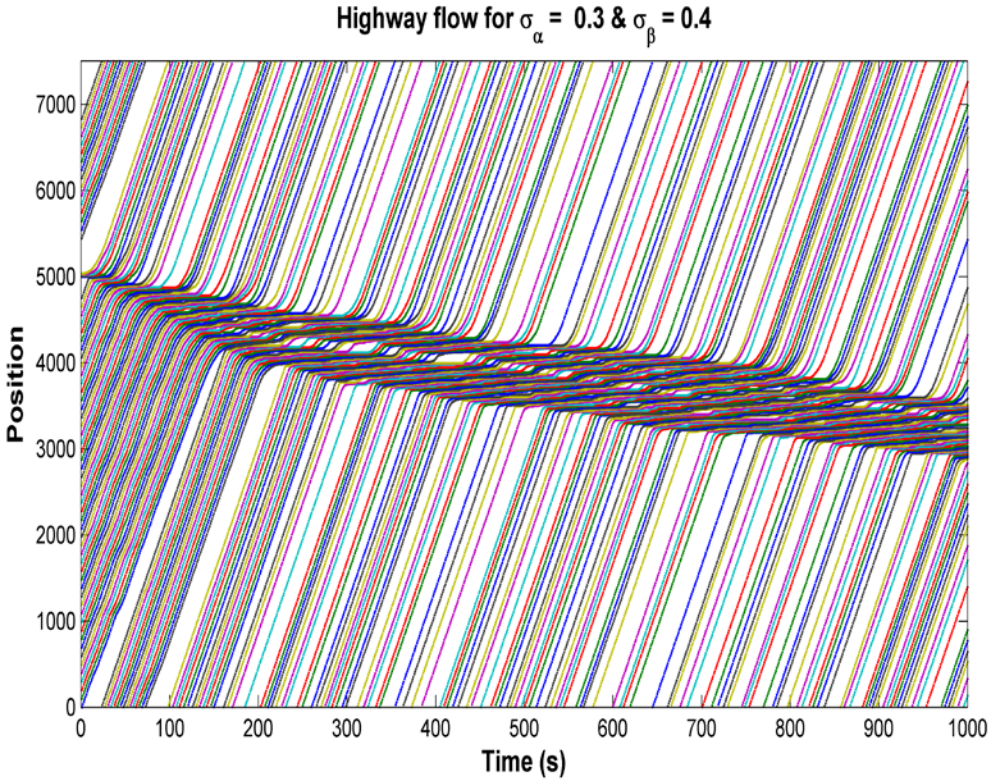

Figure C-3: Congestion shape caused by α = N (0.4, 0.3) and β = N (0.4, 0.4)

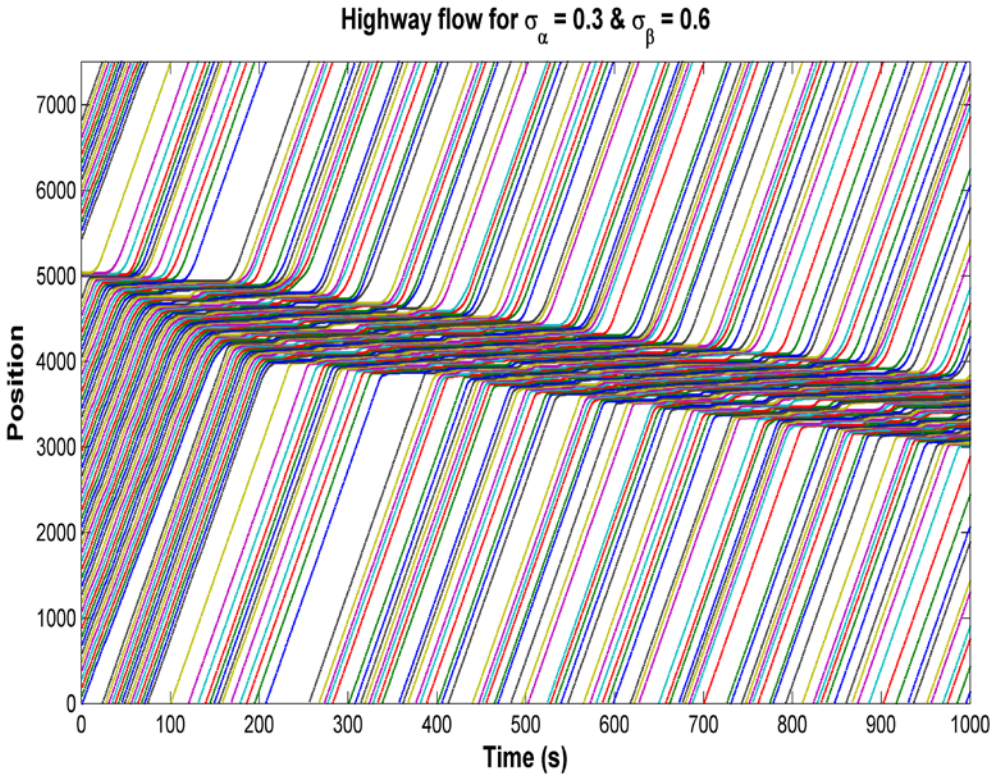

Figure C-4: Congestion shape caused by α = N (0.4, 0.3) and β = N (0.4, 0.6)

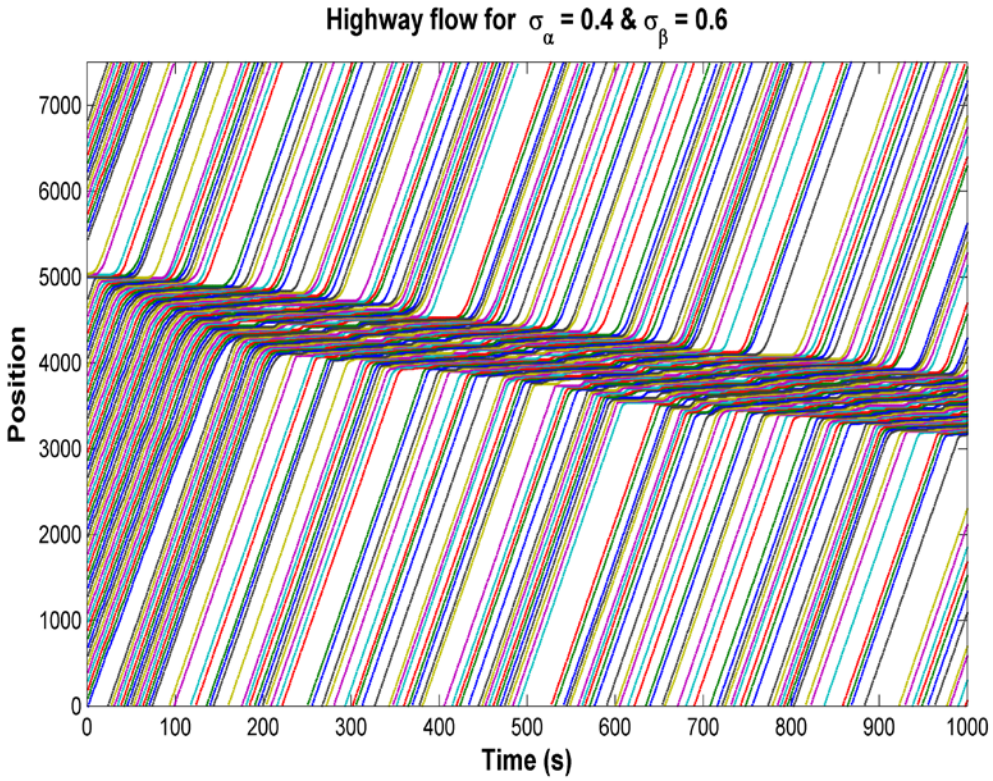

Figure C-5: Congestion shape caused by α = N (0.4, 0.4) and β = N (0.4, 0.6)

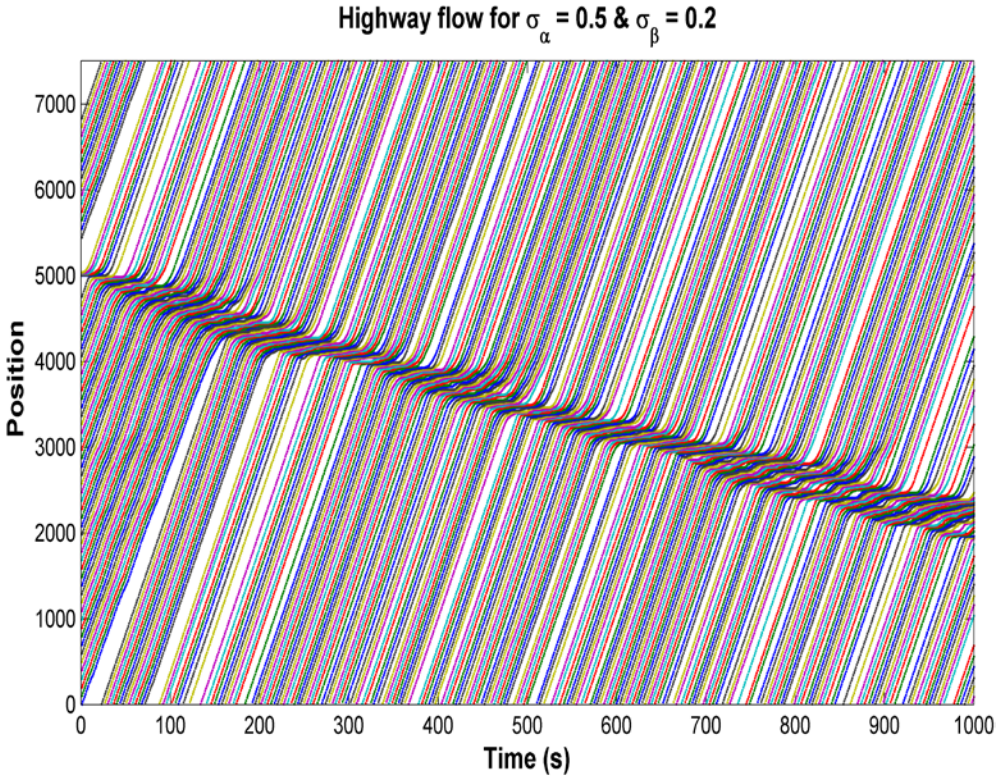

Figure C-6: Congestion shape caused by α = N (0.4, 0.5) and β = N (0.4, 0.2)

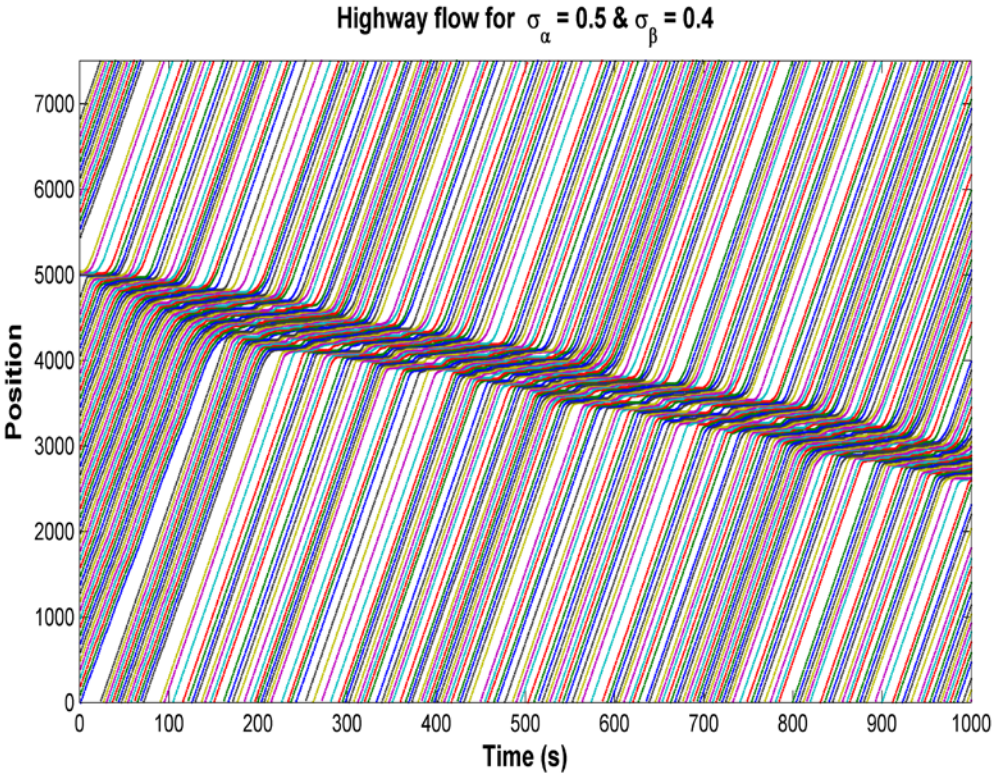

Figure C-7: Congestion shape caused by α = N (0.4, 0.5) and β = N (0.4, 0.4)

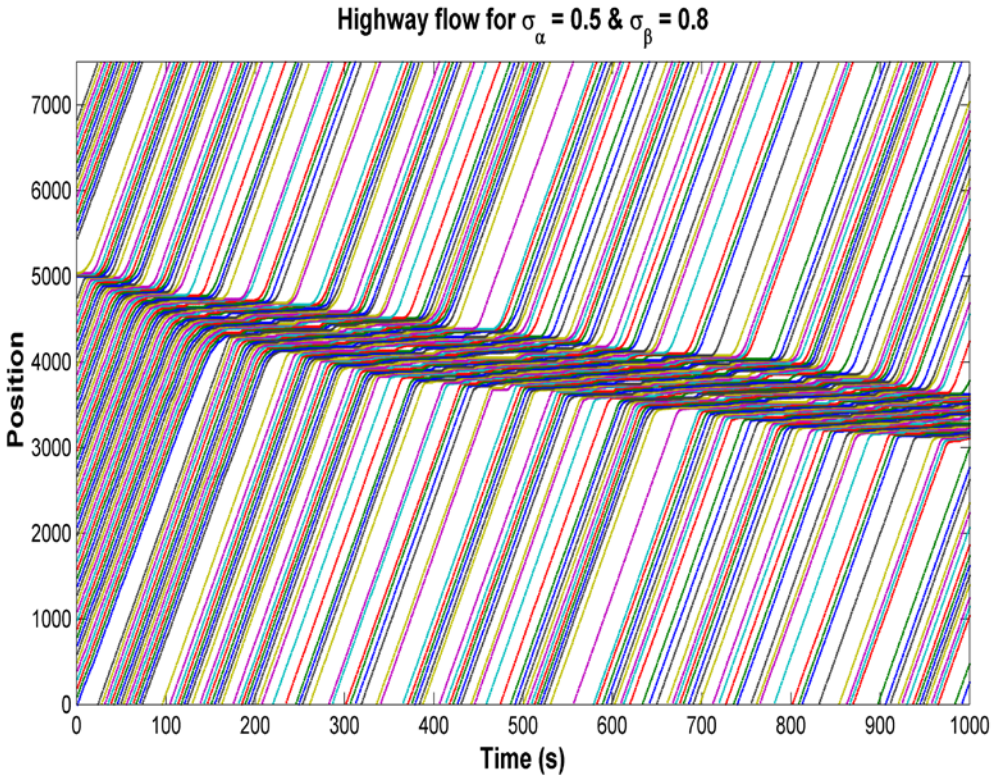

Figure C-8: Congestion shape caused by α = N (0.4, 0.5) and β = N (0.4, 0.8)

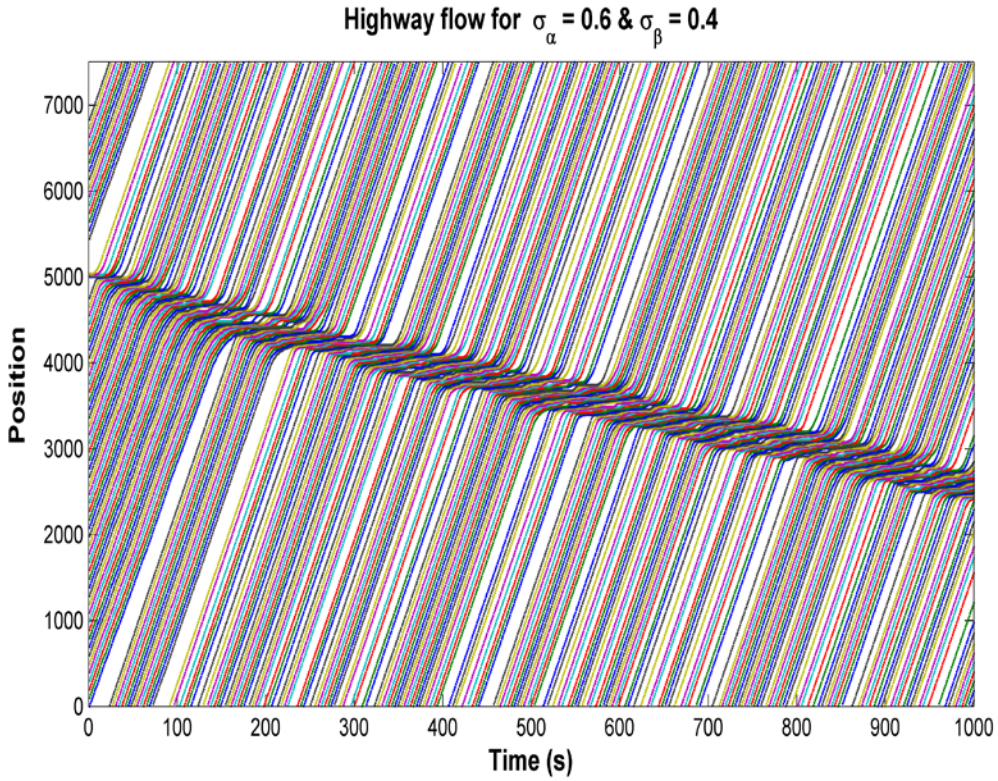

Figure C-9: Congestion shape caused by α = N (0.4, 0.6) and β = N (0.4, 0.4)

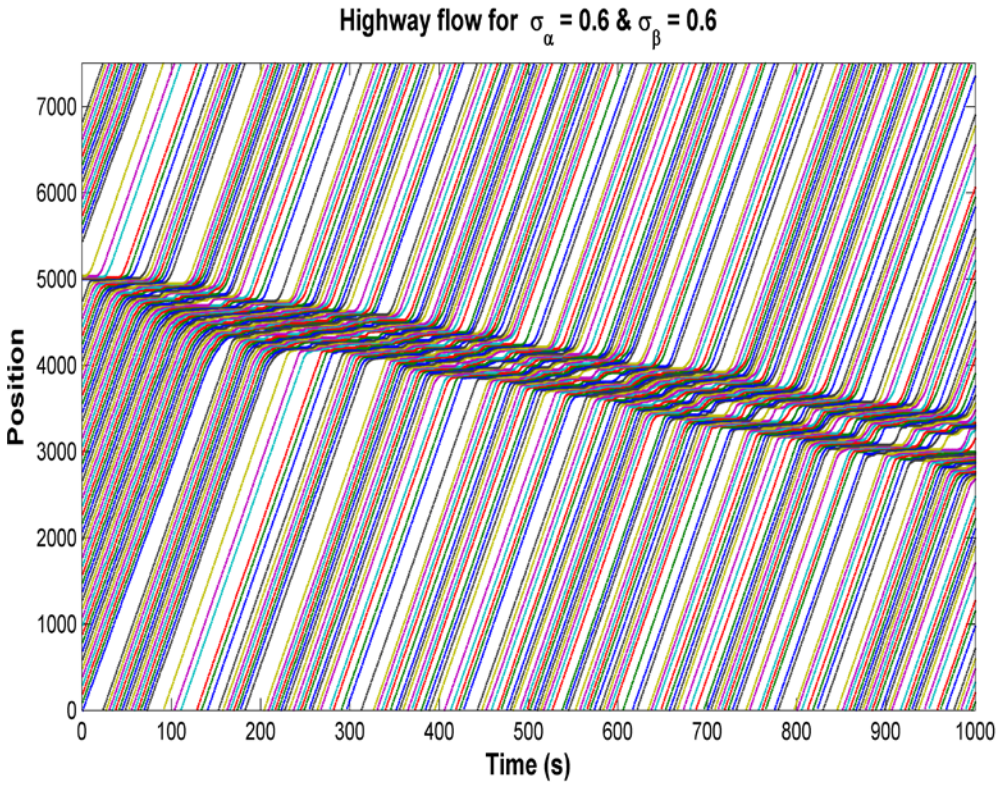

Figure C-10: Congestion shape caused by α = N (0.4, 0.6) and β = N (0.4, 0.6)

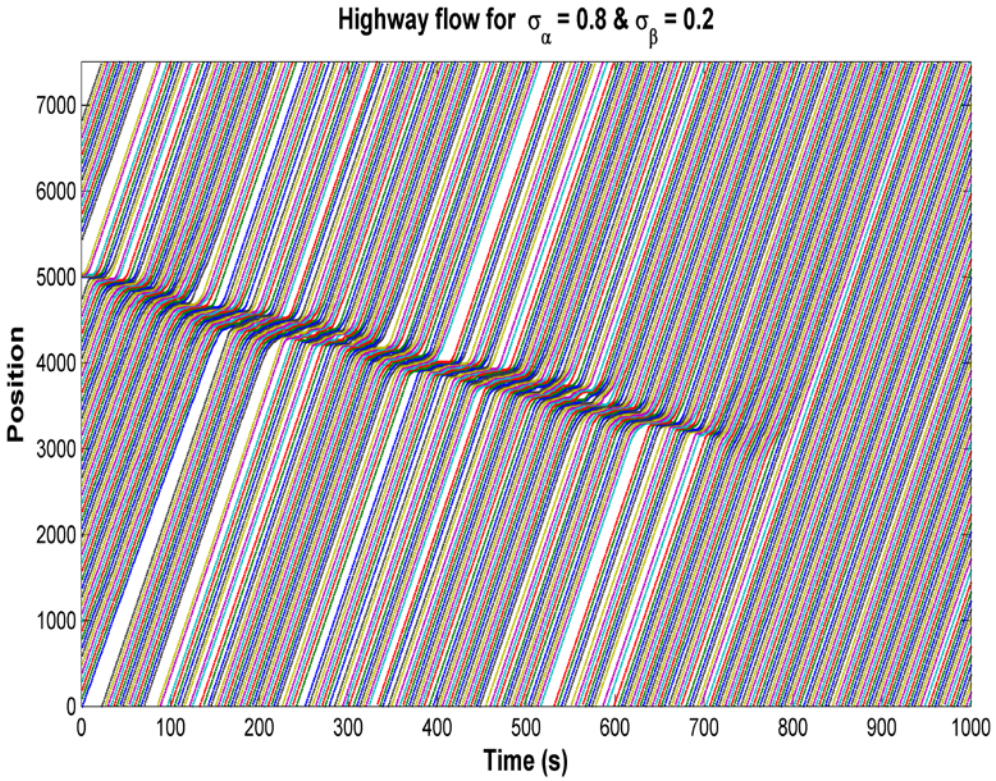

Figure C-11: Congestion shape caused by α = N (0.4, 0.8) and β = N (0.4, 0.2)

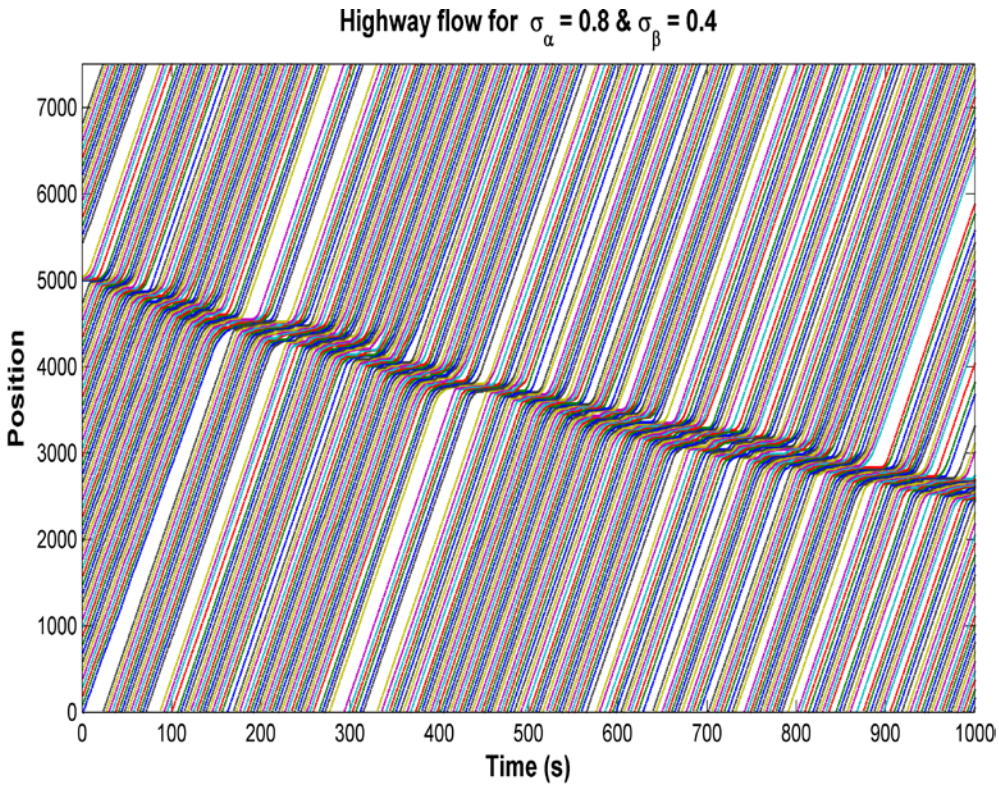

Figure C-12: Congestion shape caused by α = N (0.4, 0.8) and β = N (0.4, 0.4)

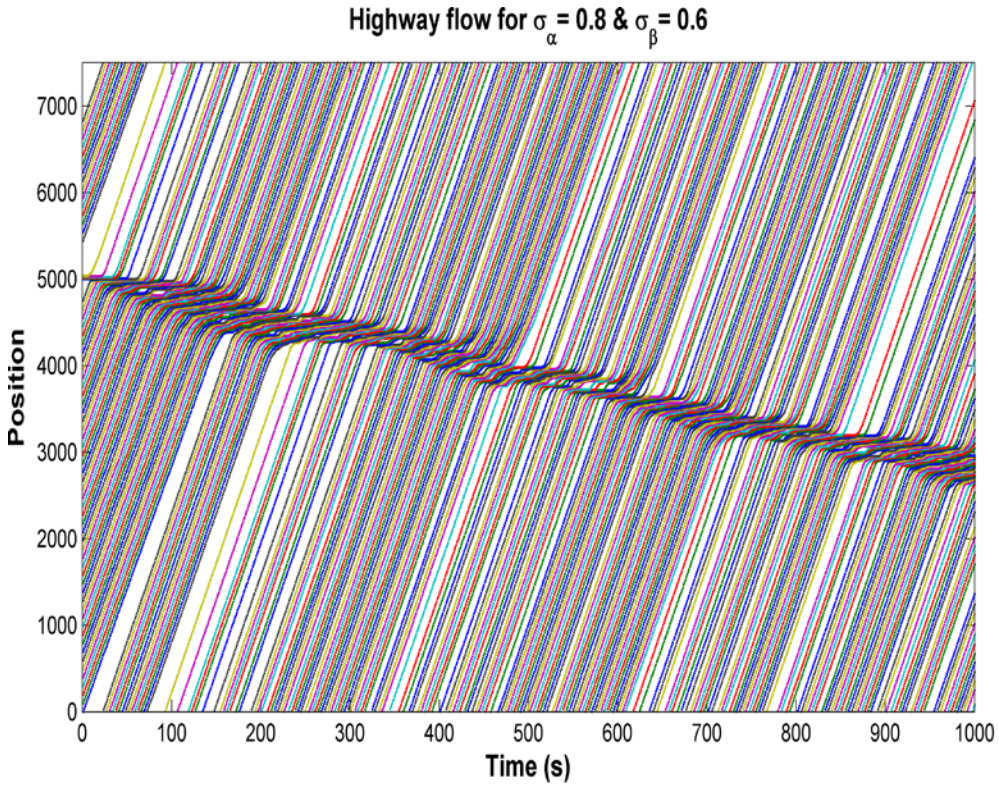

Figure C-13: Congestion shape caused by α = N (0.4, 0.8) and β = N (0.4, 0.6)

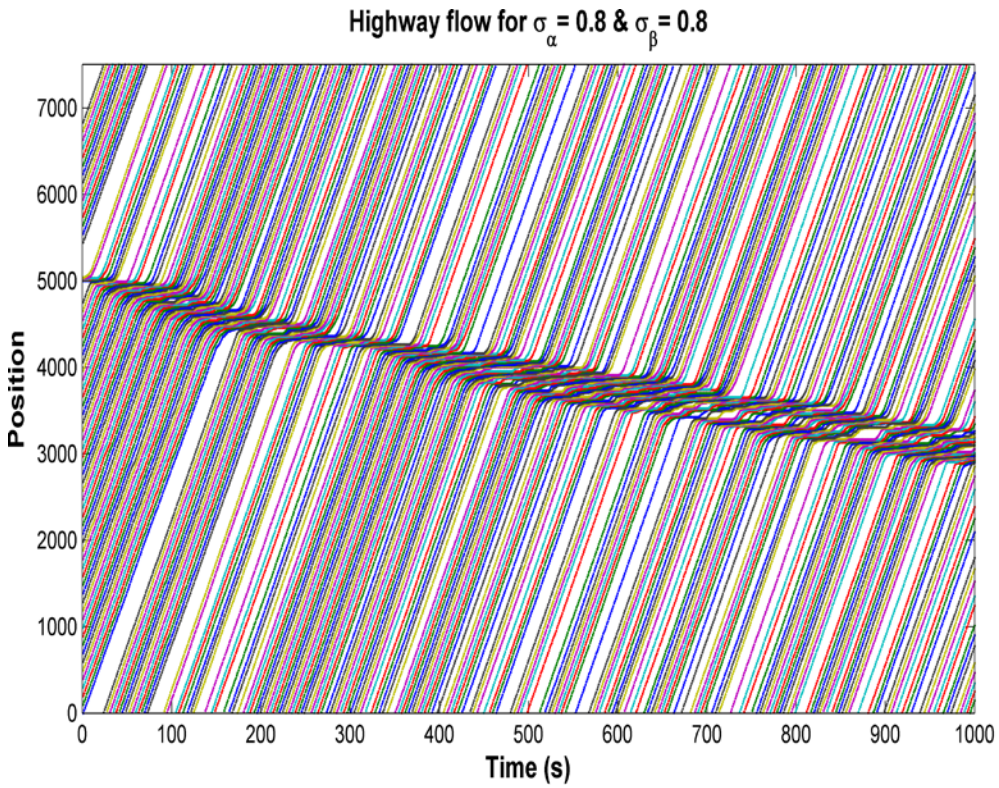

Figure C-14: Congestion shape caused by α = N (0.4, 0.8) and β = N (0.4, 0.8)

Appendix (D)

$$E1 = \begin{cases} O1 & if\ p(YES) \otimes \alpha 3 \\ Z & other\ else \end{cases} \quad \text{(D-1)}$$

$$E2 = \begin{cases} O1 & if\ p(YES) \otimes \alpha 1 \otimes \beta 1 \\ O2 & if\ p(YES) \otimes (\alpha \geq \beta) \\ Z & other\ else \end{cases} \quad \text{(D-2)}$$

$$E3 = \begin{cases} O2 & if\ (\alpha 1 \otimes \beta 1) \oplus (\alpha 2 \otimes \overline{\beta 3}) \\ O3 & if\ p(YES) \otimes (\alpha \geq \beta) \\ Z & other\ else \end{cases} \quad \text{(D-3)}$$

$$E4 = \begin{cases} O3 & if\ p(YES) \otimes \alpha 1 \otimes \beta 1 \\ O4 & if\ p(YES) \otimes \alpha 2 \otimes \overline{\beta 3} \\ O5 & if p(YES) \otimes \alpha 3 \\ Z & other\ else \end{cases} \quad \text{(D-4)}$$

$$E5 = \begin{cases} O5 & if\ p(YES) \otimes \alpha 1 \otimes \beta 1 \\ O6 & if\ p(YES) \otimes (\alpha \geq \beta) \\ Z & other\ else \end{cases} \quad \text{(D-5)}$$

$$E6 = \begin{cases} O6 & if\ p(YES) \otimes \alpha 1 \otimes \beta 1 \\ O7 & if\ p(YES) \otimes (\alpha \geq \beta) \\ Z & other\ else \end{cases} \quad \text{(D-6)}$$

$$E7 = \begin{cases} O7 & if\ p(YES) \otimes \alpha 1 \otimes \beta 1 \\ O8 & if\ p(YES) \otimes (\alpha \geq \beta) \\ Z & other\ else \end{cases} \quad \text{(D-7)}$$

$$E8 = \begin{cases} O9 & if\ p(YES) \otimes \alpha 1 \otimes \beta 1 \\ O10 & if\ p(YES) \otimes (\alpha \geq \beta) \\ Z & other\ else \end{cases} \quad \text{(D-8)}$$

$$E9 = \begin{cases} O10 & if\ p(YES) \otimes \alpha 1 \otimes \beta 1 \\ O11 & if\ p(YES) \otimes (\alpha \geq \beta) \\ Z & other\ else \end{cases} \quad \text{(D-9)}$$

$$E10 = \begin{cases} O12 & if\ p(YES) \otimes (\alpha \geq \beta) \\ Z & other\ else \end{cases} \quad \text{(D-10)}$$

$$E11 = \begin{cases} O1 & if\ (\alpha 2 \otimes \overline{\beta 3}) \oplus \alpha 3 \\ Z & other\ else \end{cases} \quad \text{(D-11)}$$

$$E12 = \begin{cases} O1 & if\ \alpha 1 \otimes \beta 1 \oplus (\alpha 2 \otimes \overline{\beta 3}) \\ O2 & if\ \alpha 3 \\ Z & other\ else \end{cases} \quad \text{(D-12)}$$

$$E13 = \begin{cases} O2 & if\ \alpha 1 \otimes \beta 1 \\ O3 & if\ (\alpha 2 \otimes \overline{\beta 3}) \oplus \alpha 3 \\ Z & other\ else \end{cases} \quad \text{(D-13)}$$

$$E14 = \begin{cases} O3 & if\ \alpha 1 \otimes \beta 1 \\ O4 & if\ (\alpha 2 \otimes \overline{\beta 3}) \oplus \alpha 3 \\ Z & other\ else \end{cases} \quad \text{(D-14)}$$

$$E15 = \begin{cases} O4 & if\ \alpha 1 \otimes \beta 1 \\ O6 & if\ (\alpha 2 \otimes \overline{\beta 3}) \oplus \alpha 3 \\ Z & other\ else \end{cases} \quad \text{(D-15)}$$

$$E16 = \begin{cases} O7 & if\ \alpha 1 \otimes \beta 1 \oplus (\alpha 2 \otimes \overline{\beta 3}) \\ O6 & if\ \alpha 3 \\ Z & other\ else \end{cases} \quad \text{(D-16)}$$

$$E17 = \begin{cases} NO1 & if\ \overline{\alpha 3} \otimes \beta 3 \\ Z & other\ else \end{cases} \quad \text{(D-17)}$$

$$E18 = \begin{cases} O1 & if\ \alpha 1 \otimes \beta 1 \\ O2 & if\ (\alpha 2 \otimes \overline{\beta 3}) \oplus \alpha 3 \\ Z & other\ else \end{cases} \quad \text{(D-18)}$$

$$E19 = \begin{cases} O2 & if\ \alpha 1 \otimes \beta 1 \\ O3 & if\ \alpha 2 \otimes \overline{\beta 3} \\ O4 & if\ \alpha 3 \\ Z & other\ else \end{cases} \quad \text{(D-19)}$$

$$E20 = \begin{cases} O3 & if\ \alpha 1 \otimes \beta 1 \\ O4 & if\ \alpha 2 \otimes \overline{\beta 3} \\ O5 & if\ \alpha 3 \\ Z & other\ else \end{cases} \quad \text{(D-20)}$$

$$E21 = \begin{cases} O5 & if\ \alpha 1 \otimes \beta 1 \\ O6 & if\ (\alpha 2 \otimes \overline{\beta 3}) \oplus \alpha 3 \\ Z & other\ else \end{cases} \quad \text{(D-21)}$$

$$E22 = \begin{cases} O6 & if\ \alpha 1 \otimes \beta 1 \\ O7 & if\ (\alpha 2 \otimes \overline{\beta 3}) \oplus \alpha 3 \\ Z & other\ else \end{cases} \quad \text{(D-22)}$$

$$E23 = \begin{cases} O7 & if\ \alpha 1 \otimes \beta 1 \\ O8 & if\ (\alpha 2 \otimes \overline{\beta 3}) \oplus \alpha 3 \\ Z & other\ else \end{cases} \quad \text{(D-23)}$$

$$E24 = \begin{cases} O10 & if\ \alpha \geq \beta \\ Z & other\ else \end{cases} \quad \text{(D-24)}$$

$$E25 = \begin{cases} O8 & if\ \alpha \geq \beta \\ Z & other\ else \end{cases} \quad \text{(D-25)}$$

$$E26 = \begin{cases} NO2 & if\ \overline{\alpha 3} \\ Z & other\ else \end{cases} \quad \text{(D-26)}$$

$$E27 = \begin{cases} O7 & if\ \alpha \geq \beta \\ Z & other\ else \end{cases} \quad \text{(D-27)}$$

$$E28 = \begin{cases} O6 & if\ \alpha \geq \beta \\ Z & other\ else \end{cases} \quad \text{(D-28)}$$

$$E29 = \begin{cases} O5 & if\ \alpha \geq \beta \\ Z & other\ else \end{cases} \quad \text{(D-29)}$$

$$E30 = \begin{cases} O4 & if\ \alpha \geq \beta \\ Z & other\ else \end{cases} \quad \text{(D-30)}$$

$$E31 = \begin{cases} O2 & if\ \alpha \geq \beta \\ Z & other\ else \end{cases} \quad \text{(D-31)}$$

$$E32 = \begin{cases} NO2 & if\ \alpha 1 \otimes \overline{\beta 1} \\ NO1 & if\ \overline{\alpha 3} \otimes \beta 3 \\ O1 & if\ \alpha 3 \\ Z & other\ else \end{cases} \quad \text{(D-32)}$$

Appendix (E)

Table E-1: Capacity and Traffic flow for different speeds

Velocity	20	40	60	80	100	120	140
Max-Capacity	310	183	130	101	82	69	60
Experiment Capacity	69	69	69	69	69	69	69
Capacity rate	0.22	0.377	0.53	0.683	0.84	1	1.15
Max-Traffic flow	372	439.2	468	484.8	492	496.8	504
Traffic flow	79	162	244	324	383	345	
Traffic flow rate	0.212	0.369	0.521	0.668	0.778	0.694	